Assessing the *in vitro* toxicity of engineered and airborne nanoceramics - contribution to the safe production and use of nanomaterials in the ceramic industry

Maria João Bessa

D

2022

U. PORTO

Maria João Moura Gonçalves Moutinho de Bessa

Assessing the *in vitro* toxicity of engineered and airborne nanoceramics - contribution to the safe production and use of nanomaterials in the ceramic industry

Thesis for application to the Doctoral degree in Biomedical Sciences; Doctorate of University of Porto (Institute of Biomedical Sciences Abel Salazar)

Supervisor: Sónia Alexandra Teixeira Fraga
Category: Auxiliary Researcher/Invited Assistant Professor;
Affiliation: Dept. of Environmental Health, National Institute of Health Dr. Ricardo Jorge, Porto, Portugal/ Faculty of Medicine of the University of Porto, Porto, Portugal

Co-Supervisor: João Paulo Fernandes Teixeira
Category: Auxiliary Researcher
Affiliation: Dept. of Environmental Health, National Institute of Health Dr. Ricardo Jorge, Porto, Portugal

Co-Supervisor: Blanca Laffon Lage
Category: Full Professor
Affiliation: Dept. of Psychology, University of A Coruña, Spain

Declaration of Honor

I declare that this thesis is my own and has not been previously submitted to another course or curricular unit, in ICBAS-UP or another institution. References to other authors (statements, ideas, thoughts) scrupulously respect the rules of attribution and are duly indicated in the text and bibliographic references, according to the rules of reference. I am aware that the practice of plagiarism and self-plagiarism is an academic illicit.

Porto, 01 July 2022

Assinado por: **Maria João Moura Gonçalves Moutinho de Bessa**
Num. de Identificação: 14174493
Data: 2022.07.04 10:54:40+01'00'

CHAVE MÓVEL

Maria João Moura Gonçalves Moutinho de Bessa

A todos aqueles que me ajudaram a manter a minha mente focada no que realmente importa.

To all of those that helped me keep my mind focused on what really matters.

"I have been impressed with the urgency of doing. Knowing is not enough; we must apply. Being willing is not enough; we must do."
Leonardo da Vinci

Acknowledgments

These last years have been a long road of hard work, dedication, and perseverance. But I could never forget those who accompanied me on this journey. I owe all of you my deepest gratitude for making this a rewarding and priceless experience.

I would like to begin with a special tribute to my supervisor Dr. Sónia Fraga, for her continuous support and patient guidance throughout my PhD. Alongside me, Dr. Sónia assisted me in overcoming all obstacles, but no less important was also present to celebrate all victories together. I am beyond grateful!

My sincere thanks also go to my co-supervisor, Dr. João Paulo Teixeira, who provided me an unforgettable opportunity to join his research team eight years ago, and since then he never stopped believing in me and what I am capable of, and always persuade me to do more and better.

To Prof. Blanca Laffon, a warm thanks for her guidance and kind words of strength and encouragement.

I would also like to extend my acknowledgements to Prof. Eduardo Jorge Sousa da Rocha, Full Professor, my Mentor Co-Supervisor at the ICBAS of the University of Porto, which tutored me in the PhD from the start on behalf of the institution. I am extremely grateful for his generous insights and valuable advice.

Besides my supervisors, I could not forget to mention and acknowledge the valuable assistance and contribution of Dr. Mar Viana and Dr. Apostolos Salmatonidis from the Institute of Environmental Assessment and Water Research (Barcelona, Spain), as well as Prof. Flemming R. Cassee from the National Institute for Public Health and the Environment (Bilthoven, The Netherlands).

My deepest and most grateful thanks are also extended to all Department of Environmental Health personnel from the National Institute of Health Dr. Ricardo Jorge (Porto) that accompanied me over these last years. Their constant motivation, kindness, and friendship filled my heart with warmth and joy, even in the darkest of times. Thank you for being my second family, I would never forget you!

To my closest family and friends, I would like to express my greatest appreciation for your patience and advice that helped me keep my mind focused on what really matters. Your support means the world to me, and I could not have done it without you.

x

Funding

Under the scope of this thesis, the following manuscripts were published, submitted, or will be submitted to international peer-reviewed journals:

Manuscripts in international peer-reviewed journals:

1. Bessa, M. J., Brandão, F., Querido, M. M., Costa, C., Pereira, C. C., Valdiglesias, V., Laffon, B., Carriere, M., Teixeira, J. P., & Fraga, S. (2019). Optimization of the harvesting and freezing conditions of human cell lines for DNA damage analysis by the alkaline comet assay. *Mutat Res Genet Toxicol Environ Mutagen*, *845*, 402994. https://doi.org/10.1016/j.mrgentox.2018.12.002

2. Bessa, M. J., Brandão, F., Viana, M., Gomes, J. F., Monfort, E., Cassee, F. R., Fraga, S., & Teixeira, J. P. (2020). Nanoparticle exposure and hazard in the ceramic industry: an overview of potential sources, toxicity and health effects. *Environ Res*, *184*, 109297. https://doi.org/10.1016/j.envres.2020.109297

3. Bessa, M. J., Brandão, F., Fokkens, P., Cassee, F. R., Salmatonidis, A., Viana, M., Vulpoi, A., Simon, S., Monfort, E., Teixeira, J. P., & Fraga, S. (2021). Toxicity assessment of industrial engineered and airborne process-generated nanoparticles in a 3D human airway epithelial *in vitro* model. *Nanotoxicology*, *15*(4), 542-557. https://doi.org/10.1080/17435390.2021.1897698

4. Viana, M., Salmatonidis, A., Bezantakos, S., Ribalta, C., Moreno, N., Córdoba, P., Cassee, F. R., Boere, J., Fraga, S., Teixeira, J. P., Bessa, M. J., & Monfort, E. (2021). Characterizing the Chemical Profile of Incidental Ultrafine Particles for Toxicity Assessment Using an Aerosol Concentrator. *Ann Work Expo Health*, *65*(8), 966-978. https://doi.org/10.1093/annweh/wxab011

5. Bessa, M. J., Brandão, F., Fokkens, P. H. B., Leseman, D., Boere, A. J. F., Cassee, F. R., Salmatonidis, A., Viana, M., Vulpoi, A., Simon, S., Monfort, E., Teixeira, J. P., & Fraga, S. (2021). *In vitro* Toxicity of Industrially Relevant Engineered Nanoparticles in Human Alveolar Epithelial Cells: Air-Liquid Interface versus Submerged Cultures. *Nanomaterials (Basel)*, *11*(12), 3225. https://doi.org/10.3390/nano11123225

6. Bessa, M. J., Brandão, F., Fokkens, P., Leseman, D., Boere, J., Cassee, F. R., Salmatonidis, A., Viana, M., Monfort, E., Fraga, S. & Teixeira, J. P. (2022). Unveiling the toxicity of fine and nano-sized airborne particles generated from industrial thermal spraying processes in human alveolar epithelial cells. *Int J Mol Sci*, *23*(8), 4278. https://doi.org/10.3390/ijms23084278

Manuscripts submitted to international peer-reviewed journals:
1. Bessa, M. J., Brandão, F., Rosário, F., Moreira, L., Reis, A.T., Valdiglesias, V., Laffon, B., Fraga, S., & Teixeira, J. P. (2022). Assessing the *in vitro* toxicity of airborne (nano)particles to the human respiratory system: from basic to advanced models [under review].

Conference abstracts:
1. Bessa, M. J., Brandão, F., Querido, M., Costa, C., Teixeira, J. P., & Fraga, S. (2017). Freezing procedure optimization of two human cell lines for comet assay analysis. *Mutagenesis, 32*(6), e23. https://doi.org/10.1093/mutage/gex037
2. Fraga, S., Bessa M. J., Brandão F., Fokkens P., Boere J., Leseeman D., Salmatonidis A., Viana M., Cassee F., & Teixeira, J. P. (2018). Toxicity of ceramic nanoparticles in human alveolar epithelial A549 cells at the air-liquid interface. *Toxicol Lett, 295*, S214. https://doi.org/10.1016/j.toxlet.2018.06.924

This thesis describes research conducted at the Dept. of Environmental Health from the National Institute of Health Dr. Ricardo Jorge (INSA; Porto, Portugal), the National Institute for Public Health and the Environment (RIVM; Bilthoven, The Netherlands), and at the Institute of Environmental Assessment and Water Research (IDAEA; Barcelona, Spain).

I certify that the research described is original and that any parts of the work that have been conducted in collaboration are clearly indicated.

In compliance with what is stated in Decree-Law no. 204/2018 of October 23, it is hereby declared that the author of this thesis participated in the creation and execution of the experimental work leading to the results shown, as well as in their interpretation and writing of the respective manuscripts. The manuscripts provided in this thesis were not previously included in other theses and correspond to their integral versions.

Under the current legislation is not allowed the reproduction of any part of this thesis.

Under the frame of the work developed in the current dissertation, the following awards were received:

1. 2018 - Applied *In Vitro* Toxicology – Mary Ann Liebert Inc. Best Poster presentation award at the 20th International Congress on *In Vitro* Toxicology (ESTIV), Berlin, Germany: Bessa M. J., Fraga F., Brandão F., Fokkens P., Boere J., Leseman D., Salmatonidis A., Viana M., Cassee F., & Teixeira J. P.. Pairwise toxicity evaluation of ceramic nanoparticles in submerged and air-liquid interface cultures of human alveolar epithelial A549 cells.

2. 2019 - 2020 IACOBUS award for the best paper: Bessa, M. J., Brandão, F., Querido, M. M., Costa, C., Pereira, C. C., Valdiglesias, V., Laffon, B., Carriere, M., Teixeira, J. P., & Fraga, S. (2019). Optimization of the harvesting and freezing conditions of human cell lines for DNA damage analysis by the alkaline comet assay. *Mutat Res Genet Toxicol Environ Mutagen*, *845*, 402994. https://doi.org/10.1016/j.mrgentox.2018.12.002

Resumo

As tecnologias avançadas usadas na indústria cerâmica têm um forte potencial para a formação e emissão de (nano)partículas em suspensão no ar, o que significa que os trabalhadores dessas indústrias correm um grande risco de exposição a essas partículas. No entanto, os estudos toxicológicos destas (nano)partículas são ainda escassos, principalmente de partículas ambientais libertadas em indústrias como as do setor cerâmico. De modo a abordar este assunto pertinente, o presente trabalho teve como objetivo avaliar a toxicidade, usando concentrações relevantes do ponto de vista ocupacional, de partículas emitidas durante duas tecnologias de pulverização térmica industrial [pulverização por plasma à pressão atmosférica (APS) e pulverização oxicombustível de alta velocidade (HVOF)], bem como de quatro nanopartículas de engenharia [ENP; óxido de estanho (SnO_2), óxido de antimónio-estanho (ATO; $Sb_2O_3 \bullet SnO_2$), óxido de cério (CeO_2) e óxido de zircónio (ZrO_2)] utilizadas como matéria-prima na manufatura de produtos cerâmicos. Dois modelos *in vitro* do sistema respiratório humano foram expostos às partículas selecionadas: i) células epiteliais alveolares A549 mantidas sob condições submersas ou na interface ar-líquido (ALI); ii) culturas tridimensionais (3D) avançadas de epitélio respiratório das vias aéreas superiores (MucilAir™) em condições de ALI. Os principais parâmetros de toxicidade avaliados incluíram a integridade da membrana plasmática, atividade metabólica, stress oxidativo, resposta inflamatória e genotoxicidade.

Na generalidade, as partículas geradas pelos dois processos de pulverização térmica causaram maior toxicidade comparativamente às ENP, muito provavelmente devido à sua maior complexidade e composição química, apresentando níveis elevados de elementos metálicos como crómio (Cr) e níquel (Ni). Entre os dois processos de pulverização térmica avaliados, as partículas derivadas do processo de HVOF foram mais citotóxicas do que as emitidas durante o processo de APS. Para ambos os processos de pulverização, tanto as partículas finas (PGFP) como as nanopartículas (PGNP) originadas foram capazes de induzir efeitos genotóxicos. No entanto, enquanto as partículas emitidas por APS levaram ao aumento dos níveis de fosforilação de histona 2AX (H2AX), as partículas de HVOF causaram lesões oxidativas no DNA do tipo 8-oxo-guanina (8-oxo-G). Por um lado, as células epiteliais alveolares humanas foram mais sensíveis à ação das ENP quanto cultivadas em condições de ALI e expostas às ENP sob a forma de aerossol,

do que quando expostas em condições submersas às ENP dispersas em meio de cultura sem soro bovino fetal, particularmente as ZrO_2 NP. Por outro lado, as culturas avançadas MucilAir™, que melhor recapitulam caraterísticas fisiológicas observadas *in vivo* como o transporte mucociliar, um importante mecanismo de defesa, foram mais resistentes às partículas emitidas por HVOF e às ENP, comparativamente às culturas epiteliais alveolares humanas convencionais. Deste modo, os modelos 3D de culturas do epitélio respiratório humano das vias aéreas superiores apresentaram uma resposta mais atenuada, enquanto as culturas convencionais de células A549 foram mais sensíveis às (nano)partículas estudadas.

O presente trabalho destaca assim o perigo das (nano)partículas libertadas durante processos industriais ou utilizadas como matéria-prima para a manufatura de cerâmicas. Não apenas as propriedades físico-químicas das partículas, mas também as condições de exposição, i.e. o modelo celular *in vitro* usado e o tipo de exposição, tiveram um papel determinante nos efeitos biológicos observados. Estes resultados reforçam a importância do uso de modelos *in vitro* fisiologicamente relevantes no estudo de toxicidade de (nano)partículas, para uma melhor extrapolação dos resultados para o Homem.

Palavras-chave: tecnologias da indústria cerâmica; partículas geradas por processos industriais; nanopartículas de engenharia; avaliação do perigo; testagem *in vitro* de toxicidade por inalação; culturas submersas; culturas 3D; interface ar-líquido.

Abstract

Advanced ceramic technologies have a strong potential for airborne (nano)particle formation and emission, meaning that workers of those industries are at great risk of exposure to these particles. However, toxicological data of these (nano)particles is lacking, particularly for airborne particles released within sectors such as the ceramic industry. To address this relevant topic, the present work aimed to assess the toxicity of occupationally relevant doses of industrially process-generated particles emitted during two industrial thermal spraying technologies [atmospheric plasma spraying (APS) and high velocity oxy-fuel (HVOF)], as well as of four engineered nanoparticles [ENP; tin oxide (SnO_2), antimony-tin oxide (ATO; $Sb_2O_3 \bullet SnO_2$), cerium oxide (CeO_2) and zirconium oxide (ZrO_2)] used as raw materials for ceramics manufacture. Two human respiratory *in vitro* systems, either conventional alveolar epithelial A549 cultures under submerged or air-liquid interface (ALI) conditions, or advanced three-dimensional (3D) upper airway epithelium (MucilAir™) cultures at ALI were exposed to the selected particles. Major toxicity endpoints including plasma membrane integrity, metabolic activity, oxidative stress, inflammatory response, and genotoxicity were assessed.

Overall, the tested process-generated particles seem to be more toxic compared to the ENP, most likely due to their higher chemical complexity and composition [elevated levels of metallic elements like chromium (Cr) and nickel (Ni)]. Among the two evaluated thermal spraying processes, particles derived from HVOF were more cytotoxic than those emitted from APS. Either fine (PGFP) and ultrafine (PGNP) particles from both spraying processes were able to induce measurable genotoxic effects. While APS particles lead to increased levels of histone 2AX (H2AX) phosphorylation, HVOF particles caused 8-oxo-7,8-dihydroguanine (8-oxo-G) oxidative DNA lesions. ENP were more toxic to human alveolar epithelial cultures when aerosolised than in liquid suspension, particularly ZrO_2 NP. On the other hand, advanced MucilAir™ cultures, that better mimic *in vivo* physiological features, such as the mucociliary defence mechanisms, were quite resistant to both HVOF-derived particles and ENP aerosols. Thus, while 3D human upper airway epithelial cultures exhibited attenuated responses, the conventional A549 cultures were more sensitive to the studied (nano)particles.

The present work highlights the hazard of industrially derived (nano)particles, either intentionally used or incidentally released into the workplace air during advanced ceramic processes. Importantly, particles' physicochemical properties alongside the testing conditions (cell model and type of exposure) played a determinant role in the observed biological responses. These findings reinforce the importance of using physiologically relevant *in vitro* models in (nano)particle toxicity studies, for better data extrapolation to humans.

Keywords: ceramic technology; process-generated particles; engineered nanoparticles; hazard assessment; *in vitro* inhalation toxicity testing; submerged cultures; 3D cultures; air-liquid interface.

Table of Contents

List of Figures

8-oxo-G	8-oxo-7,8-dihydroguanine
γ-H2AX	Gamma-H2AX; phosphorylated form of histone H2AX
ALI	Air-liquid interface
APS	Atmospheric plasma spraying
ATO	Antimony-tin oxide
DMSO	Dimethyl sulfoxide
DNA	Deoxyribonucleic acid
EC_{50}	Half-maximal effective concentration
ENP	Engineered nanoparticle(s)
FBS	Fetal bovine serum
HVOF	High velocity oxy-fuel spraying
IC_{50}	Half-maximal inhibitory concentration
IL-8	Interleukin-8
LDH	Lactate dehydrogenase
MCP-1	Monocyte chemoattractant protein-1
MMAD	Mass median aerodynamic diameter
NM	Nanomaterial(s)
NP	Nanoparticle(s)
NRV	Nano-reference value(s)
OEL	Occupational exposure limit(s)
PGFP	Process-generated fine particle(s)
PGNP	Process-generated nanoparticle(s)
PM	Particulate matter
ROS	Reactive oxygen species
VACES	Versatile aerosol concentration enrichment system

This thesis is organised into three different chapters:

Chapter I – General Introduction

The first chapter is divided into two sections:

- Theoretical Background: This section includes two literature reviews. The first one provides a state-of-art on the occupational exposure to nanoparticles in the ceramic industry and their impact on human health, describing possible sources and exposure scenarios, the existing case studies, and the toxicological potential of airborne nanoparticles used or generated in the ceramic industry workplace. The second review explores the existing pulmonary *in vitro* models already employed for nanotoxicity assessment, from basic cell lines to more advanced cell culture models.
- Thesis Main Goals: The general and specific objectives of the thesis are provided in this section.

Chapter II – Original Research

This chapter is divided into two main sections:

- Process-Generated (Nano)Particles: Collection, Sampling, and Characterisation: Herein, an original paper on the collection, sampling, and characterisation of the fine (PGFP) and nano-sized (PGNP) process-generated particles incidentally released during two industrial processes of thermal spraying of ceramic coatings is included.

- *In Vitro* Toxicity Assessment of the Airborne Process-Generated and Engineered (Nano)Particles: This section includes four published articles. The first article refers to a protocol optimisation study on the comet assay for assessing *in vitro* genotoxicity, while the remaining three rely on the *in vitro* toxicity assessment of the (nano)particles

under study, using conventional and advanced *in vitro* models and exposure conditions.

Chapter III – Integrated Discussion, Conclusions and Final Considerations

This chapter is divided into two sections:

- <u>Integrated Discussion</u>: This contains an overall discussion of the results obtained from the experimental work performed under the framework of this PhD thesis, towards answering the research questions set out in the present thesis.
- <u>Conclusions and Final Considerations</u>: The main take-home messages from the research project and the study impact for advancing the knowledge in the field are given in this section.

Chapter VI – References

The last chapter includes the bibliographic references cited along with the dissertation.

Chapter I.

General Introduction

A. Theoretical Background

Ceramic Industry: An Overview

Throughout the history to the present, the ceramic industry has been offering a wide range of applications with great impact in our daily lives, going from traditional ceramics such as tableware, pottery, sanitary ware, bricks, and tiles, to more advanced materials with electrical, optical, magnetic and structural properties (Carter *et al.*, 2007; Munz *et al.*, 2000). Indeed, advanced ceramics have a huge impact on cutting-edge technologies in the areas of energy and the environment, transport, life sciences, and communication (Matizamhuka, 2018; Salamon, 2014). Accordingly, the ceramic industry is an industrial branch with a great impact on the global economy. As depicted in **Figure 1**, according to the *European Ceramic Industry Association*, the European industries play a major role in worldwide ceramics manufacture, with a production value of around 30 billion euros per year (Cerame Unie - The European Ceramic Industry Association, 2021), accounting for 23 % of the worldwide production. Indeed, most of the ceramic companies, as well as the most qualified employees, are located in Europe. Over 200,000 people work in these industries, whose leading countries are Austria, France, Germany, Italy, Poland, Portugal, Spain, and the United Kingdom (Cerame Unie - The European Ceramic Industry Association, 2021)
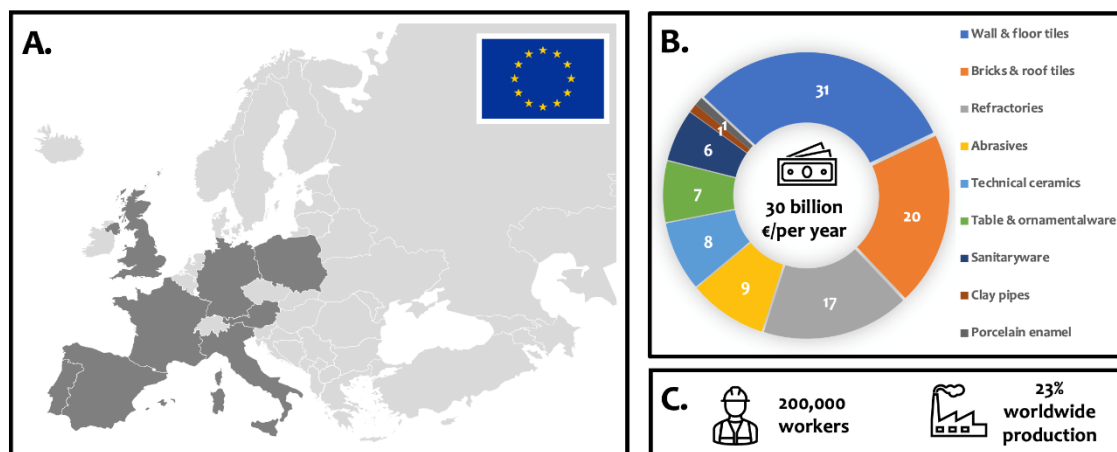
Figure 1. The European ceramic industry: facts and numbers: (**A**) main leading countries in ceramics manufacture (dark grey), (**B**) main ceramic sectors and their contribution for the ceramic production value (%), and (**C**) the estimated number of direct jobs and percentage of ceramic worldwide production [Adapted from Cerame Unie - The European Ceramic Industry Association (2021)].

Nanotechnology, Nanomaterials and the Ceramic Industry

The ceramic industry has been benefitting from nanotechnology innovation processes and advanced materials (Bessa *et al.*, 2020). Many nanomaterials (NM) such as carbon-based NM (*e.g.*, carbon nanotubes, carbon black, graphene) (Ahmad *et al.*, 2015), metal oxide nanoparticles (NP) (*e.g.*, TiO_2, Al_2O_3, CeO_2, SiO_2 NP) (Cain *et al.*, 2001; da Silva *et al.*, 2017; Lee *et al.*, 2010; Manivasakan *et al.*, 2010), nano-sized clays and nanocomposites (Palmero, 2015) have been applied in varied ceramic processes due to their unique properties. The specific nanoscale features of NM (size range 1–100 nm) (European Commission, 2011; Riego Sintes *et al.*, 2019) allow to explore and combine innovative functionalities, which will enable enhanced tribological, mechanical, thermal, and/or electrical properties of the nano-based ceramics. At the same time, several processes employed in the ceramic industry, such as ceramics firing, fracturing, glazing, spraying, inkjet printing, laser-based processes, and deposition techniques may lead to the release of coarse and fine particulate matter (PM) (Fonseca *et al.*, 2016; Fonseca *et al.*, 2015; Salmatonidis *et al.*, 2018a; Salmatonidis *et al.*, 2019; Salmatonidis *et al.*, 2020; Salmatonidis *et al.*, 2018b; Viana *et al.*, 2017; Viana *et al.*, 2021) to the workplace air. This means that ceramic workers are at high risk of exposure to airborne fine (< 2.5 µm mass median aerodynamic diameter [MMAD]) and ultrafine (< 0.1 µm MMAD) particles that may be released either during the handling or manufacturing of ceramics using engineered nanoparticles (ENP) as raw materials or incidentally emitted during mechanical and combustion/heating processes (Bessa *et al.*, 2020). Epidemiological evidence shows a relationship between increased concentrations of (nano)particles in the workplace air and the occurrence of adverse health effects that include pulmonary and cardiovascular diseases (Schraufnagel, 2020). Notwithstanding, there is not enough scientific evidence on the exact risk that these particles pose to human health since the existing knowledge relies on insufficient data of the dose-response relationships and on the consequences of long-term exposure to these particles (Riediker *et al.*, 2019; Valsami-Jones *et al.*, 2015). Therefore, it is of major importance to identify scenarios of occupational exposure to airborne (nano)particles and to investigate their possible adverse effects on human health.

In Vitro Toxicity Assessment of Airborne (Nano)Particles

Most of the existing knowledge on the airborne (nano)particle-induced biological effects comes from *in vivo* and *in vitro* inhalation toxicity studies. While there are already some studies on the toxicity of ENP used as input materials in the ceramic industry, so far it has not been possible to comprehensively assess the toxicity of airborne, process-generated fine (PGFP) and nano-sized particles (PGNP) released during the manufacture of ceramics as the result of the employed industrial processes and equipment. At the same time, many of the available studies addressing the occupational or environmental hazard of NP rely on unrealistic exposure scenarios, where very high doses were tested (Krug, 2014). Beyond that, a large extent of the available nanotoxicity studies focused on using animal models to predict human responses, which is particularly challenging for the assessment of the inhalation toxicity of airborne particles considering the anatomical and physiological differences of the human and animal respiratory systems (Bakand *et al.*, 2010, 2016). Accordingly, we are progressively moving towards the use of advanced human-based *in vitro* models for predicting target-specific toxicological responses induced by (nano)particles at the cellular level to assist in the human hazard assessment (Fadeel, 2019).

Over the past few years, an increasing number of more complex *in vitro* models and exposure systems for respiratory toxicity assessment have emerged (Nossa *et al.*, 2021). Advanced human-based *in vitro* systems can be designed to combine several cell types, better mimicking what occurs *in vivo* (Miller *et al.*, 2017). In addition, novel exposure systems comprising aerosol generators and cell exposure chambers have been developed for providing a more realistic exposure scenario compared to the traditional submerged conditions (Lacroix *et al.*, 2018).

In Section A.1 is presented a literature review on occupational exposure to NP in the ceramic industry and its impact on human health. Possible sources and exposure scenarios, a summary of the existing methods for evaluation and monitoring of airborne NP in the workplace environment and proposed nano reference values (NRV) for different classes of NP are presented. Case studies on occupational exposure to airborne NP generated at different stages of the ceramic manufacturing process are described. Finally, the toxicological potential of intentional and unintentional airborne NP that have been identified in the ceramic

industry workplace environment is discussed based on the existing evidence from *in vitro* and *in vivo* inhalation toxicity studies.

In Section A.2, is presented a literature review on the existing exposure systems and available human respiratory models for *in vitro* testing, with a special focus on (nano)particulate material. A brief insight into the path of inhaled (nano)particles along the respiratory system, the defence barriers they face, and consequent adverse effects they might cause is also presented.

A.1. Nanoparticle exposure and hazard in the ceramic industry: an overview of potential sources, toxicity and health effects

Bessa M. J., Brandão F., Viana M., Gomes J. G., Monfort E., Cassee F. R., Fraga S., & Teixeira J. P.

The PhD candidate was responsible for the conceptualisation and writing of the manuscript.

Nanoparticle exposure and hazard in the ceramic industry: an overview of potential sources, toxicity and health effects

Maria João Bessa[a,b,c], Fátima Brandão[a,b], Mar Viana[d], João F. Gomes[e,f], Eliseo Monfort[g], Flemming R. Cassee[h,i], Sónia Fraga[a,b,*], João Paulo Teixeira[a,b]

[a] Instituto Nacional de Saúde Doutor Ricardo Jorge, Departamento de Saúde Ambiental, Porto, Portugal
[b] EPIUnit - Instituto de Saúde Pública, Universidade do Porto, Porto, Portugal
[c] Instituto de Ciências Biomédicas Abel Salazar, Universidade do Porto, Porto, Portugal
[d] Institute of Environmental Assessment and Water Research (IDÆA-CSIC), Barcelona, Spain
[e] CERENA, Centro de Recursos Naturais e Ambiente/Instituto Superior Técnico, Universidade de Lisboa, Lisboa, Portugal
[f] ISEL – Instituto Superior de Engenharia de Lisboa, Lisboa, Portugal
[g] Institute of Ceramic Technology (ITC), Universitat Jaume I, 12006, Castellón, Spain
[h] National Institute for Public Health and the Environment, Bilthoven, the Netherlands
[i] Institute for Risk Assessment Studies, Utrecht University, Utrecht, the Netherlands

ARTICLE INFO

ABSTRACT

The ceramic industry is an industrial sector of great impact in the global economy that has been benefiting from advances in materials and processing technologies. Ceramic manufacturing has a strong potential for airborne particle formation and emission, namely of ultrafine particles (UFP) and nanoparticles (NP), meaning that workers of those industries are at risk of potential exposure to these particles. At present, little is known on the impact of engineered nanoparticles (ENP) on the environment and human health and no established Occupational Exposure Limits (OEL) or specific regulations to airborne nanoparticles (ANP) exposure exist raising concerns about the possible consequences of such exposure.

In this paper, we provide an overview of the current knowledge on occupational exposure to NP in the ceramic industry and their impact on human health. Possible sources and exposure scenarios, a summary of the existing methods for evaluation and monitoring of ANP in the workplace environment and proposed Nano Reference Values (NRV) for different classes of NP are presented. Case studies on occupational exposure to ANP generated at different stages of the ceramic manufacturing process are described. Finally, the toxicological potential of intentional and unintentional ANP that have been identified in the ceramic industry workplace environment is discussed based on the existing evidence from *in vitro* and *in vivo* inhalation toxicity studies.

1. Introduction

Throughout history to the present, the ceramic industry has been offering a wide range of materials with great impact on our daily lives. Broadly, a ceramic material can be defined as an inorganic, heat-resistant material composed by both metallic and non-metallic compounds. Ceramics have a broad application from construction to consumer goods and are used in several industrial processes and cutting-edge technologies. Bricks, ceramic tiles, drainage pipes, sanitaryware, household appliances, table- and ornamentalware are some of their most well-known applications. Due

to their durability, strength, non-corrosive properties and ability to withstand very high temperatures, ceramics are also employed for specific uses (e.g. as enamels, abrasives and refractories) required in metallurgical processes, glass production and many other key processes across all industries (Pampuch, 2014). Advanced ceramics with unique mechanical, electrical and thermal properties emerged in the 80's having a huge impact in cutting-edge technologies. They are used to produce a variety of materials such as cutting tools, coatings, body armour, electrical and electronic equipment, engine parts and medical products (Marinescu, 2006; Munz and Fett, 2013). A significant number of the world's ceramic industries are located in
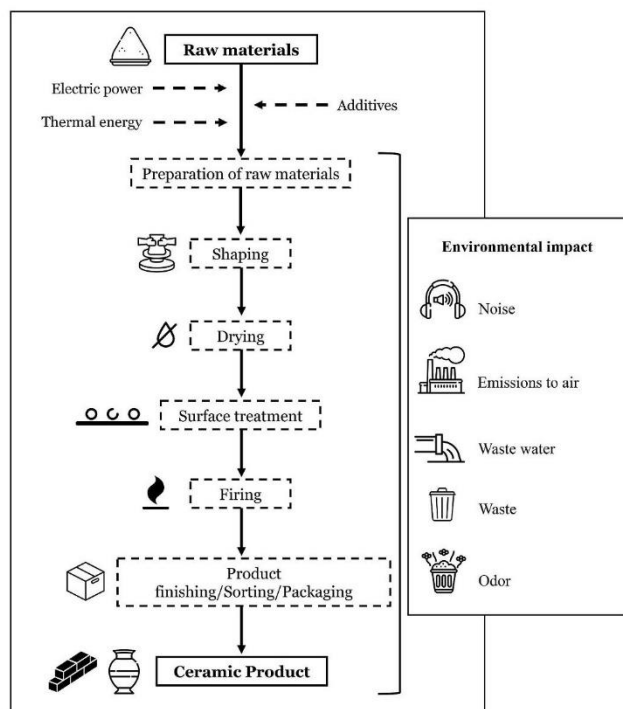
Fig. 1. Main stages of the manufacturing process of ceramic products (Adapted from European Commission (2007)).

European Union (EU) countries, with over 200 000 workers and an estimated production value of 28 billion euros per year (Cerame-Unie, 2012). Overall, EU ceramic industries account for 23% of the worldwide production, playing a significant role in the global economy (Cerame-Unie, 2012, 2015; European Commission, 2007).

In general, the main process of ceramics manufacturing is quite straightforward. Figure 1 depicts major steps of the general manufacturing process of a ceramic product, starting with the preparation of the raw materials (including addition of auxiliary agents, if needed), followed by shaping, drying, surface treatment (when applicable), firing, product finishing/sorting and packaging. As shown in Table 1, a wide range of raw materials (oxide-based and non-oxide-based), in bulk and nanoforms, are currently utilized in the ceramic industry for different purposes. Nanotechnology has already reached the ceramic sector. For many years, nanoscale ceramic materials have been used in the biomedical field as orthopaedic implants (Traykova et al., 2006). At the same time, many nanomaterials (NM) have been applied in

numerous ceramic processes. The specific nanoscale features of NM (size range 1 nm–100 nm) (European Commission, 2011) offer the opportunity to explore novel property combinations or improved tribological, mechanical or corrosion properties for nanoceramics and nanopowders (Table 1). Indeed, NM such as graphene, carbon nanotubes (CNT) and carbon black are used in the ceramic industry for their reinforcing ability (Ahmad et al., 2015; Liu et al., 2016; Wakamatsu and Salomao, 2010). Titania (TiO_2) NP are also used for ceramic glaze, in tiles or as stiffening fillers (Cain and Morrell, 2001; da Silva et al., 2017; Manivasakan et al., 2010). Alumina (Al_2O_3) NP are used for making cutting tools and are often included as polishing agents just like ceria (CeO_2) NP (Cain and Morrell, 2001). Silica (SiO_2) NP have also been incorporated in insulating ceramics due to their coolant, light transmission and fire-resistant properties in the materials (Lee et al., 2010). On the other hand, nano-sized clays have been used as catalysis, in perforation, nanocomposites and inks (Wakamatsu and Salomao, 2010). Over the last years, great attention has been given to ceramic nanocomposites due to their capacity to improve mechanical, thermal and electrical properties comparing with the conventional ceramic matrix composites (Palmero, 2015; Rathod et al., 2017). Ceramic oxides such as Al_2O_3, ZrO_2, TiO_2, Cr_2O_3 and SiO_2 are widely used as surface coating materials due to their capacity to improve resistance to wear, erosion, cavitation, fretting and corrosion (Knuuttila et al., 1998; Wang et al., 2009). Several processes for ceramics coating can be employed, for instance glazing, spraying, inkjet printing, laser-based processes and deposition techniques. These techniques often involve the injection of nanopowders that may lead to release and deposition of coarse and fine particulate matter (PM) (Fonseca et al., 2015a; Viana et al., 2017).

During the ceramic manufacturing process, the raw materials used can go through various transformation stages (Fig. 1), that may pose different risks from the environmental point of view (Monfort et al., 2014). For instance, air emissions in the ceramic industry represent a major environmental concern due to the release of PM or dust during handling and processing of raw materials, as well as from gaseous compounds released during drying, calcination and firing of the raw materials (Barros et al., 2007; Bozsin, 1974). On the other hand, water emissions arise especially from manufacture of traditional ceramics and the resulting wastewater may contain insoluble PM, inorganic or organic materials and, in some cases, heavy metals (European Commission, 2007).

The development and exponential growth of nanotechnology-based industries, with an estimation of 6 million workers in 2020 (Roco, 2011), has raised concerns in the potential health risks of exposure to engineered (ENP) or airborne nanoparticles (ANP) (Woskie, 2010). Indeed, over the last years, NP have been regarded as emerging occupational hazards (Dolez and Debia, 2015). Yet, no official estimate of the number of workers involved in the use and manipulation of NP in

Table 1
List of raw materials commonly used in the ceramic industry.

Raw materials		
Oxide-based	*Non-oxide based*	*Nanoscale*
Clays e.g. kaolinite, pyrophyllite, montmorillonite, muscovite, illite, halloysite, hydrotalcite	**Borides** magnesium (MgB_2)	**Nanoclays**
Metal oxides alumina (Al_2O_3), antimony-tin oxide (Sb_2O_3/ SnO_2), barium titanate ($BaTiO_3$), beryllia (BeO), boria (B_2O), ceria (CeO_2), chromia (Cr_2O_3), magnesia (MgO, $MgOH_2$), nickel oxide (NiO), silica (SiO_2), tin oxide (SnO_2), titania (TiO_2), urania (UO_2); zinc oxide (ZnO), zirconia (ZrO_2)	**Carbides** silicon (SiC), tungsten (WC), titanium (TiC) **Carbon-based** diamond, graphite **Fluorides** silicon (SiF) **Metals** antimony (Sb), barium (Ba), cadmium (Cd), copper (Cu), lead (Pb), silver (Ag), zinc (Zn)	**Carbon-based** carbon nanotubes (CNT), carbon black (CB), fullerenes, graphene **Carbides and nitrides** boron (BN), silicon (SiC, Si_3N_4), tungsten (WC); titanium (TiC)
Mixed oxides bismuth strontium calcium copper oxide (BSCCO), lead zirconate titanate (Pb [$ZrxTi_{1-x}]O_3$), partially stabilized zirconia (PSZ), silicon aluminum oxynitride (Sialon), yttrium barium copper oxide (YBCO)	**Nitrides** boron (BN), silicon (Si_3N_4) **Sulfides** calcium (CaS), calcium ytterbium (CaYb2S4), ytterbium (Yb_2S_3)	**Metal and metal-oxide nanoparticles** alumina (Al_2O_3), ceria (CeO_2), copper oxide (CuO), silica (SiO_2), titania (TiO_2), tin oxide (SnO_2), zinc oxide (ZnO), zirconia (ZrO_2), magnesia (MgO), yttria (Y_2O_3)
Minerals calcite ($CaCO_3$), feldspar, quartz, magnesite ($MgCO_3$), wollastonite ($CaSiO_3$); lithium carbonate (Li_2CO_3)		**Nanocomposites** e.g. silicon carbide/silicon nitride (SiC/Si_3N_4) composites

10

the ceramic industry is currently available. This industrial sector is a relevant case of ENP and airborne particle exposure due to the increased likelihood of personal exposure to potentially hazardous materials during processing of raw materials and product manufacturing, where a wide range of nano- and bulk materials are used (Salmatonidis et al., 2019b).

The identification and characterization of NP exposure scenarios dictates the first stage of the workplace exposure assessment to these substances (Seipenbusch et al., 2014). The risk of occupational exposure to ANP strongly depends on its emissions levels, dispersion into the work environment and its eventual transformation within emission and exposure (Maynard and Kuempel, 2005). So far, it has not yet been possible to comprehensively assess the toxicity and establish the hazard of ENP and ANP, in particular, those derived from industrial ceramic processes. Nevertheless, there are several studies in the literature evidencing adverse effects of ANP exposure on human health in occupational settings. In fact, both airborne ultrafine particles (UFP; < 100 nm) and NP have been associated with cardiopulmonary health effects through a series of key biological mechanisms (Stone et al., 2017).

This review provides a broad overview of the current knowledge on the workplace exposure to ENP and ANP in the ceramic industry and their potential adverse effects to the human health. Thus, this paper outlines possible NP sources and exposure scenarios in ceramic industrial settings, illustrated by a group of published case studies. A summary description of the existing methods for ANP's workplace exposure measurement, as well as the current legislation, i.e. occupational exposure limits (OEL) and existing Nano Reference Values (NRV), will also be provided and discussed. The present work will also bring together the current knowledge of the biological and adverse health effects from exposure to some NP, in particular those that are used as input materials and/or are representative of chemical elements found in the ceramic occupational setting. The literature search was conducted across two electronic databases: NCBI (Pubmed) and Science Direct. Gray literature was identified using internet-wide search engines (Google and Google Scholar). The following search terms were used: occupational health, occupational exposure, nanoparticles emissions, ultrafine particles emissions, ceramic, industrial settings and indoor air.

2. Nanomaterials in the context of the ceramic industry

2.1. Occupational exposure to airborne nanoparticles

2.1.1. Sources and possible exposure scenarios

Occupational exposure to NP can occur from a number of different sources including: (1) production/synthesis, (2) handling/transport, (3) use/application, (4) fracturing and abrasion and (5) waste recycling/disposal (Schneider et al., 2011). The risk of aerosol particle exposure is dependent on the type of source, rate of particle transport and its removal or accumulation in the work environment, which is greatly influenced by factors such as indoor and outdoor activities, ventilation system, room design, among others (Hämeri et al., 2009; Salmatonidis et al., 2019b). The most common scenarios of aerosol NP emissions at industrial workplaces are often associated with mechanical (e.g. high-energy drilling) and combustion/heating processes (e.g. firing), thermal coating techniques (e.g. thermal spray coating), flame-based powder generation and indoor air quality-related aerosols (e.g. office machinery, cleaning fluids, infiltration of ambient nanoaerosols) (Hämeri et al., 2009). Additionally, the use of nanopowders as input materials is obviously a risk factor for the presence of ANP in the workplace air. In this context, exposure scenarios related to the manufacture and use of fullerenes, CNT, metal and metal oxide NP have been already identified and reported by Aitken et al. (2004).

Inhalation is considered the predominant route of exposure to ANP in occupational settings. However, ingestion and skin absorption exposure are also possible routes for NP during the manufacturing, use and disposal (Oberdorster et al., 2005). The smaller the particles the

deeper they can penetrate into the lung (Heal et al., 2012; Oberdörster, 2000), eventually reaching the bloodstream and translocating to other organs (Fröhlich and Salar-Behzadi, 2014; Magdolenova et al., 2012; Vallyathan and Gwinn, 2006). Due to the high potential for fine and UFP release associated with the input materials and processes employed in ceramic industries, workers are likely exposed to these agents, which raise concerns on worker's health related to the poor indoor air quality (Aitken et al., 2004; Hristozov and Malsch, 2009).

At present, few studies on NP exposure in the ceramic industry exist. Most of ceramic raw materials are in the powder form. Therefore, when processing these materials, particularly in handling, transport, storage and mechanical treatment operations, fine particulate suspensions are generated in the air (Monfort et al., 2006). Moreover, high-energy processes such as laser ablation (LA), laser sintering (LS), physical vapour deposition (PVD), inkjet printing, plasma thermal spraying and glazing have a high potential for airborne particle formation and release to the workplace air (Fonseca et al., 2015b, 2016; Salmatonidis et al., 2018, 2019a; Viana et al., 2017). Machining processes (e.g. cutting, drilling, grinding) also possess a great potential for ANP release to the workplace environment as illustrated by manufacture of functionally graded materials by friction stir processing to produce aluminium (Al) alloys reinforced with SiC particles (Gandra et al., 2011). Fire and combustion processes are also highly associated with dispersion of combustible NP in the air, representing a greater risk (Hodson et al., 2009). For instance, NP containing metal oxide such as Al, cadmium (Cd), chromium (Cr), and copper (Cu) have been associated with welding processes (Donaldson et al., 2005).

To sum up, the two major potential sources that may contribute to workplace exposure to ANP in the ceramic industry includes the use of nanopowders as input materials for ceramics production and airborne, process-generated NP released during the manufacture of ceramics as the result of the employed industrial processes and equipment (Fig. 2). Due to the limited information on the ANP occupational exposure, these materials cannot be considered safe without thorough investigation regarding their exposure levels and toxicity, which is a current research gap. In section 2.1.3. will be explained in detail the available studies found in the literature regarding ANP occupational exposure in the ceramic industry.

2.1.2. Methods for workplace exposure evaluation

To identify and characterize workplace exposure scenarios, two approaches can be adopted: studies at real workplaces or laboratory simulations of workplaces/work processes. The advantage of the first approach is to obtain data under real work conditions, however, is a time-consuming approach due to the numerous background aerosols. On the other hand, simulated workplace environments allow a clear differentiation of the aerosol's source, i.e. between background or particles unintentionally produced during the manufacturing process (Kuhlbusch et al., 2011). Measurement of worker's exposure to ANP can be performed using traditional industrial hygiene approaches that include: i) static (area) sampling, where samplers are placed at the source location, and ii) personal sampling, where samplers are fixed in the worker's breathing zone (Hodson et al., 2009). Accordingly, the available instrumentation for ANP exposure assessment can be divided into stationary, portable and personal (Table 2). Stationary equipment is the most accurate, however it only gives information at a single location at time. On the other hand, portable equipment, though easy to transport has lower accuracy and particle size resolution than the stationary equipment. In turn, personal equipment allows to monitor exposure levels in worker's breathing zone and are small and lightweight enough to be carried over an 8-h shift, without compromising any activity carried out by the worker (Asbach et al., 2017; Tsai et al., 2012). Generally, personal sampling is considered the preferred method since it provides an accurate representation of the worker's exposure regarding inhalable, thoracic or respirable particle fractions (Stebounova et al., 2018). Table 2 presents a general overview of the existing

Workplace exposure to (nano)particles in the ceramic industry
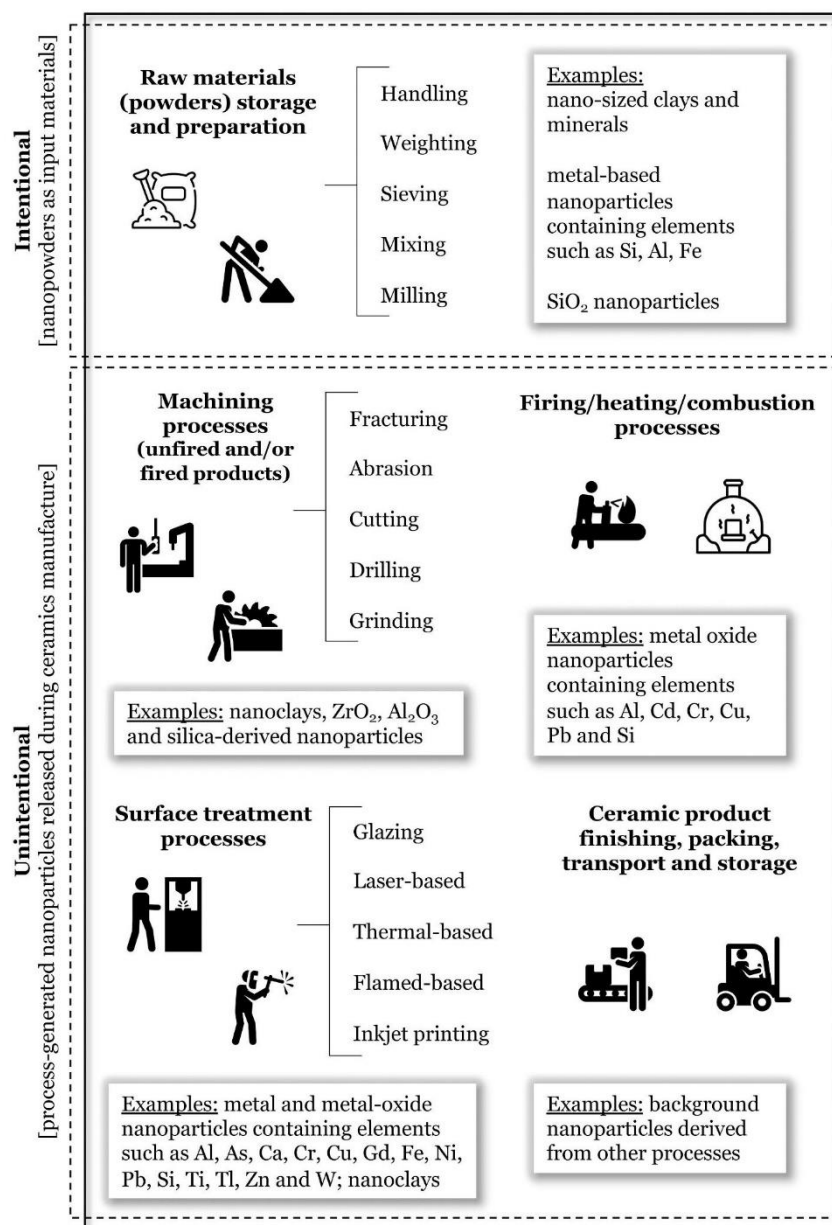
Fig. 2. Overview of potential scenarios of intentional and/or unintentional workplace exposure to nanoparticles in the ceramic industry.

methods and available instrumentation for ANP quantification. Time-resolving instruments (direct-reading) allow real-time determinations of parameters such as particle number concentration, particle size distribution or lung deposited surface area (LDSA) concentration, while time-integrating equipments are used for sampling material onto substrates and filters for posterior analysis on particle chemical composition and/or morphology (Kuhlbusch et al., 2011; O'Shaughnessy, 2013). The main drawback of direct-reading measurements is the limited instrument sensitivity to detect small particles (Asbach et al., 2017; Todea et al., 2015). Thus, the type of assessment (ambient- *vs* worker-oriented monitoring) and equipment used will greatly condition parameters to be assessed and quality of the obtained data. However, regardless the selected method for exposure monitoring, sampling

conditions (start time, duration and frequency) are also critical for an accurate and reliable assessment of workers exposure. Furthermore, exposure measurements must take place before and during production and/or processing in order to understand the variation between ANP background levels and those found during the manufacturing activities (Hodson et al., 2009).

Despite exposure and air quality standards for particles being based on mass, when it comes to ANP or UFP, mass might not be the most meaningful metric due to the poor accuracy for measuring low mass concentrations in comparison with coarser particles (Oberdörster, 2010). At the same time, there is also an ongoing debate around NP dose metrics to be used in toxicological studies (Oberdörster et al., 2005, 2007; Paur et al., 2011; Riediker et al., 2019; Wittmaack, 2006,

12

Table 2
Existing methods and instruments used for airborne nanoparticle quantification.

	Parameters	Stationary equipment	Portable equipment	Personal equipment
Time-Resolving Instruments	Particle number concentration Particle LDSA concentration Particle size distribution Mean particle size	CPC NSAM Electrical mobility analysis (SMPS, DMPS, DMA) and Inertial separation	Hand-held CPC Downsize NSAM PAMS, DMA	DisCmini Nano Tracer (e.g. Aerasense Nanoparticle monitor)
Time-Integrating Instruments	Physicochemical analysis	Filter sampling Electrostatic sampling	Hand-held ESPnano	Thermophoretic sampling (thermal precipitator sampler) Sampling on different filtration media (PENS, NanoBadge, Personal NRD)

Condensation Particle Counter (CPC); Nanoparticle Surface Area Monitor (NSAM); Scanning Mobility Particle Sizer (SMPS); Differential Mobility Particle Sizer (DMPS); Differential Mobility Analyser (DMA); Portable Aerosol Mobility Spectrometer (PAMS); Personal Nanoparticle Sampler (PENS); Nanoparticle Respiratory Deposition (NRD).

2007). Features such as surface area, morphology and chemical composition have been found to play a relevant role in the responses to inhaled UFP and ANP (Oberdörster et al., 2005; Stone et al., 2017). While some hold the view that NP-induced effects seem to be more strongly associated with size than mass (Oberdörster, 2010; Singh, 2015), other authors postulate that depending on NP physicochemical features and mode of action, particle surface area might be the most biologically-relevant metric (Schmid and Stoeger, 2016). At present, there is no available instrument capable of measuring the ANP surface area. However, LDSA concentration is a surface-area related parameter that can be determined that corresponds to the fraction of the airborne particle surface area concentration deposited in the lung (Todea et al., 2015) that is more easily measured than total surface area (Geiss et al., 2016). The particle lung deposition estimated by LDSA is an important aspect to take into consideration in occupational assessment, being influenced by parameters such as particle size, surface chemistry, distribution, breathing pattern and lung morphology rather than particle mass concentration (Reche et al., 2015).

Measurement of workplace exposure is thus essential to identify ANP sources and exposure levels, to implement control measures to efficiently reduce the exposure, contributing for the prevention of potential risks for worker's health. In this regard, mathematical/computational modelling can also be helpful to estimate exposure assessment through the analysis of the transport and fate of particles within the workplace environment (Schneider et al., 2011). Control banding (CB) is also of interest to manage workplace risks associated with occupational exposure to NM. Considering NM particularities, specific CB tools for NM have been developed (e.g. Stoffenmanager Nano, Nanosafer, CB Nanotool), with exposure assessments and derived risk levels (bands) based on different concepts and assumptions, and outputs in different formats (Liguori et al., 2016; Schulte et al., 2010; van Broekhuizen et al., 2012a).

2.1.3. Occupational exposure limits (OEL)

Occupational exposure limits (OEL) aim to protect from levels of exposure to airborne chemicals and particles that may endanger human health (Schenk and Johanson, 2010; Schulte et al., 2010). These are mostly derived from extrapolation of animal data to human, with all the related uncertainties and limitations of this estimate. A common procedure towards the definition of OEL in case of uncertain and insufficient data is the use of uncertainty factors (Schenk and Johanson, 2010). Currently, no official OEL for NP have been establish by any regulatory agency (Mihalache et al., 2017), mostly due to the uncertainty of ANP impact on human health (van Broekhuizen et al., 2012b). Notwithstanding, some organizations have provided guidance on benchmark levels. The Dutch Social and Economic Council has proposed Nano Reference Values (NRV) as a provisional substitute for OEL (Table 3) and preventive measures to control exposure to NP in the workplace environment. NRV are calculated based on the background-corrected number of NP with the diameter of 100 nm and a mass of 0.1 mg/m^3 (Mihalache et al., 2017) and not derived from any toxicological and epidemiological data. Accordingly, they constitute a precautionary risk management tool for NM handling or processing in the workplace, but they do not guarantee that exposures below those values are safe as they are built on presumable health effects (van Broekhuizen et al., 2012a).

Pietroiusti and colleagues have compiled a number of proposed OEL for several ENP recommended by different institutions worldwide (Pietroiusti and Magrini, 2014; Pietroiusti et al., 2018). The World Health Organization (WHO) has also released guidance on protection of workers health from manufactured NP exposure based on the existing evidence of NP effects on human health, where a list of proposed OEL is also presented (World Health Organization, 2017). Altogether, these compilations demonstrate the efforts and progresses made over the past years to establish and define concrete and coherent OEL for NP. Nevertheless, there is still much work ahead, particularly in defining

Table 3
Provisional Nano Reference Values (NRV) for four classes of engineered nanoparticles (ENP) (Adapted from Social and Economic Council (2012)).

Type of Nanomaterial (NM)	Nano Reference Value (NRV) (for long-term exposure)	Examples
Rigid, biopersistent nanofibres	0.01 fibres.cm^{-3}	Carbon nanotubes, metal oxide fibres
Biopersistent granular NM (density > 6000 Kg cm^{-3})	20 000 particles.cm^{-3}	Silver, gold, cerium oxide, cobalt oxide, iron/iron oxide, lead, antimony pentoxide, tin oxide
Biopersistent granular and fibre from NM (density < 6000 Kg cm^{-3})	40 000 particles.cm^{-3}	Aluminium oxide, silicon oxide, tin, titanium oxide, zinc oxide, nanoclay
Non-biopersistent granular NM	Applicable OEL	e.g. Sodium chloride

ANP-derived OEL in the context of industrial activities such as in the ceramic sector. The ongoing discussions on the metrics to be used for future "nano-OEL", i.e. mass-based or particle number-based, is also making difficult their successful implementation. While mass-based OEL are suitable for bulk materials, values for materials at the nanoscale seem to be rather high (Schulte et al., 2010). An additional limitation for the creation of nano-OEL is that NM are usually measured as primary NP and these are frequently presented in the workplace environments as micro-sized agglomerates, which may impar the correct classification for these OEL (Mihalache et al., 2017).

2.2. Airborne nanoparticle release and exposure in the ceramic industry: case studies

Just in recent years, studies on workplace exposure to ANP in ceramic industry settings began to emerge in the literature. This chapter focus on the existing case studies of ultrafine and ANP emissions during different stages of the ceramic manufacturing process, which are summarized in Table 4.

2.2.1. Firing process

The pioneering work of Voliotis et al. (2014) investigated the size, concentration and elemental composition of particles emitted during the different stages of the ceramic firing process, i.e. before and after ceramics painting and glazing, in a traditional small-sized pottery studio. This study showed that when the kiln reached temperatures above 600 °C most of the emitted particles were in the nanometer range. The size of the emitted ANP varied between 30 and 70 nm during the first stage of the firing process, where the ceramics were unpainted and unglazed, with a peak concentration around 6.5×10^5 particles/cm^3. In the second stage of the firing process, where the ceramics were painted and glazed, the mean particle size ranged from 15 to 40 nm and their particle number concentration peaked at 1.2×10^6/cm^3. Elemental analysis by Energy-Dispersive X-ray (EDX) spectroscopy of individual particles collected during the two firing stages revealed that the main element found was Si, emitted by the clay, whereas the second firing stage mostly generated particles containing Pb and Cu derived from the pigments used for glazing (Voliotis et al., 2014).

2.2.2. Surface treatment processes

In the ceramic industry, the use of laser-based techniques to improve ceramics surface properties is becoming widespread. The high-energy nature of these lasers may entail some risks of NP generation and emission. Fonseca and co-workers have investigated particle emissions during two processes using laser technology, laser sintering (LS) and laser ablation (LA) of ceramic tiles. In the first study, particle measurements were performed at laboratory scale both at the emission source, a 3 m long pilot plant-scale furnace, and at the worker's breathing zone (Fonseca et al., 2015b). ANP emissions were found to be highly dependent on temperature and tile chemical composition and induced by thermal and nucleation processes. Primary ANP emissions with a particle mean diameter of 18 nm reached concentrations up to 6.7×10^6 particles/cm^3. In the indoor area (breathing zone), particles decreased in number, mass and LDSA concentration but they were still

present at high concentrations and in a size range of 13–27 nm. In the workers' breathing zone, the collected particles presented diameters larger than in the furnace but smaller than the background air. The highest concentrations of metals including Zn, Pb, Cu, Cr, As and Ti have been found in the UFP fraction (Fonseca et al., 2015b). In a second study, the authors addressed ANP formation and release mechanisms from tile sintering using high power CO$_2$ lasers but at industrial scale in a 7 m long industrial furnace (Fonseca et al., 2016). They have underlined the difficulty to directly extrapolate particle emissions obtained at laboratory scale to industrial scale due to three main reasons: (1) Fuel: laboratory furnaces are electric, while industrial furnaces are gas-powered; (2) Gas flow: inside industrial furnaces it is much higher than in laboratory furnaces; and (3) Area: a larger working area is expected in industrial than in laboratory settings resulting in a higher particle dispersion and consequently lower particle concentrations in the breathing zone. According to this workplace exposure evaluation, new particle formation from gaseous precursors occurred during thermal treatments in both red clay and porcelain ceramic materials. This phenomenon was independent of the laser treatment. Generation and emission of ultrafine and nano-sized airborne particles occurred during the sintering process of the ceramic facility under study, and the measured exposure concentrations exceeded NRV (Fonseca et al., 2016).

Salmatonidis et al. (2018) investigated the mechanisms behind ANP formation and emission during pulsed LA of four types of ceramic tiles, using two different laser setups: near-infrared laser widely used for engraving, and mid-infrared laser generally employed for cutting and welding. These authors considered the influence of the ceramic material properties, process parameters and lasers wavelength on the formation and release of ANP, characterizing them in terms of size, particle number and mass concentration both at laboratory and pilot-plant-scale. Regardless the laser wavelength used and type of ceramic tile, a high particle number concentration of ANP, from 3.5×10^4/cm^3 to 2.5×10^6/cm^3, was released. Particles of SiO$_2$ and Al$_2$O$_3$ with sizes superior to 10 nm were formed and released during the LA process of the ceramic tiles. ANP emissions were associated with different mechanisms including nucleation and melting, which highly contributed to the particle number concentration observed. In addition, the ceramic surface and chemical properties exerted a great effect on the particle number and mass emissions of ANP (Salmatonidis et al., 2018).

Viana et al. (2017) evaluated airborne UFP (< 100 nm) and NP (< 50 nm) emissions during atmospheric plasma spraying (APS) of ceramic coatings at industrial-scale pilot level. Plasma spraying was performed inside a closed chamber located inside the worker's room, where the breathing zone was 1.5 m away. Particle size ranged between 10 and 700 nm and ultrafine emissions were higher than initial background concentrations, reaching up to 3.7×10^6 particles/cm^3 and 2.0×10^6/cm^3 inside the spraying chamber and at workers' area, respectively. These results demonstrate the hazardous potential of these airborne particles in ceramic industrial environments. In this study, it has also been applied a risk prevention protocol consisting of (1) improved air circulation in the plasma chamber and delayed door-opening system, (2) improvement of the sealing of the extraction system ducts and (3) air exchange rates (forced ventilation in the worker area). These

14

Table 4
Summary of the available case studies on ultrafine and airborne nanoparticle release and exposure in the ceramic industry.

References	Ceramic manufacturing process	Experimental settings	Sampling type	Evaluated parameters	Main findings	Identified elements/particles
Voliotis et al. (2014)	Firing	Industrial scale (traditional small-sized pottery studio)	Stationary; location: emissions source (kiln)	Particle size distribution and concentration; elemental composition	First firing stage: mean size ranged 30–70 nm; peak number concentration 6.5×10^5 cm^{-3}; Second firing stage: mean size ranged from 15–40 nm; peak number concentration 1.2×10^6 cm^{-3}	Silicon (Si), lead (Pb) and copper (Cu)
(Fonseca et al., 2015b)	Laser sintering and ablation	Laboratory pilot-plant scale furnace	Stationary; locations: emissions source (furnace), indoor (breathing zone) and outdoor air	Particle size distribution; particle formation and emission mechanisms; LDSA; chemical characterization	Nanoparticle emissions: 9.7×10^5 particles cm^{-3}; mean diameter of 18 nm; spherical-shaped morphology (TEM images) Ablation emissions: mean diameter 80 nm; Breathing zone: 2.6×10^6 particles cm^{-3}, LDSA $= 2.3 \times 10^3$ µm^2 cm^{-3}, mean size range 13–27 nm; mean diameter of 8–18 nm in the furnace, mean diameter size of 38 nm in the background air.	Zinc (Zn), lead (Pb), copper (Cu), chromium (Cr), arsenium (As) and thallium (Tl) found in the ultrafine fraction.
Fonseca et al. (2016)	Laser ablation	Industrial pilot-plant scale furnace	Stationary; locations: emissions source (furnace), indoors (breathing zone), exhaust tube (connecting the emission source to outdoor air)	Particle size distribution; particle number and diameter; LDSA; chemical characterization	Emission source: ultrafine and nanoparticle emissions reaching up to 1.0×10^7 .cm^{-3}; diameter range: 14, 12 and 58 nm for red clay, porcelain tiles, and background air particles, respectively, with spherical and irregularly shaped morphologies (TEM images); Exposure concentrations to ultrafine and nanoparticles generated in this workplace would exceed the NRV.	Quartz (SiO$_2$) was the main inorganic component released from both tiles; metal oxide NP of zinc (Zn), chromium (Cr), aluminium (Al) and iron (Fe); other components found in both tiles: calcium carbonate (CaCO$_3$), zinc oxide (ZnO)
Viana et al. (2017)	Atmospheric plasma spraying	Industrial pilot-plant scale furnace	Stationary; locations: inside (worker's room) and outside spraying chamber, outdoor air	Particle size distributions; particle number, mass and concentrations; LDSA	Inside the spraying chamber: ultrafine emissions concentration up to 3.7×10^6 cm^{-3}; diameter range 28–45 nm; spherical and irregularly shaped morphologies (TEM images) Worker area (potential breathing zone): 2.0×10^6 cm^{-3}, diameter range 33–48 nm Ultrafine emissions were mainly process-related	Zirconia-Yttria (ZrO$_2$–Y$_2$O$_3$) nanoparticles, gadolinium (Gd)- based engineered nanoparticles, mineral (Ca) particles
Salmatonidis et al. (2018)	Laser ablation (two different laser setups: near-IR and mid-IR)	Laboratory and pilot-plant scale	Stationary; locations: emission source, near-field, far-field, outdoor air	Particle size, number and mass concentration; chemical characterization	High particle number concentrations were detected: (3.5×10^4cm^{-3} to 2.5×10^6 .cm^{-3}) for all types of tiles and under both laser setups; Spherical shape; Particle number and mass emissions were dependent on the tile surface characteristics and chemical properties.	Silica (SiO$_2$)nanoparticles
(Salmatonidis et al., 2019a,)	Thermal spraying coating	Industrial scale	Stationary; locations: near-field (inside spraying booths), far-field	Particle size distribution; Particle number concentration, size-segregated mass concentrations; LDSA	Inside spraying booths: high particle number ($> 10^6$ cm^{-3}, 30–40 nm) and mass (60–600 µgPM1 m^{-3}) concentration; Worker area: 10^4–10^5cm^{-3} particle number, 40–65 nm and 44–87 µg PM$_1$.m^{-3} mass concentration; Irregularly-shaped nanoparticles with small diameters were detected inside (31–41 nm) and outside (40–64 nm) the spraying booths; Inhaled dose rates: 353×10^6–1024×10^6min^{-1}, with 70% of deposition occurring in the alveolar region.	Metal-containing particles: nickel (Ni), chromium (Cr), tungsten (W)
(Ribalta et al., 2019a)	Handling of powder materials	Pilot-plant	Stationary and personal; locations: worker area (breathing zone), indoor, outdoor	Particle mass and number concentration; LDSA; chemical characterization	Particle number concentration during handling: 15 033–40 498. cm^{-3}; different particle shapes (prismatic and platy) (TEM images); LDSA during background: 27–101 µm^2 cm^{-3}, LDSA during materials handling: 22–42 µm^2 cm^{-3}. High degree of correlation between dustiness and exposure concentrations was found during handling.	Silicon (Si), aluminium (Al), iron (Fe), oxygen (O), calcium (Ca), silica (SiO$_2$)nanoparticles

7

Table 4 (*continued*)

References	Ceramic manufacturing process	Experimental settings	Sampling type	Evaluated parameters	Main findings	Identified elements/particles
(Ribalta et al., 2019b)	Packaging of raw materials	Industrial scale	Stationary and personal; locations: three packing lines	Particle mass and number concentrations; LDSA	LDSA during packaging: $5.4\text{-}11.8 \times 10^5\ \mu m^2\ min^{-1}$ Particles depositing mainly in the alveoli (51–64%) followed by head airways (27–41%) and trachea bronchi (7–10%)	Silica (SiO_2), alumina (Al_2O_3), iron oxide (Fe_2O_3), titania (TiO_2), potassium oxide (K_2O), magnesium oxide (MgO), sodium oxide (Na_2O), calcium oxide (CaO) and lithium oxide (Li_2O).

Lung Deposited Surface Area (LDSA); Nano Reference Value (NRV); Infrared (IR); Transmission Electron Microscopy (TEM).

measures proved to be effective in reducing UFP concentrations in the workers area (Viana et al., 2017).

Recently, Salmatonidis and colleagues have evaluated particle emission and its impact on worker's exposure during thermal spraying of ceramic coatings onto metallic surfaces (Salmatonidis et al., 2019a). Several parameters were analysed including particle number and mass concentrations, LDSA, mean diameter, and size distributions of NP, fine and coarse particles. Inside the thermal spraying booths, high particle number ($> 10^6/cm^3$) and mass concentrations (60–600 µg PM_1/m^3) have been detected. Those particles were transported towards the worker area, increasing the concentrations in this region by one order of magnitude in terms of number ($10^4\text{-}10^5$ particles/cm^3), and up to a factor of 4 in terms of mass (44–100 µg PM $<$ 1 µm/m^3) contributing for the potential worker's exposure to these particles (Salmatonidis et al., 2019a). Characterization of the emitted ANP found at the workers area revealed that they were irregularly-shaped, mostly between 26 and 90 nm and constituted by metals such as nickel (Ni), Cr and tungsten (W). ANP generation and emission were mainly associated with mechanical attrition, but also melting-evaporation-condensation of the feedstock materials. Inhaled dose rates ranged from 353×10^6 - 1024×10^6 particles/min, where 70% of particle deposition was estimated to occur in the alveolar region (Salmatonidis et al., 2019a).

2.2.3. Handling and packaging of ceramic materials

Ribalta et al. evaluated the workers personal exposure to airborne particles during handling of five highly used ceramic materials with different characteristics (silica sand, three types of quartz and kaolin), as well as material dustiness, at pilot-plant-scale (Ribalta et al., 2019a). Dustiness measures the predisposition of a material to generate airborne dust during the handling and constitutes a relevant parameter to be taken into account in the context of ANP exposure evaluation in occupational settings. In this study, several parameters were evaluated including particle mass, number concentration, LDSA and particle size distribution. All ceramic materials under study presented a great impact on workers exposure regarding inhalable and respirable mass and images of Transmission Electron Microscopy (TEM) supported the presence of ANP in the form of aggregates (300 nm - 1 µm). In terms of mean inhalable mass concentrations, higher levels were consistently found during materials handling under high-energy settings compared to background levels. Nonetheless, in terms of particle number concentrations, no major differences were found before (background levels) and during materials handling. Moreover, a correlation between exposure concentration and dustiness has been demonstrated under the conditions and materials used, strengthening the idea that dustiness is a relevant parameter for the prediction of worker exposure (Ribalta et al., 2019a).

Ribalta et al. have also investigated the effectiveness of source enclosure in particle release during packaging of ceramic raw materials (Ribalta et al., 2019b). Worker's exposure was monitored during the packaging process of seven ceramic materials in three packaging lines equipped with different levels of source containment: low (L), medium (M) and high (H). As expected, real-time measurements showed that packaging lines L and M significantly increased exposure concentrations, while non-significant increases were detected in line H. These findings demonstrated the effectiveness of source enclosure as a mitigation strategy in the case of packaging of ceramic materials. The ICRP human respiratory tract model revealed that particle deposition occurred mainly in the alveoli (51–64%) followed by head airways (27–41%) and trachea bronchi (7–10%). In this study, different risk assessment tools (Stoffenmanager, ART, NanoSafer) were also employed to test the effectiveness of source containment. The comparison between the results from different risk assessment tools and the measured exposure concentrations evidenced that all of the tools overestimated exposure concentrations, by factors of 1.5–8. These findings underline the limitations of the available risk assessment tools to predict real scenario exposure levels and the urgent need to improve them.

2.2.4. General remarks

All of the aforementioned case studies evidence the relevance of studying fine, ultrafine and ANP process-generated emissions in ceramic workplaces and their impact on worker air exposure. Even though the number of workers in each of the case studies is not especially high (ranging approximately between 2 and 10 workers/activity) (Salmatonidis et al., 2019b; Viana et al., 2017; Voliotis et al., 2014), there are two main factors supporting the relevance of these exposures: (1) the fact that particles are rapidly transported across the industrial facilities (Ribalta et al., 2019a, 2019b), impacting workers active in other tasks different from the ones assessed in the case studies, and therefore not wearing any personal protective equipment (PPE), and (2) the increasing number and type of activities during which process-generated NP are being identified (see the recent case studies above), which indicates that this type of particles may be more frequent in industrial scenarios than previously thought. Overall, the reported observations and findings emphasize the importance of the risk assessment and the implementation of prevention procedures to improve occupational air quality in ceramic industrial settings.

3. Human health effects of exposure to intentional and unintentional nanoparticles in the ceramic industry: what do we know so far?

In spite of the great number of studies addressing the issue of NP toxicity, many challenges remain to identify the health impact of exposure to these materials. In fact, inconsistent and often conflicting data regarding the safety of NP are found in the literature. Consequently, relatively little is known about their effects on human health. Despite their distinct origins, NM and UFP share many similarities in terms of their physicochemical properties and *in vitro* mode of action (MoA) (Stone et al., 2017). Accumulating evidence shows that exposure to ambient air PM is associated with negative health outcomes and nano-sized (ultrafine) particles are likely to play an important role. The lung is a main target for inhaled NP though they may also translocate into the bloodstream triggering nonspecific interactions with secondary organs and systemic tissues (Oberdörster et al., 2005). Indeed, exposure to nano-sized particles has been widely associated with impaired lung function and inflammation, vascular dysfunction and adverse acute respiratory and cardiovascular effects (Stone et al., 2017). In turn, these adverse effects are strongly linked with different diseases such as lung cancer (Knaapen et al., 2004), bronchitis, acute asthma (Kreyling et al., 2006), cardiac infection, hypertension, atherosclerosis, ischemia and cardiac arrhythmia (Brook et al., 2004; Kelly and Fussell, 2015; Schulz et al., 2005; Shannahan et al., 2012), among others. In the context of the ceramic industry, many reports show that occupational exposure to ceramic dusts and fibres is associated with chronic bronchitis, chronic obstructive pulmonary disease, reduced lung function, wheezing, breathlessness and dry cough (Jaakkola et al., 2011; Kargar et al., 2013; Trethowan et al., 1995).

From the *in vitro* and *in vivo* studies conducted so far, NP mechanisms of action start to be unravelled. Major mechanisms involved in NP-induced pulmonary toxicity events already described in the literature include: (1) ineffective clearance of NP; (2) intracellular uptake/internalization of NP; (3) impairment of lung macrophage phagocytosis; (4) loss of plasma membrane integrity; (5) mitochondrial dysfunction; (6) oxidative stress (ROS generation, glutathione depletion, lipid peroxidation); (7) cytokine production and activation of inflammatory signalling cascades; (8) genotoxicity (DNA and chromosomal damage, altered DNA methylation and repair); (9) altered cell cycle regulation, among others (Bakand et al., 2012; Li et al., 2010; Paur et al., 2011; Pietroiusti et al., 2018; Stone et al., 2017).

Singh et al. reviewed several aspects related to cellular uptake and possible toxicity mechanisms of ceramic NP for drug delivery applications. In this paper, aspects related to the mechanisms of NP internalization, possibly through passive uptake or simple adhesive interactions, accumulation in phagosomes, pattern of subcellular distribution (e.g. cytoplasm, mitochondria, lipid vesicles or nucleus) and its relation to observed adverse biological outcomes (e.g. organelle and genetic material damage, cell death) are discussed (Singh et al., 2016).

Over the years, more and more NM have been introduced in the ceramic industry. At the same time, as previously described, NP emissions can arise from multiple processes employed in the ceramic industry that neither produce nor use NM, which are referred as process-generated nanoparticles (PGNP). Below, a major overview of the existing *in vitro* and *in vivo* pulmonary toxicology studies of representative ENP and PGNP found in ceramic occupational settings (described in section 2.2) will be presented.

Clays are one of the most common materials applied in the ceramic sector. Lately, there has been a wide implementation of nano-sized clays in the industry, which raises concerns for the potential risks of these NM for the exposed workers health. *In vitro* studies have shown that nanoclays exposure (e.g. montmorillonite) decreases cell viability and induces changes in morphology and cell-cell interactions in human lung epithelial cells (Wagner et al., 2017a, 2017b, 2018). Stueckle et al. also evaluated the effects of pre- and post-incinerated forms of uncoated and organomodified nanoclays in mice and observed that pulmonary inflammation and toxicity relies on coating presence and incineration status. The obtained data revealed that coated and incinerated nanoclays induced less inflammation and granuloma formation in mice than pristine montmorillonite (Stueckle et al., 2018).

Metals and metal oxides NP are also commonly utilized in the ceramic industry. Brunner et al. (2006) evaluated the toxicity of CeO_2, TiO_2, ZrO_2 and ZnO NP in human lung mesothelioma (MSTO) exposed to 0–30 ppm for 3- and 6-days. Among the tested NP, ZnO NP were the most cytotoxic, while CeO_2, ZrO_2 and TiO_2 NP induced analogous responses in MSTO cells. Similar findings were observed by Xia et al. that have compared the effects of ZnO and CeO_2 NP in human bronchial epithelial cells (BEAS-2B). These authors found that ZnO NP induced greater cytotoxicity and cell death through generation of ROS and induction of inflammation than CeO_2 NP, whose exposure suppressed ROS production and induced resistance to an exogenous source of oxidative stress in BEAS-2B cells (Xia et al., 2008). Lanone et al. have also comparatively assessed the toxicity of Al_2O_3, CeO_2, TiO_2, ZrO_2, CuO and ZnO NP up to 5000 μg/mL at 24 h after exposure in human alveolar epithelial (A549) and macrophage (THP-1) cell lines. While exposure to Al_2O_3, CeO_2, TiO_2 and ZrO_2 NP caused a moderate toxicity in both cell lines, incubation with CuO and ZnO NP markedly decreased cell viability of A549 and THP-1 cells (Lanone et al., 2009). Moreover, Kim et al. also evaluated Al_2O_3, CeO_2, TiO_2 and ZnO NP cytotoxicity to human lung cells and found out that ZnO NP were the most cytotoxic with regard to cell proliferation, viability, membrane integrity and colony formation endpoints. On the other hand, Al_2O_3, CeO_2 and TiO_2 NP did not significantly affect cell proliferation and viability, being Al_2O_3 NP the least toxic NP tested (Kim et al., 2010).

Regarding the CeO_2 NP, there is some controversy around its toxicological potential in pulmonary cell models. While some studies have demonstrated that exposure to CeO_2 NP decrease cell viability, induce oxidative stress (Eom and Choi, 2009a; Lin et al., 2006b; Park et al., 2008b) and affect DNA integrity (De Marzi et al., 2013) of human lung epithelial cells, others reported no signs of cytotoxicity following exposure to these NP (Park et al., 2008a).

Monocultures are a convenient but a rather simplified model that can be less sensitive to predict toxicity than more advanced cell culture models. Three-dimensional (3D) cultures with a fully differentiated epithelium, more than one cell type, and with a morphology and genome wide expression similar to that observed *in vivo* have been shown to closely mimic human exposure to aerosolized NP (Clippinger et al., 2016), offering a good alternative to *in vivo* testing. In addition, lung cell models grown and exposed to aerosols at the air-liquid interface (ALI) are increasingly being recognized as a more realistic system to address the toxicity of inhaled agents compared to the

17

classical submerged exposures (Lacroix et al., 2018). In this regard, Kupper et al. investigated the toxicity of CeO$_2$ NP in human lung epithelial A549 and BEAS-2B cell lines under submerged conditions but also in 3D cultures of human bronchial epithelium (MucilAir™ cultures) at ALI conditions. The obtained results showed that CeO$_2$ NP did not induce cytotoxicity, as assessed by the LDH release assay, but caused a concentration-dependent increase in DNA damage levels in BEAS-2B exposed cells, while exposure of A549 cells to CeO$_2$ NP induced a minimal increase in LDH and a distinct increase in DNA damage. On the other hand, none of these responses were observed in MucilAir™-exposed cells, where minimal translocation of CeO$_2$ NP across the 3D barrier was detected (Kuper et al., 2015). The mucociliary clearance appeared to prevent aerosolized CeO$_2$ NP to reach the respiratory epithelial cells in the 3D airway cultures. Nevertheless, toxic responses such as cytotoxicity (e.g. loss of viability and plasma membrane integrity), inflammation responses, recruitment of alveolar macrophages and neutrophils were observed *in vivo*, in the lung tissue of rats exposed to CeO$_2$ NP by intratracheal instillation (Ma et al., 2011), nose-only (Srinivas et al., 2011) and whole-body inhalation (Keller et al., 2014) to CeO$_2$ NP.

TiO$_2$ NP are widely used in the industry and consumer products worldwide due to their high stability, anticorrosive and photocatalytic properties (Shi et al., 2013). Still, the International Agency for Research on Cancer (IARC) has classified bulk TiO$_2$ as possibly carcinogenic to humans (group 2 B) (Baan, 2007), which raised concerns about the genotoxic potential of TiO$_2$ in the nanoform. At present, the toxicological potential of TiO$_2$ NP is controversial. According to the previously mentioned *in vitro* cytotoxicity studies, TiO$_2$ NP seem to moderately affect lung cell lines. However, several *in vitro* studies have shown that TiO$_2$ NP can cause DNA damage and impair DNA repair mechanisms in lung cells. In this regard, Biola-Clier et al. compared the response of bronchial (BEAS-2B) and alveolar (A549) epithelial cells upon exposure to 1–100 μg/mL of TiO$_2$ NP in terms of DNA integrity. Both cell lines exhibited similar responses, i.e., moderate cell death, oxidative DNA damage and impaired DNA repair. So far, no consistent *in vivo* genotoxic profile has been established for TiO$_2$ NP, with the route of exposure and dose influencing the genotoxic outcome (Chuang et al., 2014). Several *in vivo* inhalation and instillation studies showed negative genotoxicity outcomes for TiO$_2$ NP (Lindberg et al., 2012; Naya et al., 2012). At the same time, Relier et al. found that only under overload conditions (3 instillations of 10 mg/kg) TiO$_2$_NM105 (rutile-anatase) induced delayed genotoxicity in lung, associated with persistent inflammation (Relier et al., 2017). In fact, the lung inflammation is the most common adverse outcome derived from TiO$_2$ NP exposure (Noël and Truchon, 2015).

Silica (SiO$_2$) is one of the most common and well-studied occupational hazards (Poinen-Rughooputh et al., 2016). Occupational exposure to crystalline SiO$_2$ is intimately related with the development of silicosis, a fibrotic lung disease (Leung et al., 2012). An increased risk of lung cancer has been found in groups exposed to high levels of respirable SiO$_2$ such as miners and brick, diatomaceous earth, pottery, sand and stone workers. However, carcinogenicity of inhaled crystalline SiO$_2$ has also been observed in a population with a wide variety of exposure circumstances, suggesting that the burden of cancer induced by SiO$_2$ may be much greater than previously expected (Vida et al., 2010). Micro-sized SiO$_2$ is widely used in the ceramic industry, but the use of nanosized SiO$_2$ has potential to grow in the coming years. SiO$_2$ toxicological potential was believed to be related with its crystallinity. Amorphous SiO$_2$ has been considered less harmful than crystalline SiO$_2$ (Murugadoss et al., 2017). Notwithstanding, most recent findings (Pavan et al., 2019; Pavan and Fubini, 2017; Turci et al., 2016) suggested that crystallinity per se cannot explain toxic effects of SiO$_2$, which are more linked to surface chemistry, specifically to silanol disorganization. The comparison studies show that amorphous SiO$_2$ NP can induce similar acute toxicological activity compared to crystalline SiO$_2$, but much less chronic effects (at 3-months), which can be

attributed to its lower biopersistence (Arts et al., 2007). *In vitro* studies in lung cell lines have shown decreased cell viability, increased levels of oxidative stress (e.g. ROS production, lipid peroxidation) (Akhtar et al., 2010; Eom and Choi, 2009b; Lin et al., 2006a; McCarthy et al., 2012), induction of DNA damage (Decan et al., 2016; Maser et al., 2015) and inflammatory responses (Panas et al., 2013, 2014) following exposure to SiO$_2$ NP. Most of the *in vivo* instillation and inhalation studies for amorphous SiO$_2$ NP available in the literature reported induction of inflammatory responses (Cho et al., 2007; Guichard et al., 2015) but no genotoxic responses (Guichard et al., 2015; Maser et al., 2015; Sayes et al., 2010) though *in vitro* these NP seemed to present a high toxic potential.

Copper (CuO) and nickel (NiO) oxide NP can also be used in the ceramic industry incorporated in inks for surface coating treatments. There are several studies showing a marked toxicity effect of CuO NP in lung cells lines, most of them showing a decrease in cell viability, increased DNA damage and oxidative stress (Ahamed et al., 2010; Cronholm et al., 2013; Fahmy and Cormier, 2009; Ivask et al., 2015; Karlsson et al., 2008; Midander et al., 2009; Wang et al., 2012). *In vivo*, CuO NP has been investigated in Wistar rats after short-term inhalation (STIS) exposure for 5 days/6 h per day to doses up to 13.2 mg/m^3 (Gosens et al., 2016). Twenty-four hours after the last exposure, a dose-dependent lung inflammation and cytotoxicity were observed. However, after a recovery period of 22 days, limited lung inflammation was only observed at the highest dose (Gosens et al., 2016). Cho et al. (2012) evaluated CuO, NiO and ZnO NP toxicity following intratracheal instillation in the rat. In this study, a severe pulmonary immune response with recruitment of eosinophils and neutrophils has been observed in rats exposed to the CuO and ZnO NP, while in NiO NP-exposed animals only neutrophils were recruited into the lung (Cho et al., 2012). Special attention should be given to NiO NP considering that Ni compounds are classified as carcinogenic to humans (International Agency for Research on Cancer, 2012; Mulware, 2013). Horie and his colleagues evaluated the cytotoxicity of ultrafine and fine NiO particles and observed that the UFP induced higher toxicity than the fine particles (Horie et al., 2009) and caused an acute oxidative stress response (Horie et al., 2011). Marked toxic responses including cell damage, induction of oxidative stress and activation of antioxidant systems in the lungs of rats intratracheally instilled with ultrafine NiO particles have also been reported by Horie et al. (2011), which are consistent with the marked toxic effects observed *in vitro*. Interestingly, a case report on occupational handling of a NiO NP powder by a 26-year-old female described the occurrence of Ni sensitization caused by manipulation of the nanopowder without any respiratory protection or control measures (Journeay and Goldman, 2014). This case highlights the importance of the nanotoxicological studies, and the evaluation of adverse health effects associated with these materials, particularly at industrial settings, in order to develop precautionary measures to protect workers from NP exposure and help preventing these work-related incidents.

As previously mentioned, graphene and CNT are used in the ceramic industry for their reinforcing ability. Previous toxicity studies on materials from the graphene family (e.g. graphene oxide, graphene nanosheets, among others) have shown that inhalation of these materials may potentially cause adverse biological responses. For instance, a decrease in cell viability and apoptosis in lung cells was already observed *in vitro*, while in animal studies, lung granuloma formation, inflammatory responses, pulmonary edema, severe and persistent lung injury were some of the effects caused from exposure to graphene family materials to rodents (Su et al., 2016). Regarding CNT, these are valuable industrial products. However, studies commonly suggest that human pulmonary exposure during production and manipulation might present pathogenic effects similar to asbestos fibers, due to their alike fibrous morphology (Donaldson et al., 2013; Shvedova et al., 2009). However, it is worth mentioning that depending on the diameter and rigidity of the CNT, they may present different toxicological

18

mechanisms from asbestos. For instance, while asbestos are endocytosed by mesothelial cells regardless of their diameter, CNT are internalized in a diameter- and rigidity-dependent manner, preferentially smaller diameters and higher rigidity nanotubes, which may influence their toxicity on those cells (Nagai et al., 2011; Nagai and Toyokuni, 2012). Both *in vitro* and *in vivo* studies have shown that CNT induce oxidative stress, apoptosis in different cell lines and induce cytotoxic effects in the lung (Kayat et al., 2011). Also, in animal studies, CNT have shown to be highly biopersistent, being capable to induce pulmonary inflammation, fibrosis, lung cancer after long-term inhalation and gene damage in the lung (Kobayashi et al., 2017). However, Manke et al. (2014) suggests that additional research is needed to understand if the airborne CNT generated in workplace settings are comparable in terms of size and structure to the ones generated for the *in vitro* and *in vivo* studies.

Despite the great importance of *in vitro* and *in vivo* testing, care should be taken regarding the interpretation and extrapolation to humans, particularly in case of animal inhalation toxicology area, where the anatomical and physiological differences between laboratory animals and humans could result in distinct responses to the airborne and inhalable particles (Irvin and Bates, 2003; Ware, 2008). Though, these studies might give a major clue of the possible mechanisms of toxicity that may occur in humans after exposure to such particles and the associated harmful health effects.

Due to the increasing number of workers exposed to fine and nano-sized particles of different origins and sources, further studies must be carried out for toxicity and dose-response assessment of ANP deemed relevant in occupational settings, in particular for the ceramic industry. Therefore, identification of potential sources and characterization of airborne particles emissions in terms of emitted levels, chemical composition, size distribution, etc., is of utmost importance not only for the risk assessment of exposure to these particles but also to develop plans to prevent or reduce workers exposure, namely the establishment of OEL for ANP.

4. Conclusions and future directions

Several industries are benefiting from advances provided by nanotechnology-derived materials and innovative processes. Indeed, owing their unique physicochemical properties, the utilization of NM as input materials is widespread in the industrial field. At the same time, high-energy processes aimed to enable the rapid manufacture of high-quality, innovative and cost-competitive products may also generate incidental ANP, the so-called PGNP, meaning that these workers are a susceptible population to NP exposure. At present, there is some uncertainty around the true risk of NM to the environment and human health, which raises serious public health concerns. These concerns are further aggravated by the existing epidemiological evidence linking exposure to high ambient concentrations of PM to morbidity and mortality, for which the ultrafine particle fraction seems to be an important contributor.

The ceramic industry is a paradigmatic case of potential occupational exposure to airborne nano-sized particles, mainly when high energy processes are implemented, as evidenced by the existing exposure monitoring data. Advances in the instrumentation used for ANP workplace measurements shed light on the possible exposure scenarios arising from ENP handling or from different ceramic industry activities (e.g. machining, firing, surface coating, packaging), many of them transversal to other industrial branches. This knowledge is crucial for an effective NM risk assessment and management, in particular for the implementation of risk prevention and mitigation measures for protecting workers from intentional or unintentional exposure to ANP but also for helping in the establishment of meaningful OEL for ANP. Therefore, more exposure assessment studies are needed, in particular in the ceramic industry, for a more extensive identification of workplace exposure scenarios and a more detailed characterization of the

ANP found in terms of number, size, shape, aggregation/agglomeration, chemical composition and toxicological properties. In this context, CERASAFE (http://www.cerasafe.eu/) has been a pioneering European project that contributed to innovating in the field of characterization methods relevant to environmental health and safety (EHS) issues, namely to discriminate ENP from background aerosols in the ceramic industry and good practices to guarantee that exposure to hazardous NP may be acceptable.

In parallel with exposure assessment, is urgent to fill the gaps on the knowledge of the adverse health effects derived from ANP exposure and their relation to dose to move forward our understanding of the occupational hazard of ENP and ANP. Currently, no OEL specific to NM have been officially established and adopted by the authoritative agencies, on one hand due to the vast heterogeneity and number of available NM, on the other to the limited and controversial knowledge of NM toxicity and harmful health effects. Furthermore, increasing evidence supports that the commonly used mass metrics for OEL may need to be carefully analysed and considered to be replaced by a particle number-based approach, a fact that has also been hampering the OEL developing process. Meanwhile, NRV may be considered as a provisional precautionary tool to protect the workers from NP exposure. Concerted efforts within the EU Nanosafety Cluster are being done in order to develop grouping and read-across approaches, similar to what is already well-established for conventional chemicals, that can be used to fill data gaps without further testing, with the ultimate goal of accelerating NM safety assessment and assisting in the establishment of OEL for specific NM groups. In this regard, several research projects (e.g. Gracious, NanoToxClass, PATROLS, SmartNanoTox) are contributing to NM categorization based on the joint consideration of NM physicochemical properties and modes of action. Inflammation, oxidative stress, genotoxicity are the most frequently reported responses to NM exposure as revealed by the *in vitro* and *in vivo* studies conducted so far.

In light of the current knowledge linking exposure to PM, where UFP play a major role, to the etiology of malignant and cardiovascular diseases, implementation of effective risk mitigation measures for protecting workers from (un)intentional exposure to ENP and ANP is of paramount importance in ceramic industrial settings. Health authorities, researchers, occupational health professionals and workers should cooperate to establish the most appropriate strategies to prevent and mitigate NP exposure. WHO preconizes the adoption of a precautionary approach that seek to minimize exposure to NM. Some of the recommendations to do so include assessing workers' exposure in workplaces and evaluating whether it exceeds a proposed OEL value for the specific NM, reduction of exposures to a range of NM that have been consistently detected in workplaces, control measures based on the principle of hierarchy of controls (i.e elimination of the source of exposure before implementing control measures that are more worker-dependent, with PPE being used only as a last resort). Finally, the importance of providing data on exposure and efficiency of protective measures in industrial scenarios should be highlighted, in order to help policy-makers to establish a realistic OEL, that is, with a good balance between adequate worker's health protection and achievable OEL using the current available technologies.

Authors declaration

We wish to confirm that there are no known conflicts of interest

19

associated with this publication and there has been no significant financial support for this work that could have influenced its outcome.

We confirm that the manuscript has been read and approved by all named authors and that there are no other persons who satisfied the criteria for authorship but are not listed. We further confirm that the order of authors listed in the manuscript has been approved by all of us.

We confirm that we have given due consideration to the protection of intellectual property associated with this work and that there are no impediments to publication, including the timing of publication, with respect to intellectual property. In so doing we confirm that we have follow the regulation of our institutions concerning intellectual property.

We understand that the Corresponding Author is the sole contact for the Editorial process (including Editorial Manager and direct communications with the office). She is responsible for communicating with the other authors about progress, submissions of revisions and final approval of proofs. We confirm that we have provided a current, correct email address which is accessible by the Corresponding Author and which has been configured to accept email from sonia.fraga@insa.min-saude.pt.

CRediT authorship contribution statement

Maria João Bessa: Conceptualization, Writing - original draft. **Fátima Brandão:** Writing - review & editing. **Mar Viana:** Writing - review & editing. **João F. Gomes:** Writing - review & editing. **Eliseo Monfort:** Writing - review & editing. **Flemming R. Cassee:** Writing - review & editing. **Sónia Fraga:** Conceptualization, Methodology, Writing - review & editing, Supervision. **João Paulo Teixeira:** Conceptualization, Writing - review & editing, Supervision.

Declaration of competing interest

The authors declare that they have no competing interests.

Acknowledgments

References

Ahamed, M., et al., 2010. Genotoxic potential of copper oxide nanoparticles in human lung epithelial cells. Biochem. Biophys. Res. Commun. 396, 578–583.

Ahmad, I., et al., 2015. Recent advances on carbon nanotubes and graphene reinforced ceramics nanocomposites. Nanomaterials 5, 90–114.

Aitken, R., et al., 2004. Nanoparticles: an Occupational Hygiene Review. HSE Books.

Akhtar, M.J., et al., 2010. Nanotoxicity of pure silica mediated through oxidant generation rather than glutathione depletion in human lung epithelial cells. Toxicology 276, 95–102.

Arts, J.H., et al., 2007. Five-day inhalation toxicity study of three types of synthetic amorphous silicas in Wistar rats and post-exposure evaluations for up to 3 months. Food Chem. Toxicol. 45, 1856–1867.

Asbach, C., et al., 2017. Review of measurement techniques and methods for assessing personal exposure to airborne nanomaterials in workplaces. Sci. Total Environ. 603, 793–806.

Baan, R.A., 2007. Carcinogenic hazards from inhaled carbon black, titanium dioxide, and talc not containing asbestos or asbestiform fibers: recent evaluations by an IARC Monographs Working Group. Inhal. Toxicol. 19, 213–228.

Bakand, S., et al., 2012. Nanoparticles: a review of particle toxicology following inhalation exposure. Inhal. Toxicol. 24, 125–135.

Barros, M.C., et al., 2007. Integrated pollution prevention and control for heavy ceramic industry in Galicia (NW Spain). J. Hazard Mater. 141, 680–692.

Bozsin, M., 1974. Environmental Challenges for the Ceramic Industry. Ceramic Engineering and Science. Springer, pp. 93–101.

Brook, R.D., et al., 2004. Air pollution and cardiovascular disease: a statement for healthcare professionals from the expert panel on population and prevention science of the American heart association. Circulation 109, 2655–2671.

Brunner, T.J., et al., 2006. In vitro cytotoxicity of oxide nanoparticles: comparison to asbestos, silica, and the effect of particle solubility. Environ. Sci. Technol. 40, 4374–4381.

Cain, M., Morrell, R., 2001. Nanostructured ceramics: a review of their potential. Appl. Organomet. Chem. 15, 321–330.

Cerame-Unie, 2012. The Ceramic Industry Roadmap: Paving the Way to 2050. https://www.ceramfed.co.uk/.

Cerame-Unie, 2015. Cerame-Unie 2015 Annual Report. . http://cerameunie.eu/.

Cho, W.-S., et al., 2007. Inflammatory mediators induced by intratracheal instillation of ultrafine amorphous silica particles. Toxicol. Lett. 175, 24–33.

Cho, W.S., et al., 2012. Differential pro-inflammatory effects of metal oxide nanoparticles and their soluble ions in vitro and in vivo; zinc and copper nanoparticles, but not their ions, recruit eosinophils to the lungs. Nanotoxicology 6, 22–35.

Chuang, H.C., et al., 2014. Cardiopulmonary toxicity of pulmonary exposure to occupationally relevant zinc oxide nanoparticles. Nanotoxicology 8, 593–604.

Clippinger, A.J., et al., 2016. Expert consensus on an in vitro approach to assess pulmonary fibrogenic potential of aerosolized nanomaterials. Arch. Toxicol. 90, 1769–1783.

Cronholm, P., et al., 2013. Intracellular uptake and toxicity of Ag and CuO nanoparticles: a comparison between nanoparticles and their corresponding metal ions. Small 9, 970–982.

da Silva, A.L., et al., 2017. Self-cleaning ceramic tiles coated with Nb2O5-doped-TiO2 nanoparticles. Ceram. Int. 43, 11986–11991.

De Marzi, L., et al., 2013. Cytotoxicity and genotoxicity of ceria nanoparticles on different cell lines in vitro. Int. J. Mol. Sci. 14, 3065–3077.

Decan, N., et al., 2016. Characterization of in vitro genotoxic, cytotoxic and transcriptomic responses following exposures to amorphous silica of different sizes. Mutat. Res. Genet. Toxicol. Environ. Mutagen 796, 8–22.

Dolez, P.I., Debia, M., 2015. Overview of Workplace Exposure to Nanomaterials. Nanoengineering. Elsevier, pp. 427–484.

Donaldson, K., et al., 2013. Pulmonary toxicity of carbon nanotubes and asbestos - similarities and differences. Adv. Drug Deliv. Rev. 65, 2078–2086.

Donaldson, K., et al., 2005. Combustion-derived nanoparticles: a review of their toxicology following inhalation exposure. Part. Fibre Toxicol. 2, 10.

Eom, H.J., Choi, J., 2009a. Oxidative stress of CeO2 nanoparticles via p38-Nrf-2 signaling pathway in human bronchial epithelial cell, Beas-2B. Toxicol. Lett. 187, 77–83.

Eom, H.J., Choi, J., 2009b. Oxidative stress of silica nanoparticles in human bronchial epithelial cell, Beas-2B. Toxicol. Vitro 23, 1326–1332.

European Commission, 2007. Reference Document on Best Available Techniques in the Ceramic Manufacturing Industry.

European Commission, 2011. Commission recommendation of 18 october 2011 on the definition of nanomaterial. Official Journal of the European Union 275, 38.

Fahmy, B., Cormier, S.A., 2009. Copper oxide nanoparticles induce oxidative stress and cytotoxicity in airway epithelial cells. Toxicol. Vitro 23, 1365–1371.

Fonseca, A., et al., 2015a. Workplace Exposure to Process-Generated Ultrafine and Nanoparticles in Ceramic Processes Using Laser Technology. Indoor and Outdoor Nanoparticles. Springer, pp. 159–179.

Fonseca, A.S., et al., 2015b. Ultrafine and nanoparticle formation and emission mechanisms during laser processing of ceramic materials. J. Aerosol Sci. 88, 48–57.

Fonseca, A.S., et al., 2016. Process-generated nanoparticles from ceramic tile sintering: emissions, exposure and environmental release. Sci. Total Environ. 565, 922–932.

Fröhlich, E., Salar-Behzadi, S., 2014. Toxicological assessment of inhaled nanoparticles: role of in vivo, ex vivo, in vitro, and in silico studies. Int. J. Mol. Sci. 15, 4795–4822.

Gandra, J., et al., 2011. Functionally graded materials produced by friction stir processing. J. Mater. Process. Technol. 211, 1659–1668.

Geiss, O., et al., 2016. Lung-deposited surface area concentration measurements in selected occupational and non-occupational environments. J. Aerosol Sci. 96, 24–37.

Gosens, I., et al., 2016. Organ burden and pulmonary toxicity of nano-sized copper (II) oxide particles after short-term inhalation exposure. Nanotoxicology 10, 1084–1095.

Guichard, Y., et al., 2015. Genotoxicity of synthetic amorphous silica nanoparticles in rats following short-term exposure. Part 2: intratracheal instillation and intravenous injection. Environ. Mol. Mutagen. 56, 228–244.

Hämeri, K., et al., 2009. Facing the key workplace challenge: assessing and preventing exposure to nanoparticles at source. Inhal. Toxicol. 21, 17–24.

Heal, M.R., et al., 2012. Particles, air quality, policy and health. Chem. Soc. Rev. 41, 6606–6630.

Hodson, L., et al., 2009. Approaches to Safe Nanotechnology; Managing the Health and Safety Concerns Associated with Engineered Nanomaterials. Centers for Disease Control and Prevention & National Institute for Occupational Safety and Health.

Horie, M., et al., 2011. Evaluation of acute oxidative stress induced by NiO nanoparticles in vivo and in vitro. J. Occup. Health 53, 64–74.

Horie, M., et al., 2009. Ultrafine NiO particles induce cytotoxicity in vitro by cellular uptake and subsequent Ni (II) release. Chem. Res. Toxicol. 22, 1415–1426.

Hristozov, D., Malsch, I., 2009. Hazards and risks of engineered nanoparticles for the environment and human health. Sustainability 1, 1161–1194.

International Agency for Research on Cancer, 2012. Arsenic, Metals, Fibres, and Dusts. Volume 100 C. A Review of Human Carcinogens. IARC Monographs on the Evaluation of Carcinogenic Risks to Humans. FR. International Agency for Research on Cancer, Arsenic and arsenic compounds, Lyon, pp. 41–94.

Irvin, C.G., Bates, J.H., 2003. Measuring the lung function in the mouse: the challenge of size. Respir. Res. 4, 4.

Ivask, A., et al., 2015. Toxicity of 11 metal oxide nanoparticles to three mammalian cell types in vitro. Curr. Top. Med. Chem. 15, 1914–1929.

Jaakkola, M.S., et al., 2011. Effects of occupational exposures and smoking on lung function in tile factory workers. Int. Arch. Occup. Environ. Health 84, 151–158.

Journeay, W.S., Goldman, R.H., 2014. Occupational handling of nickel nanoparticles: a case report. Am. J. Ind. Med. 57, 1073–1076.

Kargar, F., et al., 2013. Evaluation of occupational exposure of glazers of a ceramic industry to cobalt blue dye. Iran. J. Public Health 42, 868.

20

Karlsson, H.L., et al., 2008. Copper oxide nanoparticles are highly toxic: a comparison between metal oxide nanoparticles and carbon nanotubes. Chem. Res. Toxicol. 21, 1726–1732.

Kayat, J., et al., 2011. Pulmonary toxicity of carbon nanotubes: a systematic report. Nanomedicine 7, 40–49.

Keller, J., et al., 2014. Time course of lung retention and toxicity of inhaled particles: short-term exposure to nano-Ceria. Arch. Toxicol. 88, 2033–2059.

Kelly, F.J., Fussell, J.C., 2015. Air pollution and public health: emerging hazards and improved understanding of risk. Environ. Geochem. Health 37, 631–649.

Kim, I.-S., et al., 2010. Comparative cytotoxicity of Al2O3, CeO2, TiO2 and ZnO nano-particles to human lung cells. J. Nanosci. Nanotechnol. 10, 3453–3458.

Knaapen, A.M., et al., 2004. Inhaled particles and lung cancer. Part A: Mechanisms. Int. J. Canc. 109, 799–809.

Knuuttila, J., et al., 1998. Wet abrasion and slurry erosion resistance of sealed oxide coatings. Proceedings of the 15 th International Thermal spray conference 1, 145–150.

Kobayashi, N., et al., 2017. Review of toxicity studies of carbon nanotubes. J. Occup. Health 59, 394–407.

Kreyling, W.G., et al., 2006. Health implications of nanoparticles. J. Nanoparticle Res. 8, 543–562.

Kuhlbusch, T.A., et al., 2011. Nanoparticle exposure at nanotechnology workplaces: a review. Part. Fibre Toxicol. 8, 22.

Kuper, C.F., et al., 2015. Toxicity assessment of aggregated/agglomerated cerium oxide nanoparticles in an in vitro 3D airway model: the influence of mucociliary clearance. Toxicol. Vitro 29, 389–397.

Lacroix, G., et al., 2018. Air–liquid interface in vitro models for respiratory toxicology research: consensus workshop and recommendations. Applied In Vitro Toxicology 4, 91–106.

Lanone, S., et al., 2009. Comparative toxicity of 24 manufactured nanoparticles in human alveolar epithelial and macrophage cell lines. Part. Fibre Toxicol. 6, 14.

Lee, J., et al., 2010. Nanomaterials in the construction industry: a review of their applications and environmental health and safety considerations. ACS Nano 4, 3580–3590.

Leung, C.C., et al., 2012. Silicosis. The Lancet. 379, 2008–2018.

Li, J.J.e., et al., 2010. Nanoparticle-induced pulmonary toxicity. Exp. Biol. Med. 235, 1025–1033.

Liguori, B., et al., 2016. Control banding tools for occupational exposure assessment of nanomaterials — ready for use in a regulatory context? NanoImpact 2, 1–17.

Lin, W., et al., 2006a. In vitro toxicity of silica nanoparticles in human lung cancer cells. Toxicol. Appl. Pharmacol. 217, 252–259.

Lin, W., et al., 2006b. Toxicity of cerium oxide nanoparticles in human lung cancer cells. Int. J. Toxicol. 25, 451–457.

Lindberg, H.K., et al., 2012. Genotoxicity of inhaled nanosized TiO2 in mice. Mutat. Res. Genet. Toxicol. Environ. Mutagen 745, 58–64.

Liu, J., et al., 2016. Effects of pore structure on thermal conductivity and strength of alumina porous ceramics using carbon black as pore-forming agent. Ceram. Int. 42, 8221–8228.

Ma, J.Y., et al., 2011. Cerium oxide nanoparticle-induced pulmonary inflammation and alveolar macrophage functional change in rats. Nanotoxicology 5, 312–325.

Magdolenova, Z., et al., 2012. Can standard genotoxicity tests be applied to nano-particles? J. Toxicol. Environ. Health, Part A. 75, 800–806.

Manivasakan, P., et al., 2010. Effect of TiO2 nanoparticles on properties of silica re-fractory. J. Am. Ceram. Soc. 93, 2236–2243.

Manke, A., et al., 2014. Potential occupational risks associated with pulmonary toxicity of carbon nanotubes. Occupational Medicine and Health Affairs 2, 1000165.

Marinescu, I.D., 2006. Handbook of Advanced Ceramics Machining. CRC Press.

Maser, E., et al., 2015. In vitro and in vivo genotoxicity investigations of differently sized amorphous SiO2 nanomaterials. Mutat. Res. Genet. Toxicol. Environ. Mutagen 794, 57–74.

Maynard, A.D., Kuempel, E.D., 2005. Airborne nanostructured particles and occupational health. J. Nanoparticle Res. 7, 587–614.

McCarthy, J., et al., 2012. Mechanisms of toxicity of amorphous silica nanoparticles on human lung submucosal cells in vitro: protective effects of fisetin. Chem. Res. Toxicol. 25, 2227–2235.

Midander, K., et al., 2009. Surface characteristics, copper release, and toxicity of nano- and micrometer-sized copper and copper(II) oxide particles: a cross-disciplinary study. Small 5, 389–399.

Mihalache, R., et al., 2017. Occupational exposure limits for manufactured nanomater-ials, a systematic review. Nanotoxicology 11, 7–19.

Monfort, E., et al., 2006. Control of fugitive particulate emissions in the ceramic industry. Qualicer 2006: IX World Congress on Ceramic Tile Quality, Castellón, Cámara oficial de comercio. industria y navegación, pp. PBC 137–PBC 150.

Monfort, E., et al., 2014. La evolución energética del sector español de baldosas cerámicas. Boletín de la Sociedad Española de Cerámica y Vidrio 53, 111–120.

Mulware, S.J., 2013. Trace elements and carcinogenicity: a subject in review. 3 Biotech 3, 85–96.

Munz, D., Fett, T., 2013. Ceramics: Mechanical Properties, Failure Behaviour, Materials Selection. Springer Science & Business Media.

Murugadoss, S., et al., 2017. Toxicology of silica nanoparticles: an update. Arch. Toxicol. 91, 2967–3010.

Nagai, H., et al., 2011. Diameter and rigidity of multiwalled carbon nanotubes are critical factors in mesothelial injury and carcinogenesis. Proc. Natl. Acad. Sci. Unit. States Am. 108, E1330–E1338.

Nagai, H., Toyokuni, S., 2012. Differences and similarities between carbon nanotubes and asbestos fibers during mesothelial carcinogenesis: shedding light on fiber entry me-chanism. Canc. Sci. 103, 1378–1390.

Naya, M., et al., 2012. In vivo genotoxicity study of titanium dioxide nanoparticles using comet assay following intratracheal instillation in rats. Regul. Toxicol. Pharmacol. 62, 1–6.

Noël, A., Truchon, G., 2015. Inhaled titanium dioxide nanoparticles: a review of their pulmonary responses with particular focus on the agglomeration state. Nano LIFE 5, 1450008.

O'Shaughnessy, P.T., 2013. Occupational health risk to nanoparticulate exposure. Environ. Sci. Processes Impacts. 15, 49–62.

Oberdörster, G., 2000. Pulmonary effects of inhaled ultrafine particles. Int. Arch. Occup. Environ. Health 74, 1–8.

Oberdorster, G., 2010. Safety assessment for nanotechnology and nanomedicine: concepts of nanotoxicology. J. Intern. Med. 267, 89–105.

Oberdorster, G., et al., 2005. Principles for characterizing the potential human health effects from exposure to nanomaterials: elements of a screening strategy. Part. Fibre Toxicol. 2, 8.

Oberdörster, G., et al., 2005. Nanotoxicology: an emerging discipline evolving from studies of ultrafine particles. Environ. Health Perspect. 113, 823–839.

Oberdörster, G., et al., 2007. Concepts of nanoparticle dose metric and response metric. Environ. Health Perspect. 115 A290-A290.

Palmero, P., 2015. Structural ceramic nanocomposites: a review of properties and pow-ders' synthesis methods. Nanomaterials 5, 656–696.

Pampuch, R., 2014. An Introduction to Ceramics. Springer.

Panas, A., et al., 2014. Silica nanoparticles are less toxic to human lung cells when de-posited at the air-liquid interface compared to conventional submerged exposure. Beilstein J. Nanotechnol. 5, 1590–1602.

Panas, A., et al., 2013. Screening of different metal oxide nanoparticles reveals selective toxicity and inflammatory potential of silica nanoparticles in lung epithelial cells and macrophages. Nanotoxicology 7, 259–273.

Park, B., et al., 2008a. Hazard and risk assessment of a nanoparticulate cerium oxide-based diesel fuel additive - a case study. Inhal. Toxicol. 20, 547–566.

Park, E.J., et al., 2008b. Oxidative stress induced by cerium oxide nanoparticles in cul-tured BEAS-2B cells. Toxicology 245, 90–100.

Paur, H.-R., et al., 2011. In-vitro cell exposure studies for the assessment of nanoparticle toxicity in the lung - a dialog between aerosol science and biology. J. Aerosol Sci. 42, 668–692.

Pavan, C., et al., 2019. The puzzling issue of silica toxicity: are silanols bridging the gaps between surface states and pathogenicity? Part. Fibre Toxicol. 16, 1–10.

Pavan, C., Fubini, B., 2017. Unveiling the variability of "quartz hazard" in light of recent toxicological findings. Chem. Res. Toxicol. 30, 469–485.

Pietroiusti, A, et al., 2018. Nanomaterial exposure, toxicity, and impact on human health. Wiley Interdiscip Rev Nanomed Nanobiotechnol 10, e1513.

Pietroiusti, A., Magrini, A., 2014. Engineered nanoparticles at the workplace: current knowledge about workers' risk. Occup. Med. (Lond.) 64, 319–330.

Poinen-Rughooputh, S., et al., 2016. Occupational exposure to silica dust and risk of lung cancer: an updated meta-analysis of epidemiological studies. BMC Publ. Health 16, 1137.

Rathod, V.T., et al., 2017. Polymer and ceramic nanocomposites for aerospace applica-tions. Appl. Nanosci. 7, 519–548.

Reche, C., et al., 2015. Determinants of aerosol lung-deposited surface area variation in an urban environment. Sci. Total Environ. 517, 38–47.

Relier, C., et al., 2017. Study of TiO2 P25 nanoparticles genotoxicity on lung, blood, and liver cells in lung overload and non-overload conditions after repeated respiratory exposure in rats. Toxicol. Sci. 156, 527–537.

Ribalta, C., et al., 2019a. On the relationship between exposure to particles and dustiness during handling of powders in industrial settings. Ann Work Expo Health 63, 107–123.

Ribalta, C., et al., 2019b. Health risk assessment from exposure to particles during packing in working environments. Sci Total Environ. 671, 474–487.

Riediker, M., et al., 2019. Particle toxicology and health - where are we? Part. Fibre Toxicol. 16, 19.

Roco, M.C., 2011. The Long View of Nanotechnology Development: the National Nanotechnology Initiative at 10 Years. Springer.

Salmatonidis, A., et al., 2019a. Workplace exposure to nanoparticles during thermal spraying of ceramic coatings. Annals of Work Exposures and Health 63, 91–106.

Salmatonidis, A., et al., 2019b. Effectiveness of nanoparticle exposure mitigation mea-sures in industrial settings. Int. J. Hyg Environ. Health 222, 926–935.

Salmatonidis, A., et al., 2018. Nanoparticle formation and emission during laser ablation of ceramic tiles. J. Aerosol Sci. 126, 152–168.

Sayes, C.M., et al., 2010. Changing the dose metric for inhalation toxicity studies: short-term study in rats with engineered aerosolized amorphous silica nanoparticles. Inhal. Toxicol. 22, 348–354.

Schenk, L., Johanson, G., 2010. Use of uncertainty factors by the SCOEL in their deri-vation of health-based occupational exposure limits. Crit. Rev. Toxicol. 40, 791–798.

Schmid, O., Stoeger, T., 2016. Surface area is the biologically most effective dose metric for acute nanoparticle toxicity in the lung. J. Aerosol Sci. 99, 133–143.

Schneider, T., et al., 2011. Conceptual model for assessment of inhalation exposure to manufactured nanoparticles. J. Expo. Sci. Environ. Epidemiol. 21, 450–463.

Schulte, P.A., et al., 2010. Occupational exposure limits for nanomaterials: state of the art. J. Nanoparticle Res. 12, 1971–1987.

Schulz, H., et al., 2005. Cardiovascular effects of fine and ultrafine particles. J. Aerosol Med. 18, 1–22.

Seipenbusch, M., et al., 2014. Chapter 4 - from source to dose: emission, transport, aerosol dynamics and dose assessment for workplace aerosol exposure. In: Vogel, U. (Ed.), Handbook of Nanosafety. Academic Press, San Diego, pp. 135–171.

Shannahan, J.H., et al., 2012. Manufactured and airborne nanoparticle cardiopulmonary interactions: a review of mechanisms and the possible contribution of mast cells.

21

Inhal. Toxicol. 24, 320–339.

Shi, H., et al., 2013. Titanium dioxide nanoparticles: a review of current toxicological data. Part. Fibre Toxicol. 10, 15.

Shvedova, A.A., et al., 2009. Mechanisms of pulmonary toxicity and medical applications of carbon nanotubes: two faces of Janus? Pharmacol. Ther. 121, 192–204.

Singh, A.K., 2015. Engineered Nanoparticles: Structure, Properties and Mechanisms of Toxicity. Academic Press.

Singh, D., et al., 2016. Ceramic nanoparticles: recompense, cellular uptake and toxicity concerns. Artif Cells Nanomed Biotechnol 44, 401–409.

Srinivas, A., et al., 2011. Acute inhalation toxicity of cerium oxide nanoparticles in rats. Toxicol. Lett. 205, 105–115.

Stebounova, L.V., et al., 2018. Particle concentrations in occupational settings measured with a nanoparticle respiratory deposition (NRD) sampler. Ann Work Expo Health 62, 699–710.

Stone, V., et al., 2017. Nanomaterials versus ambient ultrafine particles: an opportunity to exchange toxicology knowledge. Environ. Health Perspect. 125, 106002.

Stueckle, T.A., et al., 2018. Short-term pulmonary toxicity assessment of pre- and post-incinerated organomodified nanoclay in mice. ACS Nano 12, 2292–2310.

Su, W.C., et al., 2016. Deposition of graphene nanomaterial aerosols in human upper airways. J. Occup. Environ. Hyg. 13, 48–59.

Todea, A.M., et al., 2015. Accuracy of electrical aerosol sensors measuring lung deposited surface area concentrations. J. Aerosol Sci. 89, 96–109.

Traykova, T., et al., 2006. Bioceramics as nanomaterials. Nanomedicine 1, 91–106.

Trethowan, W., et al., 1995. Study of the respiratory health of employees in seven European plants that manufacture ceramic fibres. Occup. Environ. Med. 52, 97–104.

Tsai, C.-J., et al., 2012. Novel active personal nanoparticle sampler for the exposure assessment of nanoparticles in workplaces. Environ. Sci. Technol. 46, 4546–4552.

Turci, F., et al., 2016. Revisiting the paradigm of silica pathogenicity with synthetic quartz crystals: the role of crystallinity and surface disorder. Part. Fibre Toxicol. 13, 32.

Vallyathan, V., Gwinn, M.R., 2006. Nanoparticles: health effects-pros and cons. Environ. Health Perspect. 1818–1825.

van Broekhuizen, P., et al., 2012a. Workplace exposure to nanoparticles and the application of provisional nanoreference values in times of uncertain risks. J. Nanoparticle Res. 14, 770.

van Broekhuizen, P., et al., 2012b. Exposure limits for nanoparticles: report of an international workshop on nano reference values. Ann. Occup. Hyg. 56, 515–524.

Viana, M., et al., 2017. Workplace exposure and release of ultrafine particles during atmospheric plasma spraying in the ceramic industry. Sci. Total Environ. 599–600, 2065–2073.

Vida, S., et al., 2010. Occupational exposure to silica and lung cancer: pooled analysis of two case-control studies in Montreal, Canada. Cancer Epidemiol. Biomark. Prev. 19, 1602–1611.

Voliotis, A., et al., 2014. Nanoparticle emissions from traditional pottery manufacturing. Environ. Sci. Process Impacts 16, 1489–1494.

Wagner, A., et al., 2017a. Toxicity evaluations of nanoclays and thermally degraded byproducts through spectroscopical and microscopical approaches. Biochim. Biophys. Acta Gen. Subj. 1861, 3406–3415.

Wagner, A., et al., 2017b. Early assessment and correlations of nanoclay's toxicity to their physical and chemical properties. ACS Appl. Mater. Interfaces 9, 32323–32335.

Wagner, A., et al., 2018. Incineration of nanoclay composites leads to byproducts with reduced cellular reactivity. Sci. Rep. 8, 10709.

Wakamatsu, M., Salomao, R., 2010. Ceramic nanoparticles: what else do we have to know? International Ceramic Review 59, 28–33.

Wang, Y., et al., 2009. Laser surface remelting of plasma sprayed nanostructured Al2O3–13wt% TiO2 coatings on titanium alloy. Appl. Surf. Sci. 255, 8603–8610.

Wang, Z., et al., 2012. CuO nanoparticle interaction with human epithelial cells: cellular uptake, location, export, and genotoxicity. Chem. Res. Toxicol. 25, 1512–1521.

Ware, L.B., 2008. Modeling Human Lung Disease in Animals. American Physiological Society.

Wittmaack, K., 2006. In search of the most relevant parameter for quantifying lung inflammatory response to nanoparticle exposure: particle number, surface area, or what? Environ. Health Perspect. 115, 187–194.

Wittmaack, K., 2007. Dose and Response Metrics in Nanotoxicology: Wittmaack Responds to Oberdoerster et al. and Stoeger et al. Environ. Health Perspect. 115, A291–A292.

World Health Organization, 2017. WHO Guidelines from Potential Risks on Protecting Workers of Manufactured Nanomaterials.

Woskie, S., 2010. Workplace practices for engineered nanomaterial manufacturers. Wiley Interdisciplinary Reviews: Nanomedicine and Nanobiotechnology. 2, 685–692.

Xia, T., et al., 2008. Comparison of the mechanism of toxicity of zinc oxide and cerium oxide nanoparticles based on dissolution and oxidative stress properties. ACS Nano 2, 2121–2134.

22

A. 2. Assessing the *in vitro* toxicity of airborne (nano)particles to the human respiratory system: from basic to advanced models

Bessa M. J., Brandão F., Rosário F., Moreira L., Reis A. T., Valdiglesias, V., Laffon, B., Fraga S., & Teixeira J. P.

The PhD candidate was responsible for the conceptualisation and writing of the manuscript.

Assessing the *in vitro* toxicity of airborne (nano)particles to the human respiratory system: from basic to advanced models

Maria João Bessa[1,2,3,4], Fátima Brandão[1,2,3], Fernanda Rosário[1,2,3], Luciana Moreira[1,2,3], Ana Teresa Reis[1,2,3], Vanessa Valdiglesias[5,6], Blanca Laffon[6,7], Sónia Fraga[1,2,3]*, & João Paulo Teixeira[1,2,3]

[1] Department of Environmental Health, National Institute of Health Dr. Ricardo Jorge, Porto, Portugal

[2] EPIUnit-Instituto de Saúde Pública, Universidade do Porto, Porto, Portugal

[3] Laboratório para a Investigação Integrativa e Translacional em Saúde Populacional (ITR), Porto, Portugal

[4] Instituto de Ciências Biomédicas Abel Salazar (ICBAS), Universidade do Porto, Porto, Portugal

[5] Universidade da Coruña, Grupo NanoToxGen, Centro de Investigacións Científicas Avanzadas (CICA), Departamento de Biología, Facultad de Ciencias, A Coruña, Spain

[6] Instituto de Investigación Biomédica de A Coruña (INIBIC), A Coruña, Spain;

[7] Universidade da Coruña, Grupo DICOMOSA, Centro de Investigacións Científicas Avanzadas (CICA), Departamento de Psicología, Facultad de Ciencias de la Educación, A Coruña, Spain.

* Correspondence: sonia.fraga@insa.min-saude.pt; Tel.: (+351) 223 401147

Abstract: *In vitro* testing has long been used to assess the hazard of airborne particulates and other pollutants. Current efforts are being done for developing physiologically relevant human-based *in vitro* models for reliably and accurately predict *in vivo* human responses, ranging from mono- or coculture of various respiratory cell types in two- or three-dimensional culture systems or even more sophisticated systems such as lung-on-a-chip devices. Simultaneously, the exposure conditions are also known to strongly influence cell responses *in vitro*. So far, most of the pulmonary *in vitro* studies have been carried out using cell lines under submerged conditions but is now widely accepted that cells cultured and exposed under air-liquid interface (ALI) conditions represent a more realistic exposure scenario. Accordingly, choosing the most suitable cellular model and exposure conditions to answer a particular question is of extreme importance when designing *in vitro* pulmonary toxicity studies. This review provides an overview of the existing exposure systems and human respiratory models for *in vitro* testing, with a special focus on (nano)particulate material. A brief insight into the path of inhaled (nano)particles

along with the respiratory system, the defense barriers they face, and consequent adverse effects they might cause will be also presented.

Keywords: nanoparticles, respiratory models, *in vitro*, submerged cultures, air-liquid interface, toxicity testing

1. Introduction

Nanotechnology is an emerging field that offers insightful and innovative approaches and applications in many areas (De Jong *et al.*, 2008; Thiruvengadam *et al.*, 2018). Indeed, nanoparticle (NP) production and use are increasing exponentially, making environmental and human exposure to these particles inevitable (Malakar *et al.*, 2021). Multiple efforts have been made to understand the health implications from manipulation and exposure of these nanoscale materials. Growing evidence has shown that due to their small size and increased surface area, NP might cause harmful effects since they can easily cross the biological barriers and reach the systemic circulation, where they can be distributed and translocated to vital organs (Jia *et al.*, 2020). Inhalation is the main route of entrance for (nano)particles (Oberdorster *et al.*, 2015) and it is estimated that solid (nano)particles half-life in the human alveolar region based on the clearance mechanism is around 700 days, which constitutes a threat to the respiratory system (Hagens *et al.*, 2007).

Over the past few years, many *in vitro* and *in vivo* studies have explored the effects of micro- and nano-sized materials in different lung-related models [reviewed in (Fytianos *et al.*, 2016; Kumar *et al.*, 2017; Nahar *et al.*, 2013; Wick *et al.*, 2015; Wiemann *et al.*, 2016)]. From these studies, multiple hallmarks of (nano)particle-induced pulmonary toxicity have been identified, including particle internalization pathways, oxidative stress, genotoxicity, cell cycle alterations, and dysregulation of signaling cascades, among others (Bakand *et al.*, 2012; Li *et al.*, 2010; Paur *et al.*, 2011; Pietroiusti *et al.*, 2018). Several of these mechanisms are associated with the occurrence of negative health outcomes such as impaired lung function and inflammation, vascular dysfunction, and severe acute respiratory and cardiovascular effects (Stone *et al.*, 2017). These adverse effects are strongly linked with different diseases including lung cancer, bronchitis, and acute asthma, cardiac infection and arrhythmia, hypertension, atherosclerosis, and ischemia (Brook *et al.*, 2004;

Kelly *et al.*, 2015; Knaapen *et al.*, 2004; Kreyling *et al.*, 2006; Schulz *et al.*, 2005; Shannahan *et al.*, 2012).

As will be described later on, *in vivo* animal studies using rodents are commonly used to investigate (nano)particle pulmonary toxicity. However, data obtained from these studies are not easily extrapolated for predicting the effects of micro- and nano-sized materials inhalation in humans (Movia *et al.*, 2017; Movia *et al.*, 2020). Many *in vitro* models have proven to be good candidates to assess (nano)particle respiratory toxicity (Clippinger *et al.*, 2016; Clippinger *et al.*, 2018). In recent years, several efforts have been made towards the development and/or improvement of physiologically more relevant *in vitro* systems for inhalation toxicology testing of particles (Fröhlich, 2018).

The main purpose of this review is to provide an overview of the existing pulmonary *in vitro* models and exposure conditions for identifying and evaluating (nano)particle hazards, as reliable alternatives to animal testing. The main differences between human and rodents' respiratory systems, as well as the main adverse health effects from exposure to airborne (nano)particles, are also addressed as a prelude.

2. Human respiratory system and how it differs from rodents

Based on its structure, size and function, the respiratory tract can be divided into: (1) upper respiratory tract, which includes the extrathoracic region (nasal cavity, mouth, pharynx, and larynx), and (2) lower respiratory tract, which includes the tracheobronchiolar (trachea to terminal bronchioles) and pulmonary (terminal bronchioles to alveolar sacs) regions (Harkema *et al.*, 2012; Ionescu, 2013). While the upper respiratory tract allows the passage of the air and protects the lower respiratory regions from external aggressions (Thomas, 2013), the lower tract is where the gas exchange takes place (Weibel *et al.*, 2005). Along the respiratory tract, cell types and morphology vary (**Figure 1**), which can also be affected by pulmonary disease (Whitsett *et al.*, 2015a). As shown in **Figure 1**, the upper airways are lined with a pseudostratified epithelium that is composed of ciliated, secretory (goblet and club cells), neuro-endocrine, and basal cells, the latter acting as progenitor cells for the various cell types of the airway epithelium (Crapo *et al.*, 1982; Hiemstra *et al.*, 2015). The bronchioles are lined by ciliated cuboidal epithelium, with a small number of non-ciliated club cells that are more dominant in the distal part (Khan *et al.*, 2018). In addition, the alveolar epithelium is very important for maintaining lung

homeostasis and is constituted by cuboidal alveolar epithelial type 1 cells (AEC1) and type 2 cells (AEC2). A thin layer of AEC1 cells covers most of the alveolar surface and allows efficient gas exchange between blood and alveoli (Braakhuis *et al.*, 2015; Stone *et al.*, 1992). AEC2 are the progenitor cells of AEC1 and produce the pulmonary surfactant critical to control surface tension and prevent the alveoli collapse during the ventilation mechanisms (Stone *et al.*, 1992; Whitsett *et al.*, 2015b).
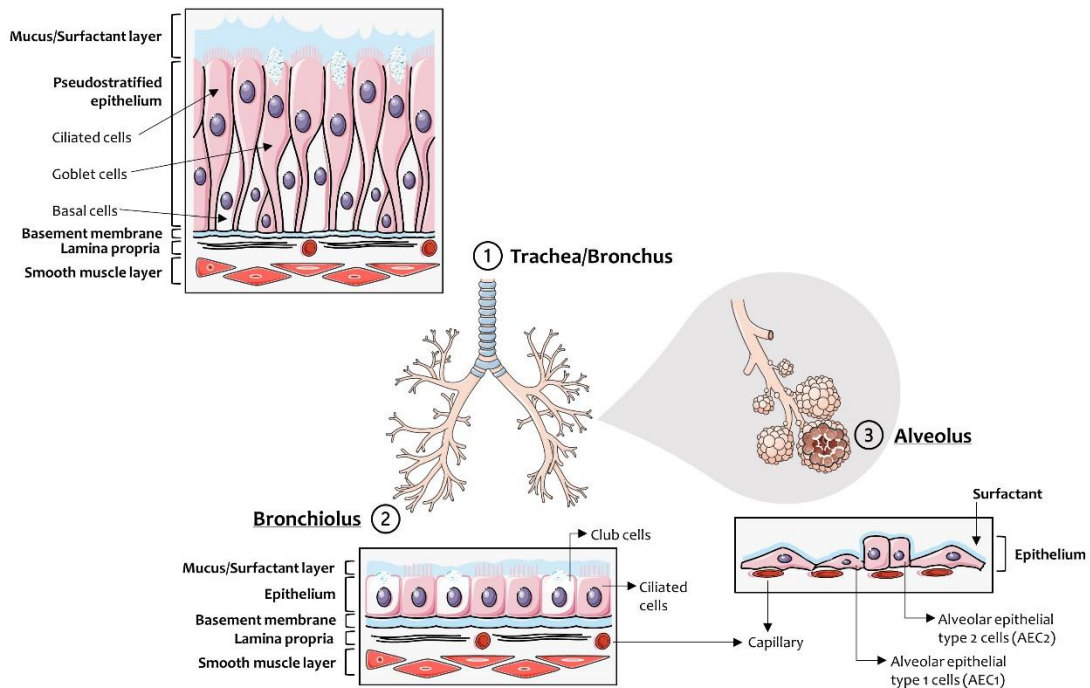
Figure 1. Respiratory tract: cell types and morphology. This illustration was created including images obtained from Smart Servier Medical Art (www.smart.servier.com) CC BY 3.0.

The defense mechanisms of the airways and lung comprise the cough reflex, the epithelial barrier and lining fluid, the mucociliary escalator, humoral factors - such as antimicrobial peptides, peptides surfactant and complement proteins - and cells that elicit immune responses, namely epithelial cells, macrophages, monocytes, dendritic cells, neutrophils, natural killer cells, and mast cells (Hastedt *et al.*, 2016; Rothen-Rutishauser *et al.*, 2008). In the large airways, the epithelial lining fluid is composed of a superficial mucus layer overlying a periciliary liquid layer that is responsible for mucociliary clearance through physical unidirectional cilia movement and removal of deposited particles and gases dissolved in the mucus from the respiratory tract (Schuster *et al.*, 2013). In turn, the alveolar surface is covered by pulmonary surfactant that also plays a pivotal role in the clearance of inhaled toxicants, including

aerosolized (nano)particles (Wohlleben *et al.*, 2016). The alveolar surfactant is composed of a complex mixture of lipids (90 %, mainly phospholipids), and proteins (10 %), that include specific surfactant proteins, albumin, and immunoglobulins. Moreover, there are additional mechanisms that contribute to the lung epithelial defense. Those include the activation of metabolic enzymes such as the cytochrome P450 family (Lingappan *et al.*, 2017) and/or activation of nuclear factor erythroid 2–related factor 2 (Nrf2)-mediated transcription factors, which are involved in the protection against oxidative damage by inhaled hazardous substances through the disruption of the Kelch-like erythroid cell-derived protein with Cap 'n' Collar (CNC) homology (ECH)-associated protein (KEAP)-1 mediated repression, glutathione (GSH)- and thioredoxin (TXN)-dependent antioxidant systems regulation, among other mechanisms (Mizumura *et al.*, 2020).

Considerable differences in the anatomy and physiology of the respiratory system between rodents and humans exist (**Table 1**), that must be considered when designing and interpreting inhalation toxicity studies. Indeed, their distinct respiratory tract architecture affects the airflow pattern and ventilation rates, which in turn influence the deposition, clearance, and retention of the inhaled particles (Bakand *et al.*, 2012; Clippinger *et al.*, 2018). Differences in the type and number of cells lining the airways, as well as in the mucociliary clearance also exist. For instance, the number of mucus-producing cells found in the major airways differs between species. While rodents possess nonciliated secretory cells that are important players in host defense and a low number of mucin-secreting goblet cells in the proximal airways, humans have submucosal glands and a high number of epithelial goblet cells that produce a layer of airway surface liquid that moisturizes the inhaled air and encloses potentially harmful airborne particles (Meyerholz *et al.*, 2018). Altogether, these aspects will strongly influence (nano)particle biological fate and hazard potential.

Rodents are the most frequently used animal model in inhalation toxicity studies (Movia *et al.*, 2020). Regarding NP *in vivo* testing, several studies have been already conducted in rodents that have been useful to identify important toxic properties of NP, to assess the safety and efficacy of nanomedicines, and to estimate risks to human and environmental health (He, 2016). However, there is also the flip side as many of these studies seem to be inconclusive, making data extrapolation to humans difficult (Landsiedel *et al.*, 2014b; Movia *et al.*, 2020).

Table 1. Main anatomical and physiological differences between humans and rodents respiratory system [Adapted from Harkema *et al.* (2012); Meyerholz *et al.* (2018); Rackley *et al.* (2012)].

Features	*Humans*	*Rodents*
Nose and sinus	Relatively simple nasal turbinate structure; total surface area: 150-200 cm^2.	Complex nasal turbinate structure; total surface area: 2.9 cm^2 [relative surface area (surface area/volume) 5x greater than humans].
	Accessory olfactory organs are not well developed or functional.	Presence of accessory olfactory organs.
	Olfactory epithelium ~3% of the nasal cavity.	Olfactory epithelium ~50% of the nasal cavity (well-developed sense of smell).
Pharynx and larynx	Widely disseminated and well-defined pharyngeal tonsils.	Lack of distinct pharyngeal tonsils; widely dispersed lymphoid aggregates.
	No U-shaped laryngeal cartilage and ventral pouch.	Presence of U-shaped laryngeal cartilage and ventral pouch (larger/more prominent in rats than mice).
	Absence of taste buds in this region.	Taste buds are located within the epiglottis, larynx, and pharynx.
Trachea	Trachea internal diameter of ~12 mm.	Trachea internal diameter of ~1.5 mm (mouse).
	Trachea lined by ciliated cells.	The trachea is mostly lined by non-ciliated epithelial cells.
	The submucosa contains numerous tightly packed seromucinous glands.	Submucosal glands are restricted to the proximal (closest to the larynx) trachea.
	Tracheal cartilaginous rings extend for several bronchial generations into the lung.	Tracheal cartilaginous rings are only present in the extrapulmonary airways.
Lungs	The right lung of humans is divided into three lobes, whereas the left lung has two lobes.	The right lung is divided into four lobes, whereas the left lung has one lobe.
	Dichotomous airway branching.	Monopodial airway branching.
	The respiratory zone includes respiratory bronchioles, alveolar ducts, and alveoli.	Respiratory zone includes diminutive respiratory bronchioles (if present), alveolar ducts, and alveoli.
Bronchi to terminal bronchioles	Lung parenchyma includes both bronchi and bronchioles.	Lack of well-developed respiratory bronchioles (defined by lack of cartilage and submucosal glands).
	Relatively abundant mucin-secreting goblet cells.	Less than 1 % mucous goblet cells in the epithelium of extrapulmonary bronchi (particularly in adults mice maintained under lab conditions).
Branching pattern	Symmetric (airflow pattern more susceptible to deposition at its bifurcation points).	Asymmetric or monopodial (relatively unimpeded flow).
Breathing mode	Oronasal breathers (both nasal and oral breathing).	Obligate nose breathers (all inhaled air passes through the nasopharynx on its path into the lungs).

Features	Humans	Rodents
Lung organogenesis	~week 3 during human development as the primitive lungs bud from the foregut endoderm.	~embryonic day 9 in the mouse.
	Undergo many additional rounds of branching before beginning alveolarization.	Mouse lungs develop quickly and do not begin forming alveoli until after birth.

In this regard, Mowat *et al.* (2017) reviewed 26 pairs of studies on the inhalation toxicity of 22 vehicles or pharmaceuticals belonging to various classes such as antibiotics, biologic drugs, muscarinic and adrenergic agents, where the same test material was tested in parallel in a rodent (rat or mouse) and nonrodent (dog or monkey) species. This analysis revealed that the rodent larynx, and to a lesser extent the tracheal bifurcation, are more sensitive to the inhaled xenobiotics than those of nonrodents. The anatomy and histology of the dog or monkey larynx more closely resemble those of the human, thus more importance should be conferred to these models (Mowat *et al.*, 2017).

3. Inhalation exposure and the effects of to (nano)particles on human respiratory tract

Inhalation is a primary route of exposure to ambient and workplace particulate matter (PM) (Oberdörster *et al.*, 2018; Oberdörster *et al.*, 2007). Several studies have already demonstrated an association between adverse human health effects following exposure to airborne PM, where ultrafine particles (UFP) seem to play an important role (Delfino *et al.*, 2005; Johnson *et al.*, 2021; Li *et al.*, 2016). Despite their distinct origin, UFP and NP share many similarities in terms of their physicochemical properties and modes of action (Stone *et al.*, 2017).

In the following sections, inhaled (nano)particles' path and fate, the defense mechanisms of the respiratory system, and their potential adverse health effects will be addressed (**Figure 2**).
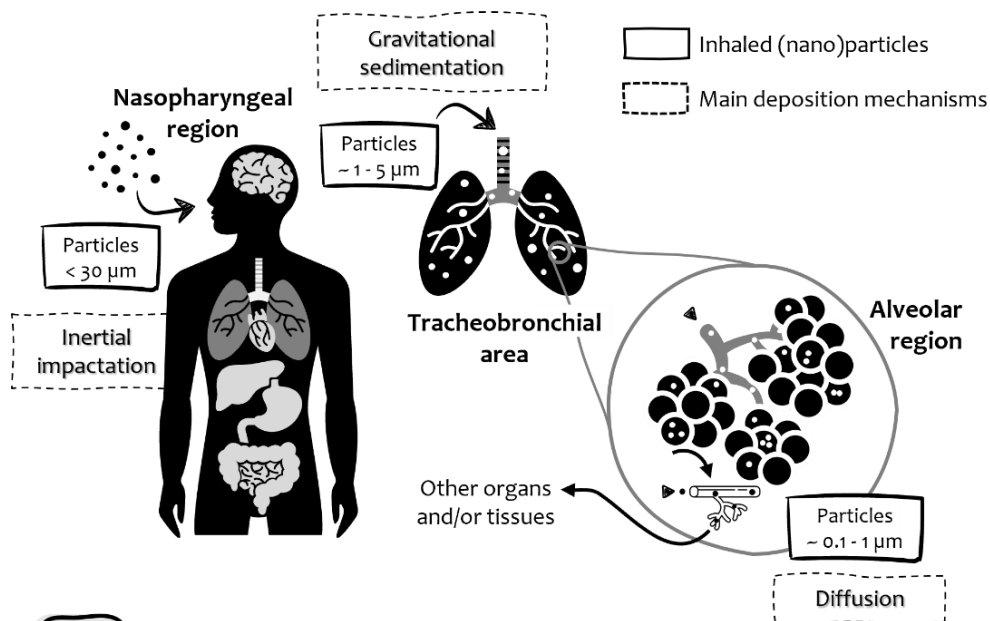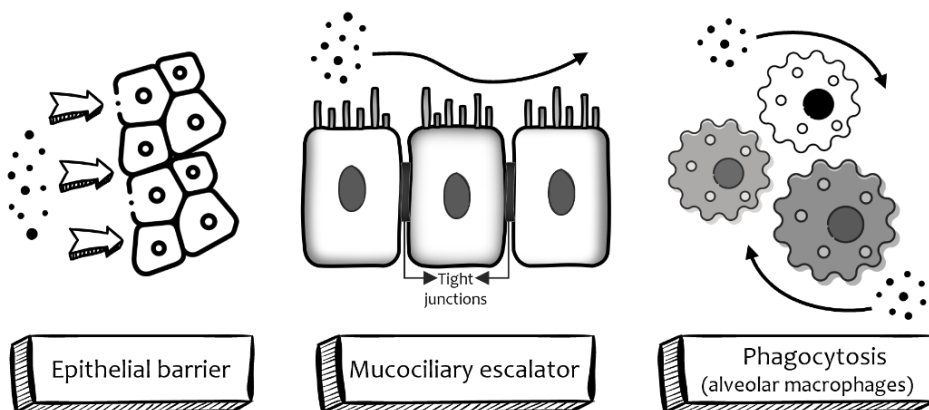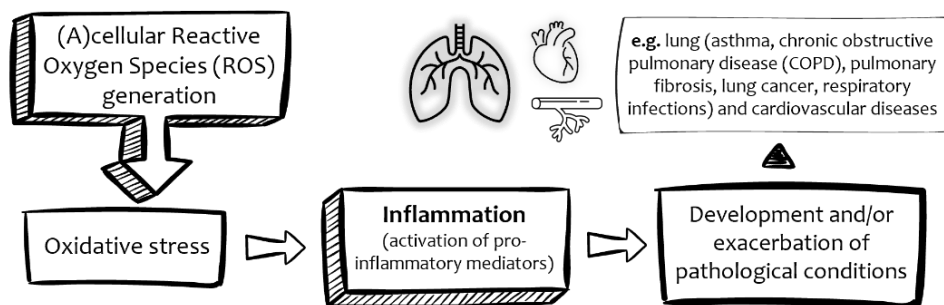
Figure 2. Inhaled particles: (1) deposition, (2) main defense mechanisms of the human respiratory system, and (3) adverse human health effects. This illustration was created including images obtained from SlidesCarnival (https://www.slidescarnival.com) CC BY 4.0.

3.1. Factors influencing the deposition of inhaled particles

As depicted in **Figure 2**, once a particle is inhaled, it enters the extrathoracic region where it meets the trachea, being conducted to the bronchi and alveolar region. Although aerosol particles are often described as spherical and monodisperse, particle collisions often originate from non-spherical aggregates and/or agglomerates (Kleinstreuer *et al.*, 2010). Indeed, deposition of inhaled particles is dependent on aerosol's physicochemical properties (Morawska *et al.*, 2021) and anatomical (diameter, length, and branching angle of airway segments) and physiological (airflow and breathing pattern) factors (Andujar *et al.*, 2011; Clippinger *et al.*, 2018). Physicochemical parameters governing particle deposition include particle size/and or size distribution, density, shape, hygroscopicity/hydrophobicity, and chemical reactions of the particle (Morawska *et al.*, 2021). In addition, lung lining fluid composition, viscosity and surface tension strongly influence particle trajectories, deposition, and biological fate. Lung morphology has a considerable influence on the deposition of (nano)particles in humans. This should be considered for the lung burden estimation from exposure to these airborne particles, particularly when comparing healthy *vs* vulnerable individuals with lung disease (Jakobsson *et al.*, 2018).

Overall, the main mechanisms for particle deposition include: interception (particle-surface contact), inertial impaction (particle sudden change in the direction of the flow), gravitational sedimentation (settling of particles under the action of gravity), diffusion (random motions of the particles, *e.g.* Brownian motion, where randomized particle motion is caused by their collision with gas molecules), and electrostatic precipitation (particle charge may potentially affect their deposition in the airways) (Bui *et al.*, 2020; Darquenne, 2020; Tsuda *et al.*, 2013). As depicted in **Figure 2**, larger particles (5–30 μm) are deposited in the nasopharyngeal region by inertial impaction, while smaller particles (1–5 μm) are deposited in the tracheobronchial area by gravitational sedimentation where they may or may not be removed by mucociliary clearance. On the other hand, nano-sized particles (0.1–1 μm) can penetrate deeper into the alveolar region, such as the alveoli where the airflow is very low, deposited by Brownian diffusion or electrostatic attraction (Bakand *et al.*, 2012; Hagens *et al.*, 2007). Once in the lung, nano-sized particles are able to translocate to the

systemic circulation, where they can reach other organs and tissues, though the exact mechanism is still poorly understood (Domb *et al.*, 2021).

Particle deposition in the respiratory system can be modeled using computational models. Two advanced and widely used models are the Multiple Path Particle Dosimetry (MPPD) (Anjilvel *et al.*, 1995) and the human respiratory tract model developed by the International Commission on Radiological Protection (ICRP) (Smith *et al.*, 2014). The MPPD is a one-dimensional (1D) whole-lung deposition model that can be used to predict regional and site-specific particle deposition, as well as particle clearance based on actual airways measurements and asymmetries. Herein, the deposited particle concentration is calculated as a function of time for the proximal and distal ends of the airway. By knowing the particle concentration at the airway proximal end, the particle concentration at the distal end can be calculated for different deposition mechanisms (Bui *et al.*, 2020; Kuempel *et al.*, 2015). This model is freely available as a dosimetry software for both rat and human respiratory tracts. The human model option includes several deposition and clearance models (Kuempel *et al.*, 2015). The ICRP, on the other hand, is a semi-empirical model, where the human respiratory tract is represented as a sequence of anatomical compartments through which aerosols pass during the inhalation and exhalation processes. This model divides the lungs into three compartments: the extrathoracic region, the tracheobronchial region, and the alveolar region. The deposition pattern is calculated for each compartment, along with the amount of clearance through different regions of the lungs post-deposition. These measurements are based on semi-empirical equations obtained from fitting of experimental data as a function of particle size and flow rate (Bui *et al.*, 2020; Guha *et al.*, 2014).

3.2. Defense mechanisms of the human respiratory system against inhaled airborne (nano)particles

The human respiratory tract possesses several defense mechanisms for inhaled airborne (nano)particles (**Figure 2**). Accordingly, (nano)particle deposition and retention in the lung is strongly influenced by the lung clearance capacity (Braakhuis *et al.*, 2015). Overall, inhaled particles in the human airways can be removed via physical (*e.g.*, translocation through the epithelium, mucociliary escalator, and phagocytosis of insoluble particles) and chemical (*e.g.*, particle dissolution, lixiviation, and protein binding) processes. While

physical clearance mechanisms differ depending on the region of the respiratory system, the chemical defenses are identical along the respiratory tract (Andujar *et al.*, 2011).

The respiratory tract is lined with epithelial cells that act as a physical barrier to external aggressors. Adhesion and paracellular transport between epithelial cells are achieved by the concerted action of intercellular tight junctions and adherent junctions that prevent inhaled airborne (nano)particles from injuring the airways and simultaneously serve as platforms for the signaling pathways involved in the regulation of gene expression, cell proliferation, and differentiation (Ganesan *et al.*, 2013). The pulmonary surfactant and cilia movements are also important components in the defense against (nano)particles. As we descend deeper in the airways, the clearance becomes slower due to the increased pathway length and decreased mucous velocity (Geiser, 2010). The surfactant film favors particle motion over the epithelial surfaces, where they can either be trapped in the mucus or recognized by phagocytic cells (macrophages, dendritic cells) located under the epithelial barrier (Hewitt *et al.*, 2021). To help these cells, a building block of structural barriers (*e.g.*, lung epithelium, basement membrane, capillary endothelium) prevents a deeper translocation of the particles into the tissue (Rothen-Rutishauser *et al.*, 2008). Nevertheless, some particles might be able to translocate the mucus layer and interact with the epithelial cells, potentially causing cell injury (Frieke Kuper *et al.*, 2015; Landsiedel *et al.*, 2014a). Once in the alveoli, where no ciliated cells and mucociliary escalator exist (Bustamante-Marin *et al.*, 2017), (nano)particles may be removed by solubilization or phagocytosed by the alveolar macrophages (Wiemann *et al.*, 2016). Particles or large agglomerates > 100 nm are easily recognized and phagocytosed, while individual (nano)particles might escape phagocyte recognition (Mühlfeld *et al.*, 2008). Individual (nano)particles might be too small to be efficiently recognized and phagocytosed by the alveolar macrophages. Therefore, by avoiding the normal phagocytic defenses in the respiratory system, (nano)particles may gain access to the systemic circulation and reach different extrapulmonary sites (Nemmar *et al.*, 2013).

Physicochemical properties of aerosol particles strongly influence their deposition but also their clearance from the human airways (Bierkandt *et al.*, 2018; Braakhuis *et al.*, 2014). For instance, charged (nano)particles seem to be more retained in the human respiratory airways due to their ability to attract

different proteins (Docter *et al.*, 2015). On the other hand, soluble particles are more easily eliminated compared to insoluble particle components (Braakhuis *et al.*, 2016). Another important aspect to take into consideration is how physiological fluids might change the physicochemical properties and behavior of (nano)particles (Urban *et al.*, 2016). Upon contact with the biological milieu of the lungs, (nano)particles will become surrounded by biomolecules such as albumin and proteins in the surfactant, which will greatly contribute to the formation of a corona around them and change their particle size and kinetics in the airways (Monopoli *et al.*, 2012). In the alveolar region, for instance, (nano)particles interact with the lipids present in the surfactant film located at the air-liquid interface (ALI) in the epithelial lining fluid covering the internal surface of the lung (Raesch *et al.*, 2015). The surfactant helps to stabilize the alveoli and promotes the clearance of inhaled particles to maintain the alveoli in a sterile- and inflammation-free environment (Kendall *et al.*, 2012). That is why the characterization of these nano-sized materials in relevant pulmonary biological fluids is so important (Wohlleben *et al.*, 2016).

3.3. Human adverse effects of (nano)particles

At the cellular level, the high surface reactivity of nano-sized particles promotes the generation of reactive oxygen species (ROS), oxidative stress, and inflammation with the release of pro-inflammatory mediators [*e.g.*, interleukin (IL)-6, IL-8, granulocyte-macrophage colony-stimulating factor (GM-CSF), tumor necrosis factor (TNF)α] (Leikauf *et al.*, 2020) (**Figure 2**). In fact, inflammation is considered a key mechanism for the occurrence of adverse health effects from exposure to inhaled particles (Donaldson *et al.*, 2001; Donaldson *et al.*, 2002), and it is usually involved in the development and/or exacerbation of several diseases such as asthma, chronic obstructive pulmonary disease (COPD), pulmonary fibrosis, respiratory infections and lung cancer (Øvrevik *et al.*, 2015; Stone *et al.*, 2017). Besides, epidemiological studies have demonstrated that individuals with pre-existing lung disease are more vulnerable to the adverse effects of fine and nano-sized particles (Geiser *et al.*, 2017). Indeed, (nano)particles have a high deposition efficiency in the lung of healthy individuals, but even higher in individuals with lung chronic disease (*e.g.*, asthma, COPD), possibly due to lung decreased clearance ability. In fact, the biopersistence of inhaled particles is a crucial aspect to consider under inflammation and tissue injury (Laux *et al.*, 2017).

Despite the close link between air pollution and human lung disease (Jiang *et al.*, 2016; Kurt *et al.*, 2016), little is known about the potential adverse health effects from inhalation of manufactured and incidental (nano)particles, with the few available reports focusing on occupational exposures. In this regard, a recent longitudinal follow-up study involving 206 nanomaterial (NM)-handling workers recruited from 14 Taiwan nanotechnology plants assessed cardiopulmonary dysfunction, inflammation, oxidative damage, and genotoxicity biomarkers, as well as antioxidant enzyme activity (Wu *et al.*, 2019). This study described no evidence of adverse health effects under the existing NP exposure levels in the workplace among these workers, except for the increase of antioxidant enzymes [*e.g.*, superoxide dismutase (SOD) and glutathione peroxidase (GPx)] (Wu *et al.*, 2019). Nevertheless, some studies indicate adverse health effects from exposure to NP. In this regard, Phillips and colleagues reported a fatal case after incidental inhalation of nickel (Ni) NP while spraying bushes for turbine bearings using a metal arc process (Phillips *et al.*, 2010). The subject, a 38-year-old healthy male, died 13 days after the accident from adult respiratory distress syndrome (ARDS). Analysis of the pulmonary tissue revealed the presence of Ni NP < 25 nm in lung macrophages, and high levels of Ni were detected in urine and renal tissue (Phillips *et al.*, 2010). Journeay *et al.* (2014) have also reported a case of Ni sensitization characterized by throat irritation, nasal congestion, and skin reactions from handling of powdered Ni NP without any kind of protective measures in a 26-year-old female chemist. Several case reports have also suggested respiratory health risks associated with inhalation of carbon NP from toner dust. Theegarten *et al.* (2010) reported a case of a 33-year-old female open office worker without any evident respiratory symptoms but who developed persistent abdominal pain, weight loss, and diarrhea from prolonged exposure to particle emissions from toner dust derived from laser printers (Theegarten *et al.*, 2010). These findings showed that following NP inhalation, the clearance mechanisms and lung barriers were overcome, and the particles were able to enter the systemic circulation and reach different extrapulmonary sites. In addition, Khatri *et al.* (2013) also described early responses to inhalation of NP emitted from photocopiers in nine healthy individuals following a six-hour period on 2-3 days in a photocopy center. These individuals were exposed to particle number levels at least 5 times higher than background levels, with a peak size distribution of 30-40 nm, and exhibited elevated urinary levels of 8-oxo-7,8-dihydroguanine (8-oxo-G), and pro-

inflammatory cytokines in nasal lavage compared to pre-exposure levels that remained elevated for up to 36 h post-exposure (Khatri *et al.*, 2013).

There are several *in vitro* and *in vivo* studies that already identified the major biological mechanisms involved in the pulmonary toxicity caused by (nano)particles, including: ineffective particle clearance, intracellular uptake/internalization, impairment of lung macrophage-mediated phagocytosis, loss of plasma membrane integrity, and mitochondrial dysfunction, oxidative stress (ROS generation, glutathione depletion, and lipid peroxidation), cytokine production and activation of inflammatory signaling cascades, DNA and chromosomal damage, altered DNA methylation and repair, and altered cell cycle regulation (Bakand *et al.*, 2016; Paur *et al.*, 2011; Pietroiusti *et al.*, 2018; Stone *et al.*, 2017). However, several aspects make the relevance of those data questionable. Most *in vitro* studies conducted so far have used rather simple models, whereas animal studies using rodents, as aforementioned, are not the most suitable model to truthfully predict human adverse effects from (nano)particles inhalation exposure. Additionally, another important issue concerning (nano)particles inhalation studies, either *in vitro* or *in vivo*, is the choice of relevant dose metrics (*e.g.*, mass, number of particles, surface area), which should be closely associated with the mechanism determining the adverse response in the target tissue/cell, and the measurement of the delivered dose (Schmid *et al.*, 2017). Not only the dose is important, but also the duration of the exposure, with most of the available studies focusing on the effects from acute exposure, while little is known about the long-term effects of chronic exposure to (nano)particles. Moreover, the clearance mechanisms play a crucial role and should be always considered in human toxicity studies. Many modeling studies are addressing this matter and a suitable estimation of these values is of major importance for a correct toxicity study planning, data interpretation, and extrapolation to real-life scenarios (Kolanjiyil *et al.*, 2013).

4. *In vitro* models for (nano)particle human respiratory toxicity assessment

For many years, *in vitro* culture systems failed to represent the complexity of multicellular organisms. Recently, more complex and physiologically relevant human *in vitro* models emerged and gained widespread acceptance (Bassi *et al.*, 2021; Sakolish *et al.*, 2016). The study of the biological effects of inhaled (nano)particles is particularly challenging and *in vitro* respiratory models have

been used as an important tool for assessing their molecular and cellular responses. At the same time, cell culture and exposure conditions should be as close as possible to the ones found *in vivo*. Several human *in vitro* models exist to represent specific areas of the respiratory tract (*e.g.*, nasal, tracheal, bronchial, and alveolar regions) (Fröhlich *et al.*, 2014; Steimer *et al.*, 2005). An ideal *in vitro* testing system for accurately predict the effects of inhaled (nano)particles would include the following features: (1) a suitable model mimicking the morphology and metabolic function of a particular healthy or vulnerable tissue/organ; (2) an exposure chamber for culture exposure to aerosolized (nano)particles; (3) a set of relevant biomarkers that would allow high-throughput evaluation of key toxicity events.

4.1. Pulmonary cell lines: mono- and co-cultures

Primary human lung epithelial cells are in theory the ideal choice for (nano)particles' testing, due to their resemblance in morphology, organization, stratification, and physiological function to the human airway epithelium (Dvorak *et al.*, 2011; Pezzulo *et al.*, 2011). However, these primary cells are difficult to establish and maintain in culture, are poorly reproducible, require complex and expensive cell culture media, and have a limited life span. This is why continuous cell lines have been widely used for *in vitro* nanotoxicology studies (Katt *et al.*, 2016). There are numerous *in vitro* lung cell lines that can be used to study the cellular interplay and cellular responses following (nano)particle exposure. Notwithstanding, since epithelial cells play a central role in the respiratory tract, providing a physical barrier to inhaled (nano)particles, these are commonly *in vitro* models for assessing (nano)toxicity. In accordance, **Table 2** presents the most widely used epithelial cell lines for *in vitro* toxicological assessment of inhaled particles (Bierkandt *et al.*, 2018; Fröhlich, 2018; Hiemstra *et al.*, 2018; Jia *et al.*, 2017; Rothen-Rutishauser *et al.*, 2008). Despite all advantages, some tumors or immortalized epithelial cell lines such as bronchial 16HBE14o, BEAS-2B, and Calu-3 cells, lack human *in vivo* characteristics such as mucociliary differentiation, the formation of an effective barrier, and have reduced metabolic capacity (Faber *et al.*, 2018). However, when grown under certain conditions, some of these cell lines may exhibit the presence of tight junctions, mucus production, cilia formation, and effective barrier function, which are important features when assessing (nano)particle toxicity.

Table 2. Human epithelial cell lines are commonly used in *in vitro* (nano)particle pulmonary toxicity studies.

Lung region	Human cell line		
	Identification	*Origin*	*Features*
Bronchial	16HBE14o	Normal bronchial epithelium; Virus transformed (adenovirus 12-simian virus 40 hybrid virus).	- Ability to form tight junctions; - Express cilia when grown at the air-liquid interface (ALI); - Retain important properties and functions of differentiated airway epithelial cells (*e.g.* mucus-secreting capacity, apical microvilli, etc.).
	BEAS-2B	Normal bronchial epithelium; Virus transformed (adenovirus 12-simian virus 40 hybrid virus).	- Do not form tight junctions; - Resemble airway basal epithelial cells, however, do not differentiate; - Poor barrier function.
	Calu-3	Lung adenocarcinoma from submucosal gland serous cells.	- Ability to form tight junctions; - Express mucins and some cilia when grown at ALI; - Reasonable barrier function.
Alveoli	A549	Lung adenocarcinoma.	- Display some characteristics of alveolar epithelial type II (AEC2) cells; - Express metabolizing phase I (cytochrome P450 isoenzymes) and phase II enzymes (transferases); - Do not form tight junctions; - Ability to produce surfactant when grown at ALI; - Poor barrier function.
	NCI-H441	Lung papillary adenocarcinoma.	- Resemble characteristics of both type II pneumocytes and club cells; - Poor barrier function.
	hAELVi	Lentivirus immortalized.	- Morphologically resemblance with alveolar type I (AEC1) cells; - Express high levels of metabolizing enzymes and transporters; - Ability to form tight junctions; - Ability to produce surfactant.

In this regard, George *et al.* (2015) compared different *in vitro* models of human lung epithelial (two bronchial cell lines, NCI-H292 and Calu-3, and one alveolar cell line, A549 cells) monocultures grown onto Transwell® inserts, and evaluated which of those models were most suitable to address the translocation of 50 nm fluorescently labeled silica (SiO_2) NP. These authors found that bronchial Calu-3 cells would be the most relevant model for assessing NP uptake

since, amongst all cells, these were able to form tight junctions, which are essential components for an effective barrier function as occurs *in vivo* (George *et al.*, 2015). Inflammation or immune responses are also very difficult to mimic in such simplistic models since these processes involve a highly coordinated network of many cell types (Joris *et al.*, 2013; Savolainen *et al.*, 2010). Some of these limitations might be overcome by using coculture models that have higher predictive power than monocultures, and more closely mimic human *in vivo* environments (Edmondson *et al.*, 2014). Besides, cocultured cells often display tight and adherent junctions (Kasper *et al.*, 2011). Therefore, these are preferred models to understand (nano)particle mechanistic behavior in more complex biological systems (Costa *et al.*, 2013). To improve the resemblance of complex human airways, coculture models have been developed using airway epithelial cells together with fibroblasts, endothelial cells, airway smooth muscle cells, as well as immune cells such as macrophages, dendritic, and mast cells. These contributed to a better understanding of toxicology and translocation mechanisms of (nano)particles (Bierkandt *et al.*, 2018; Braakhuis *et al.*, 2015).

In **Table 3** some examples of cocultures, representative of different regions of the human lung barrier, used for the evaluation of the toxic effects after (nano)particle exposure are summarized. One of the main regions that researchers try to mimic is the bronchial epithelium since it plays a critical role in biological stress responses after (nano)particle inhalation (Jia *et al.*, 2017). For a closer resemblance to the human lung–blood barrier, bronchial epithelial (*e.g.*, 16HBE14o, Calu-3), macrophage-like cells (*e.g.*, THP-1), and endothelial cells (*e.g.*, HUVEC, EA.hy 926) are commonly combined (**Table 3**). Notwithstanding, nano-sized particle deposition in the respiratory tract primarily occurs in the alveolar region (Londahl *et al.*, 2014). Therefore, alveolar epithelial cells are relevant models for the toxicity of inhalable (nano)particles, particularly in the assessment of particle retention and translocation through these cells (Leibrock *et al.*, 2019). For this purpose, *in vitro* models representative of the alveolar-capillary and/or air-blood barrier are also explored in (nano)toxicity assessments. The air-blood barrier is mainly composed of alveolar epithelial cells and macrophages, that work as a structural and immunological barrier, to external aggressors such as fine and nano-sized particles (Kletting *et al.*, 2018).

Table 3. Pulmonary (nano)particle toxicity studies using coculture models mimicking relevant human lung barriers.

Human lung barrier	Coculture model (cell lines used)	(Nano)particles tested	Main findings	References
Alveolar-capillary barrier	NCI-H441 and ISO-HAS-1.	SiO$_2$ NP (0.6 - 6000 µg/mL; submerged conditions; 4 h exposure + 20 h recovery period).	Release of IL-6 and IL-8 (early inflammatory events); upregulation of apoptosis markers.	Kasper *et al.* (2011)
Air-blood barrier	NCI-H441 and HPMECST1.6R.	CuO and TiO$_2$ NP (25 µg/mL) and PM 10 (22.5 µg/mL) (submerged conditions; 24 h exposure).	Significant modulation of pro-inflammatory (*e.g.*, IL-6 and IL-8) proteins.	Bengalli *et al.* (2013)
Alveolar epithelial barrier	A549, THP-1 and HMC-1.	SiO$_2$-Rhodamine NP (10 mg/L; ALI conditions; 24 h exposure).	Lower levels of ROS and IL-8.	Klein *et al.* (2013)
Alveolar epithelial barrier	A549, MDDC and MDM.	MWCNT (1.15 µg/cm^2; ALI conditions; repeated exposure: 3 days).	No cytotoxicity, alterations in cell morphology, or increase in pro-inflammatory markers.	Chortarea *et al.* (2015)
Lung–blood barrier	Biculture of 16HBE14o and THP-1; triculture of 16HBE14o, THP-1, and HLMVEC.	TiO$_2$, Ag and SiO$_2$ NP (1-243 µg/mL; submerged conditions; 24 h exposure).	Biculture: TiO$_2$ and Ag NP but not pristine SiO$_2$ NP induced cytotoxic effects at relative high doses (83-243 µg/mL); Triculture: no considerable changes were observed.	Smulders *et al.* (2015)
Alveolar epithelial barrier	A549 and THP-1.	CeO$_2$ and TiO$_2$ NP (1-20 µg/cm^2; submerged and ALI conditions; 24 h exposure).	Inflammation, decreased cell viability, and oxidative stress were observed at ALI; more predictive of *in vivo* effects.	Loret *et al.* (2016); Loret *et al.* (2018)
Air epithelial barrier	hAELVi and THP-1.	Ag (7.25 µg) and starch (41.25 µg) NP	Cocultures form functional diffusion	Kletting *et al.* (2018)

Human lung barrier	Coculture model (cell lines used)	(Nano)particles tested	Main findings	References
		(ALI conditions; 24 h exposure).	barriers under ALI conditions.	
Air–blood barrier	Biculture of A549 and EA.hy926; triple coculture of A549, THP-1, and EA.hy926.	Ambient PM 2.5 collected from Shanghai city (China) (20-180 µg/mL; ALI conditions; 24 h exposure).	Stronger inflammatory responses and ICAM-1 and caveolin-1 mRNA expression in triculture than in biculture system.	Wang *et al.* (2019)
Lung epithelial barrier	hAELVi and huAEC.	CeO_2 NP (0.1-200 µg/mL; ALI conditions; 24 h exposure).	CeO_2 NP induced no toxicity, while ZnO NP were toxic at concentrations between 10–50 µg/mL.	Leibrock *et al.* (2019)
Air–blood barrier	A549, THP-1, HMC-1 and EA.hy926.	Ag NM (spherical particles, PVP coated nanowires) (0.05-5 µg/cm^2; ALI conditions; 6 and 24 h exposure).	Increased cytotoxicity; increased mRNA levels of the pro-apoptotic gene CASP7, anti-oxidant enzyme HMOX-1, and pro-inflammatory mediators; induction of the NF-kB nuclear translocation.	Fizesan *et al.* (2019)
Lung–blood barrier	Calu-3, THP-1, and EA.hy926.	Ag NP (coated with tannic acid) (3-30 µg/cm^2; submerged conditions; 24 h exposure).	NP cellular uptake and translocation of Ag NP through the modeled barrier; mild cytotoxicity and reduced secretion of IL-6, IL-8, and TNF-α.	Zhang *et al.* (2019)
Air-blood barrier	A549, EA.hy 926 and THP-1.	Citrate-capped Au (50 mg/mL), $Ag-SiO_2$ (0.50 mg/mL), and CuO (1.5 mg/mL) NP (ALI conditions; 4 h exposure).	Induced more oxidative stress and higher IL-8 levels.	Wang *et al.* (2020)

For the alveolar region, A549 is the most frequently used cell line for the assessment of (nano)particle toxicity. These cells are often used either as

monocultures or in cocultures with other cell lines, for instance, immune cells such as macrophages (Fröhlich, 2018). Alveolar macrophages, in turn, are important regulators of the inflammatory processes in the lung and can ingest nano-sized particles as a clearance defense mechanism (Geiser, 2010). THP-1 cells are a commonly used cell line for investigating *in vitro* the function and regulation of monocytes and macrophages.

Increasing evidence supports the higher relevance of cocultures compared to monocultures (**Table 3**). Kasper *et al.* investigated the cytotoxic and inflammatory responses of monodisperse 30 nm amorphous SiO_2 NP in conventional monocultures *vs* coculture models representative of the alveolar-capillary barrier. Although lower cytotoxic effects in terms of cell viability, membrane integrity, and Trans-Epithelial Electrical Resistance (TEER) were observed in cocultures compared to monocultures, significantly increased levels of inflammatory (*e.g.*, IL-6 and IL-8) and apoptotic markers (*e.g.*, phosphorylation of the p53-protein at Ser15, Ser46 and Ser392) were found. These authors clearly defended that these cocultures were more suitable compared to conventional monocultures to represent alveolar regions of the human lung since they mimic the early inflammatory events that take place in the pulmonary alveoli (Kasper *et al.*, 2011). In addition, Wang *et al.* (2020) assessed the toxicity of aerosolized citrate-capped gold (Au), 15 % silver on silica (Ag-SiO_2) and copper oxide (CuO) NP on triple-cocultures of human alveolar epithelial A549, endothelial EA.hy 926 cells, and THP-1 differentiated macrophages cultured under ALI conditions (4 h; 3.5 mg/m^3). These authors compared these results with monocultures of A549, EA.hy 926, and THP-1 cells and observed that NP induced more oxidative stress (15 % Ag-SiO_2) and higher IL-8 levels (15 % Ag-SiO_2, CuO) in coculture than in A549 monocultures, whereas a similar response in terms of ROS and IL-8 responses after CuO NP exposure was observed between triple cocultures *vs* EA.hy 926 endothelial cells (Wang *et al.*, 2020). Moreover, Loret *et al.* (2016) also compared the effect of poorly soluble cerium oxide (CeO_2) and titanium oxide (TiO_2) NP in monocultures *vs* cocultures of A549 and THP-1 cells and found that cocultures were not only more sensitive than monocultures (Loret *et al.*, 2016) but also more predictive of the *in vivo* pulmonary toxicity of CeO_2 and TiO_2 NP in the rat (Loret *et al.*, 2018). These authors stated that for each dose metric used (mass/alveolar surface or mass/macrophage), the A549 and THP-1 cocultures at ALI conditions were more predictive of *in vivo* effects regarding biological activation levels (Loret *et al.*, 2018). As the number of different cell

lines in the coculture increases, it comes closer to human *in vivo* conditions. For instance, Wang *et al.* (2019) assessed the toxicity mechanisms of urban ambient PM < 2.5 μm (PM 2.5) exposure in three *in vitro* model approaches of increasing complexity: (1) monocultures of A549 alveolar epithelial cells, THP-1 differentiated macrophages, and EA.hy926 endothelial human cells, all seeded in the apical chamber of Transwell® inserts; (2) bicultures of A549 cells and EA.hy926 endothelial cells cultured in the apical chamber and basolateral chamber, respectively; (3) triple cocultures of A549 and THP-1 cells cultured in the apical side, and EA.hy926 endothelial cells seeded in the basolateral chamber. These authors not only observed that PM 2.5 were able to cross through the epithelial barrier and deposited in the endothelium, but also concluded that triple cocultures were a more sensitive and realistic model than the biculture system to assess the impact of these ambient particles on the cardiopulmonary system. Thus, triple cocultures have a greater cellular interaction when compared to the simpler cultures, which better resemble tissues *in vivo* (Wang *et al.*, 2019). Besides, Fizesan *et al.* (2019) used a tetraculture model of the alveolar barrier consisting of A549, THP-1, HMC mast (in the apical compartment), and EA.hy926 endothelial (in the basolateral side) cells for the exposure to aerosolized Ag NM (two spherical shape particles and one PVP-coated Ag nanowire) using a VitroCell® Cloud exposure system. These authors highlighted the capacity of this tetraculture model to secrete both anti- and pro-inflammatory cytokines (IL-12p70, IL-13, IL-1β, IL-2, IL-4, and IL-8) after exposure to Ag NM, reflecting complex biological responses that naturally occur in the native respiratory epithelia (Fizesan *et al.*, 2019). More recently, human alveolar epithelial lentivirus immortalized (hAELVi) cells combined with THP-1 alveolar macrophages (Kletting *et al.*, 2018) or human airway epithelial cells (huAEC) (Leibrock *et al.*, 2019) have been found to form a functional diffusion barrier under ALI conditions, constituting promising models to study the effect of inhalable NP (**Table 3**).

4.2. Advanced respiratory cell cultures

For the assessment of (nano)particle toxicity in the respiratory tract, advanced three-dimensional (3D) *in vitro* tissue models have been emerging as appealing and promising systems over the traditional two-dimensional (2D) cultures and animal experiments. These models contain different cell types in various orientations and numbers that should be organized in a structure that

reflects the tissue of interest (*e.g.*, nasal, bronchiolar, alveolar). Indeed, these models can either mimic organ-relevant normal or diseased state physiology (Jackson *et al.*, 2016). Advanced multi-cellular 3D lung tissue models better reflect cellular interactions observed *in vivo* and, therefore, allow for the investigation of the cellular interplay between different cell types following (nano)particle inhalation exposure. Exposing lung 3D tissue models cultured at ALI to aerosolized particles allows for even more human-relevant and higher resemblance *in vivo* exposure scenarios to (nano)particles (Lacroix *et al.*, 2018). As depicted in **Table 4**, the human respiratory tissue already available in the market, including: MucilAir™ and SmallAir™ from Epithelix Sàrl, EpiAirway™ and EpiAlveolar™ from MatTek Corporation, and Micro-Lung™ and Metabo-Lung™ from Cardiff University. Commercial tissue models provided by companies such as MatTek and Epithelix Sàrl, are established from biopsies of individuals either healthy or with respiratory diseases. These models are highly differentiated, mucus-producing and ciliated cultures, with well-developed tight junctions and good epithelial resistance that are able to maintain their characteristics over long periods of time (up to several months), which is a major advantage over other cellular models. Micro-Lung™ and Metabo-Lung™ from Cardiff University, on the other hand, are not commercially available (Clippinger *et al.*, 2018). The Micro-Lung™ model uses normal human bronchial epithelial (NHBE) cells isolated from surgical patients and post-mortem donors (Prytherch *et al.*, 2015), while the Metabo-Lung™ takes advantage of NHBE cells cocultured with human primary hepatocytes for assessing the role of metabolism (Prytherch *et al.*, 2011). Although these models have a great potential for evaluating (nano)particle toxicity, to the best of our knowledge there are no studies in the literature yet. There are also in the market advanced 3D lung cancer models such as OncoCilAir™, which combines a functional reconstituted human airway epithelium, human lung fibroblasts, and lung adenocarcinoma cells (Benainous *et al.*, 2018), that have been applied for the study of the controlled and targeted delivery of nanotherapeutics. Notwithstanding, despite all the efforts in the development of advanced and robust 3D *in vitro* cell cultures, as reliable alternatives tools to animal testing, these have not been approved nor validated for the *in vitro* testing of any (nano)particles or NM so far (Pfuhler *et al.*, 2020).

Table 4. Advanced 3D *in vitro* models of human respiratory tissues.

Model		Features
MucilAir™ (Epithelix Sàrs)	nasal, tracheal, or bronchial epithelial model.	- Isolated from human biopsies of the nasal cavity, trachea, and bronchi; - Constituted by basal, goblet, and ciliated cells; - Under ALI conditions display tight junctions, cilia beating and mucus production, cytokines, chemokines, and metalloproteinases secretion, and expression of specific respiratory epithelia cytochromes (*e.g.*, P450); - Effective barrier model for the assessment of the permeability/absorption of several compounds across the human airway epithelium.
SmallAir™ (Epithelix Sàrs)	small airway model.	- Isolated from the distal lung; - Constituted by epithelial cells, a large number of club cells, and fewer goblet and ciliated cells; - Presents a much thinner epithelium (compared to MucilAir™).
EpiAirway™ (MatTek Corporation)	tracheal/bronchial epithelium model.	- Derived from normal tracheal and bronchial epithelial cells; - Constituted by mucus-producing goblet cells, ciliated cells with actively beating cilia, basal cells, and club cells (club).
EpiAlveolar™ (MatTek Corporation)	lower respiratory tract tissue model.	- Constituted by alveolar epithelial cells and monocyte-derived macrophages (apical side) and pulmonary endothelial cells (basolateral side).
Micro-Lung™ (Cardiff University)	bronchial epithelium model.	- Isolated from surgical patients and post-mortem donors; - Constituted by normal human bronchial epithelial (NHBE) cells, basal, serous, club, goblet, and ciliated cells.
Metabo-Lung™ (Cardiff University)	lung-liver model.	- Coculture of NHBE cells with primary human hepatocytes, which allows the biotransformation of inhaled toxicants in an *in vivo*-like manner.

Table 5 presents an overview of existing *in vitro* studies on the pulmonary toxicity of (nano)particles using the advanced 3D lung *in vitro* models from Epithelix Sàrl and MatTek Corporation. In the literature, the majority of studies performed so far were done in MucilAir™ human bronchial epithelial culture models. In this regard, Firke Kuper *et al.* (2015) comparatively investigated the toxicity of aggregated CeO_2 NP in MucilAir™ bronchial cultures and in BEAS-2B and A549 cell lines. In the MucilAir™ cultures, no signs of marked toxicity were observed most likely due to the presence of the mucociliary apparatus that prevented NP from reaching the respiratory epithelial cells. On the other hand, these authors found a clear dose-dependent genotoxicity on BEAS-2B and A549 cells after 24 h exposure to CeO_2 NP (33-333 µg/cm^2) (Frieke

Kuper *et al.*, 2015). Di Cristo *et al.* also reported no signs of morphological alterations or cytotoxic effects after repeated exposure of MucilAir™ cultures for 12 weeks, 5 days per week to SiO_2 NP (0.90 to 55 µg/cm^2), which they also attributed to the mucociliary clearance (Di Cristo *et al.*, 2020).

As previously mentioned, MucilAir™ cultures can be established from diseased tissues, which offers the possibility to investigate the effects of NP in primary cultures from individuals with respiratory diseases. In this context, Chortarea and colleagues evaluated the pulmonary toxicity of occupational relevant doses (10 µg/cm^2 for 5 weeks/5 days per week) of multiwalled carbon nanotubes (MWCNT) in MucilAir™ bronchial cultures from healthy and asthmatic donors. Although no cytotoxicity or morphological changes were observed, chronic MWCNT exposure induced a pro-inflammatory and oxidative stress response in both types of cultures, accompanied by elevated cilia beating frequency and alteration of the mucociliary clearance. However, the magnitude and duration of the observed effects were higher in the asthmatic compared to healthy cells, indicating that individuals with asthma may be more susceptible to adverse effects from chronic MWCNT exposure (Chortarea *et al.*, 2017). Donor variability is an important aspect that should be considered when designing and interpreting data of primary culture-based studies. In this regard, Kooter *et al.* (2017) examined the toxicity of aerosolized CuO NP bronchial airway MucilAir™ cultures from four donors. Despite no major cytotoxicity, an increase in IL-6 and Monocyte Chemoattractant Protein (MCP)-1 release after 24 h of exposure was observed, being the MCP-1 release levels different among donors (Kooter *et al.*, 2017). Dankers *et al.* (2018) investigated the pro-inflammatory potential of six metal oxide NP (CeO_2, Mn_2O_3, CuO, ZnO, Co_3O_4, and WO_3; 27–108 µg/mL) in MucilAir™ cultures and dendritic cells (DC). In MucilAir™ cultures, higher secretion of IL-6, IL-8, and MCP-1 pro-inflammatory cytokines was found after 24 h of exposure to CuO NP droplets, while only exposure (48 h) to Mn_2O_3 NP upregulated all the evaluated DC maturation biomarkers (HLA-DR, CD80, CD83, and CD86). Interestingly, these authors addressed the potential interaction between epithelial cells and DC by exposing the latter to the MucilAir™-exposed cultures media, and found that only Mn_2O_3 NP triggered DC maturation, suggesting the process is not dependent on epithelial cells stimulation (Dankers *et al.*, 2018).

Recently, these models have been explored to assess the toxicity of occupationally relevant NP. In this regard, George *et al.* evaluated the toxicity of

thermonuclear fusion released-like milled tungsten (W) NP, tungstate (WO_4^{2-}) and tungsten carbide cobalt particles alloy (WC-Co), in MucilAir™ cultures exposed for 24 h to the particles, whose effects were monitored up to 28 days after exposure. These occupational NP had a minor impact in MucilAir™ bronchial cultures since they did not induce significant alterations on their metabolic activity and viability; however, a decrease in the barrier integrity and a transient increase of IL-8 levels at 24 and 96 h after initial exposure were detected (George *et al.*, 2019). Recently, Bessa *et al.* (2021) also assessed the toxicity of two engineered NP [ENP; antimony-tin oxide (ATO) and zirconium oxide (ZrO_2) NP] used as input materials in advanced ceramics, and two fractions [fine <2.5 μm (PGFP) and nano-sized <0.2 μm (PGNP)] of particles released during thermal spraying of ceramic coatings onto metal surfaces, in MucilAir™ cells under ALI conditions. These cultures were exposed for three consecutive days to the aerosolized particles, and cyto-, genotoxicity, and pro-inflammatory responses were assessed. The obtained results showed that PGFP and PGNP exhibited higher toxicity than ENP in mass per area unit, although the presence of mucociliary apparatus in the advanced 3D *in vitro* bronchial cultures seemed to substantially attenuate the toxic effects (Bessa *et al.*, 2021a).

Fewer studies exist on the effects of NP in human small airway models. Based on previous *in vivo* findings that showed Ag NP deposition in the small airway epithelium following inhalation (Seiffert *et al.*, 2016), Guo *et al.* (2018) investigated the effects of the same Ag NP in reconstituted 3D primary human small airway epithelial cell cultures (SmallAir™) under ALI conditions using the same *in vivo* doses. The data obtained showed DNA damage, cell cycle changes, and oxidative stress in response to the aerosolized Ag NP. They also found a good correlation between *in vivo – in vitro* transcriptional changes in immune-related genes, that were of similar magnitude in response to Ag in the ionic (Ag^+) or in the nanoform (Guo *et al.*, 2018). More recently, Barasova *et al.* (2020) evaluated the effects of repeated exposure over 3 weeks to occupational doses (1–30 μg/cm^2) of two MWCNT- Mitsui-7 and Nanocyl-, in EpiAlveolar™ cultures constituted by human alveolar epithelial cells, pulmonary endothelial cells, and fibroblasts. In parallel, EpiAlveolar™ were cocultured with human monocyte-derived macrophages (MDM) to assess their potential role in the pro-inflammatory and profibrotic response. These authors found that Nanocyl induced less pronounced toxicity than Mitsui-7 in EpiAlveolar™ cultures, whereas

EpiAlveolar™ + MDM cocultures showed pro-inflammatory responses at later time points compared to EpiAlveolar™ cultures (Barosova *et al.*, 2020).

Table 5. Overview of the existing pulmonary (nano)particle toxicity studies using advanced 3D *in vitro* models.

Pulmonary 3D model	(Nano)particles tested	Experimental design	Biological endpoints assessed	Main findings	References
MucilAir™ (Epithelix Sàrs)	CeO$_2$ NP	ALI (droplet) exposure; responses assessed after 3, 24, 48 h.	Cytotoxicity (TEER, LDH release); Inflammation (IL-8, MCP-1, sICAM-1, IL-1α, TNFα); Genotoxicity (comet assay and HO-1 expression).	No major toxic effects were observed.	Frieke Kuper *et al.* (2015)
	MWCNT	Cultures from healthy and asthmatic donors; ALI exposure (ALICE system); cells exposed 5 weeks/5 days per week; responses assessed at weeks 1, 3, and 5.	Cell morphology Cytotoxicity (LDH release); Inflammation (IL-8, IL-6, IP-10 and TGF-β); Oxidative Stress (HMOX-1 and SOD-2 gene expression).	Increased cilia beating frequency; alterations in the mucociliary clearance, no cytotoxicity or morphological changes, (pro)inflammatory and oxidative stress responses after chronic exposure.	Chortarea *et al.* (2017)
	CuO NP	ALI exposure (Vitrocell® system); Cells exposed for 2 days (two periods of 1 h/day); responses assessed 24 h after exposure.	Cytotoxicity (LDH release); Gene expression of inflammatory markers (MCP-1, IL-8, and IL-6).	No major cytotoxicity; Increased expression of inflammation markers (MCP-1 and IL-6).	Kooter *et al.* (2017)
	CeO$_2$, Mn$_2$O$_3$, CuO, ZnO, Co$_3$O$_4$ and WO$_3$ NP	ALI (droplet) exposure (MucilAir cultures: 24 h; DC cultures: 48 h); responses assessed after 24 h (MucilAir) and 48 h (DC).	Cytotoxicity (LDH release); Inflammation (MCP-1, IL-6, IL-8); DC maturation surface markers (HLA-DR, CD80, CD83, and CD86)	MucilAir™ cultures: inflammatory responses (increased levels of IL-6, IL-8, and MCP-1) after CuO NP exposure; DC cultures: Mn$_2$O$_3$ NP upregulated all the assessed maturation biomarkers.	Dankers *et al.* (2018)
	Milled W NP	ALI exposure; single 24 h exposure; responses	Cell viability (Trypan blue); Metabolic activity (resazurin assay);	Decrease in barrier integrity; no effect on	George *et al.* (2019)

Pulmonary 3D model	(Nano)particles tested	Experimental design	Biological endpoints assessed	Main findings	References
		assessed following exposure and up to 28 days.	Inflammation (IL-8).	metabolic activity or cell viability; transient increase in IL-8 secretion at 24 and 96 h after initial exposure.	
	SiO₂ NP	ALI (droplet) exposure (Vitrocell® Cloud system); daily exposure for 5 times per week, up to 12 weeks.	Cell viability (Alamar Blue); Barrier integrity (TEER).	No changes in the barrier integrity; no cytotoxic effects.	Di Cristo *et al.* (2020)
	ATO and ZrO₂ NP; PGFP (<2.5 µm) and PGNP (0.200 µm) particle fractions derived from high velocity oxy-fuel spraying.	ALI (droplet) exposure (Vitrocell® Cloud system); responses assessed after 24, 48, and 72 h.	Cytotoxicity (LDH release and WST-1 metabolic activity); Genotoxicity (Comet assay); Inflammation (IL-8 and MCP-1).	Mild cytotoxicity at early time points (24 h), cellular recovery at late time points (72 h), and no major genotoxicity for ATO and ZrO₂ NP; PGFP affected cell viability, while PGNP caused increased oxidative DNA damage.	Bessa *et al.* (2021a)
SmallAir™ (Epithelix Sàrs)	Ag NP	ALI exposure (Cultex® RFS system); 3 exposure times (7, 20, and 60 min); responses assessed at 6 or 24 h.	Cytotoxicity (lactate and LDH release); Alterations in immune-related gene expression (real-time PCR analysis for mRNA gene expression).	Minimal cytotoxicity and significant upregulation in the expression of inflammatory-related genes (*e.g.* IL1R2).	Guo *et al.* (2018)
EpiAlveolar™ (MatTek Corporation)	MWCNT	ALI (droplet) exposure (Vitrocell® Cloud system); repeated exposure (3 weeks).	Cytotoxicity (LDH release); Inflammation (IL-1β, TNF-α and IL-8); Profibrotic response (TGF-β, fibronectin, and COL1 release).	Barrier integrity and release of pro-inflammatory and profibrotic markers.	Barosova *et al.* (2020)

ALI: Air-liquid interface; ALICE: Air-liquid interface cell exposure; ATO: Antimony-tin oxide; COL1: Collagen 1; DC: Dendritic cells; LDH: Lactate dehydrogenase; IL1R2: Interleukin 1 Receptor Type 2; MWCNT: Multiwalled carbon nanotubes; PCR: Polymerase chain reaction; PGFP: Process-generated fine particles; PGNP: Process-generated nanoparticles; RFS: Radial flow system; TEER: Transepithelial electrical resistance

4.3. Lung Spheroids/Organoids

Spheroids and organoids are 3D structures composed of multiple cells that cluster together into self-organized aggregates. Both terms are often used interchangeably in the literature, though some differences exist between the two. Spheroids are simple spherical and scaffold-free cellular models, which are typically obtained from mature single-cell suspensions (Zanoni *et al.*, 2020). On the other hand, organoids are complex clusters derived from organ-specific cells that self-assemble within a scaffold such as gels made of a complex mixture of different extracellular matrix (ECM) proteins, including laminin, fibronectin, collagen, and heparin sulphate (*e.g.*, Matrigel), though not all organoids are formed within an ECM (Gkatzis *et al.*, 2018). Organoids may be generated from adult or embryonic stem cells (Hofer *et al.*, 2021). One curious aspect of these particular 3D structures is they can be maintained for prolonged periods of time without karyotype changes (Kar *et al.*, 2021). In the respiratory field, organoids are valuable models to mimic the complex environment of the respiratory mucosa and the relationship among different cell types. Indeed, human lung organoids have been successfully established from epithelial progenitor cells derived from embryonic (Miller *et al.*, 2018) or adult lung (Tan *et al.*, 2017; Zacharias *et al.*, 2018), and from human pluripotent stem cells (hPSC) (Chen *et al.*, 2017; Gotoh *et al.*, 2014; Yamamoto *et al.*, 2017). The establishment of alveolar organoids from cocultures of epithelial progenitor cells with mesenchymal or endothelial cells or cocultures of mesenchymal cells with fetal lung tissue or hPSC (Wilkinson *et al.*, 2016) has been already reported.

While lung spheroids/organoids are good models to investigate pulmonary injury and repair mechanisms, their 3D spherical nature and matrix components represent technical challenges for application under ALI conditions (Hiemstra *et al.*, 2018). Another limitation is that lung movements during the gas exchange are difficult to simulate in lung spheroid/organoid models (Li *et al.*, 2020). Notwithstanding, human lung spheroids or organoids have been used in the fields of regenerative medicine, lung disease modeling, and drug efficacy testing (Archer *et al.*, 2021; Cores *et al.*, 2020; Tan *et al.*, 2017). Organotypic lung cultures are also valuable models for toxicological studies, namely for nanotoxicity assessment (Prasad *et al.*, 2021).

So far, very few studies have been carried out for NP testing in human-derived lung spheroids/organoids. In this regard, Sambale *et al.* (2015)

comparatively investigated the effects of ZnO and TiO$_2$ NP in human alveolar epithelial A549 cells either in the traditional 2D monolayer cultures or in 3D spheroids. Interestingly, spheroids NP exposure was conducted after or during their formation. Overall, A549 cells displayed lower resistance to ZnO NP induced toxicity (up to 100 µg/mL) in the form of spheroids compared to 2D monolayers, while exposure to TiO$_2$ NP (up to 150 µg/mL) was non-toxic to 2D cultures but caused a minor decrease in A549 spheroids viability and affected spheroid formation, with several smaller spheroids being formed instead of a single larger spheroid (Sambale et al., 2015). On the other hand, Kabadi *et al.* (2019) investigated the effects of different types of carbon-based materials (MWCNT, M120 carbon black NP, or crocidolite asbestos fibers; 0.5–10 µg/mL) in scaffold-free 3D spheroids established from IMR-90 human lung fibroblasts, BEAS-2B lung bronchial epithelial and THP-1 monocytic cells. MWCNT were the most cytotoxic to the spheroid-like triple cocultures by day 7, causing more than 40 % decrease in cell viability at the highest tested concentration. Moreover, gene expression analysis carried out after 4 and 7 days of exposure to the tested materials revealed significant upregulation of ECM components (collagens and decorin), cytokines (*e.g.*, IL-1β and IL-6), growth factors, and matrix metalloproteases (MMP) related genes (Kabadi et al., 2019). More recently, Liu *et al.* (2021) assessed the toxicity of nano-carbon black and nano-SiO$_2$ in alveolar type 2 epithelial cell-like cells (ATL), either in 2D monolayers or 3D organoids assembled in Matrigel scaffolds, which were previously differentiated from hPSC cells. Herein, the toxicity of the nano-carbon black was evaluated in ATL 2D monolayers, while the nano-SiO$_2$ effects were assessed in ATL 3D organoids. Nano-carbon black (1-100 ng/mL) did not induce oxidative stress in ATL 2D cultures nor decreased cell viability after 6 h and 7 days of exposure, respectively. As for nano-SiO$_2$ (1-100 ng/mL), a significant increase in ROS generation was observed in ATL 3D organoids at 6 h after exposure, although did not affect organoid viability neither the gene expression of the investigated markers at 14 days after exposure (Liu *et al.*, 2021).

4.4. Lung-on-a-chip

Lately, mechanically active microdevices combining the capability of cell culture models with microfluidics have been developed to reconstitute tissue-tissue interfaces crucial to resemble organ function. These are named "organ-on-a-chip" and are gaining more and more power in drug screening and toxicology applications as low-cost alternatives to animal testing and clinical studies. The first

lung-on-a-chip was reported by Huh and colleagues, who developed a biomimetic microsystem that replicates key structural, functional, and mechanical properties of the human alveolar-capillary interface (Huh *et al.*, 2010). This model consists of a microfluidic system with two microchannels separated by a thin, flexible and porous membrane coated with fibronectin or collagen to resemble the ECM, and human alveolar epithelial and pulmonary microvascular endothelial cells cultured on opposite sides of the membrane (**Figure 3**). To simulate the *in vivo* environment of the alveolar space and gas exchange conditions, epithelial cells were exposed at the ALI. Moreover, this biologically inspired human breathing lung-on-a-chip microdevice has been successfully used to evaluate SiO_2 NP transport across this *in vitro* alveolar-capillary barrier, intracellular ROS production, and inflammatory responses (Huh *et al.*, 2010). After exposure to SiO_2 NP aerosols it was observed: (1) high levels of intercellular adhesion molecule (ICAM)-1 expression from the underlying endothelium cells; (2) increased endothelial capture of circulating neutrophils, promotion of their migration across the permeable membrane (tissue-tissue interface), and accumulation onto epithelial surface; (3) breathing-induced physiological mechanical forces; (4) increased absorption of SiO_2 NP from the airspace to the microvascular channel; (5) accentuated pro-inflammatory activities and development of acute lung inflammation; and (6) a steady increase in ROS production (Huh *et al.*, 2010; Huh, 2015).
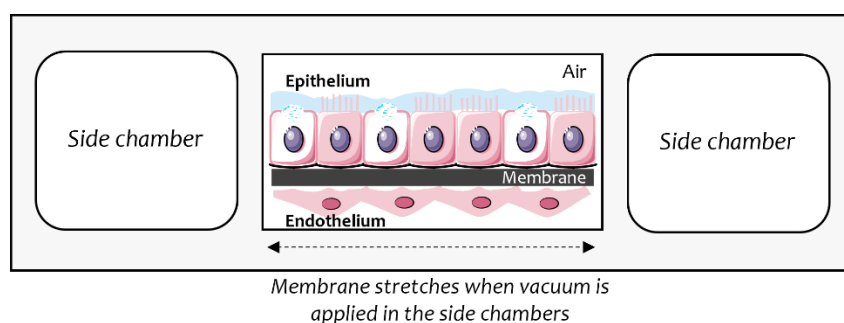

Membrane stretches when vacuum is
applied in the side chambers

Figure 3. Microfabricated human breathing-inspired lung-on-a-chip microfluidic device [Adapted from Huh *et al.* (2010)]. The device simulates physiological breathing movements by applying a vacuum into the side chambers causing a stretch of the membrane. This illustration was created including images obtained from Smart Servier Medical Art (www.smart.servier.com) CC BY 3.0.

Meanwhile, many other lung-on-a-chip devices emerged, as reported by Punde *et al.* (2015), Stucki *et al.* (2015), Blume *et al.* (2015), Rahimi *et al.* (2016), Yang *et al.* (2018), among other research groups. However, nanotoxicity studies using lung-on-a-chip models are still scarce. Recently, Zhang *et al.* (2018)

assembled a lung-on-a-chip model, reproducing the alveolar-capillary barrier, using three parallel channels: (1) alveolar channel with human pulmonary alveolar epithelial cells (HPAEpiC) to embody the alveolar side of the alveolar-capillary barrier; (2) vessel channel with human endothelial cells (HUVEC) to represent the capillaries, and (3) ECM channel with Matrigel membrane sandwiching between the alveolar and vessel channels. In this study, epithelial cells were exposed for 24 h to TiO_2 NP and zinc oxide (ZnO) NP that were injected into the alveolar channel. Both NP induced dose-dependent toxicity on the epithelial and endothelial cells, including ROS generation and apoptosis, however, ZnO NP were more toxic than TiO_2 NP. According to these authors, this lung-on-a-chip model was demonstrated to be a versatile model for assessing the NP induced pulmonary injury (Zhang *et al.*, 2018). Moreover, Meghani and colleagues designed an alveolus-epithelium-on-a-chip device with in-built sensors that allow the monitorization of pH-responsive ZnO quantum dots (QD)-loaded human serum albumin (HSA) NP. This model comprised lung cancer cells and stromal cells such as fibroblasts along with a collagen ECM. Results showed a significant internalization of the NP under the coculture conditions within this newly developed lung-on-a-chip model (Meghani *et al.*, 2020).

4.4. Exposure conditions: submerged vs air-liquid interface

Most *in vitro* studies done so far for assessing the pulmonary toxicity of (nano)particles were performed using thin (mono)layers of lung cells cultured under submerged conditions, where (nano)particles to be tested were added directly into the cell culture medium (Lacroix *et al.*, 2018). NP dispersion in complex media such as cell culture medium is likely to change their original physicochemical properties (Kendall *et al.*, 2015; Moore *et al.*, 2015; Moore *et al.*, 2019), which may influence particle-cell and cell-cell interactions, thus strongly affecting lung cells' responses. Indeed, the interaction of particles with cell culture media components often leads to the formation of a protein corona (Monopoli *et al.*, 2011), which together with media salts and osmolarity may affect particle stability and make particles more prone to aggregation and/or agglomeration (Falahati *et al.*, 2019; Teeguarden *et al.*, 2007). Another major limitation of submerged cultures is that molecular and cellular features such as expression of key transporters and proteins, cilia formation, mucus, and surfactant secretion may be affected (Acosta *et al.*, 2016). At the same time, dose deposition is hard to control as, depending on their density, particles might remain in suspension

and/or interact with the material (*e.g.*, plastic) where cells were seeded, which will have an impact on the actual dose that cells are exposed to (Lenz *et al.*, 2013). For all the aforementioned, it is widely accepted that *in vitro* cell exposure to (nano)particles under the classic submerged conditions does not properly and effectively mimic the cellular and physiological features observed in inhalation exposures *in vivo*, and consequently, the responses observed might also be different from the ones occurring in the *in vivo* situation (Blank *et al.*, 2009; Lacroix *et al.*, 2018). To overcome the major drawbacks associated with submerged cultures, innovative approaches have emerged over the past years to more accurately control dosimetry and deposition (Polk *et al.*, 2016; Secondo *et al.*, 2017).

The human airways are not fully covered with pulmonary fluid but rather under ALI conditions, to allow efficient gas exchange between cells and the environment. Cells from the human respiratory system (*e.g.*, nasal or bronchial epithelial cells) cultured under ALI conditions become properly polarized and might secrete surfactant, improving the resemblance to the *in vivo* situation, which is not possible to achieve in fully immersed environments (Barosova *et al.*, 2020). So, *in vitro* exposure systems able to deliver aerosolized (nano)particles to the surface of cells cultured under ALI conditions constitute a more reliable alternative for conducting pulmonary nanotoxicity studies. **Table 6** depicts the existing aerosol exposure systems available for (nano)particle aerosol generation and cell exposure at ALI. The normal setup generally involves an aerosol generator from powders/dusts or liquid droplets, connections, and peripherals to an exposure chamber with controlled temperature and humidity conditions. Compared to submerged exposures, particle aerosolization and exposure at ALI, where the apical liquid in cultured cells is negligible, seem to have a lower impact on particle original properties (Fujitani *et al.*, 2015; Polk *et al.*, 2016). However, these exposure systems require more expertise to set up and operate, being considerably more expensive than the traditional submerged studies (Braakhuis *et al.*, 2015). Some of the available systems are equipped with a quartz crystal microbalance (QCM) for monitoring dose deposition in the nanogram range, which is a great advantage for controlling deposition over time (Ding *et al.*, 2020). Notwithstanding, some systems present some technical limitations. In systems where particle deposition is based on sedimentation and gravitation, such as the Vitrocell® and CULTEX® systems, the maximum deposited doses achieved remain generally lower than the levels found in the ambient (Bierkandt *et al.*, 2018).

Table 6. Aerosol generation and exposure systems for cells cultured under air-liquid interface (ALI) conditions.

Aerosol exposure system	Developer/ Manufacturer	Features
Minucell	Tippe *et al.* (2002)	- Uses direct flow allowing a greater particle deposition onto cells.
Electrostatic Aerosol *in vitro* Exposure system (EAVES)	de Bruijne *et al.* (2009)	- Uses electrostatic precipitation for particle deposition onto cells.
Air-Liquid Interface Cell Exposure (ALICE)	Lenz *et al.* (2009)	- Uses dense cloud of droplets generated and transported through an exposure chamber at a specific flow rate, allowing uniform and efficient depositions of particle aerosols; - Considered an optimal system to screen NP' toxicity, particularly in pharmaceutical industries where suspension-based aerosolized NP are used in the drug formulations (Duret *et al.*, 2012).
NAVETTA	Frijns *et al.* (2017)	- Applies an electrostatic field to improve particle deposition efficiency, allowing a much higher deposition rate when compared to other ALI setups.
Nano Aerosol Chamber *In vitro* Toxicity (NACIVT)	Jeannet *et al.* (2015)	- Uses direct flow in a continuous air stream, enabling a more efficient and uniform deposition of airborne (nano)particles onto cells; - Computer-controlled temperature and humidity environment, which allows long term exposures and helps to prevent cellular stress during exposure; - Compact and easy to transport; - High throughput system; - Commercially available.
MicroSprayer® Aerosolizer	Penn-Century™ (2021)	- Commercially available manual aerosolizer; - Model IA-1C: requires a very small number of NP to reach the target dose; - Leads to the formation of droplets, affecting the homogeneous deposition of particles onto cells; - Requires high flow rates for effective particle deposition, which might damage cells by shear stress.
CULTEX®	Aufderheide *et al.* (1999)	- Uses electrostatic precipitation for NP deposition onto cells, ensuring close contact between the tested aerosol and cells without any interference of the culture medium; - Available as Radial Flow System (RFS) and RFS Compact versions;

Aerosol exposure system	Developer/ Manufacturer	Features
		- Popular system among the commercially available.
Vitrocell®	Aufderheide *et al.* (2004)	- Modified CULTEX® system; - Three available setups: Cloud® system, powder chamber, and automated exposure station; - Offers exposure chambers for 6, 12, and 24 well-plates; - Most used among the commercially available.
XposeALI®	Inhalation Sciences (2021)	- Models adapted to aerosolize dry powders; - Commercially available.

Particle-specific efficacy of deposition and deposition rate of these aerosol generator devices have considerable variations (*e.g.*, XposeALI®). In addition, a large loading of particles and/or long-term exposure may also be problematic as particle physicochemical characteristics (*e.g.*, ALICE system) might be affected and particle agglomeration and/or aggregation might occur (Upadhyay *et al.*, 2018). Most of the available systems only allow short, single-exposure experiments through a nano aerosol deposition chamber for efficient and quantitative deposition of nanoparticles, whereas the nano aerosol chamber *in vitro* toxicity (NACIVT) system allows a continuous air-stream (Clippinger *et al.*, 2016).

Several studies have already addressed (nano)particles toxicity in human respiratory cells under submerged *vs* ALI conditions. The great majority of the studies support the view that ALI cultures seem to be more resistant than submerged cultures to the effects induced by (nano)particles *in vitro* exposure. In this regard, Lenz *et al.* (2013) compared the cellular responses to ZnO NP (0.7 and 2.5 μg/cm^2; immediately and 2 h after exposure) in terms of oxidative stress [(heme oxygenase 1 (HMOX1), SOD-2 and glutamate-cysteine synthetase, catalytic subunit (GCS) transcription markers expression] and pro-inflammatory (IL-8, IL-6, and GM-CSF levels) responses in human alveolar epithelial A549 cells cultured under ALI or submerged conditions. Overall, a similar response to ZnO NP was observed in A549 cells exposed under both conditions. However, while no significant changes in oxidative stress were observed for most markers in both cultures, lower levels of pro-inflammatory responses were detected in A549 cells exposed at ALI (Lenz *et al.*, 2013). Ghio and colleagues also compared the impact of ambient air pollution particles, collected in North Carolina outside the United States Environmental

Protection Agency (EPA) Human Studies Facility, under submerged and ALI conditions on normal human bronchial epithelial (NHBE) cells by assessing pro-inflammatory (IL-8 and IL-6 levels) and oxidative stress (HOX1 and COX2 expression) markers up to 21 days. These authors showed that in NHBE cells exposed at ALI, the tested particles induced reduced biological effects compared to submerged cultures, likely due to the higher oxygen availability in ALI cultures (Ghio *et al.*, 2013).

The comparison of the biological responses of A549 cells under ALI (using a Vitrocell® system equipped with electrodes to enhance deposition by applying an electrostatic field, named ALIDA) or submerged conditions was assessed after exposure to two amorphous SiO_2 NP produced by different synthesis methods (Aerosil200 produced by flame synthesis, and 50 nm SiO_2 NP produced by the Stöber method). For ALI conditions, the attained deposited doses were 52 µg/cm^2 and 117 µg/cm^2, for Aerosil200 and 50 nm SiO_2 NP, respectively, whereas in submerged conditions both NP were tested as liquid suspensions of 15.6 µg/cm^2. The amorphous SiO_2 NP aerosols were generated by two different methods: electrospray and atomizer. The electrospray method was only applicable for 50 nm SiO_2 NP since it allowed the generation of an aerosol containing monodisperse NP. However, the deposited mass and surface dose of the particles was too low to induce cellular responses. On the other hand, the atomizer was applicable for both types of amorphous SiO_2 particles; nevertheless, deposition of particle aggregates was observed, and therefore higher mass and surface doses were attained, which led to the induction of significant biological effects on lung cells. Overall, both types of amorphous SiO_2 NP induced similar cellular responses in both culture systems, although submerged exposure to 50 nm SiO_2 NP triggered stronger responses at much lower doses (Panas *et al.*, 2014).

ALI exposure seems to be a particularly suitable approach when evaluating the toxicity of poorly soluble NP. In this regard, Loret *et al.* (2016) evaluated the biological effects of four poorly soluble NP - one CeO_2 NP and three TiO_2 NP -, in A549 alveolar cell monocultures or in coculture with alveolar macrophages (THP-1) using different exposure methods, i.e. the cultures were exposed for 24 h to the aerosolized NP in inserts or to the NP liquid suspensions either in inserts or plates. They found that the final deposited doses were reached within 3 h in the inserts, either under ALI or submerged conditions, and within 24 h in the plates. While cocultures were more sensitive than monocultures, decreased cell viability, oxidative stress and inflammatory responses were observed at lower doses in

cultures exposed under ALI compared to the conventional submerged conditions (Loret *et al.*, 2016).

Recently, Medina-Reyes *et al.* (2020) compared the cytototoxicity, genotoxicity and oxidative stress in A549 cells exposed to TiO_2 nanofibers and NP under ALI (using a Vitrocell® Cloud system; 2 and 10 µg/cm^2 for 1 or 4 h and maintained in culture for 24, 48 and 72 h) and submerged conditions (1-50 µg/cm^2 for 24, 48 and 72 h). Overall, these authors found that cytotoxicity of TiO_2 nanofibers and NP was similar in ALI and submerged cultures, although uptake was higher in submerged than in ALI cultures. However, TiO_2 nanofibers induced higher DNA double-strand breaks (DSB) in A549 cultured under ALI than in submerged conditions, while TiO_2 NP induced similar levels of DSB in both culture conditions (Medina-Reyes *et al.*, 2020). Diabaté *et al.* (2021) evaluated the *in vitro* toxicity of CeO_2 and TiO_2 NP in A549 monocultures cultured under ALI conditions *vs* cocultures of A549 with THP-1 macrophages under submerged conditions. These authors observed that cells under ALI conditions were more sensitive to NP-induced toxicity when compared to those cultured under submerged conditions, i.e., lower doses of deposited NP (0.2 and 1 µg/cm^2) were sufficient to induce adverse outcomes at ALI, as also documented in rodent experiments (Diabaté *et al.*, 2021). Similar results were observed in a study by Bessa *et al.* (2021), where more pronounced cytotoxicity in A549 cells exposed to aerosolized ATO, CeO_2, and ZrO_2 NP using a VitroCell® workstation system was observed up to 4 h exposure when compared to A549 submerged cells exposed 24 h to the same NP as a liquid suspension. Overall, A549 cells under ALI conditions were more vulnerable to NP aerosols exposure. For instance, although an increased primary DNA damage regardless of the exposure mode was observed, A549 cells seemed to be more sensitive to the genotoxic effects of ZrO_2 NP aerosols than to the same NP in a liquid medium (Bessa *et al.*, 2021b).

5. Conclusions and future perspectives

Over the years, inhalation toxicology studies in rodents have been useful to assess (nano)particle hazard and identify important toxic properties. However, many of these studies lead to inconclusive results making extrapolations to humans questionable and dubious. Beyond that, these studies are moderate to severely distressful to animals, raising ethical and welfare concerns. *In vitro* models, on the other hand, offer highly controlled cellular environments that can be easily scaled and replicated and allow the evaluation of the (nano)particle

biological hazards in real-time. This is where the *in vitro* respiratory models stand out as a promising alternative to animal testing, in particular those that successfully recapitulate the complexity and physiology of the human respiratory system. An ideal strategy should rely on conventional *in vitro* systems as initial screening tools and moving on to advanced *in vitro* models, using accurate exposure systems and dosimetry strategies closer to real (nano)particle inhalation scenarios. Exploring the intricacies behind the complexity and sensitivity of the *in vitro* cell models, as well as the exposure system, is essential to perceive the magnitude of the toxicity response to (nano)particle exposure. Therefore, more efforts are urgently needed to validate and approve these *in vitro* methods.

References

Acosta, M. F., Muralidharan, P., Meenach, S. A., Hayes, D, S, M. B., & Mansour, H. M. (2016). In Vitro Pulmonary Cell Culture in Pharmaceutical Inhalation Aerosol Delivery: 2-D, 3-D, and In Situ Bioimpactor Models. *Curr Pharm Des*, *22*(17), 2522-2531. https://doi.org/10.2174/1381612822666160202142104

Andujar, P., Lanone, S., Brochard, P., & Boczkowski, J. (2011). Respiratory effects of manufactured nanoparticles. *Rev Mal Respir*, *28*(8), e66-75. https://doi.org/10.1016/j.rmr.2011.09.008

Anjilvel, S., & Asgharian, B. (1995). A Multiple-Path Model of Particle Deposition in the Rat Lung. *Fundamental and Applied Toxicology*, *28*(1), 41-50. https://doi.org/10.1006/faat.1995.1144

Archer, F., Bobet-Erny, A., & Gomes, M. (2021). State of the art on lung organoids in mammals. *Veterinary research*, *52*(1), 77-77. https://doi.org/10.1186/s13567-021-00946-6

Aufderheide, M., & Mohr, U. (1999). CULTEX--a new system and technique for the cultivation and exposure of cells at the air/liquid interface. *Exp Toxicol Pathol*, *51*(6), 489-490. https://doi.org/10.1016/s0940-2993(99)80121-3

Aufderheide, M., & Mohr, U. (2004). A modified CULTEX system for the direct exposure of bacteria to inhalable substances. *Exp Toxicol Pathol*, *55*(6), 451-454. https://doi.org/10.1078/0940-2993-00348

Bakand, S., & Hayes, A. (2016). Toxicological Considerations, Toxicity Assessment, and Risk Management of Inhaled Nanoparticles. *Int J Mol Sci*, *17*(6). https://doi.org/10.3390/ijms17060929

Bakand, S., Hayes, A., & Dechsakulthorn, F. (2012). Nanoparticles: a review of particle toxicology following inhalation exposure. *Inhal Toxicol*, *24*(2), 125-135. https://doi.org/10.3109/08958378.2010.642021

Barosova, H., Maione, A. G., Septiadi, D., Sharma, M., Haeni, L., Balog, S., O'Connell, O., Jackson, G. R., Brown, D., Clippinger, A. J., Hayden, P., Petri-Fink, A., Stone, V., & Rothen-Rutishauser, B. (2020). Use of EpiAlveolar Lung Model to Predict Fibrotic Potential of Multiwalled Carbon Nanotubes. *ACS Nano*, *14*(4), 3941-3956. https://doi.org/10.1021/acsnano.9b06860

Bassi, G., Grimaudo, M. A., Panseri, S., & Montesi, M. (2021). Advanced Multi-Dimensional Cellular Models as Emerging Reality to Reproduce In Vitro the Human Body Complexity. *International Journal of Molecular Sciences*, *22*(3), 1195. https://doi.org/10.3390/ijms22031195

Benainous, H., Kilin, V., Huang, S., Wiszniewski, L., Wolf, J.-P., Bonacina, L., Constant, S., & Mas, C. (2018). OncoCilAir™: A physiological in vitro platform to assess the efficacy and the toxicity of lung cancer therapeutics. *Toxicology Letters*, *295*, S122. https://doi.org/10.1016/j.toxlet.2018.06.670

Bengalli, R., Mantecca, P., Camatini, M., & Gualtieri, M. (2013). Effect of nanoparticles and environmental particles on a cocultures model of the air-blood barrier. *Biomed Res Int*, *2013*, 801214. https://doi.org/10.1155/2013/801214

Bessa, M. J., Brandão, F., Fokkens, P., Cassee, F. R., Salmatonidis, A., Viana, M., Vulpoi, A., Simon, S., Monfort, E., Teixeira, J. P., & Fraga, S. (2021a). Toxicity assessment of industrial engineered and airborne process-generated nanoparticles in a 3D human airway epithelial in vitro model. *Nanotoxicology*, 1-16. https://doi.org/10.1080/17435390.2021.1897698

Bessa, M. J., Brandão, F., Fokkens, P. H. B., Leseman, D. L. A. C., Boere, A. J. F., Cassee, F. R., Salmatonidis, A., Viana, M., Vulpoi, A., Simon, S., Monfort, E., Teixeira, J. P., & Fraga, S. (2021b). In Vitro Toxicity of Industrially Relevant Engineered Nanoparticles in Human Alveolar Epithelial Cells: Air–Liquid Interface versus Submerged Cultures. *Nanomaterials*, *11*(12), 3225. https://doi.org/10.3390/nano11123225

Bierkandt, F. S., Leibrock, L., Wagener, S., Laux, P., & Luch, A. (2018). The impact of nanomaterial characteristics on inhalation toxicity. *Toxicol Res (Camb)*, *7*(3), 321-346. https://doi.org/10.1039/c7tx00242d

Blank, F., Gehr, P., & Rothen-Rutishauser, B. (2009). In vitro human lung cell culture models to study the toxic potential of nanoparticles. In *Nanotoxicity: From in vitro, in vivo models to health risks* (pp. 379-395). https://doi.org/10.1002/9780470747803.ch19

Blume, C., Reale, R., Held, M., Millar, T. M., Collins, J. E., Davies, D. E., Morgan, H., & Swindle, E. J. (2015). Temporal Monitoring of Differentiated Human Airway Epithelial Cells Using Microfluidics. *PLoS One*, *10*(10), e0139872. https://doi.org/10.1371/journal.pone.0139872

Braakhuis, H. M., Kloet, S. K., Kezic, S., Kuper, F., Park, M. V., Bellmann, S., van der Zande, M., Le Gac, S., Krystek, P., Peters, R. J., Rietjens, I. M., & Bouwmeester, H. (2015). Progress and future of in vitro models to study translocation of nanoparticles. *Arch Toxicol*, *89*(9), 1469-1495. https://doi.org/10.1007/s00204-015-1518-5

Braakhuis, H. M., Oomen, A. G., & Cassee, F. R. (2016). Grouping nanomaterials to predict their potential to induce pulmonary inflammation. *Toxicol Appl Pharmacol*, *299*, 3-7. https://doi.org/10.1016/j.taap.2015.11.009

Braakhuis, H. M., Park, M. V., Gosens, I., De Jong, W. H., & Cassee, F. R. (2014). Physicochemical characteristics of nanomaterials that affect pulmonary inflammation. *Part Fibre Toxicol*, *11*(1), 18. https://doi.org/10.1186/1743-8977-11-18

Brook, R. D., Franklin, B., Cascio, W., Hong, Y., Howard, G., Lipsett, M., Luepker, R., Mittleman, M., Samet, J., & Smith Jr, S. C. (2004). Air pollution and cardiovascular disease: a statement for healthcare professionals from the Expert Panel on Population and Prevention Science of the American Heart Association. *Circulation*, *109*(21), 2655-2671. https://doi.org/10.1161/01.CIR.0000128587.30041.C8

Bui, V. K. H., Moon, J.-Y., Chae, M., Park, D., & Lee, Y.-C. (2020). Prediction of Aerosol Deposition in the Human Respiratory Tract via Computational Models: A Review with Recent Updates. *Atmosphere*, *11*(2), 137. https://doi.org/10.3390/atmos11020137

Bustamante-Marin, X. M., & Ostrowski, L. E. (2017). Cilia and Mucociliary Clearance. *Cold Spring Harbor perspectives in biology*, *9*(4), a028241. https://doi.org/10.1101/cshperspect.a028241

Chen, Y.-W., Huang, S. X., de Carvalho, A. L. R. T., Ho, S.-H., Islam, M. N., Volpi, S., Notarangelo, L. D., Ciancanelli, M., Casanova, J.-L., Bhattacharya, J., Liang, A. F., Palermo, L. M., Porotto, M., Moscona, A., & Snoeck, H.-W. (2017). A three-dimensional model of human lung development and disease from pluripotent stem cells. *Nature Cell Biology*, *19*(5), 542-549. https://doi.org/10.1038/ncb3510

Chortarea, S., Barosova, H., Clift, M. J. D., Wick, P., Petri-Fink, A., & Rothen-Rutishauser, B. (2017). Human Asthmatic Bronchial Cells Are More Susceptible to Subchronic Repeated Exposures of Aerosolized Carbon Nanotubes At Occupationally Relevant Doses Than Healthy Cells. *ACS Nano*, *11*(8), 7615-7625. https://doi.org/10.1021/acsnano.7b01992

Chortarea, S., Clift, M. J., Vanhecke, D., Endes, C., Wick, P., Petri-Fink, A., & Rothen-Rutishauser, B. (2015). Repeated exposure to carbon nanotube-based aerosols does not affect the functional properties of a 3D human epithelial airway model. *Nanotoxicology*, *9*(8), 983-993. https://doi.org/10.3109/17435390.2014.993344

Clippinger, A. J., Ahluwalia, A., Allen, D., Bonner, J. C., Casey, W., Castranova, V., David, R. M., Halappanavar, S., Hotchkiss, J. A., Jarabek, A. M., Maier, M., Polk, W., Rothen-Rutishauser, B., Sayes, C. M., Sayre, P., Sharma, M., & Stone, V. (2016). Expert consensus on an in vitro approach to assess pulmonary fibrogenic potential of aerosolized nanomaterials. *Arch Toxicol*, *90*(7), 1769-1783. https://doi.org/10.1007/s00204-016-1717-8

Clippinger, A. J., Allen, D., Jarabek, A. M., Corvaro, M., Gaca, M., Gehen, S., Hotchkiss, J. A., Patlewicz, G., Melbourne, J., Hinderliter, P., Yoon, M., Huh, D., Lowit, A., Buckley, B., Bartels, M., BeruBe, K., Wilson, D. M., Indans, I., & Vinken, M. (2018). Alternative approaches for acute inhalation toxicity testing to address global regulatory and non-regulatory data requirements: An international workshop report. *Toxicol In Vitro*, *48*, 53-70. https://doi.org/10.1016/j.tiv.2017.12.011

Cores, J., Dinh, P.-U. C., Hensley, T., Adler, K. B., Lobo, L. J., & Cheng, K. (2020). A pre-investigational new drug study of lung spheroid cell therapy for treating pulmonary fibrosis. *Stem Cells Translational Medicine*, *9*(7), 786-798. https://doi.org/10.1002/sctm.19-0167

Costa, E. C., Gaspar, V. M., Marques, J. G., Coutinho, P., & Correia, I. J. (2013). Evaluation of nanoparticle uptake in co-culture cancer models. *PLoS One*, *8*(7), e70072-e70072. https://doi.org/10.1371/journal.pone.0070072

Crapo, J. D., Barry, B. E., Gehr, P., Bachofen, M., & Weibel, E. R. (1982). Cell number and cell characteristics of the normal human lung. *Am Rev Respir Dis*, *126*(2), 332-337. https://doi.org/10.1164/arrd.1982.126.2.332

Dankers, A. C. A., Kuper, C. F., Boumeester, A. J., Fabriek, B. O., Kooter, I. M., Grollers-Mulderij, M., Tromp, P., Nelissen, I., Zondervan-Van Den Beuken, E. K., & Vandebriel, R. J. (2018). A practical approach to assess inhalation toxicity of metal oxide nanoparticles in vitro. *J Appl Toxicol*, *38*(2), 160-171. https://doi.org/10.1002/jat.3518

Darquenne, C. (2020). Deposition mechanisms. *Journal of aerosol medicine and pulmonary drug delivery*, *33*(4), 181-185. https://doi.org/10.1089/jamp.2020.29029.cd

de Bruijne, K., Ebersviller, S., Sexton, K. G., Lake, S., Leith, D., Goodman, R., Jetters, J., Walters, G. W., Doyle-Eisele, M., Woodside, R., Jeffries, H. E., & Jaspers, I. (2009). Design and testing of Electrostatic Aerosol in Vitro Exposure System (EAVES): an alternative exposure system for particles. *Inhal Toxicol*, *21*(2), 91-101. https://doi.org/10.1080/08958370802166035

De Jong, W. H., & Borm, P. J. A. (2008). Drug delivery and nanoparticles:applications and hazards. *Int J Nanomedicine*, *3*(2), 133-149. https://doi.org/10.2147/ijn.s596

Delfino, R. J., Sioutas, C., & Malik, S. (2005). Potential role of ultrafine particles in associations between airborne particle mass and cardiovascular health. *Environmental health perspectives*, *113*(8), 934-946. https://doi.org/10.1289/ehp.7938

Di Cristo, L., Boccuni, F., Iavicoli, S., & Sabella, S. (2020). A Human-Relevant 3D In Vitro Platform for an Effective and Rapid Simulation of Workplace Exposure to Nanoparticles: Silica Nanoparticles as Case Study. *Nanomaterials*, *10*(9), 1761. https://doi.org/10.3390/nano10091761

Diabaté, S., Armand, L., Murugadoss, S., Dilger, M., Fritsch-Decker, S., Schlager, C., Béal, D., Arnal, M.-E., Biola-Clier, M., Ambrose, S., Mülhopt, S., Paur, H.-R., Lynch, I., Valsami-Jones, E., Carriere, M., & Weiss, C. (2021). Air–Liquid Interface Exposure of Lung Epithelial Cells to Low Doses of Nanoparticles to Assess Pulmonary Adverse Effects. *Nanomaterials*, *11*(1), 65. https://doi.org/10.3390/nano11010065

Ding, Y., Weindl, P., Lenz, A. G., Mayer, P., Krebs, T., & Schmid, O. (2020). Quartz crystal microbalances (QCM) are suitable for real-time dosimetry in nanotoxicological studies using VITROCELL®Cloud cell exposure systems. *Part Fibre Toxicol*, *17*(1), 44. https://doi.org/10.1186/s12989-020-00376-w

Docter, D., Westmeier, D., Markiewicz, M., Stolte, S., Knauer, S., & Stauber, R. (2015). The nanoparticle biomolecule corona: lessons learned–challenge accepted? *Chemical Society Reviews*, *44*(17), 6094-6121. https://doi.org/10.1039/C5CS00217F

Domb, A. J., Sharifzadeh, G., Nahum, V., & Hosseinkhani, H. (2021). Safety Evaluation of Nanotechnology Products. *Pharmaceutics*, *13*(10), 1615. https://doi.org/10.3390/pharmaceutics13101615

Donaldson, K., Stone, V., Seaton, A., & MacNee, W. (2001). Ambient particle inhalation and the cardiovascular system: potential mechanisms. *Environmental health perspectives*, *109 Suppl 4*(Suppl 4), 523-527. https://doi.org/10.1289/ehp.01109s4523

Donaldson, K., & Tran, C. L. (2002). Inflammation caused by particles and fibers. *Inhal Toxicol*, *14*(1), 5-27. https://doi.org/10.1080/089583701753338613

Duret, C., Wauthoz, N., Merlos, R., Goole, J., Maris, C., Roland, I., Sebti, T., Vanderbist, F., & Amighi, K. (2012). In vitro and in vivo evaluation of a dry powder endotracheal insufflator device for use in dose-dependent preclinical studies in mice. *Eur J Pharm Biopharm*, *81*(3), 627-634. https://doi.org/10.1016/j.ejpb.2012.04.004

Dvorak, A., Tilley, A. E., Shaykhiev, R., Wang, R., & Crystal, R. G. (2011). Do airway epithelium air-liquid cultures represent the in vivo airway epithelium transcriptome? *Am J Respir Cell Mol Biol*, *44*(4), 465-473. https://doi.org/10.1165/rcmb.2009-0453OC

Edmondson, R., Broglie, J. J., Adcock, A. F., & Yang, L. (2014). Three-dimensional cell culture systems and their applications in drug discovery and cell-based biosensors. *Assay Drug Dev Technol*, *12*(4), 207-218. https://doi.org/10.1089/adt.2014.573

Faber, S. C., & McCullough, S. D. (2018). Through the Looking Glass: In Vitro Models for Inhalation Toxicology and Interindividual Variability in the Airway. *Appl In Vitro Toxicol*, *4*(2), 115-128. https://doi.org/10.1089/aivt.2018.0002

Falahati, M., Attar, F., Sharifi, M., Haertlé, T., Berret, J. F., Khan, R. H., & Saboury, A. A. (2019). A health concern regarding the protein corona, aggregation and disaggregation. *Biochim Biophys Acta Gen Subj*, *1863*(5), 971-991. https://doi.org/10.1016/j.bbagen.2019.02.012

Fizesan, I., Cambier, S., Moschini, E., Chary, A., Nelissen, I., Ziebel, J., Audinot, J. N., Wirtz, T., Kruszewski, M., Pop, A., Kiss, B., Serchi, T., Loghin, F., & Gutleb, A. C. (2019). In vitro exposure of a 3D-tetraculture representative for the alveolar barrier at the air-liquid interface to silver particles and nanowires. *Part Fibre Toxicol*, *16*(1), 14. https://doi.org/10.1186/s12989-019-0297-1

Frieke Kuper, C., Grollers-Mulderij, M., Maarschalkerweerd, T., Meulendijks, N. M., Reus, A., van Acker, F., Zondervan-van den Beuken, E. K., Wouters, M. E., Bijlsma, S., & Kooter, I. M. (2015). Toxicity assessment of aggregated/agglomerated cerium oxide nanoparticles in an in vitro 3D airway model: the influence of mucociliary clearance. *Toxicol In Vitro*, *29*(2), 389-397. https://doi.org/10.1016/j.tiv.2014.10.017

Frijns, E., Verstraelen, S., Stoehr, L. C., Van Laer, J., Jacobs, A., Peters, J., Tirez, K., Boyles, M. S. P., Geppert, M., Madl, P., Nelissen, I., Duschl, A., & Himly, M. (2017). A Novel Exposure System Termed NAVETTA for In Vitro Laminar Flow Electrodeposition of Nanoaerosol and Evaluation of Immune Effects in

Human Lung Reporter Cells. *Environ Sci Technol*, *51*(9), 5259-5269. https://doi.org/10.1021/acs.est.7b00493

Fröhlich, E. (2018). Comparison of conventional and advanced in vitro models in the toxicity testing of nanoparticles. *Artif Cells Nanomed Biotechnol*, *46*(sup2), 1091-1107. https://doi.org/10.1080/21691401.2018.1479709

Fröhlich, E., & Salar-Behzadi, S. (2014). Toxicological assessment of inhaled nanoparticles: role of in vivo, ex vivo, in vitro, and in silico studies. *Int J Mol Sci*, *15*(3), 4795-4822. https://doi.org/10.3390/ijms15034795

Fujitani, Y., Sugaya, Y., Hashiguchi, M., Furuyama, A., Hirano, S., & Takami, A. (2015). Particle deposition efficiency at air–liquid interface of a cell exposure chamber. *Journal of Aerosol Science*, *81*, 90-99. https://doi.org/10.1016/j.jaerosci.2014.10.012

Fytianos, K., Drasler, B., Blank, F., von Garnier, C., Seydoux, E., Rodriguez-Lorenzo, L., Petri-Fink, A., & Rothen-Rutishauser, B. (2016). Current in vitro approaches to assess nanoparticle interactions with lung cells. *Nanomedicine (Lond)*, *11*(18), 2457-2469. https://doi.org/10.2217/nnm-2016-0199

Ganesan, S., Comstock, A. T., & Sajjan, U. S. (2013). Barrier function of airway tract epithelium. *Tissue Barriers*, *1*(4), e24997. https://doi.org/10.4161/tisb.24997

Geiser, M. (2010). Update on macrophage clearance of inhaled micro-and nanoparticles. *J Aerosol Med Pulm Drug Deliv*, *23*(4), 207-217. https://doi.org/10.1089/jamp.2009.0797

Geiser, M., Jeannet, N., Fierz, M., & Burtscher, H. (2017). Evaluating adverse effects of inhaled nanoparticles by realistic in vitro technology. *Nanomaterials*, *7*(2), 49. https://doi.org/10.3390/nano7020049

George, I., Uboldi, C., Bernard, E., Sobrido, M. S., Dine, S., Hagege, A., Vrel, D., Herlin, N., Rose, J., Orsiere, T., Grisolia, C., Rousseau, B., & Malard, V. (2019). Toxicological Assessment of ITER-Like Tungsten Nanoparticles Using an In Vitro 3D Human Airway Epithelium Model. *Nanomaterials (Basel)*, *9*(10). https://doi.org/10.3390/nano9101374

George, I., Vranic, S., Boland, S., Courtois, A., & Baeza-Squiban, A. (2015). Development of an in vitro model of human bronchial epithelial barrier to study nanoparticle translocation. *Toxicol In Vitro*, *29*(1), 51-58. https://doi.org/10.1016/j.tiv.2014.08.003

Ghio, A. J., Dailey, L. A., Soukup, J. M., Stonehuerner, J., Richards, J. H., & Devlin, R. B. (2013). Growth of human bronchial epithelial cells at an air-liquid interface alters the response to particle exposure. *Part Fibre Toxicol*, *10*(1), 25. https://doi.org/10.1186/1743-8977-10-25

Gkatzis, K., Taghizadeh, S., Huh, D., Stainier, D. Y., & Bellusci, S. (2018). Use of three-dimensional organoids and lung-on-a-chip methods to study lung development, regeneration and disease. *European Respiratory Journal*, *52*(5). https://doi.org/10.1183/13993003.00876-2018

Gotoh, S., Ito, I., Nagasaki, T., Yamamoto, Y., Konishi, S., Korogi, Y., Matsumoto, H., Muro, S., Hirai, T., Funato, M., Mae, S., Toyoda, T., Sato-Otsubo, A., Ogawa, S., Osafune, K., & Mishima, M. (2014). Generation of alveolar epithelial spheroids via isolated progenitor cells from human pluripotent stem cells. *Stem Cell Reports*, *3*(3), 394-403. https://doi.org/10.1016/j.stemcr.2014.07.005

Guha, S., Hariharan, P., & Myers, M. R. (2014). Enhancement of ICRP's Lung Deposition Model for Pathogenic Bioaerosols. *Aerosol Science and Technology*, *48*(12), 1226-1235. https://doi.org/10.1080/02786826.2014.975334

Guo, C., Buckley, A., Marczylo, T., Seiffert, J., Romer, I., Warren, J., Hodgson, A., Chung, K. F., Gant, T. W., Smith, R., & Leonard, M. O. (2018). The small airway epithelium as a target for the adverse pulmonary effects of silver nanoparticle inhalation. *Nanotoxicology*, *12*(6), 539-553. https://doi.org/10.1080/17435390.2018.1465140

Hagens, W. I., Oomen, A. G., de Jong, W. H., Cassee, F. R., & Sips, A. J. (2007). What do we (need to) know about the kinetic properties of nanoparticles in the body? *Regul Toxicol Pharmacol*, *49*(3), 217-229. https://doi.org/10.1016/j.yrtph.2007.07.006

Harkema, J. R., Carey, S. A., Wagner, J. G., Dintzis, S. M., & Liggitt, D. (2012). 6 - Nose, Sinus, Pharynx, and Larynx. In P. M. Treuting & S. M. Dintzis (Eds.), *Comparative Anatomy and Histology* (pp. 71-94). Academic Press. https://doi.org/10.1016/B978-0-12-381361-9.00006-8

Hastedt, J. E., Bäckman, P., Clark, A. R., Doub, W., Hickey, A., Hochhaus, G., Kuehl, P. J., Lehr, C.-M., Mauser, P., & McConville, J. (2016). Scope and relevance of a pulmonary biopharmaceutical classification system AAPS/FDA/USP Workshop March 16-17th, 2015 in Baltimore, MD. https://doi.org/10.1186/s41120-015-0002-x

He, X. (2016). In Vivo Nanotoxicity Assays in Animal Models. In *Toxicology of Nanomaterials* (pp. 151-198). https://doi.org/10.1002/9783527689125.ch7

Hewitt, R. J., & Lloyd, C. M. (2021). Regulation of immune responses by the airway epithelial cell landscape. *Nature Reviews Immunology*, *21*(6), 347-362. https://doi.org/10.1038/s41577-020-00477-9

Hiemstra, P. S., Grootaers, G., van der Does, A. M., Krul, C. A. M., & Kooter, I. M. (2018). Human lung epithelial cell cultures for analysis of inhaled toxicants: Lessons learned and future directions. *Toxicol In Vitro*, *47*, 137-146. https://doi.org/10.1016/j.tiv.2017.11.005

Hiemstra, P. S., McCray, P. B., Jr., & Bals, R. (2015). The innate immune function of airway epithelial cells in inflammatory lung disease. *Eur Respir J*, *45*(4), 1150-1162. https://doi.org/10.1183/09031936.00141514

Hofer, M., & Lutolf, M. P. (2021). Engineering organoids. *Nature Reviews Materials*, *6*(5), 402-420. https://doi.org/10.1038/s41578-021-00279-y

Huh, D., Matthews, B. D., Mammoto, A., Montoya-Zavala, M., Hsin, H. Y., & Ingber, D. E. (2010). Reconstituting organ-level lung functions on a chip. *Science*, *328*(5986), 1662-1668. https://doi.org/10.1126/science.1188302

Huh, D. D. (2015). A human breathing lung-on-a-chip. *Ann Am Thorac Soc*, *12 Suppl 1*, S42-44. https://doi.org/10.1513/AnnalsATS.201410-442MG

Inhalation Sciences. (2021). *XposeALI ® - 3D in vitro cell exposure.* https://inhalation.se/products/xposeali-cell-exposures/

Ionescu, C. M. (2013). The human respiratory system. In *The Human Respiratory System* (pp. 13-22). Springer. https://link.springer.com/book/10.1007/978-1-4471-5388-7

Jackson, E. L., & Lu, H. (2016). Three-dimensional models for studying development and disease: moving on from organisms to organs-on-a-chip and organoids. *Integrative biology : quantitative biosciences from nano to macro*, *8*(6), 672-683. https://doi.org/10.1039/c6ib00039h

Jakobsson, J. K. F., Aaltonen, H. L., Nicklasson, H., Gudmundsson, A., Rissler, J., Wollmer, P., & Löndahl, J. (2018). Altered deposition of inhaled nanoparticles in subjects with chronic obstructive pulmonary disease. *BMC Pulm Med*, *18*(1), 129. https://doi.org/10.1186/s12890-018-0697-2

Jeannet, N., Fierz, M., Kalberer, M., Burtscher, H., & Geiser, M. (2015). Nano aerosol chamber for in-vitro toxicity (NACIVT) studies. *Nanotoxicology*, *9*(1), 34-42. https://doi.org/10.3109/17435390.2014.886739

Jia, J., Wang, Z., Yue, T., Su, G., Teng, C., & Yan, B. (2020). Crossing Biological Barriers by Engineered Nanoparticles. *Chem Res Toxicol*, *33*(5), 1055-1060. https://doi.org/10.1021/acs.chemrestox.9b00483

Jia, Y. Y., Wang, Q., & Liu, T. (2017). Toxicity Research of PM2.5 Compositions In Vitro. *Int J Environ Res Public Health*, *14*(3). https://doi.org/10.3390/ijerph14030232

Jiang, X.-Q., Mei, X.-D., & Feng, D. (2016). Air pollution and chronic airway diseases: what should people know and do? *Journal of thoracic disease*, *8*(1), E31-E40. https://doi.org/10.3978/j.issn.2072-1439.2015.11.50

Johnson, N. M., Hoffmann, A. R., Behlen, J. C., Lau, C., Pendleton, D., Harvey, N., Shore, R., Li, Y., Chen, J., & Tian, Y. (2021). Air pollution and children's health—a review of adverse effects associated with prenatal exposure from fine to ultrafine particulate matter. *Environmental health and preventive medicine*, *26*(1), 1-29. https://doi.org/10.1186/s12199-021-00995-5

Joris, F., Manshian, B. B., Peynshaert, K., De Smedt, S. C., Braeckmans, K., & Soenen, S. J. (2013). Assessing nanoparticle toxicity in cell-based assays: influence of cell culture parameters and optimized models for bridging the in vitro-in vivo gap. *Chem Soc Rev*, *42*(21), 8339-8359. https://doi.org/10.1039/c3cs60145e

Journeay, W. S., & Goldman, R. H. (2014). Occupational handling of nickel nanoparticles: a case report. *Am J Ind Med*, *57*(9), 1073-1076. https://doi.org/10.1002/ajim.22344

Kabadi, P. K., Rodd, A. L., Simmons, A. E., Messier, N. J., Hurt, R. H., & Kane, A. B. (2019). A novel human 3D lung microtissue model for nanoparticle-induced cell-matrix alterations. *Part Fibre Toxicol*, *16*(1), 15. https://doi.org/10.1186/s12989-019-0298-0

Kar, S. K., Wells, J. M., Ellen, E. D., te Pas, M. F. W., Madsen, O., Groenen, M. A. M., & Woelders, H. (2021). Organoids: a promising new in vitro platform in livestock and veterinary research. *Veterinary research*, *52*(1), 43. https://doi.org/10.1186/s13567-021-00904-2

Kasper, J., Hermanns, M. I., Bantz, C., Maskos, M., Stauber, R., Pohl, C., Unger, R. E., & Kirkpatrick, J. C. (2011). Inflammatory and cytotoxic responses of an alveolar-capillary coculture model to silica nanoparticles: comparison with conventional monocultures. *Part Fibre Toxicol*, *8*(1), 6. https://doi.org/10.1186/1743-8977-8-6

Katt, M. E., Placone, A. L., Wong, A. D., Xu, Z. S., & Searson, P. C. (2016). In Vitro Tumor Models: Advantages, Disadvantages, Variables, and Selecting the Right Platform [Review]. *Front Bioeng Biotechnol*, *4*(12). https://doi.org/10.3389/fbioe.2016.00012

Kelly, F. J., & Fussell, J. C. (2015). Air pollution and public health: emerging hazards and improved understanding of risk. *Environ Geochem Health*, *37*(4), 631-649. https://doi.org/10.1007/s10653-015-9720-1

Kendall, M., Hodges, N. J., Whitwell, H., Tyrrell, J., & Cangul, H. (2015). Nanoparticle growth and surface chemistry changes in cell-conditioned culture medium. *Philosophical transactions of the Royal Society of London. Series B, Biological sciences*, *370*(1661), 20140100-20140100. https://doi.org/10.1098/rstb.2014.0100

Kendall, M., & Holgate, S. (2012). Health impact and toxicological effects of nanomaterials in the lung. *Respirology*, *17*(5), 743-758. https://doi.org/10.1111/j.1440-1843.2012.02171.x

Khan, Y. S., & Lynch, D. T. (2018). Histology, Lung.

Khatri, M., Bello, D., Gaines, P., Martin, J., Pal, A. K., Gore, R., & Woskie, S. (2013). Nanoparticles from photocopiers induce oxidative stress and upper respiratory tract inflammation in healthy volunteers. *Nanotoxicology*, *7*(5), 1014-1027. https://doi.org/10.3109/17435390.2012.691998

Klein, S. G., Serchi, T., Hoffmann, L., Blömeke, B., & Gutleb, A. C. (2013). An improved 3D tetraculture system mimicking the cellular organisation at the alveolar barrier to study the potential toxic effects of particles on the lung. *Part Fibre Toxicol*, *10*, 31. https://doi.org/10.1186/1743-8977-10-31

Kleinstreuer, C., & Zhang, Z. (2010). Airflow and Particle Transport in the Human Respiratory System. *Annu Rev Fluid Mech*, *42*(1), 301-334. https://doi.org/10.1146/annurev-fluid-121108-145453

Kletting, S., Barthold, S., Repnik, U., Griffiths, G., Loretz, B., Schneider-Daum, N., de Souza Carvalho-Wodarz, C., & Lehr, C.-M. (2018). Co-culture of human alveolar epithelial (hAELVi) and macrophage (THP-1) cell lines. *Altex*. https://doi.org/10.14573/altex.1607191

Knaapen, A. M., Borm, P. J., Albrecht, C., & Schins, R. P. (2004). Inhaled particles and lung cancer. Part A: Mechanisms. *Int J Cancer*, *109*(6), 799-809. https://doi.org/10.1002/ijc.11708

Kolanjiyil, A. V., & Kleinstreuer, C. (2013). Nanoparticle mass transfer from lung airways to systemic regions--Part I: Whole-lung aerosol dynamics. *J Biomech Eng*, *135*(12), 121003. https://doi.org/10.1115/1.4025332

Kooter, I. M., Gröllers-Mulderij, M., Duistermaat, E., Kuper, F., & Schoen, E. D. (2017). Factors of concern in a human 3D cellular airway model exposed to aerosols of nanoparticles. *Toxicol In Vitro*, *44*, 339-348. https://doi.org/10.1016/j.tiv.2017.07.006

Kreyling, W. G., Semmler-Behnke, M., & Möller, W. (2006). Health implications of nanoparticles. *J Nanoparticle Res*, *8*(5), 543-562. https://doi.org/10.1186/1743-8977-7-2

Kuempel, E. D., Sweeney, L. M., Morris, J. B., & Jarabek, A. M. (2015). Advances in Inhalation Dosimetry Models and Methods for Occupational Risk Assessment and Exposure Limit Derivation. *J Occup Environ Hyg*, *12*(sup1), S18-S40. https://doi.org/10.1080/15459624.2015.1060328

Kumar, V., Sharma, N., & Maitra, S. (2017). In vitro and in vivo toxicity assessment of nanoparticles. *Int Nano Lett*, *7*(4), 243-256. https://doi.org/10.1007/s40089-017-0221-3

Kurt, O. K., Zhang, J., & Pinkerton, K. E. (2016). Pulmonary health effects of air pollution. *Current opinion in pulmonary medicine*, *22*(2), 138-143. https://doi.org/10.1097/MCP.0000000000000248

Lacroix, G., Koch, W., Ritter, D., Gutleb, A. C., Larsen, S. T., Loret, T., Zanetti, F., Constant, S., Chortarea, S., Rothen-Rutishauser, B., Hiemstra, P. S., Frejafon, E., Hubert, P., Gribaldo, L., Kearns, P., Aublant, J.-M., Diabaté, S., Weiss, C., de Groot, A., & Kooter, I. (2018). Air–Liquid Interface In Vitro Models for Respiratory Toxicology Research: Consensus Workshop and Recommendations. *Appl In Vitro Toxicol*, *4*(2), 91-106. https://doi.org/10.1089/aivt.2017.0034

Landsiedel, R., Ma-Hock, L., Hofmann, T., Wiemann, M., Strauss, V., Treumann, S., Wohlleben, W., Gröters, S., Wiench, K., & van Ravenzwaay, B. (2014a). Application of short-term inhalation studies to assess the inhalation toxicity of nanomaterials. *Part Fibre Toxicol*, *11*(1), 16. https://doi.org/10.1186/1743-8977-11-16

Landsiedel, R., Sauer, U. G., Ma-Hock, L., Schnekenburger, J., & Wiemann, M. (2014b). Pulmonary toxicity of nanomaterials: a critical comparison of published in vitro assays and in vivo inhalation or instillation studies.

Nanomedicine (Lond), *9*(16), 2557-2585. https://doi.org/10.2217/nnm.14.149

Laux, P., Riebeling, C., Booth, A. M., Brain, J. D., Brunner, J., Cerrillo, C., Creutzenberg, O., Estrela-Lopis, I., Gebel, T., Johanson, G., Jungnickel, H., Kock, H., Tentschert, J., Tlili, A., Schäffer, A., Sips, A. J. A. M., Yokel, R. A., & Luch, A. (2017). Biokinetics of nanomaterials: The role of biopersistence. *NanoImpact*, *6*, 69-80. https://doi.org/10.1016/j.impact.2017.03.003

Leibrock, L., Wagener, S., Singh, A. V., Laux, P., & Luch, A. (2019). Nanoparticle induced barrier function assessment at liquid-liquid and air-liquid interface in novel human lung epithelia cell lines. *Toxicol Res (Camb)*, *8*(6), 1016-1027. https://doi.org/10.1039/c9tx00179d

Leikauf, G. D., Kim, S.-H., & Jang, A.-S. (2020). Mechanisms of ultrafine particle-induced respiratory health effects. *Experimental & Molecular Medicine*, *52*(3), 329-337. https://doi.org/10.1038/s12276-020-0394-0

Lenz, A. G., Karg, E., Brendel, E., Hinze-Heyn, H., Maier, K. L., Eickelberg, O., Stoeger, T., & Schmid, O. (2013). Inflammatory and oxidative stress responses of an alveolar epithelial cell line to airborne zinc oxide nanoparticles at the air-liquid interface: a comparison with conventional, submerged cell-culture conditions. *Biomed Res Int*, *2013*, 652632. https://doi.org/10.1155/2013/652632

Lenz, A. G., Karg, E., Lentner, B., Dittrich, V., Brandenberger, C., Rothen-Rutishauser, B., Schulz, H., Ferron, G. A., & Schmid, O. (2009). A dose-controlled system for air-liquid interface cell exposure and application to zinc oxide nanoparticles. *Part Fibre Toxicol*, *6*(1), 32. https://doi.org/10.1186/1743-8977-6-32

Li, J. J. e., Muralikrishnan, S., Ng, C.-T., Yung, L.-Y. L., & Bay, B.-H. (2010). Nanoparticle-induced pulmonary toxicity. *Exp Biol Med*, *235*(9), 1025-1033. https://doi.org/10.1258/ebm.2010.010021

Li, N., Georas, S., Alexis, N., Fritz, P., Xia, T., Williams, M. A., Horner, E., & Nel, A. (2016). A work group report on ultrafine particles (American Academy of Allergy, Asthma & Immunology): Why ambient ultrafine and engineered nanoparticles should receive special attention for possible adverse health outcomes in human subjects. *The Journal of allergy and clinical immunology*, *138*(2), 386-396. https://doi.org/10.1016/j.jaci.2016.02.023

Li, Y., Wu, Q., Sun, X., Shen, J., & Chen, H. (2020). Organoids as a Powerful Model for Respiratory Diseases. *Stem Cells Int*, *2020*, 5847876. https://doi.org/10.1155/2020/5847876

Lingappan, K., Maity, S., Jiang, W., Wang, L., Couroucli, X., Veith, A., Zhou, G., Coarfa, C., & Moorthy, B. (2017). Role of Cytochrome P450 (CYP)1A in Hyperoxic Lung Injury: Analysis of the Transcriptome and Proteome. *Sci Rep*, *7*(1), 642-642. https://doi.org/10.1038/s41598-017-00516-x

Liu, S., Yang, R., Chen, Y., Zhao, X., Chen, S., Yang, X., Cheng, Z., Hu, B., Liang, X., Yin, N., Liu, Q., Wang, H., Liu, S., & Faiola, F. (2021). Development of Human Lung Induction Models for Air Pollutants' Toxicity Assessment. *Environmental Science & Technology*, *55*(4), 2440-2451. https://doi.org/10.1021/acs.est.0c05700

Londahl, J., Moller, W., Pagels, J. H., Kreyling, W. G., Swietlicki, E., & Schmid, O. (2014). Measurement techniques for respiratory tract deposition of airborne nanoparticles: a critical review. *J Aerosol Med Pulm Drug Deliv*, *27*(4), 229-254. https://doi.org/10.1089/jamp.2013.1044

Loret, T., Peyret, E., Dubreuil, M., Aguerre-Chariol, O., Bressot, C., le Bihan, O., Amodeo, T., Trouiller, B., Braun, A., Egles, C., & Lacroix, G. (2016). Air-liquid interface exposure to aerosols of poorly soluble nanomaterials induces different biological activation levels compared to exposure to suspensions. *Part Fibre Toxicol*, *13*(1), 58. https://doi.org/10.1186/s12989-016-0171-3

Loret, T., Rogerieux, F., Trouiller, B., Braun, A., Egles, C., & Lacroix, G. (2018). Predicting the in vivo pulmonary toxicity induced by acute exposure to poorly soluble nanomaterials by using advanced in vitro methods. *Part Fibre Toxicol*, *15*(1), 25. https://doi.org/10.1186/s12989-018-0260-6

Malakar, A., Kanel, S. R., Ray, C., Snow, D. D., & Nadagouda, M. N. (2021). Nanomaterials in the environment, human exposure pathway, and health effects: A review. *Science of The Total Environment*, *759*, 143470. https://doi.org/10.1016/j.scitotenv.2020.143470

Medina-Reyes, E. I., Delgado-Buenrostro, N. L., Leseman, D. L., Deciga-Alcaraz, A., He, R., Gremmer, E. R., Fokkens, P. H. B., Flores-Flores, J. O., Cassee, F. R., & Chirino, Y. I. (2020). Differences in cytotoxicity of lung epithelial cells exposed to titanium dioxide nanofibers and nanoparticles: Comparison of air-liquid interface and submerged cell cultures. *Toxicol In Vitro*, *65*, 104798. https://doi.org/10.1016/j.tiv.2020.104798

Meghani, N., Kim, K. H., Kim, S. H., Lee, S. H., & Choi, K. H. (2020). Evaluation and live monitoring of pH-responsive HSA-ZnO nanoparticles using a lung-on-a-chip model. *Arch Pharm Res*, *43*(5), 503-513. https://doi.org/10.1007/s12272-020-01236-z

Meyerholz, D. K., Suarez, C. J., Dintzis, S. M., & Frevert, C. W. (2018). 9 - Respiratory System. In P. M. Treuting, S. M. Dintzis, & K. S. Montine (Eds.), *Comparative Anatomy and Histology (Second Edition)* (pp. 147-162). Academic Press. https://doi.org/10.1016/B978-0-12-802900-8.00009-9

Miller, A. J., Hill, D. R., Nagy, M. S., Aoki, Y., Dye, B. R., Chin, A. M., Huang, S., Zhu, F., White, E. S., Lama, V., & Spence, J. R. (2018). In Vitro Induction and In Vivo Engraftment of Lung Bud Tip Progenitor Cells Derived from Human Pluripotent Stem Cells. *Stem Cell Reports*, *10*(1), 101-119. https://doi.org/10.1016/j.stemcr.2017.11.012

Mizumura, K., Maruoka, S., Shimizu, T., & Gon, Y. (2020). Role of Nrf2 in the pathogenesis of respiratory diseases. *Respir Investig*, *58*(1), 28-35. https://doi.org/10.1016/j.resinv.2019.10.003

Monopoli, M. P., Aberg, C., Salvati, A., & Dawson, K. A. (2012). Biomolecular coronas provide the biological identity of nanosized materials. *Nat Nanotechnol*, *7*(12), 779-786. https://doi.org/10.1038/nnano.2012.207

Monopoli, M. P., Walczyk, D., Campbell, A., Elia, G., Lynch, I., Baldelli Bombelli, F., & Dawson, K. A. (2011). Physical−Chemical Aspects of Protein Corona: Relevance to in Vitro and in Vivo Biological Impacts of Nanoparticles. *J Am Chem Soc*, *133*(8), 2525-2534. https://doi.org/10.1021/ja107583h

Moore, T. L., Rodriguez-Lorenzo, L., Hirsch, V., Balog, S., Urban, D., Jud, C., Rothen-Rutishauser, B., Lattuada, M., & Petri-Fink, A. (2015). Nanoparticle colloidal stability in cell culture media and impact on cellular interactions [10.1039/C4CS00487F]. *Chemical Society Reviews*, *44*(17), 6287-6305. https://doi.org/10.1039/C4CS00487F

Moore, T. L., Urban, D. A., Rodriguez-Lorenzo, L., Milosevic, A., Crippa, F., Spuch-Calvar, M., Balog, S., Rothen-Rutishauser, B., Lattuada, M., & Petri-Fink, A. (2019). Nanoparticle administration method in cell culture alters particle-cell interaction. *Sci Rep*, *9*(1), 900-900. https://doi.org/10.1038/s41598-018-36954-4

Morawska, L., & Buonanno, G. (2021). The physics of particle formation and deposition during breathing. *Nature Reviews Physics*, *3*(5), 300-301. https://doi.org/10.1038/s42254-021-00307-4

Movia, D., Bruni-Favier, S., & Prina-Mello, A. (2020). In vitro Alternatives to Acute Inhalation Toxicity Studies in Animal Models-A Perspective. *Front Bioeng Biotechnol*, *8*, 549. https://doi.org/10.3389/fbioe.2020.00549

Movia, D., Di Cristo, L., Alnemari, R., McCarthy, J. E., Moustaoui, H., Lamy de la Chapelle, M., Spadavecchia, J., Volkov, Y., & Prina-Mello, A. (2017). The curious case of how mimicking physiological complexity in in vitro models of the human respiratory system influences the inflammatory responses. A preliminary study focused on gold nanoparticles. *Journal of Interdisciplinary Nanomedicine*, *2*(2), 110-130. https://doi.org/10.1002/jin2.25

Mowat, V., Alexander, D. J., & Pilling, A. M. (2017). A Comparison of Rodent and Nonrodent Laryngeal and Tracheal Bifurcation Sensitivities in Inhalation Toxicity Studies and Their Relevance for Human Exposure. *Toxicol Pathol*, *45*(1), 216-222. https://doi.org/10.1177/0192623316678695

Mühlfeld, C., Gehr, P., & Rothen-Rutishauser, B. (2008). Translocation and cellular entering mechanisms of nanoparticles in the respiratory tract. *Swiss Med Wkly*, *138*(27-28), 387-391. https://pubmed.ncbi.nlm.nih.gov/18642134/

Nahar, K., Gupta, N., Gauvin, R., Absar, S., Patel, B., Gupta, V., Khademhosseini, A., & Ahsan, F. (2013). In vitro, in vivo and ex vivo models for studying particle deposition and drug absorption of inhaled pharmaceuticals. *European journal of pharmaceutical sciences*, *49*(5), 805-818. https://doi.org/10.1016/j.ejps.2013.06.004

Nemmar, A., Holme, J. A., Rosas, I., Schwarze, P. E., & Alfaro-Moreno, E. (2013). Recent advances in particulate matter and nanoparticle toxicology: a review of the in vivo and in vitro studies. *Biomed Res Int*, *2013*, 279371. https://doi.org/10.1155/2013/279371

Oberdorster, G., Castranova, V., Asgharian, B., & Sayre, P. (2015). Inhalation Exposure to Carbon Nanotubes (CNT) and Carbon Nanofibers (CNF): Methodology and Dosimetry. *J Toxicol Environ Health B Crit Rev*, *18*(3-4), 121-212. https://doi.org/10.1080/10937404.2015.1051611

Oberdörster, G., & Kuhlbusch, T. A. J. (2018). In vivo effects: Methodologies and biokinetics of inhaled nanomaterials. *NanoImpact*, *10*, 38-60. https://doi.org/10.1016/j.impact.2017.10.007

Oberdörster, G., Stone, V., & Donaldson, K. (2007). Toxicology of nanoparticles: A historical perspective. *Nanotoxicology*, *1*(1), 2-25. https://doi.org/10.1080/17435390701314761

Øvrevik, J., Refsnes, M., Låg, M., Holme, J. A., & Schwarze, P. E. (2015). Activation of Proinflammatory Responses in Cells of the Airway Mucosa by Particulate Matter: Oxidant- and Non-Oxidant-Mediated Triggering Mechanisms. *Biomolecules*, *5*(3), 1399-1440. https://doi.org/10.3390/biom5031399

Panas, A., Comouth, A., Saathoff, H., Leisner, T., Al-Rawi, M., Simon, M., Seemann, G., Dossel, O., Mulhopt, S., Paur, H. R., Fritsch-Decker, S., Weiss, C., & Diabate, S. (2014). Silica nanoparticles are less toxic to human lung cells when deposited at the air-liquid interface compared to conventional submerged exposure. *Beilstein J Nanotechnol*, *5*, 1590-1602. https://doi.org/10.3762/bjnano.5.171

Paur, H.-R., Cassee, F. R., Teeguarden, J., Fissan, H., Diabate, S., Aufderheide, M., Kreyling, W. G., Hänninen, O., Kasper, G., & Riediker, M. (2011). In-vitro cell exposure studies for the assessment of nanoparticle toxicity in the lung - A dialog between aerosol science and biology. *J Aerosol Sci*, *42*(10), 668-692. https://doi.org/10.1016/j.jaerosci.2011.06.005

Penn-Century™. (2021). *Penn-Century™ - Exclusive manufacturer of the MicroSprayer® Aerosolizer*. https://penncentury.com/products/

Pezzulo, A. A., Starner, T. D., Scheetz, T. E., Traver, G. L., Tilley, A. E., Harvey, B.-G., Crystal, R. G., McCray Jr, P. B., & Zabner, J. (2011). The air-liquid interface and use of primary cell cultures are important to recapitulate the transcriptional profile of in vivo airway epithelia. *Am J Physiol Lung Cell Mol Physiol*, *300*(1), L25-L31. https://doi.org/10.1152/ajplung.00256.2010

Pfuhler, S., van Benthem, J., Curren, R., Doak, S. H., Dusinska, M., Hayashi, M., Heflich, R. H., Kidd, D., Kirkland, D., Luan, Y., Ouedraogo, G., Reisinger, K., Sofuni, T., van Acker, F., Yang, Y., & Corvi, R. (2020). Use of in vitro 3D tissue models in genotoxity testing: Strategic fit, validation status and way forward. Report of the working group from the 7th International Workshop on Genotoxicity Testing (IWGT). *Mutat Res Genet Toxicol Environ Mutagen*, *850-851*, 503135. https://doi.org/10.1016/j.mrgentox.2020.503135

Phillips, J. I., Green, F. Y., Davies, J. C., & Murray, J. (2010). Pulmonary and systemic toxicity following exposure to nickel nanoparticles. *Am J Ind Med*, *53*(8), 763-767. https://doi.org/10.1002/ajim.20855

Pietroiusti, A., Stockmann-Juvala, H., Lucaroni, F., & Savolainen, K. (2018). Nanomaterial exposure, toxicity, and impact on human health. *Wiley Interdiscip Rev Nanomed Nanobiotechnol*. https://doi.org/10.1002/wnan.1513

Polk, W. W., Sharma, M., Sayes, C. M., Hotchkiss, J. A., & Clippinger, A. J. (2016). Aerosol generation and characterization of multi-walled carbon nanotubes exposed to cells cultured at the air-liquid interface. *Part Fibre Toxicol*, *13*, 20. https://doi.org/10.1186/s12989-016-0131-y

Prasad, M., Kumar, R., Buragohain, L., Kumari, A., & Ghosh, M. (2021). Organoid Technology: A Reliable Developmental Biology Tool for Organ-Specific Nanotoxicity Evaluation. *Frontiers in cell and developmental biology*, *9*, 696668-696668. https://doi.org/10.3389/fcell.2021.696668

Prytherch, Z., & BéruBé, K. (2015). 3-dimensional cell and tissue culture models of the human respiratory system: Approaches for in vitro safety testing and drug discovery. http://orca.cardiff.ac.uk/id/eprint/76320

Prytherch, Z., Job, C., Marshall, H., Oreffo, V., Foster, M., & BéruBé, K. (2011). Tissue-Specific stem cell differentiation in an in vitro airway model. *Macromol Biosci*, *11*(11), 1467-1477. https://doi.org/10.1002/mabi.201100181

Punde, T. H., Wu, W. H., Lien, P. C., Chang, Y. L., Kuo, P. H., Chang, M. D., Lee, K. Y., Huang, C. D., Kuo, H. P., Chan, Y. F., Shih, P. C., & Liu, C. H. (2015). A biologically inspired lung-on-a-chip device for the study of protein-induced lung inflammation. *Integr Biol (Camb)*, *7*(2), 162-169. https://doi.org/10.1039/c4ib00239c

Rackley, C. R., & Stripp, B. R. (2012). Building and maintaining the epithelium of the lung. *J Clin Invest*, *122*(8), 2724-2730. https://doi.org/10.1172/jci60519

Raesch, S. S., Tenzer, S., Storck, W., Rurainski, A., Selzer, D., Ruge, C. A., Perez-Gil, J., Schaefer, U. F., & Lehr, C. M. (2015). Proteomic and Lipidomic Analysis of Nanoparticle Corona upon Contact with Lung Surfactant Reveals Differences in Protein, but Not Lipid Composition. *ACS Nano*, *9*(12), 11872-11885. https://doi.org/10.1021/acsnano.5b04215

Rahimi, R., Htwe, S. S., Ochoa, M., Donaldson, A., Zieger, M., Sood, R., Tamayol, A., Khademhosseini, A., Ghaemmaghami, A. M., & Ziaie, B. (2016). A paper-based in vitro model for on-chip investigation of the human respiratory system [10.1039/C6LC00866F]. *Lab on a Chip*, *16*(22), 4319-4325. https://doi.org/10.1039/C6LC00866F

Rothen-Rutishauser, B., Blank, F., Mühlfeld, C., & Gehr, P. (2008). In vitro models of the human epithelial airway barrier to study the toxic potential of

particulate matter. *Expert Opin Drug Metab Toxicol*, *4*(8), 1075-1089. https://doi.org/10.1517/17425255.4.8.1075

Sakolish, C. M., Esch, M. B., Hickman, J. J., Shuler, M. L., & Mahler, G. J. (2016). Modeling Barrier Tissues In Vitro: Methods, Achievements, and Challenges. *EBioMedicine*, *5*, 30-39. https://doi.org/10.1016/j.ebiom.2016.02.023

Sambale, F., Lavrentieva, A., Stahl, F., Blume, C., Stiesch, M., Kasper, C., Bahnemann, D., & Scheper, T. (2015). Three dimensional spheroid cell culture for nanoparticle safety testing. *J Biotechnol*, *205*, 120-129. https://doi.org/10.1016/j.jbiotec.2015.01.001

Savolainen, K., Alenius, H., Norppa, H., Pylkkänen, L., Tuomi, T., & Kasper, G. (2010). Risk assessment of engineered nanomaterials and nanotechnologies—a review. *Toxicology*, *269*(2-3), 92-104. https://doi.org/10.1016/j.tox.2010.01.013

Schmid, O., & Cassee, F. R. (2017). On the pivotal role of dose for particle toxicology and risk assessment: exposure is a poor surrogate for delivered dose. *Part Fibre Toxicol*, *14*(1), 52. https://doi.org/10.1186/s12989-017-0233-1

Schulz, H., Harder, V., Ibald-Mulli, A., Khandoga, A., Koenig, W., Krombach, F., Radykewicz, R., Stampfl, A., Thorand, B., & Peters, A. (2005). Cardiovascular effects of fine and ultrafine particles. *J Aerosol Med*, *18*(1), 1-22. https://doi.org/10.1089/jam.2005.18.1

Schuster, B. S., Suk, J. S., Woodworth, G. F., & Hanes, J. (2013). Nanoparticle diffusion in respiratory mucus from humans without lung disease. *Biomaterials*, *34*(13), 3439-3446. https://doi.org/10.1016/j.biomaterials.2013.01.064

Secondo, L. E., Liu, N. J., & Lewinski, N. A. (2017). Methodological considerations when conducting in vitro, air-liquid interface exposures to engineered nanoparticle aerosols. *Crit Rev Toxicol*, *47*(3), 225-262. https://doi.org/10.1080/10408444.2016.1223015

Seiffert, J., Buckley, A., Leo, B., Martin, N. G., Zhu, J., Dai, R., Hussain, F., Guo, C., Warren, J., Hodgson, A., Gong, J., Ryan, M. P., Zhang, J. J., Porter, A., Tetley, T. D., Gow, A., Smith, R., & Chung, K. F. (2016). Pulmonary effects of inhalation of spark-generated silver nanoparticles in Brown-Norway and Sprague-Dawley rats. *Respiratory research*, *17*(1), 85-85. https://doi.org/10.1186/s12931-016-0407-7

Shannahan, J. H., Kodavanti, U. P., & Brown, J. M. (2012). Manufactured and airborne nanoparticle cardiopulmonary interactions: a review of mechanisms and the possible contribution of mast cells. *Inhal Toxicol*, *24*(5), 320-339. https://doi.org/10.3109/08958378.2012.668229

Smith, J. R., Birchall, A., Etherington, G., Ishigure, N., & Bailey, M. R. (2014). A revised model for the deposition and clearance of inhaled particles in human extra-thoracic airways. *Radiat Prot Dosimetry*, *158*(2), 135-147. https://doi.org/10.1093/rpd/nct218

Smulders, S., Luyts, K., Brabants, G., Golanski, L., Martens, J., Vanoirbeek, J., & Hoet, P. H. (2015). Toxicity of nanoparticles embedded in paints compared to pristine nanoparticles, in vitro study. *Toxicol Lett*, *232*(2), 333-339. https://doi.org/10.1016/j.toxlet.2014.11.030

Steimer, A., Haltner, E., & Lehr, C.-M. (2005). Cell culture models of the respiratory tract relevant to pulmonary drug delivery. *Journal of aerosol medicine*, *18*(2), 137-182. https://doi.org/10.1089/jam.2005.18.137

Stone, K. C., Mercer, R. R., Gehr, P., Stockstill, B., & Crapo, J. D. (1992). Allometric relationships of cell numbers and size in the mammalian lung. *Am J Respir Cell Mol Biol*, *6*(2), 235-243. https://doi.org/10.1165/ajrcmb/6.2.235

Stone, V., Miller, M. R., Clift, M. J. D., Elder, A., Mills, N. L., Moller, P., Schins, R. P. F., Vogel, U., Kreyling, W. G., Alstrup Jensen, K., Kuhlbusch, T. A. J., Schwarze, P. E., Hoet, P., Pietroiusti, A., De Vizcaya-Ruiz, A., Baeza-Squiban, A., Teixeira, J. P., Tran, C. L., & Cassee, F. R. (2017). Nanomaterials Versus Ambient Ultrafine Particles: An Opportunity to Exchange Toxicology Knowledge. *Environmental health perspectives*, *125*(10), 106002. https://doi.org/10.1289/EHP424

Stucki, A. O., Stucki, J. D., Hall, S. R., Felder, M., Mermoud, Y., Schmid, R. A., Geiser, T., & Guenat, O. T. (2015). A lung-on-a-chip array with an integrated bio-inspired respiration mechanism. *Lab Chip*, *15*(5), 1302-1310. https://doi.org/10.1039/c4lc01252f

Tan, Q., Choi, K. M., Sicard, D., & Tschumperlin, D. J. (2017). Human airway organoid engineering as a step toward lung regeneration and disease modeling. *Biomaterials*, *113*, 118-132. https://doi.org/10.1016/j.biomaterials.2016.10.046

Teeguarden, J. G., Hinderliter, P. M., Orr, G., Thrall, B. D., & Pounds, J. G. (2007). Particokinetics in vitro: dosimetry considerations for in vitro nanoparticle

toxicity assessments. *Toxicol Sci*, *95*(2), 300-312. https://doi.org/10.1093/toxsci/kfl165

Theegarten, D., Boukercha, S., Philippou, S., & Anhenn, O. (2010). Submesothelial deposition of carbon nanoparticles after toner exposition: case report. *Diagn Pathol*, *5*, 77. https://doi.org/10.1186/1746-1596-5-77

Thiruvengadam, M., Rajakumar, G., & Chung, I. M. (2018). Nanotechnology: current uses and future applications in the food industry. *3 Biotech*, *8*(1), 74. https://doi.org/10.1007/s13205-018-1104-7

Thomas, R. J. (2013). Particle size and pathogenicity in the respiratory tract. *Virulence*, *4*(8), 847-858. https://doi.org/10.4161/viru.27172

Tippe, A., Heinzmann, U., & Roth, C. (2002). Deposition of fine and ultrafine aerosol particles during exposure at the air/cell interface. *J Aerosol Sci*, *33*(2), 207-218. https://doi.org/10.1016/S0021-8502(01)00158-6

Tsuda, A., Henry, F. S., & Butler, J. P. (2013). Particle transport and deposition: basic physics of particle kinetics. *Compr Physiol*, *3*(4), 1437-1471. https://doi.org/10.1002/cphy.c100085

Upadhyay, S., & Palmberg, L. (2018). Air-Liquid Interface: Relevant In Vitro Models for Investigating Air Pollutant-Induced Pulmonary Toxicity. *Toxicol Sci*, *164*(1), 21-30. https://doi.org/10.1093/toxsci/kfy053

Urban, D. A., Rodriguez-Lorenzo, L., Balog, S., Kinnear, C., Rothen-Rutishauser, B., & Petri-Fink, A. (2016). Plasmonic nanoparticles and their characterization in physiological fluids. *Colloids Surf B Biointerfaces*, *137*, 39-49. https://doi.org/10.1016/j.colsurfb.2015.05.053

Wang, G., Zhang, X., Liu, X., Zheng, J., Chen, R., & Kan, H. (2019). Ambient fine particulate matter induce toxicity in lung epithelial-endothelial co-culture models. *Toxicol Lett*, *301*, 133-145. https://doi.org/10.1016/j.toxlet.2018.11.010

Wang, Y., Adamcakova-Dodd, A., Steines, B. R., Jing, X., Salem, A. K., & Thorne, P. S. (2020). Comparison of in vitro toxicity of aerosolized engineered nanomaterials using air-liquid interface mono-culture and co-culture models. *NanoImpact*, *18*, 100215. https://doi.org/10.1016/j.impact.2020.100215

Weibel, E. R., Sapoval, B., & Filoche, M. (2005). Design of peripheral airways for efficient gas exchange. *Respir Physiol Neurobiol*, *148*(1-2), 3-21. https://doi.org/10.1016/j.resp.2005.03.005

Whitsett, J. A., & Alenghat, T. (2015a). Respiratory epithelial cells orchestrate pulmonary innate immunity. *Nat Immunol*, *16*(1), 27-35. https://doi.org/10.1038/ni.3045

Whitsett, J. A., & Weaver, T. E. (2015b). Alveolar development and disease. *Am J Respir Cell Mol Biol*, *53*(1), 1-7. https://doi.org/10.1165/rcmb.2015-0128PS

Wick, P., Chortarea, S., Guenat, O. T., Roesslein, M., Stucki, J. D., Hirn, S., Petri-Fink, A., & Rothen-Rutishauser, B. (2015). In vitro-ex vivo model systems for nanosafety assessment. *European Journal of Nanomedicine*, *7*(3), 169-179. https://doi.org/10.1515/ejnm-2014-0049

Wiemann, M., Vennemann, A., Sauer, U. G., Wiench, K., Ma-Hock, L., & Landsiedel, R. (2016). An in vitro alveolar macrophage assay for predicting the short-term inhalation toxicity of nanomaterials. *J Nanobiotechnology*, *14*, 16. https://doi.org/10.1186/s12951-016-0164-2

Wilkinson, D. C., Alva-Ornelas, J. A., Sucre, J. M. S., Vijayaraj, P., Durra, A., Richardson, W., Jonas, S. J., Paul, M. K., Karumbayaram, S., Dunn, B., & Gomperts, B. N. (2016). Development of a Three-Dimensional Bioengineering Technology to Generate Lung Tissue for Personalized Disease Modeling. *Stem Cells Translational Medicine*, *6*(2), 622-633. https://doi.org/10.5966/sctm.2016-0192

Wohlleben, W., Driessen, M. D., Raesch, S., Schaefer, U. F., Schulze, C., Vacano, B., Vennemann, A., Wiemann, M., Ruge, C. A., Platsch, H., Mues, S., Ossig, R., Tomm, J. M., Schnekenburger, J., Kuhlbusch, T. A., Luch, A., Lehr, C. M., & Haase, A. (2016). Influence of agglomeration and specific lung lining lipid/protein interaction on short-term inhalation toxicity. *Nanotoxicology*, *10*(7), 970-980. https://doi.org/10.3109/17435390.2016.1155671

Wu, W.-T., Li, L.-A., Tsou, T.-C., Wang, S.-L., Lee, H.-L., Shih, T.-S., & Liou, S.-H. (2019). Longitudinal follow-up of health effects among workers handling engineered nanomaterials: a panel study. *Environmental Health*, *18*(1), 107. https://doi.org/10.1186/s12940-019-0542-y

Yamamoto, Y., Gotoh, S., Korogi, Y., Seki, M., Konishi, S., Ikeo, S., Sone, N., Nagasaki, T., Matsumoto, H., Muro, S., Ito, I., Hirai, T., Kohno, T., Suzuki, Y., & Mishima, M. (2017). Long-term expansion of alveolar stem cells derived from human iPS cells in organoids. *Nature Methods*, *14*(11), 1097-1106. https://doi.org/10.1038/nmeth.4448

Yang, X., Li, K., Zhang, X., Liu, C., Guo, B., Wen, W., & Gao, X. (2018). Nanofiber membrane supported lung-on-a-chip microdevice for anti-cancer drug

testing. *Lab on a Chip*, *18*(3), 486-495. https://doi.org/10.1039/C7LC01224A

Zacharias, W. J., Frank, D. B., Zepp, J. A., Morley, M. P., Alkhaleel, F. A., Kong, J., Zhou, S., Cantu, E., & Morrisey, E. E. (2018). Regeneration of the lung alveolus by an evolutionarily conserved epithelial progenitor. *Nature*, *555*(7695), 251-255. https://doi.org/10.1038/nature25786

Zanoni, M., Cortesi, M., Zamagni, A., Arienti, C., Pignatta, S., & Tesei, A. (2020). Modeling neoplastic disease with spheroids and organoids. *Journal of Hematology & Oncology*, *13*(1), 97. https://doi.org/10.1186/s13045-020-00931-0

Zhang, F., Aquino, G. V., Dabi, A., & Bruce, E. D. (2019). Assessing the translocation of silver nanoparticles using an in vitro co-culture model of human airway barrier. *Toxicol In Vitro*, *56*, 1-9. https://doi.org/10.1016/j.tiv.2018.12.013

Zhang, M., Xu, C., Jiang, L., & Qin, J. (2018). A 3D human lung-on-a-chip model for nanotoxicity testing. *Toxicol Res*, *7*(6), 1048-1060. https://doi.org/10.1039/C8TX00156A

Workers dealing with advanced ceramic technologies may be at (increased) risk of exposure to a broad variety of airborne (nano)particles. Indeed, not only nanoscale powders are being used for ceramics production, but also in the high-temperature processing of ceramic materials, there is a high potential for particle release into the workplace environment. Nevertheless, the inhalation hazard of these airborne particles remains poorly understood.

The main goal of the present work was to investigate the *in vitro* toxicity of occupationally relevant doses of airborne (nano)particles relevant to the ceramic industry: i) process-generated fine particles (PGFP; <2.5 µm MMAD) and NP (PGNP; <0.2 µm MMAD) collected at an industrial-scale metallurgy workshop during two widely employed thermal spraying processes for ceramic coating of metallic surfaces - atmospheric plasma spraying (APS) and high velocity oxy-fuel spraying (HVOF)-, and ii) ENP used as input materials for ceramics manufacture, in particular metal oxide NP that are amongst the most used [tin oxide (SnO_2), antimony-tin oxide (ATO; $Sb_2O_3 \bullet SnO_2$), cerium oxide (CeO_2) and zirconium oxide (ZrO_2)] (**Figure 2**).
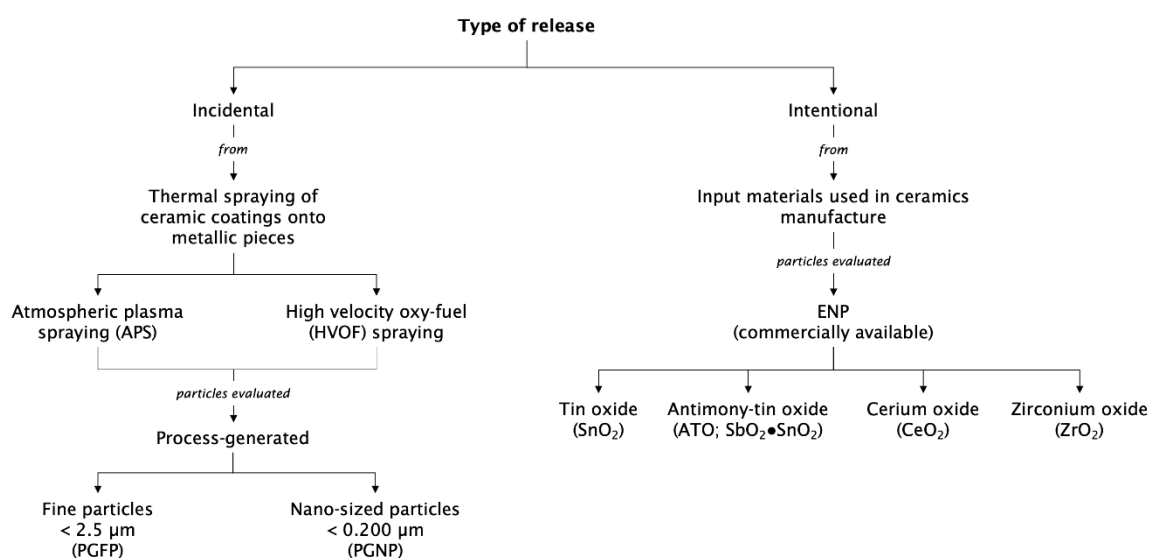

Figure 2. Schematic representation of the (nano)particles studied in the present work.

In this thesis, two human respiratory *in vitro* models of different complexity were selected for airborne particle toxicity testing: i) alveolar epithelial A549 cells, a widely used lung model for toxicity testing, and ii) reconstituted epithelia from upper airways 3D cultures (MucilAir™). The exposure conditions can considerably

affect the (nano)particles' toxicological potential. Accordingly, cells were exposed to liquid suspensions of the airborne particles under the traditional submerged conditions or to the aerosolised particles at the air-liquid interface (ALI), a more realistic approach for assessing the toxicity of airborne particles *in vitro*.

To achieve the proposed main goal, specific objectives were established as follows:

1.   To characterise the physicochemical properties of the airborne particles emitted during APS and HVOF spraying of ceramic coatings onto metallic surfaces and of the selected ENP;

2.   To optimise the harvesting and freezing procedures of human cells for DNA damage analysis using the comet assay;

3.   To investigate the toxicity of APS- and HVOF-derived particles (PGFP and PGNP fractions) in human alveolar epithelial-like cultures exposed under submerged conditions;

4.   To investigate and compare the toxicity of ENP in human alveolar epithelial-like cultures exposed under submerged *vs* ALI conditions;

5.   To assess and compare the toxicity of process-generated particles (PGFP and PGNP fractions) and ENP in advanced 3D cultures of human upper airway epithelium (MucilAir™) under ALI conditions;

6.   To compare the hazard of APS- and HVOF-derived particles (PGFP and PGNP fractions) with ENP.

Chapter II.

Original Research

A. Process-Generated (Nano)Particles: Collection, Sampling and Characterisation

Herein is presented an original research paper on the collection, sampling and characterisation of airborne particles incidentally released during high-energy industrial processes of thermal spraying of ceramic coatings at an industrial-scale metallurgy workshop (Chapter II, section A.1.). Two high-energy thermal spraying processes were appraised: i) APS, which is characterised by high temperatures and lower projection velocities, in this particular case of two feedstock materials containing a titanium oxide (TiO_2) – aluminium oxide (Al_2O_3) blend and a chromium (Cr) – nickel (Ni) blend; and ii) HVOF, which is characterised by lower temperatures but higher velocities, and where a feedstock material containing tungsten carbide (WC) – chromium carbon (CrC) – Ni – cobalt (Co) blend was used. The collected PGFP and PGNP fractions were tested for toxicity using conventional human alveolar epithelial-like cultures and advanced human 3D upper airway epithelium (MucilAir™) cultures (Chapter II, Section B.).

A.1. Characterising the chemical profile of incidental ultrafine particles using an aerosol concentrator

Viana M., Salmatonidis A., Bezantakos S., Ribalta C., Moreno N., Córdoba P., Cassee F. R., Boere J., Fraga S., Teixeira J. P., Bessa M. J., & Monfort E.

The PhD candidate contributed for the reviewing and editing of the manuscript.

BOHS
The Chartered Society for
Worker Health Protection

OXFORD

Original Article

Characterizing the Chemical Profile of Incidental Ultrafine Particles for Toxicity Assessment Using an Aerosol Concentrator

M. Viana[1],[*],[○], A. Salmatonidis[1], S. Bezantakos[2], C. Ribalta[1], N. Moreno[1],[○],
P. Córdoba[1], F.R. Cassee[3], J. Boere[3], S. Fraga[4],[5], J.P. Teixeira[4],[5], M.J. Bessa[4],[5]
and E. Monfort[6]

[1]IDAEA-CSIC, Barcelona, Spain [2]Université du Littoral Côte d' 'Opale, Dunkerque, France [3]RIVM, Bilthoven, The Netherlands [4]Department of Environmental Health, National Institute of Health Dr Ricardo Jorge, Porto, Portugal [5]EPIUnit-Instituto de Saúde Pública, Universidade do Porto, Porto, Portugal [6]ITC, Castellón, Spain

* Author to whom correspondence should be addressed. E-mail: mar.viana@idaea.csic.es

Abstract

Incidental ultrafine particles (UFPs) constitute a key pollutant in industrial workplaces. However, characterizing their chemical properties for exposure and toxicity assessments still remains a challenge. In this work, the performance of an aerosol concentrator (Versatile Aerosol Concentration Enrichment System, VACES) was assessed to simultaneously sample UFPs on filter substrates (for chemical analysis) and as liquid suspensions (for toxicity assessment), in a high UFP concentration scenario. An industrial case study was selected where metal-containing UFPs were emitted during thermal spraying of ceramic coatings. Results evidenced the comparability of the VACES system with online monitors in terms of UFP particle mass (for concentrations up to 95 μg UFP/m^3) and between filters and liquid suspensions, in terms of particle composition (for concentrations up to 1000 μg/m^3). This supports the applicability of this tool for UFP collection in view of chemical and toxicological characterization for incidental UFPs. In the industrial setting evaluated, results showed that the spraying temperature was a driver of fractionation of metals between UF (<0.2 μm) and fine (0.2–2.5 μm) particles. Potentially health hazardous metals (Ni, Cr) were enriched in UFPs and depleted in the fine particle fraction. Metals vaporized at high temperatures and concentrated in the UF fraction through nucleation processes. Results evidenced the need to understand incidental particle formation mechanisms due to their direct implications on particle composition and, thus, exposure. It is advisable that personal exposure and subsequent risk assessments in occupational settings should include dedicated metrics to monitor UFPs (especially, incidental).

What's important about this paper

Our work addresses the challenge of characterizing the bulk chemical composition of ultrafine particles in occupational settings, for exposure and toxicity assessments. We tested the performance of an aerosol concentrator (VACES) to simultaneously sample ultrafine particles (UFPs) on filter substrates and as liquid suspensions, in a high UFP concentration scenario. An industrial case study was selected where metal-bearing UFPs were emitted. We report the chemical exposures characterized in the industrial facility, and evidence the comparability of the VACES system with online monitors for UFP particle mass (up to 95 µg UFP/m³) as well as between UFP chemical composition on filters and in suspension. This supports the applicability of this tool for UFP collection in view of chemical and toxicological characterization of exposures to incidental UFPs in workplace settings.

Graphical Abstract
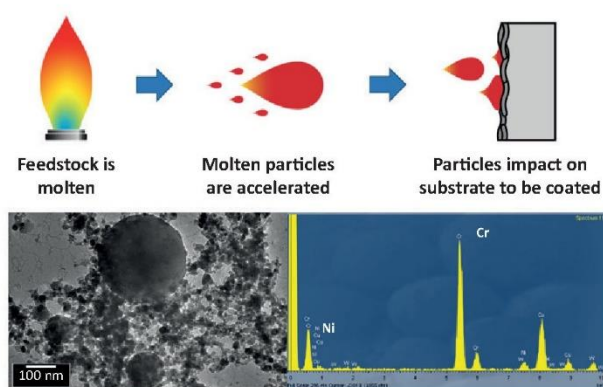
Keywords: morphology; new particle formation; metal nanoparticles; nanoparticles; occupational; versatile aerosol concentrator; workplace

Highlights

- The VACES system is a useful tool for UFP sampling in high-concentration settings.
- UFP collected simultaneously on filters and in suspension showed good comparability.
- UFP chemical profiles were characterized.
- Health-hazardous metals Ni and Cr accumulated in UFPs.
- Understanding emission mechanisms is key to identifying exposure sources.

Introduction

While the adverse health effects and burden of exposure to coarse and fine atmospheric particles are described in detail in the literature (Lelieveld *et al.*, 2015; Cohen *et al.*, 2017; Burnett *et al.*, 2018; Pope et al., 2019; among others), significant gaps still remain regarding nanoparticles (NPs) and ultrafine particles (UFPs, <100 nm) despite their ability to penetrate deeper in the respiratory tract (Oberdörster, 2001; Oberdörster *et al.*,

2007). UFPs are a key pollutant in urban and industrial areas, in occupational and ambient air, resulting from anthropogenic sources such as internal combustion engines and other sources of thermo-degradation (Terzano *et al.*, 2010; Morawska *et al.*, 2017).

In occupational industrial settings, efforts to evaluate environmental health and safety implications of UFP are frequently based on physical particle properties such as particle number concentration or size distribution (Gonzalez-Pech *et al.*, 2019; Oberbek *et al.*, 2019; among

others). When referring to engineered nanomaterials (ENMs), the body of literature reporting physical properties is large (Maynard *et al.*, 2004; Maynard and Aitken, 2007; Hämeri *et al.*, 2009; Kuhlbusch *et al.*, 2011; Brouwer *et al.*, 2012; Hristozov *et al.*, 2012; Falk *et al.*, 2016; among many others). However, chemical properties (e.g. metal content) and sources are also determinants of health risks (Perrone *et al.*, 2010; Billet *et al.*, 2018; Shao *et al.*, 2018; Gerlofs-Nijland *et al.*, 2019). Literature on workplace UFP chemical composition is currently relatively scarce (Ntziachristos *et al.*, 2007; Terzano *et al.*, 2010; Viana et al., 2015, 2014; Corsini *et al.*, 2017; Ozgen *et al.*, 2017; Mendes *et al.*, 2018; Gonzalez-Pech *et al.*, 2019), one of the reasons being that it is frequently difficult to obtain enough released material for a proper characterization and more so for toxicological testing (Kuhlbusch *et al.*, 2018). As a result, the characterization of bulk UFP chemical composition for exposure and toxicity assessments still remains a challenge, evidenced by an increasing interest in assessing the concentrations and physico-chemical properties of incidental UFPs in workplaces (Curwin and Bertke, 2011; Stone *et al.*, 2017; Viitanen *et al.*, 2017; Gonzalez-Pech *et al.*, 2019; Keyter *et al.*, 2019).

The present work aimed to assess the applicability of a Versatile Aerosol Concentration Enrichment System (VACES; Kim *et al.*, 2001; Geller *et al.*, 2002; Freney *et al.*, 2006; Liu *et al.*, 2019) for collection of airborne UFPs in occupational settings, in view of UFP toxicity assessment (reported elsewhere, Bessa *et al.*, 2021). The case study selected was a thermal spraying facility where two different types of technologies were used to spray ceramic coatings (Salmatonidis *et al.*, 2019a), in the framework of SIINN-ERANET project CERASAFE (Safe Production and Use of Nanomaterials in the Ceramic Industry). Advanced ceramic materials and processing technologies have a strong potential for incidental formation and release of UFP into workplace air (Fonseca *et al.*, 2015; Viana *et al.*, 2017; Ribalta *et al.*, 2019b; Salmatonidis et al., 2019a, 2019b; Bessa *et al.*, 2020). The use of the VACES system provided a unique opportunity to collect particles, simultaneously, on filter substrates for chemical characterization and as suspensions for toxicity assessments (discussed elsewhere; Bessa *et al.*, 2021). The target analyses (in this case, toxicity and chemical characterization) determine the need for different sample preparations (Stone *et al.*, 2017). In addition to testing the applicability of the tool, our work aimed to generate new information on the chemical composition of incidental metallic UFPs, as well as of fine (PM$_{2.5}$) and coarse (PM$_{2.5-10}$) aerosols, emitted during plasma spraying of ceramic materials onto metal substrates. The results obtained contribute to the growing body of literature on

chemical profiling of occupational exposures to incidental UFPs, specifically of metal-containing UFPs, and provide the basis for toxicity and subsequent risk assessment of the particles emitted during this kind of industrial activity. Studies on exposure to incidental UFP in occupational settings are paramount for the design of effective health and safety protocols, which should include incidental UFPs as a key potential health risk.

Materials and methods

Site description

Measurements were carried out at an industrial-scale metallurgy workshop (T.M. Comas) in the vicinity of Barcelona (Spain), in November 2017. Particle emissions were monitored during spraying of ceramic powders onto metal surfaces to produce thermal-resistant coatings (Ribalta *et al.*, 2019a; Salmatonidis *et al.*, 2019a). The spraying activities were representative of the usual operating conditions in the plant, which were concurrent to other activities (welding, laser cladding, among others) in nearby sections of the plant. The layout of the spraying facilities is described in Fig. 1: three spraying booths were located in an area of approximately 240 m² (14 m wide × 17 m in length), including a central area for worker transit (referred to as the worker area). The operators worked both inside and outside the booths during spraying. The booth doors were frequently open while spraying due to the need to introduce new pieces to be coated. Workers wore personal protective equipment (FFP3 masks) inside the booths but removed them every time they stepped in the worker area. As a result, they were exposed to particles originating inside the booths and to those transported and formed in the worker area.

The operational characteristics of each of the spraying activities and booths are reported elsewhere (Ribalta *et al.*, 2019b; Salmatonidis *et al.*, 2019a). The main difference between booths #1 and #3, relevant for this work, are:

- Booth #1: high spraying temperatures (5–20 × 10³°C) and low spraying velocities (200–500 m/s). Spraying technique: atmospheric plasma spraying (APS).
- Booth #3: high spraying velocities (425–1500 m/s) and lower temperatures (2.9 × 10³°C). Spraying technique: high velocity oxy fuel (HVOF).

Ultrafine particle sampling, characterization and monitoring

A VACES (Kim *et al.*, 2001; Geller *et al.*, 2002; Liu *et al.*, 2019) was used to collect aerosols in three size fractions: coarse (PM$_{2.5-10}$), fine + UF (PM$_{2.5}$) and quasi-UF
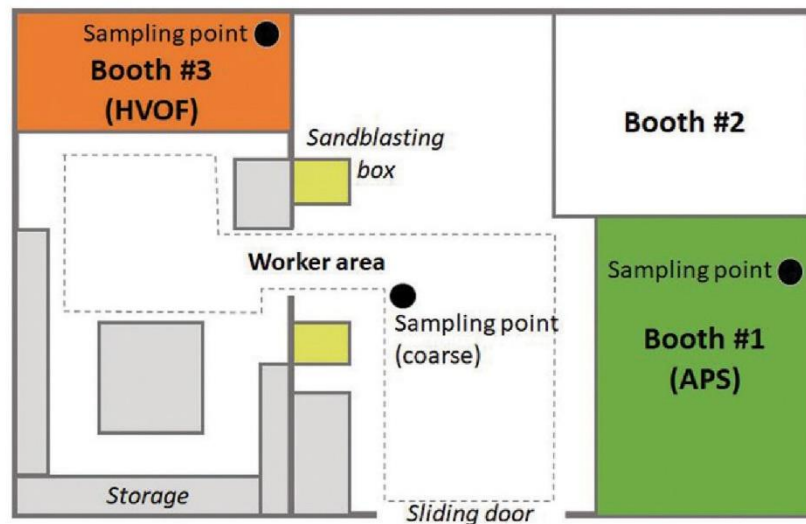
Figure 1. Schematic representation of the thermal spraying facility.

(<0.2 µm; referred to as UF in this manuscript) particles. The fine particle mass concentrations were calculated indirectly by subtraction of the UF from the fine + UF size fraction. In short, a single-nozzle virtual impactor collects the coarse fraction, whereas the fine fraction is collected by drawing air samples through two parallel lines. The fine size fractions go through a saturation–condensation system, which grows particles to 2–3 µm droplets, and then concentrate them by virtual impaction (Liu *et al.*, 2019). The VACES system has been validated for ambient aerosol (Kim *et al.*, 2001; Ning *et al.*, 2006; Ntziachristos *et al.*, 2007) and at (relatively low) UFP mass concentrations (e.g. 2.7 µg/m³; Ntziachristos *et al.*, 2007). The present work presents an application in indoor air and for high UFP concentrations (up to 95 µg/m³; see Section 3.1).

The VACES enriches ambient particles by a factor of 20–40, depending on the output flow rate required (Ntziachristos *et al.*, 2007). In the present study, the VACES operated at 110 l/min, resulting in a concentration enrichment factor of 31. The experimental enrichment factor of the VACES is similar to what theoretically expected, based on its operating flows, for all particles sizing above 50 nm, irrespective of whether they are hydrophobic or not (Kim *et al.*, 2001). Time-integrated aerosol samples were collected over 8-hr shifts from indoor air: fine and UF particles were collected directly from inside the spraying booths, and the coarse fraction was sampled from the worker area given that no primary coarse particle emissions were expected to be generated inside the booths. Even if particle agglomeration were considered due to the high particle number

emissions, this was not expected to result in coarse mode particles inside the booths. Particle samples were collected simultaneously on Teflon filters for elemental analysis and gravimetric determination. and in a BioSampler (SKC Inc.) using de-ionized water (the sample flowing directly through the liquid) for toxicity testing (Bessa *et al.*, 2021). Additional sets of Teflon filters were placed after the BioSamplers to collect aerosols potentially not retained in the sampler due to lower sampling efficiency linked to particle size and/or composition. Particle losses in the biosamplers ranged between 1.8 and 4.6%, lower than the usual 5%. In total, 18 filter samples (8-h) were collected: 6 from booth #1 (three collecting the concentrated aerosol flow and three downstream of the BioSampler), and 12 from booth #3 (same as in booth #1, on two different days). The complexity of the VACES instrument and the need to minimize any interference with the plant's production process limited the collection of a larger number of samples, as is usual in occupational real-world studies. However, the industrial production monitored is typically repetitive and the samples collected are considered fully representative of the 8-hr shifts. Based on the limited data availability, the comparisons between different cases (e.g. booths, Figs. 2, 3 and 6) should be considered descriptive and not based on statistical analyses.

Particle mass concentrations were determined on the Teflon filters after conditioning at constant temperature and relative humidity by gravimetry (microbalance XP105DR Mettler Toledo; sensitivity ±10 µg). Filters were then acid digested (5 ml HF, 2.5 ml HNO₃, 2.5 ml HClO₄) according to Querol *et al.* (2001) and the
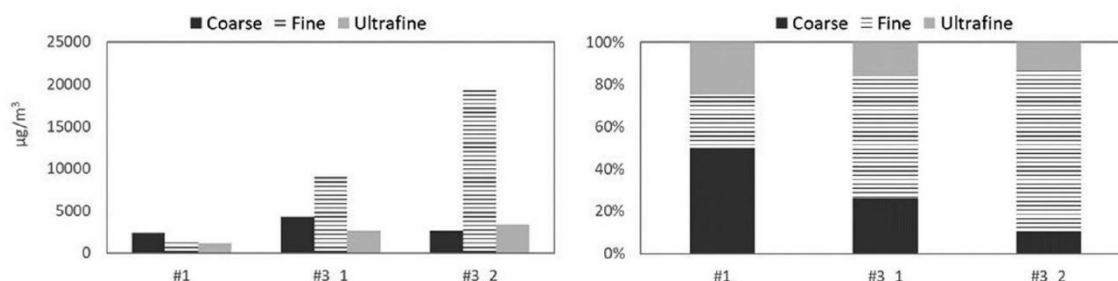
Figure 2. Absolute and relative particle mass contributions from the size fractions measured (coarse, fine and UF) to the total aerosol mass. Concentrations reported in the y-axis as measured (concentrated, by a factor of 31; µg/m³). The x-axis shows the three 8-h aerosol samples collected (sample #1 during APS spraying in booth #1, and samples #3_1 and #3_2 during HVOF spraying in booth #3 on two different days).
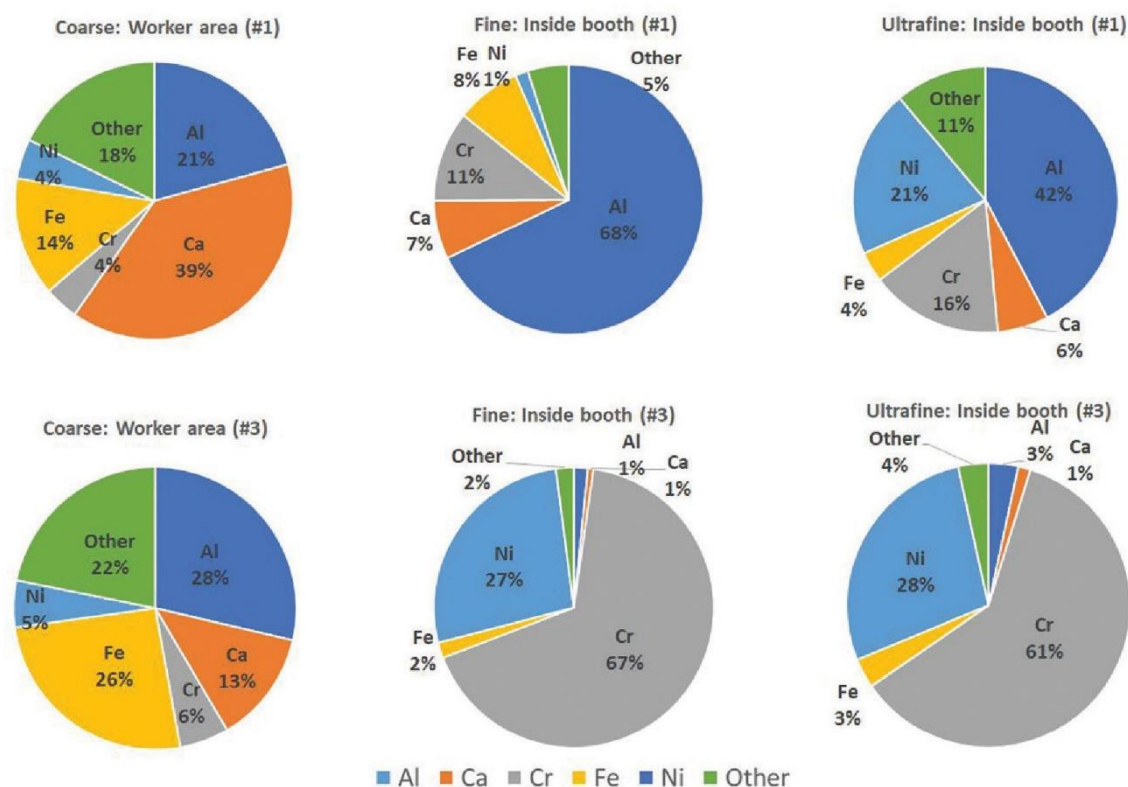

Figure 3. Size-resolved chemical composition (in %) of coarse, fine and UF particles in the worker area and inside the spraying booths.

extracts analysed by Inductively Coupled Plasma Mass Spectrometry (ICP-MS) and Inductively Couple Plasma Optical Emission Spectrometry (ICP-OES). The elemental composition was also determined directly on the Teflon filters by Energy Dispersive X-Ray Fluorescence Spectrometer (EDXRF). Three different analytical techniques were used for quality-control purposes. The elements determined were Li, Ti, V, Cr, Mn, Co, Ni, Cu,

Zn, As, Se, Rb, Sr, Y, Zr, Nb, Mo, Cd, Sn, Sb, Cs, Ba, La, Ce, W, Tl and Pb. Finally, particle morphology was characterized by Transmission Electron Microscopy (TEM) at the Barcelona University.

In parallel to particle collection, particle mass, number concentrations and size distributions were recorded continuously with a NanoScan-SMPS (Nanoscan SMPS Nanoparticle Sizer 3910, TSI Inc. USA; 10–420 nm; 60-s

99

time resolution) and a MiniWRAS aerosol spectrometer (Mini Wide Range Aerosol Spectrometer model 1371, GRIMM Aerosol Technik Ainring GmbH & Co.; 10 nm to 35 µm; 6-s time resolution). The results from the online measurements carried out in the plant are reported elsewhere (Ribalta *et al.*, 2019b; Salmatonidis *et al.*, 2019a).

Feedstock characterization

A portion of the raw feedstock materials was acid-digested in duplicate by using a two-step digestion method devised by Querol *et al.* (2001) to retain volatile elements. This consisted of weighing ca. 0.1 g powdered sample into a PFTE vial and adding Primar grade concentrated HNO_3 to pre-digest the organic fraction. This was followed by addition of concentrated Primar grade HF: HNO_3:$HClO_4$ mixture and evaporation on a hot plate at 240°C, the purpose being digestion of mineral phases. The concentrations of major elements in the acid digests were determined using Inductively Coupled Plasma Atomic-Emission Spectrometry (ICP-AES, Iris advantage Radial ER/S device from Thermo Jarrell-Ash). Trace elements were analysed by Inductively Coupled Plasma Mass Spectrometry (ICP-MS, X-SERIES II Thermo Fisher Scientific, Bremen, Germany), operating the instrument with a collision cell to remove spectral interferences and using 10 µg L-1 In as internal standard.

Results and discussion

Particle mass and number concentrations

Size-resolved particle mass concentrations sampled with the aerosol concentrator are reported in Fig. 2, for the three 8-h aerosol samples collected (sample #1 during APS spraying in booth #1, and samples #3_1 and #3_2 during HVOF spraying in booth #3 on two different days). High particle mass concentrations were collected, with the fine fraction reaching up to 19 mg/m³ (sample #3_2) while the highest UF mass concentration was 3 mg/m³ (#3_2) and the highest coarse concentration, 4 mg/m³ (#3_1) (Fig. 2, left). Assuming an aerosol concentration factor of 31 as reported by Kim *et al.* (2001), this would result in mean 8-h concentrations of up to 95, 600 and 130 µg/m³ for the UF, fine and coarse fractions, respectively. These concentrations are higher yet comparable to those reported e.g. during welding (a foundry and a machining centre; 37–54 µg UFP/m³; Gonzalez-Pech *et al.*, 2019). As shown in Fig. 2 (right), the coarse fraction was highest in relative terms in the worker area when spraying was active in booth #1 while the fine fraction was clearly dominant during spraying inside booth #3. Despite this, the high UF mass concentrations measured should be highlighted (95 µg/m³ as 8-h mean), especially due to their metal content (described below). The mean mass concentrations measured are comparable to concentrations monitored with online instruments during the same activity in other periods of time (PM₁ between 61 µg m³ booth #1 and 640 µg m³ in booth #3; Salmatonidis *et al.*, 2019a), which confirms the representativeness of the aerosol samples collected and the validity of the VACES system (in terms of mass concentrations) for high exposure scenarios. The larger contribution of coarse particles in the worker area during spraying in booth #1, compared to those from booth #3, is consistent with the major particle emission
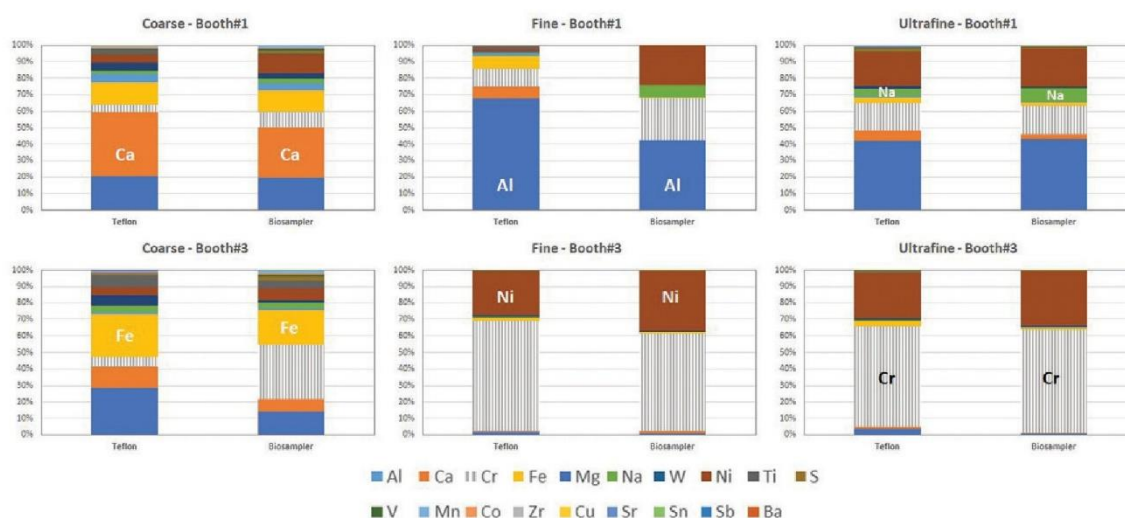

Figure 6. Relative chemical composition of coarse, fine and UF particles collected on Teflon filter substrates and in the biosamplers. Key elements are highlighted to facilitate reading.

Table 1. Element concentrations (in µg/m³) in coarse, fine and UF particles emitted from booths #1 and #3. The fine fraction was calculated indirectly from the fine + UF and UF fractions. Aerosol concentration factor: 31.

Fraction	Coarse	Coarse	Fine + UF	Fine + UF	Fine	Fine	UF	UF
Booth	#1	#3	#1	#3	#1	#3	#1	#3
Feedstock	Al/Ti/Cr/Ni	Ni/Cr/Co/W	Al/Ti/Cr/Ni	Ni/Cr/Co/W	Al/Ti/Cr/Ni	Ni/Cr/Co/W	Al/Ti/Cr/Ni	Ni/Cr/Co/W
Al	139	252	379	133	232	93	147	40
Ca	260	113	45	52	24	36	22	16
Cr	27	50	93	4534	37	3825	56	709
Fe	93	226	39	141	27	102	13	39
Mg	34	14	9.1	7.0	5.5	4.7	3.7	2.3
Na	12	35	16	21	1.6	15	15	5
W	33	54	8.4	73	2.5	58	5.9	14
Ni	31	47	76	1864	5.3	1539	71	325
Ti	16	63	7	32	5	24	2	8
S	5.6	6.9	4.8	6.9		2.1	7.5	4.8
V	0.20	0.40	0.08	0.80	0.05	0.66	0.03	0.14
Mn	1.9	2.9	2.2	3.3	0.69	2.22	1.5	1.1
Co	4.2	4.9	1.4	8.7	0.3	7.4	1.1	1.4
Zr	4.0	5.4	1.1	1.8	0.56	1.25	0.49	0.54
Cu	1.9	2.0	0.7	1.5	0.25	0.84	0.40	0.66
Sr	0.41	0.38	0.09	0.17	0.07	0.13	0.03	0.04
Sn	3.2	2.5	1.9	2.2	0.01	0.71	1.9	1.5
Sb	0.4	0.3	0.2	0.3	<0.01	0.08	0.3	0.2
Ba	1.2	1.1	0.3	0.41	<0.01	<0.01	0.01	<0.01
Sum	*668*	*882*	*686*	*6883*	*341*	*5713*	*348*	*1169*
Mass	*2377*	*3446*	*2378*	*17328*	*121.3*	*14344*	*1165*	*2985*
% det.	*28%*	*26%*	*29%*	*40%*	*28%*	*40%*	*30%*	*39%*

101

mechanisms (hypersonic impaction *vs.* melting/fusion of the feedstock material; Salmatonidis *et al.*, 2019a).

Chemical composition of the concentrated aerosol

Size-resolved particle chemical composition (in µg/m³), determined by ICP-MS and ICP-OES, is presented in Fig. 3 and Table 1 (mean results for both sampling days are presented for booth #3). The elemental composition was also determined by XFR for quality-control purposes. The inter-comparison between both analytical methods provided good results for the majority of the elements analysed, with especially high intra-method correlations for Ca, Fe, Ti, Cr, Sr, Co, Ni, W, Zn and Pb ($R^2 > 0.98$; Fig. S1 in Supporting Information), which include the main tracers of the feedstock materials sprayed (Table S1 in Supporting Information). Based on this quality control, for the following analyses the data obtained by ICP-MS and ICP-OES were used. The elemental composition analysed accounted for 26–40% of the aerosol mass determined by gravimetry (Table 1), with carbonaceous species (elemental and organic carbon), secondary inorganic species (SO_4^{2-}, NO_3^-, NH_4^+) and water accounting for the remaining aerosol mass.

Different results were obtained for the coarse fraction, on the one hand, and the fine and UF fractions, on the other (Fig. 3). UF particle composition was dominated by the elemental composition of the feedstock: in booth #1 (feedstocks ANVAL 50/50, Cr/Ni and Amdry 6228, Al_2O_3+TiO_2), major contributions were detected from Al (147 µg/m³; Table 1), Cr (56 µg/m³) and Ni (71 µg/m³); while in booth #3 (feedstock Woka 3702-1, WC, CrC, Ni, Co) the dominant elements were Cr (709 µg/m³) and Ni (325 µg/m³). Once again, the high mass concentrations of potentially health-hazardous metals measured in UFPs should be highlighted as an exposure risk in this occupational setting. The composition of the feedstock materials was obtained from the product technical specification sheets (Table S1) and from direct quantification in the laboratory (Table S2). Contributions were also detected from S to the UF fraction, which were low in comparison to other elements but high in absolute terms (4.8–7.5 µg/m³).

The chemical composition of the fine and UF fractions was highly similar during spraying in booth #3, whereas significant differences between both size fractions were observed for aerosols generated inside booth #1. In booth #1, UF particles were made up by 42% of Al, 20% of Ni and 16% of Cr, as expected based on the feedstock powders composition (Table S1). Conversely, fine particles (0.2–0.25 µm) were strongly enriched in Al (68%) and depleted in Cr (from 56 µg/m³ to 37 µg/m³ in

UF and fine particles, respectively) and Ni (from 71 µg/m³ in UF to 5 µg/m³ in fine particles), in comparison to UFPs. The reason for this different size-resolved composition could be the spraying temperature: spraying in booth #1 is characterized by high temperatures at the nozzle (5–20×10³°C), which are above the vaporization temperatures of both Ni (2800°C) and Cr (2650°C). Therefore, Ni and Cr probably volatilized during spraying in booth#1. After volatilization, the presence of Ni and Cr in UF particles could be explained as resulting from new particle formation due to condensation of the gaseous components (Byeon *et al.*, 2008), which would also explain the low concentration of these elements in fine particles. UF particle agglomerates formed by spherical Cr/Ni particles (<20 nm primary particle size; Fig. 4a) support this hypothesis. This would not be the case for booth #3, where spraying temperatures were lower at the nozzle (2.9 × 10³°C). Thus, it may be concluded that the metal content (and potential toxicity) of the UF size fraction in booth#1 was enhanced by the spraying temperature, which was not the case in booth #3. These results highlight the relevance of understanding the specifics of the particle formation mechanisms of incidental particles, as these have major and direct implications on particle composition and, thus, exposure.

Aside from this new-particle formation mechanism, UF particles containing Ni and Cr were released in both booths through fugitive emissions during handling of the feedstock powders and/or through hypersonic impaction on the surface being coated (as reported in Salmatonidis *et al.*, 2019a), which resulted in irregular-shaped particles. These were observed during spraying in booth #3 (with lower spraying temperatures, Fig. 4b) but also in booth #1 (Fig. 4c).

The case of Al requires further research: while it vaporized during spraying in booth #1 (vaporization temperature = 2327°C) and was detected forming spherical UF particles together with Ni and Cr (Fig. 4a), it was also detected as the major component in spherical particles in the fine mode (Fig. 4d). As a result, higher Al concentrations were measured in fine particles when compared to the UF mode (Fig. 3), in contrast to what was observed for Ni and Cr. Possible explanations for this behaviour could be different growth rates of Al particles when compared to Ni-Cr particles, or that Al particles formed after vaporization had a larger formation diameter than Ni-Cr ones, which would subsequently have grown by coagulation. Further research is necessary to understand this process.

Finally, the impact of particle emissions in the worker area was also evident for coarse particles, which showed similar average chemical characteristics during spraying
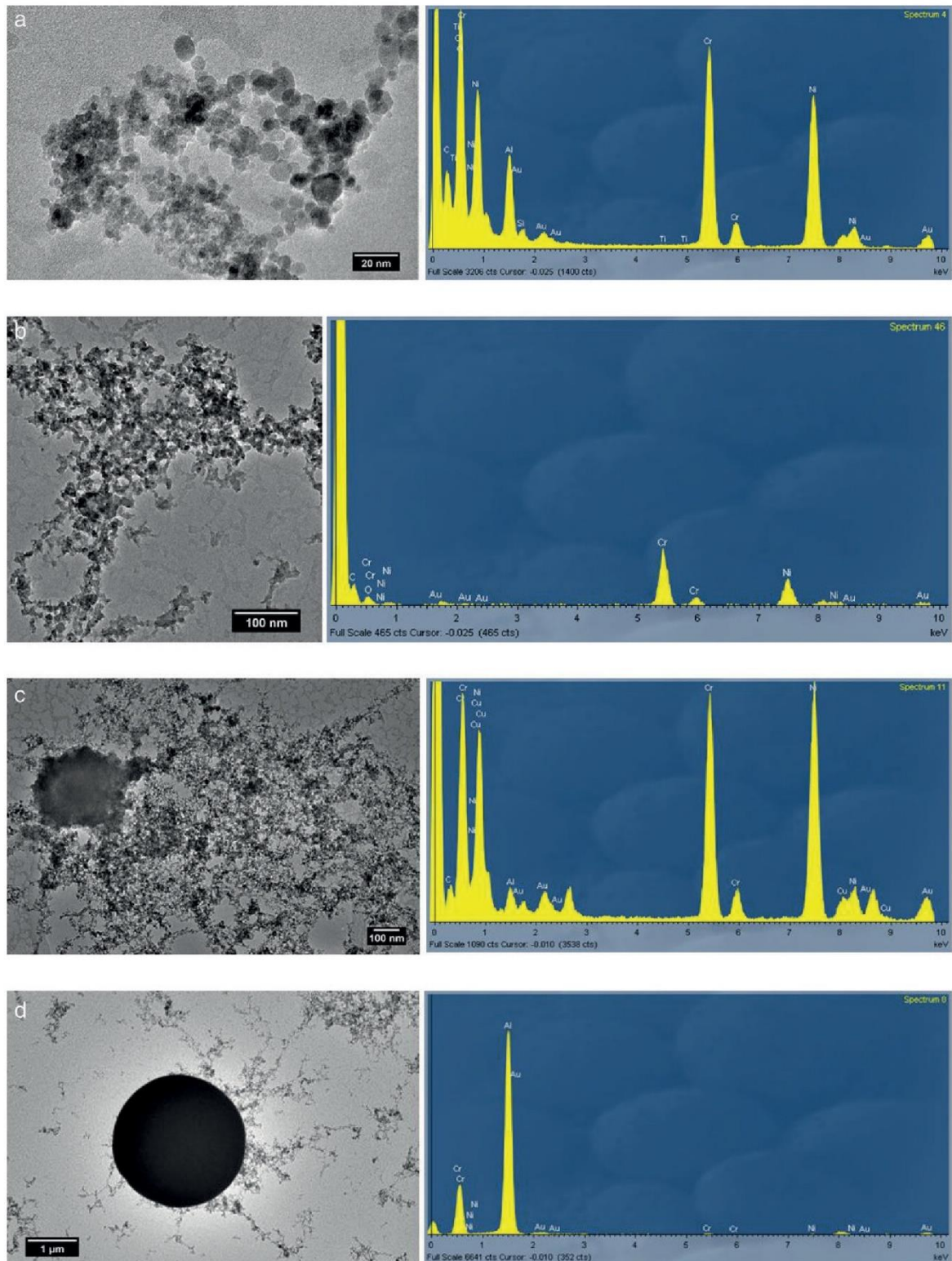
Figure 4. TEM-EDX images showing (a) spherical Cr/Ni/Al UF particles collected in booth #1; (b) irregular Cr/Ni UF particles from booth #3; (c) irregular Cr/Ni UF particles from booth #1; (d) spherical Al fine particle from booth #1.
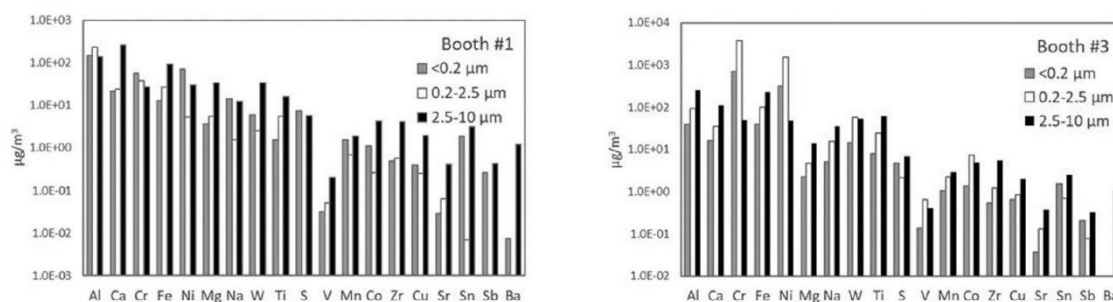
Figure 5. Distribution of the element concentrations across the three different size fractions collected (concentrated, by a factor of 31).

from both booths. Short-term impacts on coarse particle mass from the different booths were also detected, using online instrumentation (Salmatonidis *et al.*, 2019a). The main components of the coarse fraction were Al (139–252 µg/m³), Ca (113–260 µg/m³) and Fe (93–226 µg/m³), followed by S (5.6–6.9 µg/m³), Co (4.2–4.9 µg/m³), Zr (4.0–5.4 µg/m³) and Sb (0.3–0.4 µg/m³) (Fig. 3, Table 1). These tracers are not representative of the feedstock materials sprayed (with the exception of Al in booth #1), and they include markers of urban background emissions (e.g. Sb) in similar concentrations to other urban environments (Sb = 9–12 ng/m³ before aerosol concentration, versus 11 ng/m³ in urban background sites in Spain; Querol *et al.*, 2004). Thus, the chemical composition of the coarse fraction reflects the indoor background aerosol mix, influenced by outdoor infiltration (ambient air) and indoor air by emissions from diverse stages of metal processing activities in the workshop such as welding, polishing, laser processing, metal grinding, and plasma spraying, among others.

Element size distribution

Fig. 5 shows the distribution of element mass concentrations in the three size fractions collected (concentrated), during spraying in both booths. Once again, different behaviours were observed for the different types of aerosols. Based on Fig. 2, the size distribution of the aerosol mass from booth #1 was dominated by coarse particles (50% of the mass) and, as shown in Fig. 5, this aerosol mass was mainly driven by Ca, Al and Fe (260, 139 and 93 µg/m³, respectively). However, while Ca and Fe showed a coarse size distribution (Fig. 5), in the case of Al larger contributions were measured from fine and UF particles (232 and 147 µg/m³, respectively) than from coarse particles. The same was true for Ni and Cr, determined mostly in UF particles (71 and 56 µg/m³, respectively), but not for Ti (mainly coarse). Thus, for Al, Ni and Cr, the spraying activity generated

fine and UF particles from the feedstock either through volatilization of the powder and subsequent new particle formation and growth, or via primary emission during impaction of the feedstock on the surfaces to be coated (Fig. 4). Ti did not follow the same size distribution pattern, possibly due to its higher vaporization temperature (3260°C), and was thus mainly found in coarse particles (mean aggregate diameter of the feedstocks = 35–77 µm according to the technical specification sheets, Table S1).

On the other hand, elements not present in the feedstock (e.g. Ca, Fe) were mostly detected as coarse particles, probably emitted by simultaneous sources in the facility. Other elements found mainly in coarse particles and originating from cross-contamination and background aerosols were Mg, W, Co, Zr, Cu, Sn and Ba.

During spraying in booth #3 (lower temperatures and higher speeds) the majority of the elements (Al, Ca, Fe, Mg, Na, W, Ti, S, Zr, Cu, Sr, Sn, Sb, Ba) showed a dominantly coarse size distribution. However, the high Ni and Cr mass concentrations determined in fine and UF particles (Cr = 3825 µg/m³ in fine and 709 µg/m³ in UF particles; Ni = 1539 and 325 µg/m³, respectively) drove the overall aerosol mass size distribution towards the finer size fractions, as shown in Fig. 2. Fine and UF particles were probably generated from the initial powder (mean diameter of aggregates = 29.2–34.3 µm, Table S1) by direct emission during spraying (Fig. 4b), given the lower spraying temperatures applied in this booth. The dominant particle emission mechanism at lower temperatures was mechanical impaction of the feedstock onto the material being coated, which resulted in UF and fine particles (Salmatonidis *et al.*, 2019a).

As a result, it may be concluded that in the case of booth #3 the chemical composition and size distribution of the particles emitted were mainly determined by the feedstock material, while in the case of booth #1 the relative contribution from indoor background aerosols was higher. The different size distribution patterns observed for the different types of particles sampled are

thus dependent on spraying conditions (e.g. temperature, speed, duration) and also on environmental conditions (influence of indoor background particles), which in turn impact exposure.

Comparison between filter and biosampler particle composition

The aerosol concentrator uses Teflon filters downstream of the VACES and in parallel to the Biosampler to collect particulate matter for chemical analyses and gravimetric determination of the mass. The parallel filters are thus representative of the aerosol collected in the biosampler, and may be used to validate the representativeness of the chemical properties determined in view of toxicity assessments (Bessa *et al.*, 2020). Similar comparisons were carried out by Ning *et al.* (2006) and Saarikoski *et al.* (2014) for ambient aerosol, who concluded that for average concentrations ranging over four orders of magnitude (<ng/m^3 to 100s ng/m^3) very good agreements were found. In the present work this comparison was applied to indoor air aerosols, and at the opposite end of the concentration range (>1000 µg/m^3, Table 1).

Large similarities were observed between the relative particle chemical composition on the Teflon filters and in the biosampler (Fig. 6), which were especially remarkable for fine and UF particles (with the exception of fine particles in booth #1). Differences may have been expected with high contributions from water-soluble species, which was not the case as particles emitted during spraying were mainly metals and metal oxides. It should be remembered that fine and UF particles were collected directly from the inside of the spraying booths, while coarse particles were sampled from the worker area. This means that coarse particles were more influenced by indoor and outdoor background aerosols than fine and UF particles, and probably had a higher water-soluble content. As shown in Fig. 6, the relative composition of coarse particles sampled during spraying in both booths (but sampled in the worker area) showed certain differences between the Teflon and the biosampler samples which were, in any case, not large (e.g. Ca 31% versus 39% of the mass analysed in the biosampler versus Teflon samples, Al 20% versus 21%, or Fe 13% versus 14%). Finally, unexpected differences between the filter and biosampler composition were obtained for fine particles from booth #1, with higher relative contributions from Cr and Ni in the biosampler filters. This result could be due to technical issues such as lower particle collection efficiency during re-filling of the condensation water tanks during the collection of this sample, but it so far remains unexplained.

Aside from this discrepancy, our results evidence an overall good comparability between particle chemical composition on filters collected in parallel to and in the biosamplers in the VACES system, for concentrations in the range 1–1000 µg/m^3.

Summary and conclusions

An aerosol concentrator (VACES) was used to sample incidental ultrafine particles (UFPs), as well as fine (PM$_{2.5}$, including UFP) and coarse aerosols, simultaneously on filter substrates and in liquid to determine their physical–chemical properties in view of toxicological assessments. An industrial case study was selected with the aim to challenge the VACES system with high concentrations of UFPs and test its applicability in indoor industrial scenarios. Results supported the comparability of this tool with online monitors in terms of particle mass for UF, fine and coarse particles, for the high concentrations measured (up to 95 µg UFP/m^3). Similarly, our results evidence an overall good comparability between particle chemical composition on filters collected in parallel to and in the biosamplers in the VACES system, for concentrations in the range 1–1000 µg/m^3. While the large size of the instrument is challenging for deployment in industrial settings, this work evidences that representative results may be obtained as long as a sufficiently repetitive activity is monitored.

In this case study, UFP emission mechanisms and particle transformation in workplace air (vaporization of target metals and new particle formation) were assessed with a focus on particle chemistry. During thermal spraying, the spraying conditions (specifically, temperature) were a key driver of fractionation of metals (Ni, Cr) between UF and fine particle sizes. When spraying occurred at temperatures above the elemental vaporization point, the metals were found in the UF fraction as a result of new particle formation. Conversely, at lower spraying temperatures these potentially health-hazardous metals were found in coarser size fractions (fine and coarse). These mechanisms have evident health implications, as they determine the inhalation trajectory and deposition regions of ultrafine-sized Ni and Cr along the human respiratory tract. In addition to chemical properties, particle morphology (e.g. spherical coarse particles in booth #3 *vs.* irregular UFPs in booth #1) was a key element to understand particle formation mechanisms and their impact on exposure. For all size fractions, and especially for UFPs, these results evidence the need for a detailed understanding of incidental particle formation mechanisms due to their direct implications on particle composition and, thus, exposure. In

agreement with recent studies (Keyter *et al.*, 2019), it is advisable that the ultrafine size fraction (especially, incidental) should be included in personal exposure and risk assessments in occupational settings.

Acknowledgements

Funding

Authors' Contributions

M. Viana: Conceptualization, Formal analysis, Methodology, Writing – Original draft, review and editing, Supervision; A. Salmatonidis: Data curation, Formal Analysis, Writing - review and editing; S. Bezantakos: Methodology, Writing – review and editing; C. Ribalta: Data curation, Writing – review and editing; N. Moreno: Methodology, Data curation, Writing – review and editing; P. Córdoba: Methodology, Data curation, Writing – review and editing; F. Cassee: Methodology, Writing – review and editing; J. Boere: Methodology; S. Fraga: Conceptualization, Writing – review and editing; J.P Teixeira: Conceptualization; M.J. Bessa: Review and editing; E. Monfort: Writing – review and editing.

Conflict of Interest

The authors declare no conflict of interest.

References

Bessa MJ, Brandão F, Fokkens P *et al.* (2021) Toxicity assessment of industrial engineered and airborne process-generated nanoparticles in a 3D human airway epithelial in vitro model. *Nanotoxicology*; 15: 542–57. doi:10.1080/17435390.2021.1897698.

Bessa MJ, Brandão F, Viana M *et al.* (2020) Nanoparticle exposure and hazard in the ceramic industry: an overview of potential sources, toxicity and health effects. *Environ Res*; 184: 109297.

Billet S, Landkocz Y, Martin PJ *et al.* (2018) Chemical characterization of fine and ultrafine PM, direct and indirect genotoxicity of PM and their organic extracts on pulmonary cells. *J Environ Sci (China)*; 71: 168–78.

Brouwer D, Berges M, Virji MA *et al.* (2012) Harmonization of measurement strategies for exposure to manufactured nano-objects; report of a workshop. *Ann Occup Hyg*; 56: 1–9.

Burnett R, Chen H, Szyszkowicz M *et al.* (2018) Global estimates of mortality associated with longterm exposure to outdoor fine particulate matter. *Proc Natl Acad Sci USA*; 115: 9592–7.

Byeon JH, Park JH, Hwang J. (2008) Spark generation of monometallic and bimetallic aerosol nanoparticles. *J Aerosol Sci*; 39: 888–96.

Cohen AJ, Brauer M, Burnett R *et al.* (2017) Estimates and 25-year trends of the global burden of disease attributable to ambient air pollution: an analysis of data from the Global Burden of Diseases Study 2015. *Lancet*; 389: 1907–18.

Corsini E, Vecchi R, Marabini L *et al.* (2017) The chemical composition of ultrafine particles and associated biological effects at an alpine town impacted by wood burning. *Sci Total Environ*; 587–588: 223–31.

Curwin B, Bertke S. (2011) Exposure characterization of metal oxide nanoparticles in the workplace. *J Occup Environ Hyg*; 8: 580–7.

Falk A, Schimpel C, Haase A *et al.* (2016) *Research roadmap for nanosafety. Part III: Closer to the market (CTTM)*. https://zenodo.org/record/1493492.

Fonseca AS, Maragkidou A, Viana M *et al.* (2015) Process-generated nanoparticles from ceramic tile sintering: emissions, exposure and environmental release. *Sci Total Environ*; 565: 922–32.

Freney EJ, Heal MR, Donovan RJ *et al.* (2006) A single-particle characterization of a mobile Versatile Aerosol Concentration Enrichment System for exposure studies. *Part Fibre Toxicol*; 3: 8.

Geller MD, Kim S, Misra C *et al.* (2002) A methodology for measuring size-dependent chemical composition of ultrafine particles. *Aerosol Sci Technol*; 36: 748–62.

Gerlofs-Nijland ME, Bokkers BGH, Sachse H *et al.* (2019) Inhalation toxicity profiles of particulate matter: a comparison between brake wear with other sources of emission. *Inhal Toxicol*; 31: 89–98.

Gonzalez-Pech NI, Stebounova LV, Ustunol IB *et al.* (2019) Size, composition, morphology, and health implications of airborne incidental metal-containing nanoparticles. *J Occup Environ Hyg*; 16: 387–99.

Hämeri K, Lähde T, Hussein T *et al.* (2009) Facing the key workplace challenge: assessing and preventing exposure to nanoparticles at source. *Inhal Toxicol*; 21: 17–24.

Hristozov D, Maccalman L, Jensen K *et al.* (2012) *Risk assessment of engineered nanomaterials*. *Nanotoxicology*; 6: 880–98. doi:10.3109/17435390.2011.626534.

Keyter M, Van Der Merwe A, Franken A. (2019) Particle size and metal composition of gouging and lancing fumes. *J Occup Environ Hyg*; **16**: 643–55.

Kim S, Jaques PA, Chang M *et al.* (2001) Versatile concentration enrichment system (VACES) for simultaneous in vivo and in vitro evaluation of toxic effects of ultrafine, fine and course ambient particles. Part I: development and laboratory characterization. *J Aerosol Sci*; **32**: 1281–97.

Kuhlbusch TA, Asbach C, Fissan H *et al.* (2011) Nanoparticle exposure at nanotechnology workplaces: a review. *Part Fibre Toxicol*; **8**: 22.

Kuhlbusch TAJ, Wijnhoven SWP, Haase A. (2018) Nanomaterial exposures for worker, consumer and the general public. *NanoImpact*; **10**: 11–25.

Lelieveld J, Evans JS, Fnais M *et al.* (2015) The contribution of outdoor air pollution sources to premature mortality on a global scale. *Nature*; **525**: 367–71.

Liu D, Mariman R, Gerlofs-Nijland ME *et al.* (2019) Microbiome composition of airborne particulate matter from livestock farms and their effect on innate immune receptors and cells. *Sci Total Environ*; **688**: 1298–307.

Maynard AD, Aitken RJ. (2007) Assessing exposure to airborne nanomaterials: current abilities and future requirements. *Nanotoxicology*; **1**: 26–41.

Maynard AD, Baron PA, Foley M *et al.* (2004) Exposure to carbon nanotube material: aerosol release during the handling of unrefined single-walled carbon nanotube material. *J Toxicol Environ Health A*; **67**: 87–107.

Mendes L, Gini MI, Biskos G *et al.* (2018) Airborne ultrafine particles in a naturally ventilated metro station: Dominant sources and mixing state determined by particle size distribution and volatility measurements. *Environ Pollut*; **239**: 82–94.

Morawska L, Ayoko GA, Bae GN *et al.* (2017) Airborne particles in indoor environment of homes, schools, offices and aged care facilities: the main routes of exposure. *Environ Int*; **108**: 75–83.

Ning Z, Moore KF, Polidori A *et al.* (2006) Field validation of the new miniature versatile aerosol concentration enrichment system (mVACES). *Aerosol Sci Technol*; **40**: 1098–110.

Ntziachristos L, Ning Z, Geller MD *et al.* (2007) Fine, ultrafine and nanoparticle trace element compositions near a major freeway with a high heavy-duty diesel fraction. *Atmos Environ*; **41**: 5684–96.

Oberbek P, Kozikowski P, Czarnecka K *et al.* (2019) Inhalation exposure to various nanoparticles in work environment—contextual information and results of measurements. *J Nanoparticle Res*; **21**: 222.

Oberdörster G. (2001) Pulmonary effects of inhaled ultrafine particles. *Int Arch Occup Env Heal*; **74**: 1–8.

Oberdörster G, Stone V, Donaldson K. (2007) Toxicology of nanoparticles: a historical perspective. *Nanotoxicology*; **1**: 2–25.

Ozgen S, Becagli S, Bernardoni V *et al.* (2017) Analysis of the chemical composition of ultrafine particles from two domestic solid biomass fired room heaters under simulated real-world use. *Atmos Environ*; **150**: 87–97.

Perrone MG, Gualtieri M, Ferrero L *et al.* (2010) Seasonal variations in chemical composition and in vitro biological effects of fine PM from Milan. *Chemosphere*; **78**: 1368–77.

Pope CA 3rd, Coleman N, Pond ZA *et al.* (2019) Fine particulate air pollution and human mortality: 25+ years of cohort studies. *Environ Res*; **183**: 108924.

Querol X, Alastuey A, Rodriguez S *et al.* (2001) PM10 and PM2.5 source apportionment in the Barcelona Metropolitan area, Catalonia, Spain. *Atmos Environ*; **35**: 6407–19. doi:10.1016/S1352-2310(01)00361-2.

Querol X, Alastuey A, Viana MM *et al.* (2004) Speciation and origin of PM10 and PM2.5 in Spain. *J Aerosol Sci*; **35**: 1151–72.

Ribalta C, Koivisto AJ, López-Lilao A *et al.* (2019a) Testing the performance of one and two box models as tools for risk assessment of particle exposure during packing of inorganic fertilizer. *Sci Total Environ*; **650**(Pt 2): 2423–36.

Ribalta C, Koivisto AJ, Salmatonidis A *et al.* (2019b) Modeling of high nanoparticle exposure in an indoor industrial scenario with a one-box model. *Int J Environ Res Public Health*; **16**: 1695.

Saarikoski S, Carbone S, Cubison MJ *et al.* (2014) Evaluation of the performance of a particle concentrator for online instrumentation. *Atmos Meas Tech*; **7**: 2121–35.

Salmatonidis A, Ribalta C, Sanfélix V *et al.* (2019a) Workplace exposure to nanoparticles during thermal spraying of ceramic coatings. *Ann Work Expo Health*; **63**: 91–106.

Salmatonidis A, Sanfélix V, Carpio P *et al.* (2019b) Effectiveness of nanoparticle exposure mitigation measures in industrial settings. *Int J Hyg Environ Health*; **222**: 926–35.

Shao J, Wheeler AJ, Chen L *et al.* (2018) The pro-inflammatory effects of particulate matter on epithelial cells are associated with elemental composition. *Chemosphere*; **202**: 530–7.

Stone V, Miller MR, Clift MJD *et al.* (2017) Nanomaterials versus ambient ultrafine particles: an opportunity to exchange toxicology knowledge. *Environ Health Perspect*; **125**: 106002.

Terzano C, Di Stefano F, Conti V *et al.* (2010) Air pollution ultrafine particles: toxicity beyond the lung. *Eur Rev Med Pharmacol Sci*; **14**: 809–21.

Viana M, Fonseca AS, Querol X *et al.* (2017) Workplace exposure and release of ultrafine particles during atmospheric plasma spraying in the ceramic industry. *Sci Total Environ*; **599-600**: 2065–73.

Viana M, Rivas I, Querol X *et al.* (2014) Indoor/outdoor relationships and mass closure of quasi-ultrafine, accumulation and coarse particles in Barcelona schools. *Atmos Chem Phys*; **14**: 4459–72.

Viana M, Rivas I, Querol X *et al.* (2015) Partitioning of trace elements and metals between quasi-ultrafine, accumulation and coarse aerosols in indoor and outdoor air in schools. *Atmos Environ*; **106**: 392–401.

Viitanen AK, Uuksulainen S, Koivisto AJ *et al.* (2017) Workplace measurements of ultrafine particles-a literature review. *Ann Work Expo Health*; **61**: 749–58.

B. *In Vitro* Toxicity Assessment of the Airborne Process-Generated and Engineered (Nano)Particles

Prior to the *in vitro* toxicity assessment of the (nano)particles under study, protocol optimisation for establishing the most suitable proceedings for cell collection and freezing for comet assay analysis was performed. This preliminary study has been done since the *in vitro* ALI exposures were carried out at the RIVM (Bilthoven, The Netherlands), and the cells were frozen and shipped to our laboratory at INSA (Porto, Portugal) for subsequent analysis of the DNA damage caused by exposure to the tested particles. As a result of this study, an original research paper was published respecting the optimisation of the harvesting and freezing protocol procedures using two human cell lines for the assessment of DNA damage by the alkaline comet assay (Section B.1.).

Afterwards, human respiratory *in vitro* models of different complexity, a traditional lung cell line and more advanced 3D cell cultures of upper airway epithelium, were exposed to (nano)particles derived from ceramic technologies: PGFP and PGNP incidentally emitted and collected from real scenarios of thermal spraying of ceramic coatings (APS and HVOF), as well as to four commercially available ENP (SnO_2, ATO, CeO_2, and ZrO_2) used as raw materials for ceramics manufacture.

To understand the toxicity impact and the nature of the mechanisms involved, major toxicity endpoints including plasma membrane integrity, metabolic activity, oxidative stress, inflammatory response, and genotoxicity were assessed.

The following studies were performed:

- Toxicity testing of APS- and HVOF-derived PGFP and PGNP in human alveolar epithelial A549 cells under the traditional submerged conditions (Section B.2.);
- Comparative toxicity of four ENP (SnO_2, ATO, CeO_2, and ZrO_2 NP) in the human alveolar epithelial A549 cell line under submerged *vs* ALI conditions (Section B.3.);
- Comparative toxicity of two ENP (ATO and ZrO_2 NP) and HVOF-incidentally released PGFP and PGNP, in a human 3D model of upper airway epithelium (MucilAir™) cultured under ALI conditions (Section B.4.).

B.1. Optimisation of the harvesting and freezing conditions of human cell lines for DNA damage analysis by the alkaline comet assay

Bessa M. J., Brandão F., Querido M. M., Costa C., Costa Pereira C., Valdiglesias V., Laffon B., Carriere M., Teixeira J. P., & Fraga S.

The PhD candidate contributed for the methodology, investigation, formal analysis and writing of the manuscript.

Optimization of the harvesting and freezing conditions of human cell lines for DNA damage analysis by the alkaline comet assay

Maria João Bessa[a,b], Fátima Brandão[a,b], Micaela Machado Querido[a,b], Carla Costa[a,b], Cristiana Costa Pereira[a,b], Vanessa Valdiglesias[a,c], Blanca Laffon[c], Marie Carriere[d], João Paulo Teixeira[a,b,*], Sónia Fraga[a,b]

[a] EPIUnit-Instituto de Saúde Pública, Universidade do Porto, Porto, Portugal
[b] Instituto Nacional de Saúde Dr. Ricardo Jorge, Departamento de Saúde Ambiental, Porto, Portugal
[c] Universidade da Coruña, DICOMOSA Group, Department of Psychology, Area of Psychobiology, Coruña, Spain
[d] Université Grenoble-Alpes, CEA, CNRS, INAC-SyMMES, Chimie Interface Biologie pour l'Environnement, la Santé et la Toxicologie (CIBEST), France

ARTICLE INFO

ABSTRACT

The comet assay is a commonly used method for *in vitro* and *in vivo* genotoxicity assessment. This versatile assay can be performed in a wide range of tissues and cell types. Although most of the studies use samples immediately processed after collection, frozen biological samples can also be used. The present study aimed to optimize a collection and freezing protocol to minimize the DNA damage associated with these procedures in human cell line samples for comet assay analysis. This study was conducted in glial A172 and lung alveolar epithelial A549 cells. Two cell detachment methods (mechanical *vs* enzymatic) and two cryoprotective media [FBS + 10% DMSO *vs* Cell Culture Media (CCM) + 10% DMSO] were tested, and DNA damage assessed at four time points following storage at -80 °C (one, two, four and eight weeks). In both cell lines, no differences in % tail intensity were detected between fresh and frozen cells up to eight weeks, irrespective of the harvesting method and freezing medium used. However, freshly isolated A172 cells exhibited a significant lower DNA damage when resuspended in CCM + 10% DMSO, while for A549 fresh cells the preferable harvesting method was the enzymatic one since it induced less DNA damage. Although both harvesting methods and cryoprotective media tested were found suitable, our data indicate that enzymatic harvesting and cryopreservation in CCM + 10% DMSO is a preferable method for DNA integrity preservation of human cell line samples for comet assay analysis. Our data also suggest that CCM is a preferable and cost-effective alternative to FBS in cryopreservation media. This optimized protocol allows the analysis of *in vitro* cell samples collected and frozen at different locations, with minimal interference on the basal DNA strand break levels in samples kept frozen up to eight weeks.

1. Introduction

The single-cell gel electrophoresis, most commonly denominated as comet assay, is a standard method for the assessment of DNA damage and repair [1,2]. Besides its simplicity, versatility, sensitivity, speed and low cost, this assay allows the researcher to evaluate genotoxicity at a single cell level, requiring a small number of cells per analysis and enabling the detection of low levels of DNA damage [1,2]. Main fields of application of the comet assay includes the genotoxicity testing of xenobiotics (*in vitro* and *in vivo* screening), molecular epidemiology and genetic ecotoxicology studies, human biomonitoring studies to measure changes in genomic stability, and basic research studies aimed to understand the mechanisms behind DNA damage and repair [3,4]. The comet assay can be performed either *in vivo* using cells isolated from any tissue or *in vitro* using primary or immortalized cells [5].

As in any other assay, its protocol standardization is of paramount importance, especially for inter-laboratory comparisons involving different research groups. Up to date there are several studies on the influence of a number of critical steps of the comet assay protocol, including agarose concentration, lysis buffer composition and incubation

time, electrophoretic conditions (*e.g.* voltage, current and time of electrophoresis), sensitivity and specificity of the different types of endonucleases to detect oxidative lesions on DNA [6–9], among others. The comet assay has been successfully applied to a wide range of eukaryotic cells, and different protocols have been developed for specific tissues and cell types [5]. The issues surrounding collection, handling and storage of cell samples may have a profound impact on DNA integrity and on its suitability for use in downstream analysis [10]. To perform collaborative studies requiring large number of samples collected in different geographical locations or requiring multiple parameters to be analysed in different laboratories, the use of frozen cells is mandatory. Indeed, the use of frozen cells allows simultaneous analysis of a large number of samples collected over a long period of time. However, the protocol and number of freeze/thaw cycles has been found to affect genomic DNA stability [11]. This brings up the question of comparability between fresh and frozen cells since ice crystal formation during the freezing procedure can potentially affect the cell's DNA integrity. In fact, cryopreservation is a complex procedure since cells are under extreme conditions that can affect them at different levels, for instance at genomic level. Therefore, in order to avoid possible artefactual damage, it is important to establish a suitable cryopreservation protocol [12]. Composition of the cryopreservation medium, as well as the freezing process (freezing speed and storage time) are important aspects to take into account in cells/samples processing for subsequent comet assay analysis. Some studies have approached these issues using different cell models. Al-Salmani et al. [13] investigated the impact of varying the volume of the blood samples (5 mL or 250 μL frozen aliquots) and storage temperature (- 20 or - 80 °C), with or without 10% DMSO as cryoprotectant, over different time points up to one month on sample integrity, as assessed by alkaline and enzyme-modified comet assay versions. These authors observed successful DNA preservation in smaller volume of whole blood samples, stored even without cryoprotectant, at either − 20 °C or − 80 °C up to one month. Recently, Koppen et al. [14] also evaluated the cryopreservation protocol of human whole blood by comparing DNA damage between fresh and frozen samples also using both alkaline and enzyme-modified comet assay versions. No significant increase on DNA damage was detected in cryopreserved whole blood samples compared to fresh samples.

The reliability of the comet assay in measuring DNA damage in cryopreserved compared with fresh cells has been also investigated in other cell types. Duty et al. [15] examined the effect of the cryopreservation method (flash freezing *vs* programmable freezing in liquid nitrogen, both with or without cryoprotectant) on DNA integrity in sperm, as measured with the neutral comet assay. These authors reported that flash-freezing in liquid nitrogen without cryoprotectant represents the most appropriate cryopreservation method for human semen since it most closely reflects data obtained using fresh human semen samples. Fraser et al. [16] also evaluated the effect of freezing-thawing on DNA integrity of boar sperm samples by the neutral comet assay version. They showed that the freezing-thawing process affects the boar sperm DNA integrity, irrespective of the extender type and packaging material used for cryopreservation.

In *in vivo* genotoxicity testing, DNA damage analysis by the comet assay is traditionally performed using fresh samples processed immediately after tissue collection and cell isolation. However, some of the available *in vivo* genotoxicity studies have also relied on frozen samples [11]. Jackson et al. [11] have demonstrated the suitability of frozen samples of bronchoalveolar cells, lung and liver tissues for comet analysis of DNA strand break levels of mice exposed to methyl methanesulphonate (MMS), as the observed effects were similar to those detected in fresh cells. Nonetheless, different cells may exhibit different sensitivity to freezing conditions, worthwhile to investigate to ensure reliability and validity of the obtained data.

Accordingly, the present study aimed to optimize a harvesting and freezing protocol for human cell lines for DNA damage analysis by the alkaline comet assay. For the sake of comparison, two commonly used human adherent cell lines from different origins were selected for this study: A172 glial and A549 lung epithelial cells. Two harvesting methods (scraping *vs* trypsinization) were employed using two different cryopreservation media (10% DMSO in FBS *vs* 10% DMSO in cell culture media). DNA damage was assessed in those samples one, two, four and eight weeks upon freezing at - 80 °C, in parallel with fresh collected cells, in order to establish an appropriate method for sample cryopreservation for *in vitro* comet assay analysis.

2. Materials and methods

2.1. Chemicals

Triton X-100, low melting point (LMP) agarose, Tris hydrochloride (Tris − HCl) and methyl methanesulfonate (MMS) were purchased from Sigma-Aldrich (Madrid, Spain). Dimethyl sulfoxide (DMSO), sodium hydroxide (NaOH), sodium chloride (NaCl), potassium chloride (KCl) and potassium hydroxide (KOH) were bought from Merck KGaA (Darmstadt, Germany). Tris base and disodium salt dihydrate (Na$_2$EDTA) were purchased from Merck Millipore (Madrid, Spain). Normal melting point (NMP) agarose was supplied by Bioline (London, UK). Lonza BioWhitaker Dulbecco's Modified Eagle Medium (DMEM) was acquired from VWR International (Madrid, Spain). The cell culture supplements and reagents were from Gibco® and purchased to Thermo Fisher Scientific (Madrid, Spain), as well as the Invitrogen™ SYBR® Gold solution.

2.2. Cell culture

Human glioblastoma A172 (ECACC 88062428) and lung epithelial A549 (ATCC® CCL-185™) cells lines were obtained from the European Collection of Authenticated Cell Cultures (ECACC) and American Type Culture Collection (ATCC), respectively. A172 cells were cultured in DMEM supplemented with 2 mM L-Glutamine, 50 U/mL of penicillin, 50 μg/mL of streptomycin and 10% of heat-inactivated foetal bovine serum (FBS), whereas A549 cells were cultured in DMEM with 2 mM L-Glutamine, 50 U/mL of penicillin, 50 μg/mL of streptomycin, 1% of Minimum Essential Medium Non-Essential Amino Acids (MEM NEAA) and 10% heat-inactivated FBS. Cells were grown in a humidified atmosphere with 5% CO$_2$ at 37 °C.

2.3. Cell harvesting and freezing procedures

To carry out the experiments, 2×10^5 cells were seeded in 12-well plates (VWR International, Madrid, Spain) and allowed to adhere for 48 h at 37 °C and 5% CO$_2$. After this period, media were aspirated, and cells washed (2x) with phosphate buffered saline (PBS) pH 7.4. Cells were then detached mechanically with a cell scraper or enzymatically with a 0.25% Trypsin- EDTA solution (2–5 min followed by addition of PBS). The content of each well was transferred into a microtube and centrifuged for 5 min at 200 × *g*. The supernatant was discarded, and the pellet was gently resuspended in either of two cryoprotective media: (1) 90% of FBS or (2) 90% of cell culture medium (CCM), both supplemented with 10% DMSO. Samples were frozen for 1 h at − 20 °C, kept at − 80 °C, and analysed at one, two, four and eight weeks after freezing, in parallel with freshly samples collected under the very same conditions of the frozen ones. Freshly collected cells treated with 500 μM of MMS were included in every experiment as a positive control.

2.4. Alkaline comet assay

The alkaline comet assay was performed as previously described by Bessa et al. [17], with slight modifications. Briefly, freshly harvested and thawed samples (at 37 °C) cells were centrifuged for 5 min at 200 × *g*. After cell counting, 1.0×10^4 cells in PBS pH 7.4 were transferred to

a microtube and centrifuged for 5 min at $400 \times g$. Subsequently, the supernatant was discarded, and cells embedded in 100 μL of 0.6% LMP agarose and 5 μL of each cell suspension (500 cells) were placed onto dry microscope slides precoated with 1% NMP using a medium throughput 12-gel comet assay unit (Severn Biotech Ltd.®, Kidderminster, UK). After agarose solidification at 4 °C for 5 min, slides were immersed in ice-cold lysis solution (NaCl 2.5 M, Na_2EDTA 100 mM, Tris-base 10 mM, NaOH 10 M, pH 10, Triton-X 100 1%) during 1 h at 4 °C, protected from light. Slides were then washed with PBS for 5 min. For DNA unwinding, slides were immersed in electrophoresis solution (Na_2EDTA 1 mM, NaOH 0.3 M, pH 13) in the electrophoresis platform for 40 min, followed by electrophoresis in the same solution for 30 min at constant 25 V (0.9 V/cm) and 400 mA. For neutralization, slides were then washed with cold PBS (pH 7.2) and deionized H_2O for 10 min each. Then, slides were fixed with ethanol 70% and 96% for 15 min each, at room temperature and air-dried overnight. Slides were stained with 1:10,000 dilution of SYBR® Gold in TE buffer (Tris − HCl 10 mM and EDTA 1 mM, pH 7.5–8) and visualized in a Motic BA410 ELITE Series microscope equipped with a Complete EPI-Fluorescence Kit. The comets were scored using the Comet Assay IV image analysis software (Perceptive Instruments, Staffordshire, UK). At least 100 cells/experimental group (50 in each replicate gel) were scored and the mean of the percentage of DNA in the comet tail (% tail intensity) was used as DNA damage descriptor.

2.5. Statistical analysis

Results are expressed as a mean ± standard deviation (SD) from three independent experiments, each performed in duplicate. Statistical analyses were performed using the SPSS statistical package for Windows version 25.0. Data were tested for normality and homogeneity of variances by Shapiro-Wilk and Levene's tests, respectively, and were log-transformed whenever necessary. Differences in % tail intensity data between fresh and frozen cells over time were estimated using one-way analysis of variance (ANOVA) followed by post-hoc Dunnett's test for multiple comparisons. A two-way analysis of variance (ANOVA) followed by HSD Tukey test was performed to test for the effect of the harvesting method and frozen medium in DNA damage (% tail intensity). A P value < 0.05 was assumed as the level of significance.

3. Results

The present study was designed to optimize the most suitable conditions for the collection and freezing of cell lines for subsequent DNA strand break analysis by the comet assay, with minimal impact on the basal DNA damage of the cells. For this purpose, two widely used human cell models with distinct origin, molecular profiling and behaviour were chosen: a glial (A172) and a lung alveolar epithelial (A549) cell line. To understand how the freezing conditions may possibly interfere with the DNA stability of these cells, two cryoprotective media (90% of heat inactivated FBS + 10% DMSO and 90% of CCM + 10% DMSO) were tested and the DNA damage assessed after four periods of storage at - 80 °C: one, two, four and eight weeks. However, not only the freezing conditions were considered important in this study, but also the cell harvesting procedure. Therefore, two harvesting methods were evaluated: mechanical cell detachment using a scraper and enzymatic cell dissociation with a 0.25% Trypsin-EDTA solution. For sake of comparison and to assure that cells were subjected to the same experimental conditions, fresh cells were subjected to the same conditions tested for the remaining samples. DNA damage of cells was assessed by the alkaline comet assay and % of tail intensity was the chosen descriptor since it measures the relative fluorescent intensity in the head and tail [18]. The percentage of tail DNA is often considered the preferable metric since it is linearly related to DNA damage and is associated with DNA break frequency [19].

Regarding glial A172 cells, as shown in Table 1, for each of the

freezing media used no significant differences in % tail intensity of freshly collected cells were observed between the two harvesting methods. However, a significant difference (p = 0.02) was detected between fresh cells resuspended with the different freezing media, with cells collected with FBS + 10% DMSO exhibiting higher % tail intensity values compared to cells in CCM + 10% DMSO. Moreover, no differences in DNA damage were observed between fresh and frozen cells analysed at all selected time points. Overall, A172 cells harvested mechanically and frozen with FBS + 10% DMSO presented higher levels of DNA damage compared to cells frozen with CCM + 10% DMSO. This is particularly evident in eight-week frozen cells, whose % tail intensity values are significantly higher in cells detached by mechanic means compared to cells collected with 0.25% trypsin-EDTA (p = 0.03). In addition, it is important to point out that the obtained % tail DNA values of A172 cells (mean value ~ 10%) are within the range of those reported in the literature [20,21].

A similar trend was observed in alveolar epithelial A549 cells, were no significant differences were observed between fresh and frozen cells at all assessed storage periods (Table 2). Nonetheless, contrasting with A172 cells, a significant difference in % tail intensity of A549 fresh cells collected with different harvesting methods (p = 0.03) was observed, the enzymatic method being the one that induced less DNA damage (Table 2). Moreover, the obtained values of % tail DNA for A549 fresh cells (mean value ~ 5%) in the present study are also within the range of those previously reported [22–24]. Additionally, significant differences on the % tail intensity were found in two-weeks frozen cells cryopreserved with different freezing media (p = 0.03), with low levels of DNA damage in cells frozen with CCM + 10% DMSO. Furthermore, at eight weeks after freezing, significant differences in DNA damage of A549 cells between harvesting methods and cell frozen media were detected (p = 0.02). Thus, A549 cells detached enzymatically and frozen in CCM + 10% DMSO presented lower levels of % tail DNA (1.00 ± 0.67) compared to cells harvested mechanically (5.83 ± 1.30) and stored in the same cryoprotective medium (p < 0.05). In general, the mechanical harvesting of A549 cells was associated with higher levels of % tail DNA comparing to the enzymatic method, whereas cells resuspended in FBS + 10% DMSO exhibited higher levels of DNA damage than cells in CCM + 10% DMSO (Table 2). Differential sensitivity to harvesting methods and freezing media between glial A172 and human lung A549 cells was only observed in freshly collected cells but not in frozen samples. Representative images of comets of fresh and eight-week frozen A172 and A549 cells are depicted in Figs. 1 and 2, respectively. Both cells types exposed to a positive control, the alkylating agent MMS (500 μM, 1 h), exhibited a prominent tail, as expected, with % tail intensity mean values of 39.80 ± 8.58 and 33.82 ± 4.92 for A172 and A549 cells, respectively.

4. Discussion

To recover a maximum of viable cells on thawing, several aspects should be considered during the freezing procedure: i) the use of a cryoprotectant to help preventing intracellular ice crystal formation, ii) a slow cooling rate of the sample and iii) a low-temperature storage of the samples [25]. Most of the existing studies on the DNA damage analysis relied on cryopreserved cells and, in most of the cases, there is no mention regarding the freezing and storage processes [26]. Indeed, the impact of cell cryopreservation procedures on DNA integrity are commonly overlooked. In this context, Jackson et al. [11] have shown that tissue collection, cell isolation and freezing procedures may influence DNA integrity of rat lung samples. To our knowledge, our study is the first one comparing levels of in vitro DNA damage in freshly collected vs cryopreserved human cell lines using two different freezing media and harvesting methods.

Regarding cell isolation procedure, detachment of cultured cells requires enzymatic or mechanical methods that can result in harmful

Table 1

Impact of the harvesting method (HM) and freezing medium (FM) on DNA damage of fresh vs frozen A172 cells as measured by the percentage (%) of tail intensity. Cells were detached by mechanical (scraper) or enzymatic (incubation with 0.25% Trypsin-EDTA solution) means, using 90% of Heat Inactivated Foetal Bovine Serum (FBS) with 10% DMSO or 90% of cell culture medium (CCM) with 10% DMSO as freezing media. Cells were then analysed for DNA damage at different periods after freezing (one up to eight weeks).

| | | % Tail intensity | | | | Two-way ANOVA *P-value* | | |
| | HM | Mechanical | | Enzymatic | | | | |
	FM	90 % FBS + 10% DMSO	90 % CCM + 10% DMSO	90 % FBS + 10% DMSO	90 % CCM + 10% DMSO	HM	FM	HM x FM
Frozen storage duration	Fresh cells	10.27 ± 3.68	7.51 ± 2.16	11.07 ± 0.21	6.14 ± 1.10	0.86	**0.02**	0.36
	1 week	5.83 ± 2.86	4.03 ± 0.65	5.78 ± 3.23	6.44 ± 4.17	0.58	0.73	0.53
	2 weeks	10.04 ± 9.40	4.52 ± 0.65	9.74 ± 5.70	4.63 ± 1.56	0.75	0.27	0.74
	4 weeks	11.18 ± 9.90	5.58 ± 0.37	4.10 ± 0.58	8.42 ± 0.38	0.67	0.73	0.19
	8 weeks	12.11 ± 8.02	9.91 ± 5.04	6.39 ± 2.50	3.37 ± 0.39	**0.03**	0.21	0.47

Values are presented as mean ± SD of three independent experiments, each performed in duplicate. A two-way ANOVA analysis was performed to compare differences between HM and FM conditions. A P value < 0.05 was considered significant.

Table 2

Impact of the harvesting method (HM) and freezing medium (FM) on DNA damage of fresh vs frozen A549 cells as measured by the percentage (%) of tail intensity. Cells were detached by mechanical (scraper) or enzymatic (incubation with 0.25% Trypsin-EDTA solution) means, using 90% of Heat Inactivated Foetal Bovine Serum (FBS) with 10% DMSO or 90% of cell culture medium (CCM) with 10% DMSO as freezing media. Cells were then analysed for DNA damage at different periods after freezing (one up to eight weeks).

| | | % Tail intensity | | | | Two-way ANOVA *P-value* | | |
| | HM | Mechanical | | Enzymatic | | | | |
	FM	90 % FBS + 10% DMSO	90 % CCM + 10% DMSO	90 % FBS + 10% DMSO	90 % CCM + 10% DMSO	HM	FM	HM x FM
Frozen storage duration	Fresh cells	6.66 ± 1.14	5.55 ± 1.85	4.48 ± 2.60	2.96 ± 0.98	**0.03**	0.24	0.78
	1 week	7.44 ± 5.02	9.19 ± 8.86	5.62 ± 1.99	3.55 ± 0.48	0.37	0.73	0.48
	2 weeks	9.46 ± 5.74	3.29 ± 2.33	4.54 ± 2.57	2.11 ± 0.70	0.16	**0.03**	0.59
	4 weeks	11.42 ± 4.51	6.34 ± 3.12	8.90 ± 7.86	4.57 ± 3.48	0.28	0.14	0.99
	8 weeks	1.77 ± 0.95	5.83 ± 1.30 [a]	2.53 ± 1.52	1.00 ± 0.67	0.06	0.64	**0.02**

Values are presented as mean ± SD of three independent experiments, each performed in duplicate. A two-way ANOVA analysis was performed to compare differences between HM and FM conditions. A P value < 0.05 was considered significant. [a] $P < 0.05$ between HM.
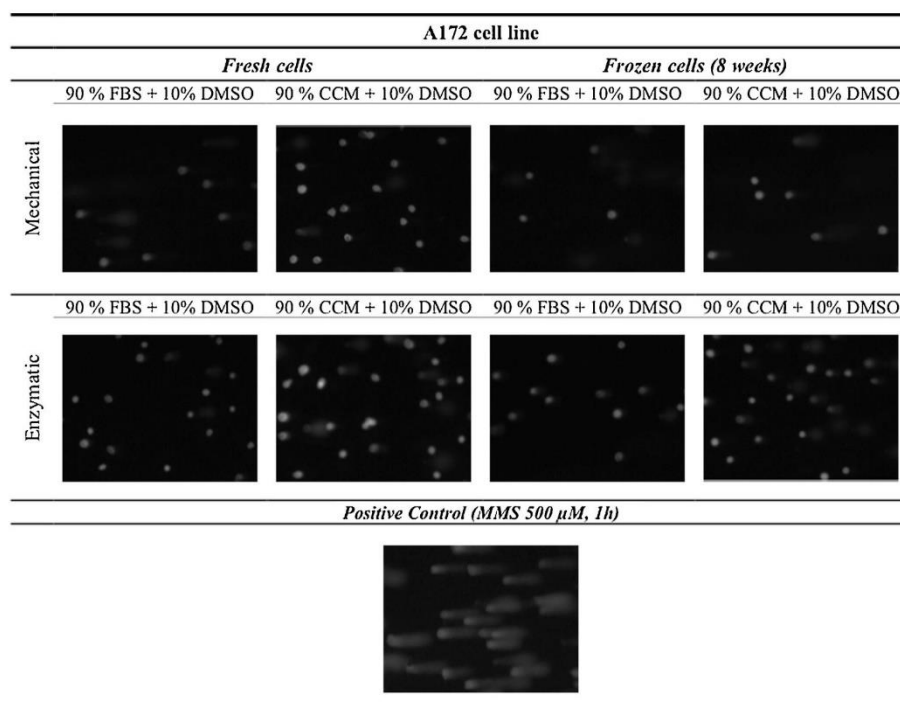

Fig. 1. Comet assay representative images (100× magnification) of fresh vs eight-week frozen A172 cells harvested using a mechanical or enzymatic method, and two cryoprotective media. As a positive control of the comet assay, cells were exposed to 500 μM of methyl methanesulfonate (MMS) for 1 h.
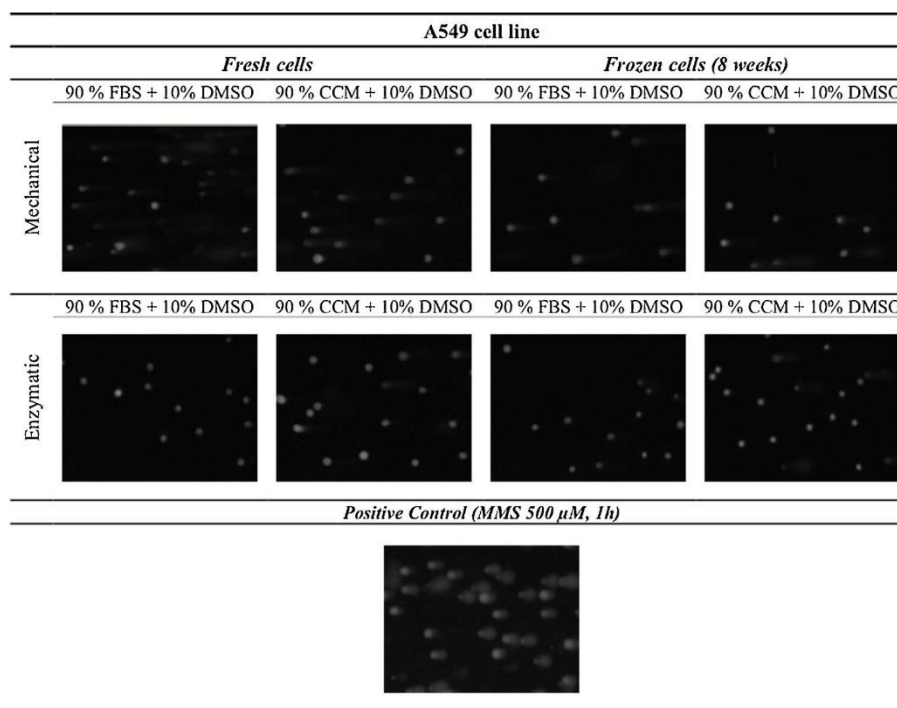
116

Fig. 2. Comet assay representative images (100× magnification) of fresh vs eight-week frozen A549 cells harvested using a mechanical or enzymatic method, and two cryoprotective media. As a positive control of the comet assay, cells were exposed to 500 μM of methyl methanesulfonate (MMS) for 1 h.

effects [27], modifying cellular morphological appearance due to the disruption of the plasma membrane [28,29]. While the mechanical dissociation yields adherent cell sheets surrounded by their extracellular matrix, the enzymatic digestion disaggregates cells that exhibit a rounded appearance [27]. Despite the limited statistical findings, our data suggest that, overall, the enzymatic procedure (0.25% trypsin-EDTA solution) is the preferable method for cell collection for comet assay analysis as those cells displayed lower levels of DNA damage comparing with scraped cells. While trypsin selectively cleaves cell adherent proteins to detach cells from the tissue surface, the EDTA content of the solution might contribute to DNA preservation. As a chelating agent, EDTA inhibits the DNase activity, preventing DNA fragmentation [30]. It has also been shown that DNA samples stored at - 80 °C in higher concentrations of EDTA remain intact for longer periods, suggesting a protective effect of EDTA [31].

Cell membranes can be highly affected by freezing due to intracellular ice crystals formation [32], which can also lead to formation of breaks in the DNA strands [33]. Our study also intended to address the effect of the freezing process on the DNA integrity over time. According to our results, no differences were detected in the DNA damage levels between fresh and frozen cells up to eight weeks in both cell lines under study. This demonstrates that the freezing process apparently did not affect DNA integrity of glial A172 and human alveolar epithelial A549 cells and did not induce more strand breaks and alkali label sites on their DNA. This finding is in accordance with previous studies in whole blood cells where no signs of deleterious effects upon DNA were obtained in cryopreserved as compared with DNA basal levels of fresh whole blood samples [14,34].

The freezing medium is usually constituted by higher serum concentrations and an anti-freezing agent [25]. FBS supplemented with 10% DMSO is a conventional freezing medium used for mammalian cells [35]. DMSO is traditionally the adopted cryoprotectant agent [36], and thus selected in the present study to constitute both cryoprotective media tested, since it helps to prevent the formation of ice crystals and protect cells from damage [26,37]. Since DMSO interacts with

hydrogen bonds present in H_2O molecules, it allows to decrease ice crystals formation during storage at freezing temperatures and, therefore, is expected to diminish the formation of DNA strand breaks [33]. Noda and his colleagues [33] demonstrated that DMSO effectively protected DNA molecules from double strand breaks induced by the freezing process, photo and γ-ray-irradiation. It is important to point out that DMSO is also used in the Polymerase Chain Reaction (PCR) due to its capacity to disrupt the secondary structure formation in the DNA template and to hydrogen bond to the major and minor grooves of the DNA molecule [38]. This hydrogen bond strength increase may contribute to a higher stability of the DNA molecules during the freezing process. These phenomena might explain the absence of increment in DNA damage of frozen cells over time that we have studied herein. Loss of damaged cells during thawing and/or washing of the frozen cells may also account for this finding.

Nevertheless, previous studies have shown that other freezing media components, in place of FBS, can as well effectively preserve mammalian cell lines [35]. In our study we compared the effectiveness of FBS and CCM to act as cryoprotective media for freezing human cell lines minimizing their DNA damage. FBS has been frequently used in freezing media due to its capacity to protect cells from the freezing process but also from mechanical damage [25,39]. This serum is broadly constituted by important biological molecules such as albumin, apolipoproteins, cholesterol, hormones (*e.g.* steroids), growth factors, vitamins, among others [39,40]. In the present study, for both *in vitro* models, cells resuspended in FBS + 10% DMSO exhibited a higher DNA damage in comparison with cells in CCM + 10% DMSO. It could be hypothesized that FBS components may contribute to this damaging effect. For instance, steroid hormones have been associated with the induction of genotoxicity such as the formation of DNA adducts or generation of reactive oxygen species [41,42]. Despite FBS being frequently used as the major constituent of freezing media for research purposes, our data indicate that the cryoprotective medium containing CCM seems to be the most appropriate choice for human cell lines, at least the ones selected. Kim et al. [43] have found that, in freezing

medium mainly composed by DMEM, lowering the % of FBS was beneficial for DNA integrity of cryopreserved fish embryonic cell lines, which is in agreement with our findings. Therefore, our study emphasizes that a paradigm shift must be taken into account in relation to the use of FBS in cryoprotective media for mammalian cells freezing, since according to our data CCM seems to be the most suitable medium to use as its associated with higher DNA quality than FBS, with the advantage of being a more cost-effective option. Despite not being assessed in the present study, another alternative to the use of FBS, and even cheaper in comparison with CCM, would be the use of PBS as a major component of the cryopreservation medium, which has been found appropriate to cryopreserve sperm [15]. Future studies should be taken to assess its effectiveness in preserving DNA integrity at $-80\,^{\circ}C$ of other types of samples, including cell line samples.

5. Conclusions

The use of frozen cells allows researchers to process many samples simultaneously, which is of great advantage for large-scale studies. However, the impact of cryopreservation on cellular morphology and physiology must be investigated to ensure data reliability and validity.

The purpose of the present study was to establish the optimal harvesting and freezing conditions for human cell line samples for subsequent analysis of DNA strand breaks by the alkaline comet assay. Although both harvesting methods and cryoprotective media tested were found suitable for this purpose, our data suggest that cells collected by the enzymatic method (0.25% trypsin-EDTA) and cryopreserved in 90% CCM + 10% DMSO presented better DNA quality. Thus, CCM is a preferable cost-effective alternative to FBS for human cell lines cryopreservation medium, at least up to eight weeks of freezing. For any cell model, this type of optimization approach is highly recommended to obtain the finest protocol conditions and understand the impact on cell's DNA integrity and on its suitability for use in downstream analysis, in this particular case of DNA damage using the comet assay. Therefore, the present data provided a further insight regarding two distinct human *in vitro* cell lines, on how to collect and frozen them for short time periods. Notwithstanding, a deeper analysis could be conducted in samples stored for longer periods to better understand the impact of this optimized protocol over time.

Declarations of interest

None.

References

[1] A.R. Collins, The comet assay for DNA damage and repair, Mol. Biotechnol. 26 (2004) 249.

[2] W. Liao, M.A. McNutt, W.G. Zhu, The comet assay: a sensitive method for detecting DNA damage in individual cells, Methods 48 (2009) 46–53.

[3] A.R. Collins, The comet assay: a heavenly method!, Mutagenesis 30 (2015) 1–4.

[4] G. Koppen, A. Azqueta, B. Pourrut, G. Brunborg, A.R. Collins, S.A.S. Langie, The next three decades of the comet assay: a report of the 11th International Comet Assay Workshop, Mutagenesis 32 (2017) 397–408.

[5] A. Azqueta, A.R. Collins, The essential comet assay: a comprehensive guide to measuring DNA damage and repair, Arch. Toxicol. 87 (2013) 949–968.

[6] A. Azqueta, K.B. Gutzkow, G. Brunborg, A.R. Collins, Towards a more reliable comet assay: optimising agarose concentration, unwinding time and electrophoresis conditions, Mutat. Res. 724 (2011) 41–45.

[7] C. Ersson, L. Moller, The effects on DNA migration of altering parameters in the comet assay protocol such as agarose density, electrophoresis conditions and durations of the enzyme or the alkaline treatments, Mutagenesis 26 (2011) 689–695.

[8] S.H. Hansen, A.J. Pawlowicz, L. Kronberg, K.B. Gutzkow, A.K. Olsen, G. Brunborg, Using the comet assay and lysis conditions to characterize DNA lesions from the acrylamide metabolite glycidamide, Mutagenesis 33 (2018) 31–39.

[9] J.M. Enciso, K.B. Gutzkow, G. Brunborg, A.K. Olsen, A. Lopez de Cerain, A. Azqueta, Standardisation of the in vitro comet assay: influence of lysis time and lysis solution composition on the detection of DNA damage induced by X-rays, Mutagenesis 33 (2018) 25–30.

[10] W. Shao, S. Khin, W.C. Kopp, Characterization of effect of repeated freeze and thaw cycles on stability of genomic DNA using pulsed field gel electrophoresis, Biopreserv. Biobank. 10 (2012) 4–11.

[11] P. Jackson, L.M. Pedersen, Z.O. Kyjovska, N.R. Jacobsen, A.T. Saber, K.S. Hougaard, U. Vogel, H. Wallin, Validation of freezing tissues and cells for analysis of DNA strand break levels by comet assay, Mutagenesis 28 (2013) 699–707.

[12] C. Lin, S. Tsai, The effect of cryopreservation on DNA damage, gene expression and protein abundance in vertebrate, Ital. J. Anim. Sci. 11 (2016).

[13] K. Al-Salmani, H.H. Abbas, S. Schulpen, M. Karbaschi, I. Abdalla, K.J. Bowman, K.K. So, M.D. Evans, G.D. Jones, R.W. Godschalk, M.S. Cooke, Simplified method for the collection, storage, and comet assay analysis of DNA damage in whole blood, Free Radic. Biol. Med. 51 (2011) 719–725.

[14] G. Koppen, S. De Prins, A. Jacobs, V. Nelen, G. Schoeters, S.A.S. Langie, The comet assay in human biomonitoring: cryopreservation of whole blood and comparison with isolated mononuclear cells, Mutagenesis 33 (2018) 41–47.

[15] S. Duty, N. Singh, L. Ryan, Z. Chen, C. Lewis, T. Huang, R. Hauser, Reliability of the comet assay in cryopreserved human sperm, Hum. Reprod. 17 (2002) 1274–1280.

[16] L. Fraser, J. Strzeżek, Effects of freezing–thawing on DNA integrity of boar spermatozoa assessed by the neutral comet assay, Reprod. Domest. Anim. 40 (2005) 530–536.

[17] M.J. Bessa, C. Costa, J. Reinosa, C. Pereira, S. Fraga, J. Fernández, M.A. Bañares, J.P. Teixeira, Moving into advanced nanomaterials. Toxicity of rutile TiO2 nanoparticles immobilized in nanokaolin nanocomposites on HepG2 cell line, Toxicol. Appl. Pharmacol. 316 (2017) 114–122.

[18] J. Bright, M. Aylott, S. Bate, H. Geys, P. Jarvis, J. Saul, R. Vonk, Recommendations on the statistical analysis of the comet assay, Pharm. Stat. 10 (2011) 485–493.

[19] D.P. Lovell, T. Omori, Statistical issues in the use of the comet assay, Mutagenesis 23 (2008) 171–182.

[20] N. Fernandez-Bertolez, C. Costa, F. Brandao, G. Kilic, J.A. Duarte, J.P. Teixeira, E. Pasaro, V. Valdiglesias, B. Laffon, Toxicological assessment of silica-coated iron oxide nanoparticles in human astrocytes, Food Chem. Toxicol. 118 (2018) 13–23.

[21] B. Laffon, N. Fernandez-Bertolez, C. Costa, E. Pasaro, V. Valdiglesias, Comparative study of human neuronal and glial cell sensitivity for in vitro neurogenotoxicity testing, Food Chem. Toxicol. 102 (2017) 120–128.

[22] W. Lin, Y. Xu, C.-C. Huang, Y. Ma, K.B. Shannon, D.-R. Chen, Y.-W. Huang, Toxicity of nano- and micro-sized ZnO particles in human lung epithelial cells, J. Nanopart. Res. 11 (2008) 25–39.

[23] J. Kain, H.L. Karlsson, L. Moller, DNA damage induced by micro- and nanoparticles–interaction with FPG influences the detection of DNA oxidation in the comet assay, Mutagenesis 27 (2012) 491–500.

[24] L. Marabini, S. Ozgen, S. Turacchi, S. Aminti, F. Arnaboldi, G. Lonati, P. Fermo, L. Corbella, G. Valli, V. Bernardoni, M. Dell'Acqua, R. Vecchi, S. Becagli, D. Caruso, G.L. Corrado, M. Marinovich, Ultrafine particles (UFPs) from domestic wood stoves: genotoxicity in human lung carcinoma A549 cells, Mutat. Res. Genet. Toxicol. Environ. Mutagen. 820 (2017) 39–46.

[25] R. Nazarpour, E. Zabihi, E. Alijanpour, Z. Abedian, H. Mehdizadeh, F. Rahimi, Optimization of human peripheral blood mononuclear cells (PBMCs) cryopreservation, Int. J. Mol. Cell. Med. 1 (2012) 88.

[26] C. Del Bo, D. Fracassetti, C. Lanti, M. Porrini, P. Riso, Comparison of DNA damage by the comet assay in fresh versus cryopreserved peripheral blood mononuclear cells obtained following dietary intervention, Mutagenesis 30 (2015) 29–35.

[27] H.E. Canavan, X. Cheng, D.J. Graham, B.D. Ratner, D.G. Castner, Cell sheet detachment affects the extracellular matrix: a surface science study comparing thermal liftoff, enzymatic, and mechanical methods, J. Biomed. Mater. Res. A. 75 (2005) 1–13.

[28] N. Fujioka, Y. Morimoto, K. Takeuchi, M. Yoshioka, M. Kikuchi, Difference in infrared spectra from cultured cells dependent on cell-harvesting method, Appl. Spectrosc. 57 (2003) 241–243.

[29] B. Chelobanov, P. Laktionov, M. Khar, E.Y. Rykova, D. Pyshnyi, I. Pyshnaya, V. Silnikov, V. Vlassov, Investigation of surface oligonucleotide binding proteins of eucaryotic cells by affinity modification with reactive oligonucleotide derivatives, Russ. Chem. B. 51 (2002) 1204–1211.

[30] R. Kotikalapudi, R.K. Patel, Comparative study of the influence of EDTA and sodium heparin on long term storage of cattle DNA, Cell J. 17 (2015) 181.

[31] D.K. Lahiri, B. Schnabel, DNA isolation by a rapid method from human blood samples: effects of MgCl2, EDTA, storage time, and temperature on DNA yield and quality, Biochem. Genet. 31 (1993) 321–328.

[32] L. Limaye, V. Kale, Cryopreservation of human hematopoietic cells with membrane stabilizers and bioantioxidants as additives in the conventional freezing medium, J. Hematother. Stem Cell Res. 10 (2001) 709–718.

[33] M. Noda, Y. Ma, Y. Yoshikawa, T. Imanaka, T. Mori, M. Furuta, T. Tsuruyama, K. Yoshikawa, A single-molecule assessment of the protective effect of DMSO against DNA double-strand breaks induced by photo-and gamma-ray-irradiation,

and freezing, Sci. Rep. 7 (2017) 8557.

[34] M.B. Akor-Dewu, N. El Yamani, O. Bilyk, L. Holtung, T.E. Tjelle, R. Blomhoff, A.R. Collins, Leucocytes isolated from simply frozen whole blood can be used in human biomonitoring for DNA damage measurement with the comet assay, Cell Biochem. Funct. 32 (2014) 299–302.

[35] M. Sasaki, Y. Kato, H. Yamada, S. Terada, Development of a novel serum-free freezing medium for mammalian cells using the silk protein sericin, Biotechnol. Appl. Biochem. 42 (2005) 183–188.

[36] R. Mallone, S.I. Mannering, B.M. Brooks-Worrell, I. Durinovic-Bello, C.M. Cilio, F.S. Wong, N.C. Schloot, I.o.D.S. T-Cell Workshop Committee, Isolation and preservation of peripheral blood mononuclear cells for analysis of islet antigen-reactive T cell responses: position statement of the T-Cell Workshop Committee of the Immunology of Diabetes Society, Clin. Exp. Immunol. 163 (2011) 33–49.

[37] G. Chen, A. Yue, Z. Ruan, Y. Yin, R. Wang, Y. Ren, L. Zhu, Comparison of the effects of different cryoprotectants on stem cells from umbilical cord blood, Stem Cells Int. 2016 (2016) 1396783.

[38] A. Hardjasa, M. Ling, K. Ma, H. Yu, Investigating the effects of DMSO on PCR

fidelity using a restriction digest-based method, J. Exp. Microbiol. Immunol. 14 (2010) 161–164.

[39] X. Zheng, H. Baker, W.S. Hancock, F. Fawaz, M. McCaman, E. Pungor, Proteomic analysis for the assessment of different lots of fetal bovine serum as a raw material for cell culture. Part IV. Application of proteomics to the manufacture of biological drugs, Biotechnol. Prog. 22 (2006) 1294–1300.

[40] M.J. Sikora, M.D. Johnson, A.V. Lee, S. Oesterreich, Endocrine response phenotypes are altered by charcoal-stripped serum variability, Endocrinology 157 (2016) 3760–3766.

[41] G. Di Sante, A. Di Rocco, C. Pupo, M.C. Casimiro, R.G. Pestell, Hormone-induced DNA damage response and repair mediated by cyclin D1 in breast and prostate cancer, Oncotarget 8 (2017) 81803.

[42] M.J. Schiewer, K.E. Knudsen, Linking DNA damage and hormone signaling pathways in cancer, Trends Endocrinol. Metab. 27 (2016) 216–225.

[43] M.S. Kim, S.T. Lee, J.M. Lim, S.P. Gong, Medium composition for effective slow freezing of embryonic cell lines derived from marine medaka (Oryzias dancena), Cytotechnology 68 (2016) 9–17.

B.2. Unveiling the toxicity of fine and nano-sized airborne particles generated from industrial thermal spraying processes in human alveolar epithelial cells

Bessa M. J., Brandão F., Fokkens P. H., Leseman D. L. A. C., Boere A. J. F., Cassee F. R., Salmatonidis A., Viana M., Monfort E., Fraga S., & Teixeira J. P.

The PhD candidate contributed for the methodology, investigation, formal analysis and writing of the manuscript.

Unveiling the toxicity of fine and nano-sized airborne particles generated from industrial thermal spraying processes in human alveolar epithelial cells

Maria João Bessa[1,2,3,4], Fátima Brandão[1,2,3,4], Paul H. B. Fokkens[5], Daan L. A. C. Leseman[5], A. John F. Boere[5], Flemming R. Cassee[5,6], Apostolos Salmatonidis[7,8], Mar Viana[7], Eliseo Monfort[9], Sónia Fraga[1,2,3*], & João Paulo Teixeira[1,2,3]

[1] Department of Environmental Health, National Institute of Health Dr. Ricardo Jorge, Porto, Portugal

[2] EPIUnit-Instituto de Saúde Pública, Universidade do Porto, Porto, Portugal

[3] Laboratório para a Investigação Integrativa e Translacional em Saúde Populacional (ITR), Porto, Portugal

[4] Instituto de Ciências Biomédicas Abel Salazar (ICBAS), Universidade do Porto, Porto, Portugal

[5] National Institute for Public Health and Environment (RIVM), Bilthoven, The Netherlands

[6] Institute for Risk Assessment Sciences (IRAS), Utrecht, The Netherlands

[7] Institute of Environmental Assessment and Water Research, Barcelona, Spanish Research Council (IDAEA-CSIC), Spain

[8] LEITAT Technological Center, C/ de la Innovació 2, 08225 Terrassa, Barcelona, Spain

9 Institute of Ceramic Technology (ITC), Universitat Jaume I, 12006 Castellón, Spain

* Correspondence: sonia.fraga@insa.min-saude.pt; Tel.: (+351) 223 401147

Abstract: High-energy industrial processes have been associated with particle release into workplace air that can adversely affect workers' health. The present study assessed the toxicity of incidental fine (PGFP) and nanoparticles (PGNP), emitted from atmospheric plasma (APS) and high velocity oxy-fuel (HVOF) thermal spraying. Lactate dehydrogenase (LDH) release, 2-(4-nitrophenyl)-2H-5-tetrazolio]-1,3-benzene disulfonate (WST-1) metabolisation, intracellular reactive oxygen species (ROS) levels, cell cycle changes, histone H2AX phosphorylation (γ-H2AX) and DNA damage were evaluated in human alveolar epithelial cells at 24 h after exposure. Overall, HVOF-particles were the most cytotoxic to human alveolar cells with cell viability half-maximal inhibitory concentration (IC_{50}) values of 20.18 $\mu g/cm^2$ and 1.79 $\mu g/cm^2$ for PGFP and PGNP, respectively. Only the highest tested concentration of APS-PGFP caused a slight decrease in cell viability. Particle uptake, cell cycle arrest at $S+G_2/M$ and γ-H2AX augmentation was observed after exposure to all tested particles. However, higher levels of γ-H2AX were found in cells exposed to APS-derived particles (~16%), while cells exposed to HVOF particles exhibited increased levels of oxidative damage (~17% tail intensity) and ROS (~184%). Accordingly, APS and HVOF particles seem to exert their genotoxic effects by

different mechanisms, highlighting that the health risks of these process-generated particles at industrial settings should not be underestimated.

1. Introduction

The ceramic industry has been benefitting from nanotechnology innovation processes and advanced materials (Bessa *et al.*, 2020). Workers from these industries are at risk of exposure to airborne fine (< 2.5 µm mass median aerodynamic diameter [MMAD]) and nano-sized (< 0.2 µm MMAD) particles that may be released either during the handling or manufacturing of ceramics using engineered nanoparticles (ENP, 1-100 nm) as raw materials or to incidentally emitted particles during mechanical and combustion/heating processes. Indeed, high-energy processes such as laser ablation, laser sintering, physical vapour deposition, inkjet printing, thermal spraying processes [*e.g.*, atmospheric plasma spraying (APS) and high velocity oxy-fuel spraying (HVOF)] and glazing represent a high potential of fine and ultrafine particle formation and release to the workplace air (Fonseca *et al.*, 2015a; Fonseca *et al.*, 2015b; Fonseca *et al.*, 2016; Ribalta *et al.*, 2019; Salmatonidis *et al.*, 2018a; Salmatonidis *et al.*, 2020; Salmatonidis *et al.*, 2018b; Viana *et al.*, 2017; Viana *et al.*, 2021).

Inhalation is the predominant route of exposure to micro- and nano-sized particles at occupational settings. Respiratory tract deposition and clearance is governed by the aerosol physics and by the anatomy and physiology of the respiratory tract (Stuart, 1984). The deeper the particles reach, the harder is their removal from the respiratory system favouring particle-cell interactions that might result in adverse health effects (Geiser *et al.*, 2010; Xing *et al.*, 2016). Many epidemiological studies already described an association between exposure to particulate matter (PM) and the occurrence of adverse health effects (Karanasiou *et al.*, 2014; Schraufnagel, 2020). Exposure to airborne particles has been associated with cardiovascular, pulmonary and neurological diseases, which leads to increased risk of mortality (Anderson *et al.*, 2012; Hamanaka *et al.*, 2018; Stone *et al.*, 2017). In the case of the ceramic industry, worker' exposure to ceramic dusts has been strongly linked to respiratory symptoms such as wheezing, breathlessness and dry cough as well as with reduced lung function, chronic bronchitis and chronic

obstructive pulmonary disease (COPD) (Jaakkola *et al.*, 2011; Kargar *et al.*, 2013; Trethowan *et al.*, 1995).

Most of the knowledge on nano(particle) toxicity comes from *in vitro* mechanistic studies. While there are many available studies on the *in vitro* toxicity of engineered nanoparticles (ENP), little is known about the *in vitro* hazard of process-generated (nano)particles. In this regard, our group has recently conducted a comparative assessment on the *in vitro* toxicity of ENP [tin oxide (Sb_2O_3) and zirconium oxide (ZrO_2) ENP] used as input materials in the ceramic industry *vs* particles collected during HVOF spraying of ceramic coatings onto metal surfaces to produce thermal-resistant coatings (Bessa *et al.*, 2021a). Overall, our data showed that human tri-dimensional (3D) bronchial cultures under air-liquid interface (ALI) conditions were rather resistant to the ENP that induced mild cytotoxicity at early timepoints (24 h), though cells rapidly recovered since no significant changes in cell viability compared to the control were observed at late timepoints (72 h). At the same time, while the fine fraction of the HVOF-derived particles significantly decreased cell viability, the ultrafine fraction significantly increased DNA oxidative damage, showing that HVOF particles exhibited higher toxicity potential compared to ENP (Bessa *et al.*, 2021a). A recent study by Cediel-Ulloa *et al.* also evaluated the *in vitro* toxicity of airborne particles emitted during gas–metal arc welding (GMAW) in a laboratory setting on primary human small airway epithelial cells (hSAEC) (Cediel-Ulloa *et al.*, 2021). These authors observed that stainless steel welding particles were more cytotoxic compared to mild steel particles and induced oxidative stress in primary human small airway epithelial cells. In addition, Pavlovska *et al.* investigated the biological effects of airborne particulates collected in woodworking and metalworking industries both on EpiAirway 3D human small airway epithelial cells exposed for 4 h (half working day), 8 h (full working day) 72 h (3 working days) and on A549 lung epithelial cells continuously exposed for 96 h. Data obtained showed that exposure to these polluting particles exerted minor acute effects on the morphology and viability of both A549 cells and EpiAirway tissues. However, a marked reduction in EpiAirway tissue viability after 8 h exposure to woodworking particles, and a slight reduction in tissue viability after 72 h of exposure to metalworking particles was observed (Pavlovska *et al.*, 2021).

Therefore, the present study aims to further explore the *in vitro* toxicity of process-generated fine (PGFP; <2.5 μm MMAD) and nano-sized particles (PGNP; <0.2 μm MMAD) incidentally emitted during two industrial thermal spraying

processes (APS and HVOF) of ceramic coatings onto metal surfaces. We hypothesise that PGNP are more toxic to human alveolar epithelial cells than PGFP. Biological endpoints including particle internalisation, plasma membrane integrity, cell metabolic activity and viability, reactive oxygen-species (ROS) levels, cell cycle analysis, histone H2AX phosphorylation and DNA damage were evaluated in human alveolar epithelial A549 cells at 24 h after exposure.

2. Results

2.1. Process-generated fine and nano-sized particles characterisation

Table 1 presents the physicochemical features of the aqueous suspensions of the tested process-generated particles, namely concentration (both in terms of mass and number of particles per mL), hydrodynamic size and oxidative potential. As shown, APS-derived aqueous suspensions were more diluted in terms of mass/mL than the HVOF ones, which somehow limited the maximum tested concentrations of the former type of particles, in particular of the PGNP fraction. For APS-derived particles, the mean hydrodynamic size value was 244 nm and 410 nm for PGFP and PGNP, respectively. At the same time, HVOF- PGFP (247 nm) and PGNP (236 nm) exhibited a similar hydrodynamic size mean value. Regarding the oxidative potential, only APS-derived PGFP demonstrated a low oxidative potential, whereas HVOF-derived particles, particularly PGNP, exhibited a high ability to produce ·OH in a cell-free environment.

Table 1. Physicochemical characteristics of the tested PGFP and PGNP particles aqueous suspensions.
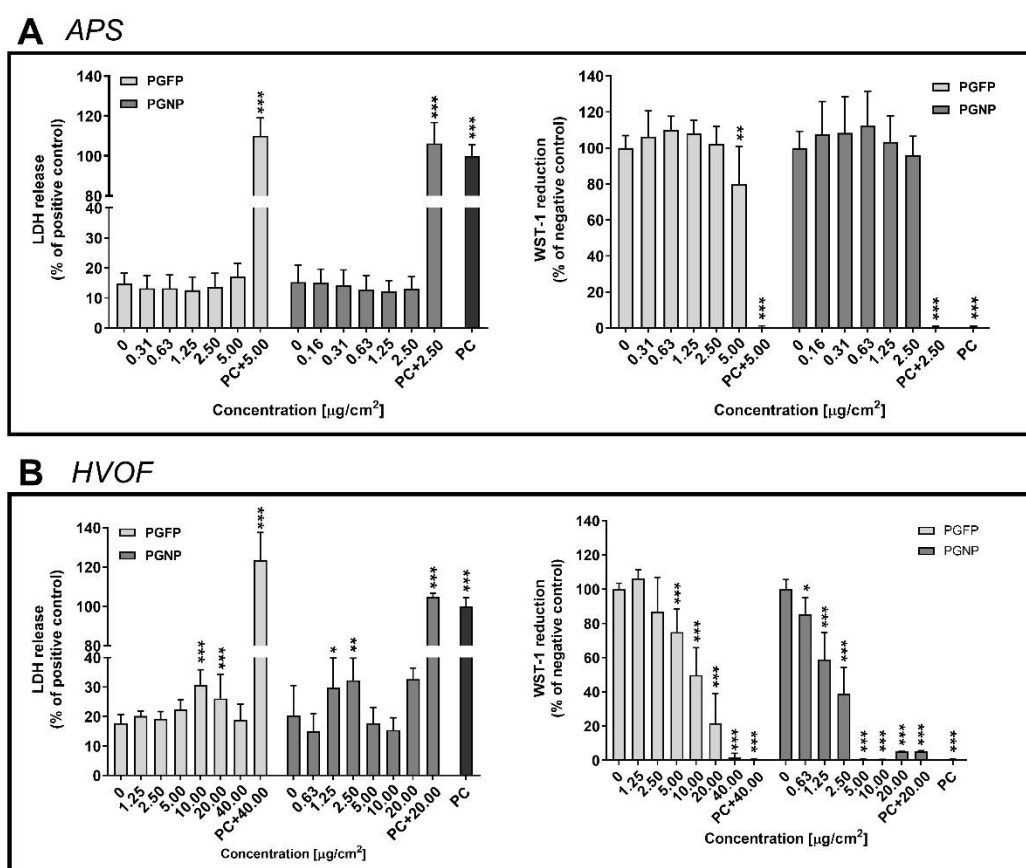
		Stock suspension concentration (mg/mL)	Stock suspension concentration (number of particles/mL)	Hydrodynamic size (nm)	Oxidative potential (A.U.)*
APS	*PGFP*	0.068	8.49×10^8	244 ± 120	3291
	PGNP	0.034	4.21×10^8	410 ± 162	5319
HVOF	*PGFP*	1.069	9.72×10^8	247 ± 116	9893
	PGNP	0.140	15.86×10^8	236 ± 86	12833

Data are presented as mean ± SD. Hydrodynamic size and concentration were measured by Nanoparticle Tracking Analysis. Oxidative potential was measured by Electronic Spin Resonance. A.U.: arbitrary units. *Negative control (ultrapure water) = 3191 A.U.; Positive control (DOFA) = 48041 A.U.

2.2. Plasma membrane integrity and cell viability

Under our experimental conditions, no differences in cell's membrane integrity and viability were found after 24 h of exposure to both fractions of APS-derived particles, comparing with the negative control (NC) (**Figure 1A**). On the other hand, the cytotoxic effects were more pronounced when cells were exposed

to particles derived from the HVOF spraying process. While a significant increase in the LDH release compared to control cells was observed after exposure to PGFP at either 10.00 μg/cm² (30.70 %) or 20 μg/cm² (26.15 %), a clear concentration-dependent decrease in cell viability was detected (**Figure 1B**). Analysis of cell viability concentration-response curves of cells exposed to HVOF-derived PGFP and PGNP revealed a half-maximal inhibitory concentration (IC$_{50}$) of 20.18 μg/cm² (CI 95 %: 11.66-34.95) and 1.79 μg/cm² (CI 95 %: 1.48-2.16), respectively.

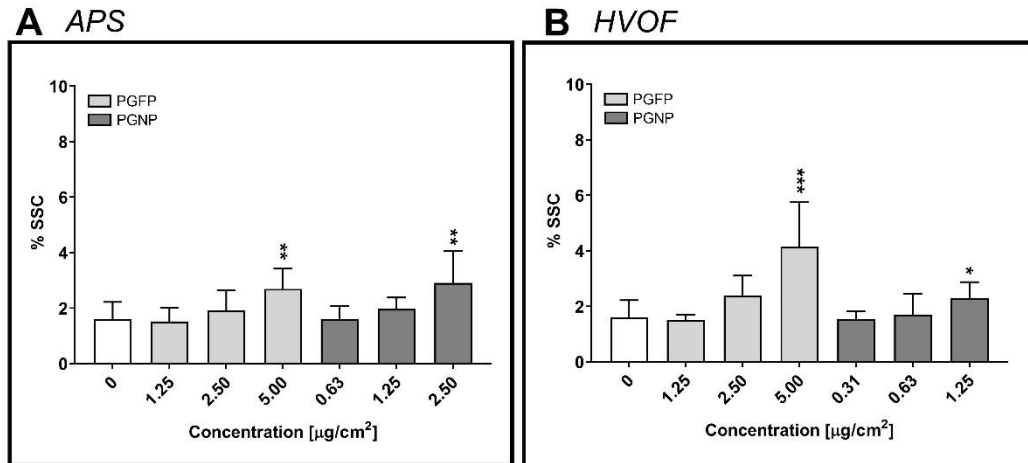**Figure 1.** Cytotoxicity of PGFP and PGNP released during APS **(A)** and HVOF **(B)** in human alveolar epithelial cells after 24 h of exposure. Data are expressed as mean ± standard deviation (n=3-4). LDH release values were normalised considering the positive control (total LDH release; cells lysed with 2 % Triton X-100), while WST-1 reduction values were normalised considering the negative control (NC). Data was analysed by the one-way analysis of variance (ANOVA) test followed by the Dunnett's post hoc test for multiple comparisons. *P ≤ 0.05, **P ≤ 0.01 and ***P ≤ 0.001 *vs* NC. PC: Positive control (LDH: 2 % Triton X-100; WST-1: 70 % EtOH).

2.3. Intracellular reactive oxygen species levels

No major effects on ROS levels were found on human alveolar epithelial cells after 24 h of exposure to APS-derived PGFP and PGNP (**Figure 2A**). On the other

hand, in cells exposed to the HVOF-particles a significant increase in the intracellular ROS levels was found for the highest tested concentrations of PGFP (176.88 ± 32.35 %) and PGNP (183.67 ± 59.06 %), when compared to the NC (**Figure 2B**).
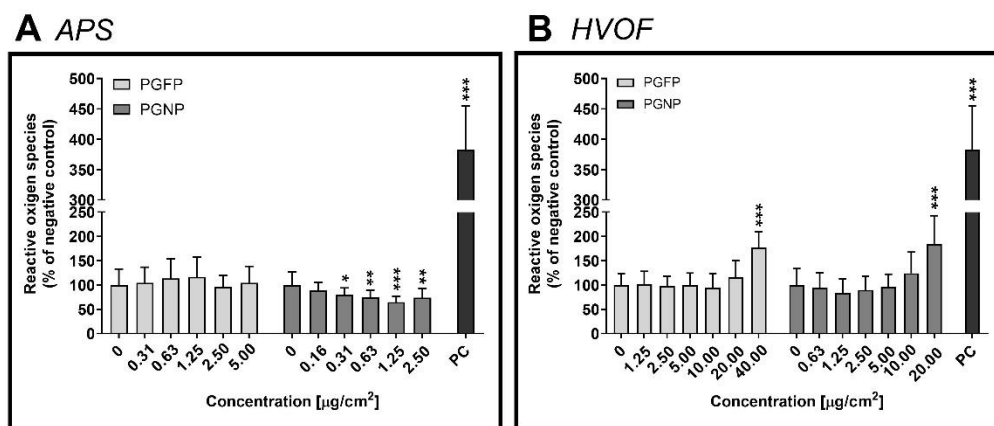
Figure 2. ROS intracellular levels in human alveolar epithelial cells after 24 h of exposure to PGFP and PGNP released during APS **(A)** and HVOF **(B)**. Data are expressed as mean ± standard deviation (n=3-4). Values were normalised considering the NC. Data was analysed by the one-way ANOVA test followed by the Dunnett's post hoc test for multiple comparisons. *$P \leq 0.05$, **$P \leq 0.01$ and ***$P \leq 0.001$ *vs* NC. PC: 25 μM AgNO$_3$.

2.4. Cellular uptake of the (nano)particles

The cellular uptake of the process-generated particles under study by human alveolar epithelial cells was estimated based on changes in the percentage of the side scatter signal (% SSC), a measure of cellular complexity, analysed by flow cytometry. As depicted in **Figure 3**, a concentration-dependent increase in cell complexity was observed in A549 cells incubated with all tested particles regardless the process and the particle fraction. For APS- and HVOF-derived particles, a significant increase in particle uptake has been detected in cells exposed to the highest tested concentrations of either PGFP or PGNP. However, the fine HVOF-derived particles have been internalised by A549 cells in a higher degree than the nano-sized fraction. At the same time, HVOF-PGFP (5 μg/cm^2; 4.16 ± 1.61 %) were internalised to a greater extent than APS-PGFP (5 μg/cm^2; 2.69 ± 0.75 %) in A549 cells.

Figure 3. Cellular uptake of PGFP and PGNP released during APS **(A)** and HVOF **(B)** by human alveolar epithelial A549 cells after 24 h of exposure, as estimated by variations of the side scatter signal (SSC). Data are expressed as mean ± standard deviation (n=3-4). Data was analysed by the one-way ANOVA test followed by the Dunnett's post hoc test for multiple comparisons. *$P \leq 0.05$, **$P \leq 0.01$ and ***$P \leq 0.001$ *vs* NC.

2.5. Cell cycle analysis

Figure 4 shows the effect of the tested process-generated particles on the human alveolar epithelial cell cycle dynamics, as assessed by flow cytometry. In the NC, most of the cells were at G_0/G_1 phase (78.04 ± 2.51 % cells), which was expected considering that cells were incubated for 24 h with FBS-free culture medium. Moreover, a concentration-dependent increase of cells in the S and G_2/M phases was observed at 24 h after exposure to all particles under study, but still with the G_0/G_1 cells representing the largest subpopulation (**Figures 4A and 4B**). As shown in **Figure 4C**, under our experimental conditions, less than 10 % of the cells undergo apoptosis (sub-G_1 population), though a concentration-dependent increase in the apoptotic cell number was observed for all tested particles, regardless the process and particle fraction.
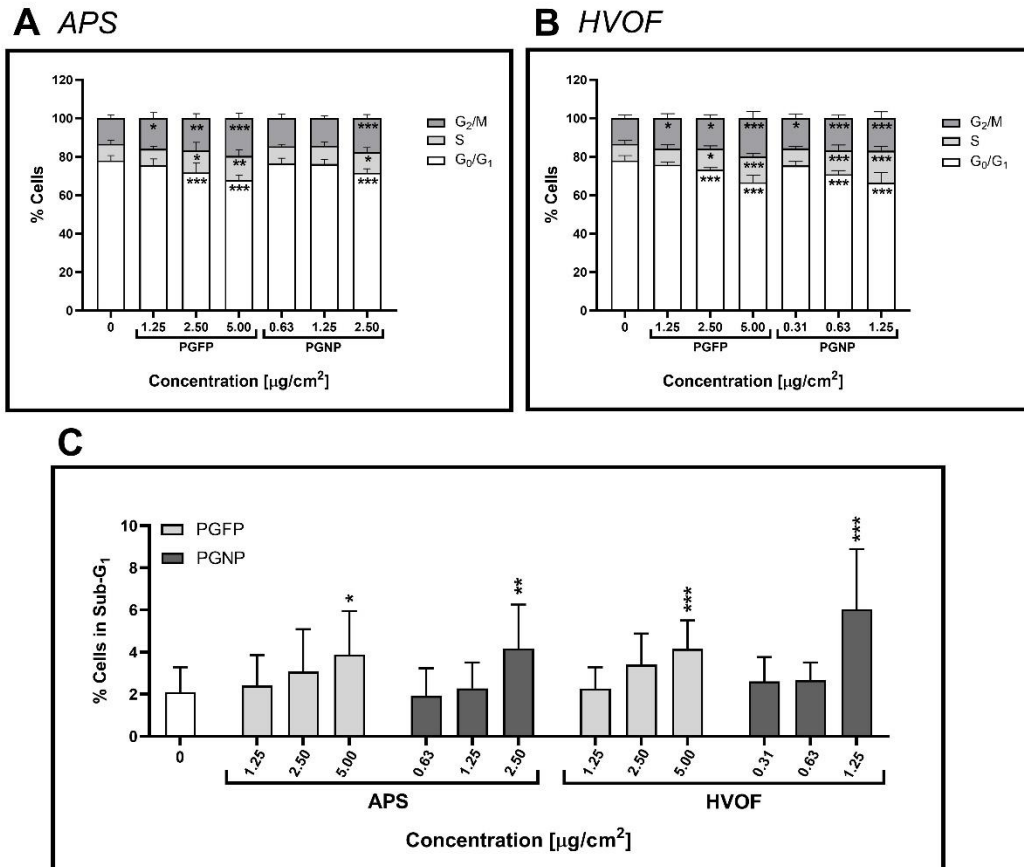
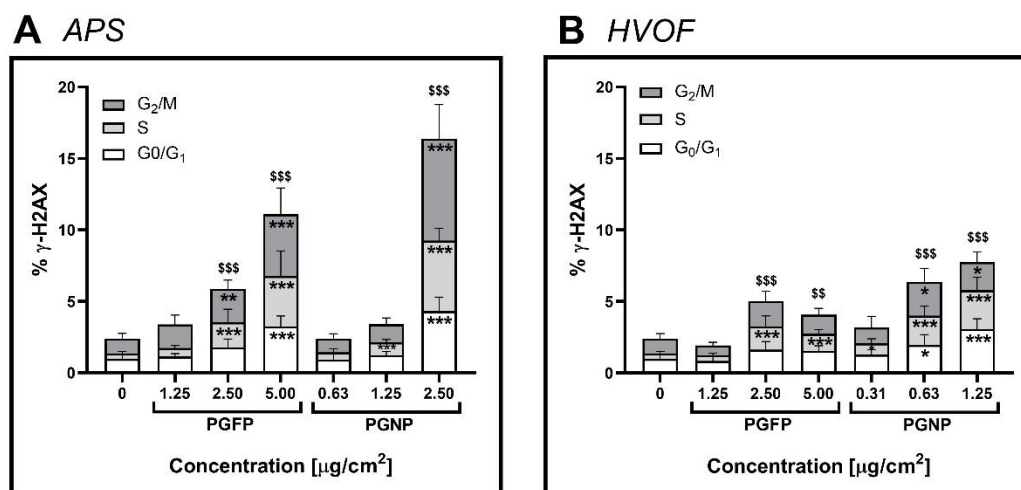**Figure 4.** Cell cycle analysis of human alveolar epithelial cells after 24 h of exposure to PGFP and PGNP released during APS **(A)** and HVOF **(B)**. The percentage of cells in the sub-G_1 phase (apoptotic cells) was also analysed **(C)**. Data are expressed as mean ± standard deviation (n=3-4). Data was analysed by one-way ANOVA followed by Dunnett's post-hoc test. *P ≤ 0.05, **P ≤ 0.01 and ***P ≤ 0.001 *vs* NC.

2.6. Histone gamma-H2AX phosphorylation

Histone gamma-H2AX phosphorylation (γ-H2AX), a biomarker for DNA double-strand breaks was assessed by flow cytometry at 24 h after exposure to the process-generated particles. As shown in **Figure 5**, a significant increase in the total γ-H2AX levels in A549 cells has been detected after exposure to any type of process-generated particles, being this increase more marked in cells incubated with the APS-derived particles (**Figure 5A**) compared to the ones exposed to the HVOF-particles (**Figure 5B**). In fact, for the APS-derived particles, PGNP (2.5 µg/cm^2: 16.39 ± 3.65 %) were more effective in causing total γ-H2AX than PGFP (5 µg/cm^2: 11.10 ± 4.14 %). Moreover, increasing levels of γ-H2AX were found for each phase of the cell cycle after 24 h exposure to the highest tested concentration of PGFP and PGNP APS-derived particles. Regarding HVOF-derived particles increasing levels

of γ-H2AX in each phase of the cell cycle were found, but in a much lower degree than APS-particles. Camptothecin (3.5 µg/mL) served as positive control (PC) and as expected caused an evident increment of the total γ-H2AX levels in cells at the different cell cycle phases compared to the NC.

Representative graphs of the cellular uptake of particles, cell cycle and γ-H2AX analyses by flow cytometry are depicted in **Figure A1**.

Figure 5. γ-H2AX in human alveolar epithelial cells after 24 h of exposure to PGFP and PGNP released during APS **(A)** and HVOF **(B)**. Data are expressed as mean ± standard deviation (n=3-4). Data were analysed by one-way ANOVA followed by Dunnett's post-hoc test. Global γ-H2AX analysis: $^{§}P \leq 0.05$, $^{§§}P \leq 0.01$ and $^{§§§}P \leq 0.001$ *vs* NC. γ-H2AX in each phase of cell cycle: $*P \leq 0.05$, $**P \leq 0.01$ and $***P \leq 0.001$ *vs* NC.

2.7. Primary and oxidative DNA damage

Figure 6 depicts the primary and oxidative DNA damage of A549 cells incubated with the APS- (**Figure 6A**) and HVOF-derived particles (**Figure 6B**). Although a slight increase in DNA strand breaks was observed for PGFP of both APS and HVOF spraying processes, as well as for HVOF-derived PGNP, those were not significant when compared to the NC. However, APS-derived PGFP significantly increased DNA FPG-sensitive sites of human alveolar epithelial cells at concentrations of 2.5 µg/cm² (7.81 ± 4.40 % tail intensity) and 5 µg/cm² (8.37 ± 2.23 % tail intensity) compared to the NC (2.90 ± 1.80 % tail intensity) (**Figure 6A**), while the nano-sized fraction did not increase oxidative DNA damage in A549 cells (**Figure 6A**). HVOF particles seem to cause higher levels of DNA oxidative damage compared to the APS-particles. As shown in **Figure 6B**, both PGFP and PGNP HVOF-derived fractions significantly increased DNA oxidation in a concentration-

dependent manner. Representative comet images of the DNA damage of human alveolar epithelial cells exposed to the highest tested concentrations of PGFP and PGNP emitted during HVOF thermal spraying process are depicted in **Figure B1**.
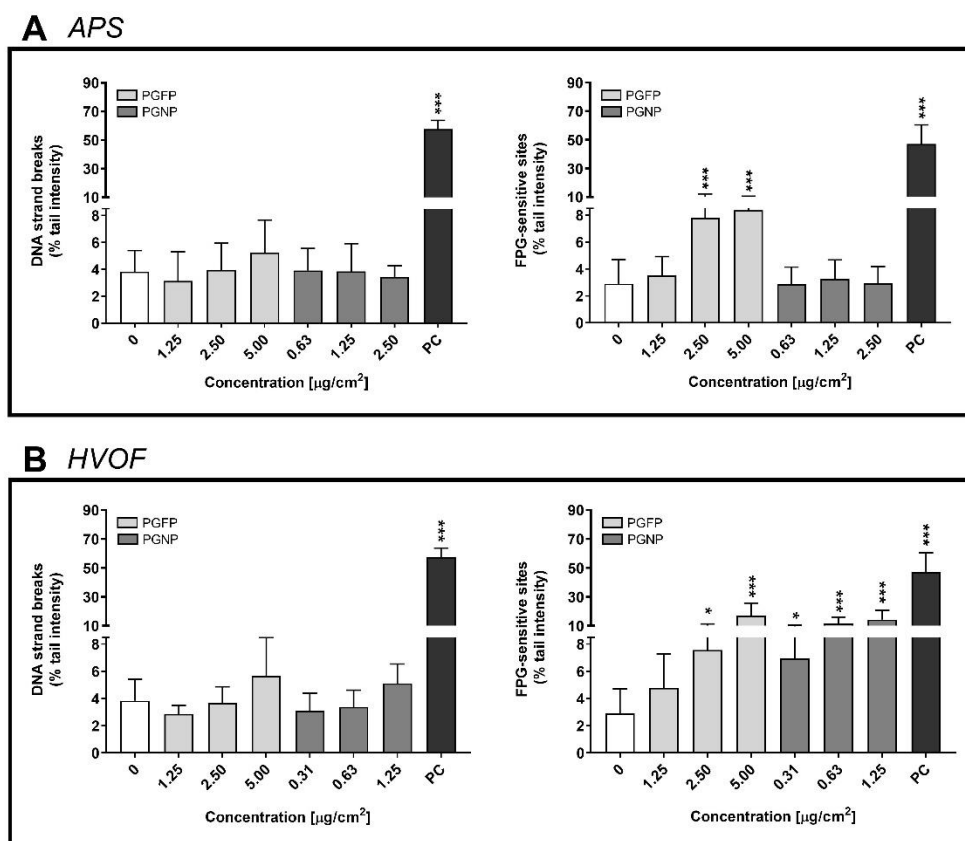

Figure 6. Primary (DNA strand breaks) and oxidative (FPG-sensitive) DNA damage in human alveolar epithelial cells after 24 h of exposure to PGFP and PGNP particles released during APS **(A)** and HVOF **(B)**. Data are expressed as mean ± standard deviation (n=3-4). Data was analysed by one-way ANOVA followed by Dunnett's post-hoc test. *$P \leq 0.05$, **$P \leq 0.01$ and ***$P \leq 0.001$ *vs* NC. PC: 500 µM MMS and 2.5 mM $KBrO_3$ for primary and oxidative DNA damage, respectively.

3. Discussion

Regardless the size fraction, HVOF-derived particles were more cytotoxic for A549 cultures than the APS-particles. Indeed, particles emitted during HVOF spraying induced a marked decrease in cell viability, with PGNP being more potent than PGFP as evidenced by its ~10x lower IC_{50} value, while only the fine fraction of APS-derived particles slightly decreased cell viability at the highest tested concentration (5 µg/cm²). In addition, only exposure to HVOF- but not to APS-emitted particles significantly increased ROS intracellular levels of A549 cells. These results are in good agreement with the highest oxidative potential of HVOF

particles compared to the APS particles. ROS are important molecules involved in redox-associated signalling pathways. While important to regulate and maintain normal physiological functions, excessive levels of intracellular ROS can activate cell death and other signalling pathways including nuclear factor-κB (NF-κB), mitogen-activated protein kinase (MAPK), phosphoinositide 3-kinase (PI3-K) that are involved in the regulation of the expression of inflammatory response genes, cell cycle arrest, DNA strand breaks and formation of 8-oxo-7,8-dihydro-2'-deoxyguanosine (8-oxo-dG) DNA adducts (Manke *et al.*, 2013; Peixoto *et al.*, 2017).

Differences in their chemical composition might have an obvious toxicological impact and may explain the observed cellular effects in A549 cells. The chemical analysis of the airborne fine and nano-sized particles under study revealed a major enrichment in potentially health hazardous metals [chromium (Cr), nickel (Ni), tungsten (W)] sourcing directly from the feedstock in both scenarios, as well as in major elements [aluminium (Al), calcium (Ca), iron (Fe)] with different possible source origins, including re-suspension of indoor dusts. Size-resolved particle chemical composition analysis by Inductively coupled plasma mass spectrometry (ICP-MS) and Inductively coupled plasma - optical emission spectrometry (ICP-OES) showed that APS-derived particles were mainly constituted by Al (68 % and 42% for PGFP and PGNP, respectively), Cr (11 and 16 % for PGFP and PGNP, respectively) and Ni (1 and 21% for PGFP and PGNP, respectively), while the HVOF generated ones were mainly constituted by Cr (61 and 67 % for PGFP and PGNP, respectively) and Ni (27 and 28 % for PGFP and PGNP, respectively), as previously reported (Viana *et al.*, 2021). These differences in composition might have contributed to particle aggregation/agglomeration of the aqueous suspensions, in particular of APS-PGNP that presented a high hydrodynamic size value.

Epidemiological and occupational studies have shown the hazard of inhalation exposure to Al, Cr, and Ni to human health. Workplace exposure to airborne particles containing these elements has been associated with several respiratory disorders such as pulmonary fibrosis, asthma, chronic obstructive lung disease, lung cancer, and cardiovascular disease (Björ *et al.*, 2008; Halasova *et al.*, 2010; Jederlinic *et al.*, 1990; Lippmann *et al.*, 2009; Park *et al.*, 2018; Phillips *et al.*, 2010; Salnikow *et al.*, 2008; Thomassen *et al.*, 2006). Several *in vivo* and *in vitro* studies have also addressed the toxicity of nanoforms of these elements. Kim *et al.* investigated the toxicity of aluminium oxide (Al_2O_3) nanoparticles (NP) following 28 days of repeated exposure by inhalation in male rats and reported a

no-observed-adverse-effect level (NOAEL) of 1 mg/m^3 (Kim *et al.*, 2018). At the same time, the existing evidence on the Al$_2$O$_3$ NP effects on human pulmonary cell lines seem to point out for minimal toxic effects caused by these NP, that were considered less toxic when compared to cerium oxide (CeO$_2$), titanium dioxide (TiO$_2$), silicon dioxide (SiO$_2$), and zinc oxide (ZnO) NP (Ivask *et al.*, 2015; Kim *et al.*, 2010; Tsaousi *et al.*, 2010; Zhang *et al.*, 2011). These findings are in line with our results showing that Al-rich APS-derived particles did not induce a marked cytotoxicity or increment in ROS levels of A549 cells.

Both tested thermal spraying derived particles, especially HVOF-emitted ones, are enriched in Cr and Ni. So far, the available *in vitro* and *in vivo* studies on Cr and Ni effects have shown pulmonary toxicity in response to exposure to these elements (Åkerlund *et al.*, 2018; IARC, 1990; Morimoto *et al.*, 2011; Roedel *et al.*, 2012; Wise *et al.*, 2002; Zhang *et al.*, 2003). In this regard, human lung cells incubated with Cr(VI) have been reported to exhibit significant levels of oxidative DNA damage (Reynolds *et al.*, 2012), as well as increasing levels of H2AX-Ser139 phosphorylation (DeLoughery *et al.*, 2014). Evidence of cell cycle arrest at G$_2$/M has been also found in alveolar A549 cells exposed for 24 h to Cr(VI) (Zhang *et al.*, 2001). On the other hand, Ding *et al.* have shown that exposure to Ni triggered G$_2$/M cell cycle arrest and proliferation blockage in human bronchial epithelial cells (BEAS-2B) (Ding *et al.*, 2009). In the nanoscale form, DNA damage accompanied by increased phosphorylation of DNA damage response associated proteins ATM serine/threonine protein kinase (Ser1981), p53 tumour protein (Ser15) and H2AX (ser139) has been reported by Mo *et al.* in BEAS-2B cells exposed to Ni NP for 24 h (Mo *et al.*, 2021).

In response to DNA damage, the cell undergoes through various checkpoint mechanisms essential to survival, but when these fail, that potentially result in a rapid cell death (Ma *et al.*, 2018). DNA damage occurring throughout interphase will elicit a cell cycle arrest which allows time for repair mechanisms to occur prior progression to subsequent phases of the cell cycle (Barnum *et al.*, 2014). For instance, depending on the cell cycle phase which a double strand break occurs, the repair mechanism used by the cell differs (Mjelle *et al.*, 2015). One mechanism of double strand break repair is through the phosphorylation-dependent recruitment of DNA damage repair factors to sites of DNA damage, such as the phosphorylation of Ser139 on histone H2AX (γ-H2AX) (Podhorecka *et al.*, 2010). In the current study, flow cytometry data showed that exposure to any type of thermal spraying-derived particles induced cell cycle arrest at S and G$_2$/M phases in human

alveolar epithelial A549 cells, most likely triggered in response to DNA damage. Indeed, following DNA damage, the S-phase checkpoint delays DNA synthesis, while the G_2 cell cycle checkpoint prevents cells from entering mitosis, inhibiting cell proliferation (Barnum *et al.*, 2014). In addition, for every particle, a concentration-dependent increase in the number of apoptotic sub-G_1 phase cells after 24 h of exposure was observed. Under our experimental conditions, an overall increase in γ-H2AX levels was found in A549 cells, especially in cells at S and G_2/M phases. Interestingly, a more prominent effect on γ-H2AX levels was observed in cells incubated with fine or nano-sized APS-derived particles. Notwithstanding, for both APS- and HVOF- derived particles, the found γ-H2AX levels were more evident at lower concentrations of PGNP when compared to PGFP. On the other hand, although both fractions of HVOF-emitted particles increased the oxidative DNA damage, in cells exposed to PGNP that effect was visible at lower concentrations. For the APS-particles, for instance, oxidative damage was only observed after 24 h exposure to the fine fraction. Therefore, our data suggest that mechanisms involved in the genotoxicity of the tested thermal spraying-emitted particles might differ between them. While APS-particles prominently cause histone H2AX phosphorylation at serine-139 as an early cellular response to the induction of DNA double-strand breaks, HVOF-particles mainly induce 8-oxo-G oxidative DNA lesions, most likely caused by the increased intracellular ROS levels observed.

We have recently reported the effect of both fractions of the HVOF-derived particles studied herein in human 3D bronchial epithelial cultures (MucilAir™) under ALI conditions (Bessa *et al.*, 2021a). We have found that PGFP aerosols affected cell viability at dose levels as low as 9 µg/cm^2, which was not seen for the aerosolised PGNP. However, exposure to PGNP (4.5 mg/cm^2) caused an increase in the oxidative DNA damage of MucilAir™ cultures. In the present study, under submerged conditions, a stronger toxic response has been observed, as both fractions of HVOF particles induced a pronounced decrease in cell viability and higher levels of oxidative DNA damage at lower concentrations after 24 h exposure of A549 cells. Differences in the magnitude of the responses to the HVOF particles within the two studies may be explained by differences in the attained deposited doses, as well as in the sensitivity of the cell models used. While aerosolised particles directly deposit on cells surface, at submerged conditions particles in suspension may react with the culture medium, agglomerate/aggregate into larger particles (Lacroix *et al.*, 2018; Loret *et al.*, 2016). On the other hand, human primary cultures under ALI conditions have been described as more resistant than the traditional 2D

monoculture models since they exhibit a higher degree of complexity, with active ciliary beating and mucus production that mimic the mucociliary clearance defence system that occurs *in vivo* (Frieke Kuper *et al.*, 2015; George *et al.*, 2019), which might have considerably attenuated the uptake and cellular effects of the HVOF-derived particles (Bessa *et al.*, 2021a). Our simplified test system does not account for differences in pulmonary deposition of PGFP and PGNP, whereas it is well-established that the smaller sizes may penetrate more deep into the lung and more efficiently reach the more vulnerable alveoli. Statements on the actual human health risk are therefore not possible, also in the absence of actual personal exposure levels.

4. Conclusions

HVOF-particles were more cytotoxic compared to APS-particles, , most likely due to differences in their elemental composition. As hypothesised, PGNP derived from HVOF were more cytotoxic to A549 cells than PGFP, while both fractions of APS-emitted particles did not induce significant cytotoxic effects in A549 cells. Notwithstanding, particles emitted from the two thermal spraying processes under study were genotoxic to human alveolar epithelial cells. While APS particles prominently lead to increased levels of H2AX phosphorylation, HVOF particles mainly caused 8-oxo-dG oxidative DNA lesions. Among the perceived genotoxicity, PGNP induced significant effects at lower concentrations for both high energy spraying processes, except regarding oxidative DNA were only PGFP emitted during APS cause measurable effects.

Our data highlight that workers from industries employing high-energy processes may be at (increased) risk of adverse health effects depending on the actual inhaled dose, i.e. exposure levels and duration. Occupational epidemiological studies are urgently needed to establish this risk, whereas a better understanding of the cellular mechanisms involved in process-generated particles-induced biological effects, ultimately contributing for controlling exposures to these particles in the workplace would facilitate reducing the health risks. The availability of information obtained from real-world exposure scenarios is deemed essential to establish realistic preventive and corrective measures adapted to the different work scenarios (manufacturing technologies and/or chemical composition of materials).

5. Materials and Methods

4.1. Chemicals

Dimethyl sulfoxide (DMSO), sodium hydroxide (NaOH), sodium chloride (NaCl), potassium chloride (KCl) and potassium hydroxide (KOH) were purchased from Merck KGaA (Darmstadt, Germany). Triton X-100, bovine serum albumin (BSA), low melting point (LMP) agarose, Tris hydrochloride (Tris-HCl), silver nitrate ($AgNO_3$), 4-(2-hydroxyethyl)piperazine-1-ethanesulfonic acid (HEPES), methyl methanesulfonate (MMS), propidium iodide (PI), Roche cytotoxicity detection kit (LDH) and cell proliferation reagent water-soluble tetrazolium (WST-1) were bought from Sigma-Aldrich (Madrid, Spain). Tris-base and disodium salt dihydrate (Na_2EDTA) were supplied from Merck Millipore (Madrid, Spain). Normal melting point (NMP) agarose was purchased from Bioline (London, UK). Potassium bromate ($KBrO_3$) and camptothecin were supplied from Alfa Aesar (Karlsruhe, Germany). Formamidopyrimidine-DNA glycosylase (FPG) was purchased from New England Biolabs (Ipswich, MA, USA). Guava ICF instrument cleaning fluid was supplied by Luminex Corporation (Austin, TX, USA). and PBS pH 7.4 flow cytometry grade from Gibco were purchased from Life Technologies Corp. (NY, USA). RNAse A from bovine pancreas (DNAse-free) from Applichem Panreac, eBioscience™ phospho-histone H2A.X (Ser139) Alexa Fluor® 488 conjugated monoclonal antibody (CR55T33), Invitrogen™ SYBR® Gold dye and CM-H_2DCFDA (General Oxidative Stress Indicator) were bought from Thermo Fisher Scientific (Madrid, Spain). All cell culture reagents were purchased from Gibco, Thermo Fisher Scientific (Madrid, Spain). All chemicals used were of high purity or analytical grade.

4.2. Fine and nano-sized particles suspensions and characterisation

Incidental process-generated fine (PGFP; <2.5 μm MMAD) and nano-sized particles (PGNP; <0.2 μm MMAD) emitted during APS and HVOF spraying were collected directly from the inside of the spraying booths at an industrial-scale mechanical workshop in the vicinity of Barcelona, as previously described (Viana *et al.*, 2021). Regarding the APS spraying, the collection was performed during the injection of a Cr/Ni (50/50) and Al_2O_3 + TiO_2 feedstock blend, while for HVOF it was performed during the injection of a tungsten carbide (WC) – chromium carbon (CrC) – Ni – cobalt (Co) feedstock blend, as described in (Viana *et al.*, 2021). Both PGFP and PGNP fractions were sampled directly as stock suspensions for toxicity testing,

using an aerosol concentration enrichment system, as previously described (Kim *et al.*, 2001). The collected samples were subjected to gamma-ray irradiation to ensure the required sterility prior to the cell incubations.

Hydrodynamic size and concentration (number of particles/mL) of the aqueous particle suspensions under study were determined by Nanoparticle Tracking Analysis (NTA) using a NanoSight LM20 (NANOSIGHT Ltd, Salisbury, United Kingdom). The particle oxidative potential (acellular ROS production) was determined by Electron Spin Resonance (ESR) based on the trapping of nanoparticle NP-induced hydroxyl radicals (OH) generated in the presence of hydrogen peroxide (H_2O_2) using DMPO (5,5-dimethyl-1-pyrroline-N-oxide) as spin trap, as previously described (Bessa *et al.*, 2021b). Briefly, particle suspensions were mixed with 0.5 M H_2O_2 and 0.05 M DMPO, followed by incubation for 15 min at 37 °C in a heated shaking water bath prior to ESR analysis. The ESR quantification was conducted with the Analysis Software (2.0 Magnettech GmbH, Berlin) on first derivation of ESR signals of DMPOeOH quartet as the average of total amplitudes and expressed in arbitrary units (A.U.) per sampled volume (Bessa *et al.*, 2021b).

4.3. Cell culture

Lung adenocarcinoma epithelial A549 cells from the American Type Culture Collection (ATCC®, CCL-185™) were cultured in RPMI 1640 medium with Glutamax™, 25 mM HEPES and supplemented with 10 % heat-inactivated foetal bovine serum (FBS), 50 U/mL penicillin and 50 µg/mL streptomycin. Cells were maintained in a humidified atmosphere with 5 % CO_2 at 37 ℃. To carry out the submerged exposure experiments, cells were seeded in 96-well (1.0×10^4 cells/well) or 24-well plates (5.0×10^4 cells/well) and allowed to adhere for 48 h at 37 ℃, 5 % CO_2.

4.4. Exposure conditions

All particle stock suspensions under study were dispersed by indirect probe sonication using a Branson sonifier (model 450) equipped with a disruptor cup horn according with the Standard Operation Procedure (SOP) for preparation of NP suspensions developed within the NanoToxClass project (NanoToxclass, 2017). The selected concentrations of each particle fraction depended on the stock's concentrations and volume available. In addition, the tested concentrations were chosen based on daily alveolar mass dose of 0.13 µg/cm^2 expected to achieve in a

worst-case occupational exposure scenario and with a maximum accumulated lifetime dose of 420 µg/cm^2, according to Paur *et al.* (2011). Accordingly, serial dilutions of the stock suspensions were carried out in incubation media (FBS-free cell culture medium) and A549 cells were exposed for 24 h at 37 ºC, 5 % CO$_2$. For APS, the tested particles concentration ranged 0.31-5.00 µg/cm^2 and 0.16-2.50 µg/cm^2 for PGFP and PGNP, respectively. While for HVOF-particles, the concentration ranged between 2.50-40.00 µg/cm^2 and 0.63-10.00 µg/cm^2 for PGFP and PGNP, respectively. At least three independent experiments with three replicates each were performed.

4.5. Cytotoxicity assessment

To assess the impact of the tested particles in human alveolar epithelial cells, two endpoints were evaluated: LDH release and WST-1 reduction, indicators of plasma membrane integrity and cell metabolic activity, respectively.

LDH release was determined using Roche Cytotoxicity Detection Kit (Roche, Mannheim, Germany), according to manufacturer's instructions. After exposure and prior to analysis, samples were carefully transferred to a 96-well round bottom plates and then centrifuged at 2210 *g* for 5 min to remove the cell debris and residual (nano)particles. Cells lysed with 2 % Triton X-100 (30 min) were used as PC. Briefly, 100 µL of freshly prepared reaction mixture was added to 100 µL of each sample and incubated up to 30 min at room temperature and protected from light. Absorbance was measured at 490 nm and 630/690 nm (reference wavelength) in a microplate reader (SpectraMax® iD3 Molecular Devices, San Jose, CA, USA). LDH release values were normalized considering the PC mean value (total LDH release).

Cell metabolic activity and viability was assessed using the WST-1 Cell Proliferation Reagent Kit (Roche, Mannheim, Germany), according to the manufacturer's instructions. After exposure and prior to analysis, cells were washed with PBS pH 7.4. Afterwards, 100 µL/well of WST-1 reagent diluted 1:10 was added for a 2 h incubation period at 37 ºC, 5 % CO$_2$. Sample's absorbance was measured at 450 nm and 630/690 nm (reference wavelength) in a microplate reader (SpectraMax® iD3 Molecular Devices, San Jose, CA, USA). WST-1 reduction values were normalized considering the NC mean value.

To test for possible particle interferences with the assays, PC was determined in the absence and in the presence of the highest tested concentration of particle liquid suspensions. None of tested particles seemed to interfere in the

conducted cytotoxicity assays since no significant differences in the PC values in the absence vs. in the presence of the highest tested concentration of PGFP and PGNP were detected.

4.6. Intracellular reactive oxygen species generation

Generation of ROS was estimated using the Invitrogen™ CM-H$_2$DCFDA General Oxidative Stress Indicator probe (Thermo Fisher Scientific, Madrid, Spain), according to manufacturer's instructions. Briefly, 1.0 x 10^4 cells/well were seeded in 96-well black clear bottom plates and medium renewed after 24 h. At 48 h post-seeding, cells were loaded with 5 µM CM-H$_2$DCFDA probe for 1 h at 37 ºC, 5 % CO$_2$. Then, the medium was aspirated, and cells exposed to the tested particles over a 24 h period. Following exposure, fluorescence was measured at 492 nm/527 nm (excitation/emission) in a microplate reader (SpectraMax® iD3 Molecular Devices, San Jose, CA, USA). ROS production was normalised considering the mean fluorescence (arbitrary units) of the NC.

4.7. Cellular uptake, cell cycle and histone gamma-H2AX phosphorylation analysis by flow cytometry

Determination of cellular particle uptake, changes in the cell cycle by determining cellular distribution in the different phases (G$_0$/G$_1$, S, G$_2$/M and Sub-G$_1$) and DNA double-strand breaks assessed via phosphorylation of the Ser-139 residue of the histone variant H2AX (γ-H2AX) were carried out by flow cytometry using a Guava® easyCyte™ flow cytometer (Merck KGaA, Darmstadt, Germany). Briefly, 5.0 x 10^4 cells/well were seeded onto 24-well plates, with medium renewal after 24 h. At 48 h post-seeding, cells were exposed to three non-cytotoxic concentrations for each particle over a 24 h period, followed by medium removal and washing of the cells with PBS pH 7.4. Cells were detached using trypsin-EDTA 0.05 %, inactivated with incubation medium and centrifuged at 900 *g* for 5 min. The supernatant was gently removed, and the cells were permeabilized and fixed with ice-cold ethanol 70 % and left overnight at -20 ºC. To remove the ethanol, samples were centrifuged, washed with PBS with 1 % BSA, and once again centrifuged at 900 g for 5 min. Then, cells were labelled with 5 µg/mL of Phospho-Histone H2A.X (Ser139) Alexa Fluor® 488 conjugated monoclonal antibody for 15 min at room temperature and protected from light, followed by a washing step with PBS with 1 % BSA and centrifugation at 900 *g* for 5 min. Prior analysis, a final 15 min staining at room

temperature with a 50 µg/mL RNAse and 50 µg/mL PI solution was performed to ensure that only nuclear DNA was stained. Acquisitions were made with approximately 5000 events/per sample and recorded at a low flow rate (0.24 µL/s). For estimating the potential of particles to enter cells, the analysis was carried out by measuring the size (forward scatter, FSC) and complexity (side scatter, SSC) of the cells, following the protocol described by Suzuki *et al.* (2007). Debris and doublets were gated out by plotting SSC-Width *vs* SSC-Area. Cell cycle analysis was performed by evaluating the relative cellular DNA content from the PI signal detection, as previously described by Rosário *et al.* (2020), while the γ-H2AX from assessing the Alexa Fluor® 488 and PI channel intensities, as described by Valdiglesias *et al.* (2011). Camptothecin at 3.5 µg/mL was used as PC to help define where cells were positive for γ-H2AX. Data were analysed using the Guava® InCyte™ Software (Merck KGaA, Darmstadt, Germany).

4.8. DNA damage assessment

Primary and oxidative DNA damage were assessed by the standard alkaline and FPG-modified comet assay versions, respectively, as previously described (Bessa *et al.*, 2021b). Minimum Information for Reporting Comet Assay procedures and results (MIRCA) recommendations were followed in this manuscript (Møller *et al.*, 2020). Briefly, 5.0×10^4 cells/well were seeded onto 24-well plates, with medium renewal after 24 h. At 48 h post-seeding, cells were exposed for 24 h to three non-cytotoxic concentrations of each tested particle. After exposure, cells were washed twice with PBS pH 7.4, scrapped and suspended in PBS pH 7.4. Cells exposed to 500 µM MMS and 2.5 mM of $KBrO_3$ for 30 min were included as PC for primary and oxidative DNA damage assessment, respectively. Cells were counted in a Neubauer's chamber and 6.0×10^3 cells were transferred to a microcentrifuge tube, centrifuged at 700 *g* for 5 min and then embedded in 100 µL of 1 % LMP agarose. Five µL of each sample were placed on microscope slides precoated with 1 % NMP using a high throughput system of 12-gel comet assay unit (Severn Biotech Ltd®, Kidderminster, UK) and placed for 5 min at 4 °C. Duplicates of each sample were added per slide. Slides were performed in triplicate, one for alkaline version and the other two for enzymatic version of the comet assay (with or without FPG-enzyme). Then slides were immersed in an ice-cold lysis solution (NaCl 2.5 M, Na_2EDTA 100 mM, Tris-base 10 mM, NaOH 10 M, pH 10, Triton-X 100 1 %) for 2 h at 4 °C. For the enzymatic version, slides were washed in freshly prepared ice-cold

buffer F solution (HEPES 400 mM, KCl 1 M, Na$_2$EDTA 5 mM, BSA 2 mg/mL, pH 8.0) (3x 5 min) at 4 °C. A 30 μL solution of buffer F or FPG-enzyme (2.7 U/mL) was added to each well and incubated for 30 min at 4 °C. For this to happen, slides were previously placed on an ice-cold metal base of a 12-gel chamber apparatus (Severn Biotech Ltd®, Kidderminster, UK) covered by a silicon rubber 12-well mould followed by a top plate and clamped. Meanwhile, slides for the alkaline version remained in lysis solution. All slides were immersed in electrophoresis solution (Na$_2$EDTA 1 mM, and NaOH 0.3 M, pH 13) in the electrophoresis platform for 40 min, followed by electrophoresis for 30 min at constant 25 V (0.9 V/cm) and 400 mA. For slides washing, these were firstly covered by cold PBS (pH 7.2) and then by deionized H$_2$O for 10 min each. At the end of electrophoresis, slides were neutralised and fixed as described elsewhere (Bessa *et al.*, 2019). For comet scoring, slides were initially hydrated in TE Buffer (Tris-HCl 10 mM and EDTA 1 mM, pH 7.5-8) and stained at room temperature with 1:10,000 dilution of SYBR® Gold in TE buffer for 40 min. Comets were visualized in a Motic BA410 ELITE Series microscope equipped with a Complete EPI-Fluorescence Kit and scored using the Comet Assay IV image analysis software (Perceptive Instruments, Staffordshire, UK). At least 100 cells/experimental group (50 in each replicate gel) were scored. The comet tail DNA percentage (% tail intensity) was used as a DNA damage descriptor.

4.9. Statistical analysis

Statistical analysis was performed using SPSS (version 26.0, Armonk, NY, USA) and GraphPad Prism (version 6.0, San Diego, CA, USA) statistical software. Experimental data were expressed as mean ± standard deviation (SD). Data were tested for normality and homogeneity of variances by Shapiro-Wilk and Levene's tests, respectively. For each assessed timepoint, differences between tested concentrations and NC were estimated using a one-way ANOVA followed by post-hoc Dunnett's test for multiple comparisons. A p value < 0.05 was considered significant.
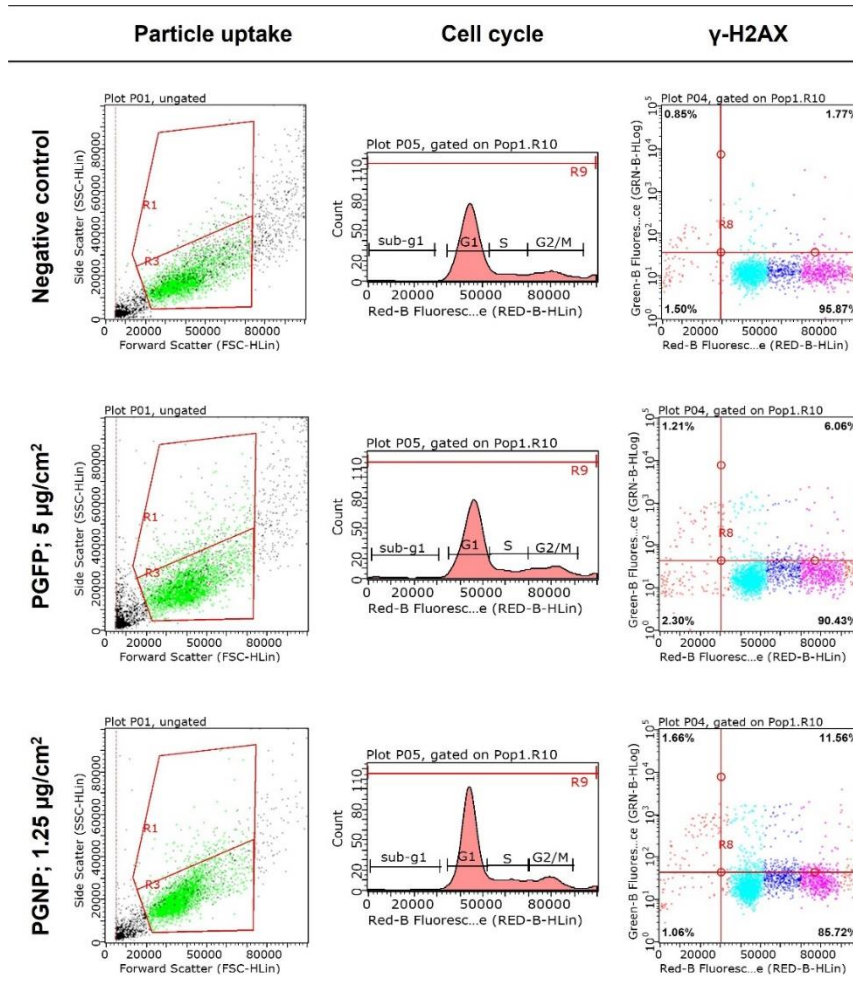
Appendix A

Figure A1. Representative flow cytometry graphs obtained for particle uptake, cell cycle and γ-H2AX analysis in human alveolar epithelial cells incubated for 24 h with the highest tested concentration of process-generated fine (PGFP) and nano-sized (PGNP) particles released during High Velocity Oxy-Fuel Spraying (HVOF).
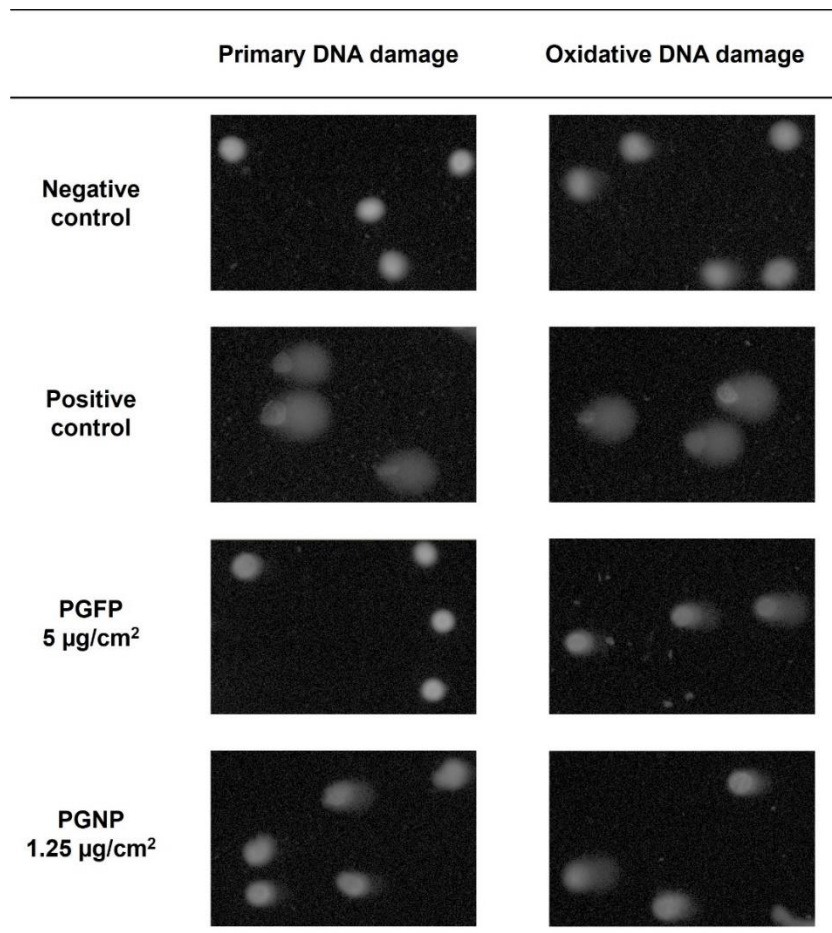
Appendix B

Figure B1. Representative comet assay images (100× magnification) of human alveolar epithelial cells exposed to the highest tested concentration of process-generated fine (PGFP) and nano-sized (PGNP) particles released during High Velocity Oxy-Fuel Spraying (HVOF), and respective experimental controls.

References

Åkerlund, E., Cappellini, F., Di Bucchianico, S., Islam, S., Skoglund, S., Derr, R., Odnevall Wallinder, I., Hendriks, G., & Karlsson, H. L. (2018). Genotoxic and mutagenic properties of Ni and NiO nanoparticles investigated by comet assay, γ-H2AX staining, Hprt mutation assay and ToxTracker reporter cell lines. *Environ Mol Mutagen*, *59*(3), 211-222. https://doi.org/10.1002/em.22163

Anderson, J. O., Thundiyil, J. G., & Stolbach, A. (2012). Clearing the air: a review of the effects of particulate matter air pollution on human health. *J Med Toxicol*, *8*(2), 166-175. https://doi.org/10.1007/s13181-011-0203-1

Barnum, K. J., & O'Connell, M. J. (2014). Cell cycle regulation by checkpoints. *Methods Mol Biol*, *1170*, 29-40. https://doi.org/10.1007/978-1-4939-0888-2_2

Bessa, M. J., Brandão, F., Fokkens, P., Cassee, F. R., Salmatonidis, A., Viana, M., Vulpoi, A., Simon, S., Monfort, E., Teixeira, J. P., & Fraga, S. (2021a). Toxicity assessment of industrial engineered and airborne process-generated nanoparticles in a 3D human airway epithelial in vitro model. *Nanotoxicology*, *15*(4), 542-557. https://doi.org/10.1080/17435390.2021.1897698

Bessa, M. J., Brandão, F., Fokkens, P. H. B., Leseman, D., Boere, A. J. F., Cassee, F. R., Salmatonidis, A., Viana, M., Vulpoi, A., Simon, S., Monfort, E., Teixeira, J. P., & Fraga, S. (2021b). In Vitro Toxicity of Industrially Relevant Engineered Nanoparticles in Human Alveolar Epithelial Cells: Air-Liquid Interface versus Submerged Cultures. *Nanomaterials (Basel)*, *11*(12). https://doi.org/10.3390/nano11123225

Bessa, M. J., Brandao, F., Querido, M. M., Costa, C., Pereira, C. C., Valdiglesias, V., Laffon, B., Carriere, M., Teixeira, J. P., & Fraga, S. (2019). Optimization of the harvesting and freezing conditions of human cell lines for DNA damage analysis by the alkaline comet assay. *Mutat Res*, *845*, 402994. https://doi.org/10.1016/j.mrgentox.2018.12.002

Bessa, M. J., Brandão, F., Viana, M., Gomes, J. F., Monfort, E., Cassee, F. R., Fraga, S., & Teixeira, J. P. (2020). Nanoparticle exposure and hazard in the ceramic industry: An overview of potential sources, toxicity and health effects. *Environmental Research*, 109297. https://doi.org/10.1016/j.envres.2020.109297

Björ, O., Damber, L., Edström, C., & Nilsson, T. (2008). Long-term follow-up study of mortality and the incidence of cancer in a cohort of workers at a primary aluminum smelter in Sweden. *Scand J Work Environ Health*, *34*(6), 463-470. https://doi.org/10.5271/sjweh.1293

Cediel-Ulloa, A., Isaxon, C., Eriksson, A., Primetzhofer, D., Sortica, M. A., Haag, L., Derr, R., Hendriks, G., Löndahl, J., Gudmundsson, A., Broberg, K., & Gliga, A. R. (2021). Toxicity of stainless and mild steel particles generated from gas–metal arc welding in primary human small airway epithelial cells. *Scientific Reports*, *11*(1), 21846. https://doi.org/10.1038/s41598-021-01177-7

DeLoughery, Z., Luczak, M. W., Ortega-Atienza, S., & Zhitkovich, A. (2014). DNA Double-Strand Breaks by Cr(VI) Are Targeted to Euchromatin and Cause ATR-Dependent Phosphorylation of Histone H2AX and Its Ubiquitination. *Toxicological Sciences*, *143*(1), 54-63. https://doi.org/10.1093/toxsci/kfu207

Ding, J., He, G., Gong, W., Wen, W., Sun, W., Ning, B., Huang, S., Wu, K., Huang, C., Wu, M., Xie, W., & Wang, H. (2009). Effects of nickel on cyclin expression, cell cycle progression and cell proliferation in human pulmonary cells. *Cancer epidemiology, biomarkers & prevention : a publication of the American Association for Cancer Research, cosponsored by the American Society of Preventive Oncology*, *18*(6), 1720-1729. https://doi.org/10.1158/1055-9965.EPI-09-0115

Fonseca, A., Viana, M., Querol, X., Moreno, N., De Francisco, I., Estepa, C., & De La Fuente, G. (2015a). Ultrafine and nanoparticle formation and emission mechanisms during laser processing of ceramic materials. *Journal of Aerosol Science*, *88*, 48-57. https://doi.org/10.1016/j.jaerosci.2015.05.013

Fonseca, A., Viana, M., Querol, X., Moreno, N., de Francisco, I., Estepa, C., & de la Fuente, G. (2015b). Workplace Exposure to Process-Generated Ultrafine and Nanoparticles in Ceramic Processes Using Laser Technology. In *Indoor and Outdoor Nanoparticles* (pp. 159-179). Springer. https://doi.org/10.1007/698_2015_422

Fonseca, A. S., Maragkidou, A., Viana, M., Querol, X., Hämeri, K., de Francisco, I., Estepa, C., Borrell, C., Lennikov, V., & de la Fuente, G. F. (2016). Process-generated nanoparticles from ceramic tile sintering: Emissions, exposure and environmental release. *Science of The Total Environment*, *565*, 922-932. https://doi.org/10.1016/j.scitotenv.2016.01.106

Frieke Kuper, C., Gröllers-Mulderij, M., Maarschalkerweerd, T., Meulendijks, N. M. M., Reus, A., van Acker, F., Zondervan-van den Beuken, E. K., Wouters, M. E. L., Bijlsma, S., & Kooter, I. M. (2015). Toxicity assessment of aggregated/agglomerated cerium oxide nanoparticles in an in vitro 3D airway model: The influence of mucociliary clearance. *Toxicology in Vitro*, *29*(2), 389-397. https://doi.org/10.1016/j.tiv.2014.10.017

Geiser, M., & Kreyling, W. G. (2010). Deposition and biokinetics of inhaled nanoparticles. *Particle and Fibre Toxicology*, *7*(1), 2. https://doi.org/10.1186/1743-8977-7-2

George, I., Uboldi, C., Bernard, E., Sobrido, M. S., Dine, S., Hagège, A., Vrel, D., Herlin, N., Rose, J., Orsière, T., Grisolia, C., Rousseau, B., & Malard, V. (2019). Toxicological Assessment of ITER-Like Tungsten Nanoparticles Using an In Vitro 3D Human Airway Epithelium Model. *Nanomaterials*, *9*(10), 1374. https://doi.org/10.3390/nano9101374

Halasova, E., Adamkov, M., Matakova, T., Kavcova, E., Poliacek, I., & Singliar, A. (2010). Lung cancer incidence and survival in chromium exposed individuals with respect to expression of anti-apoptotic protein survivin and tumor suppressor P53 protein. *European Journal of Medical Research*, *15*(2), 55. https://doi.org/10.1186/2047-783X-15-S2-55

Hamanaka, R. B., & Mutlu, G. M. (2018). Particulate Matter Air Pollution: Effects on the Cardiovascular System. *Frontiers in Endocrinology*, *9*, 680-680. https://doi.org/10.3389/fendo.2018.00680

IARC. (1990). Chromium, nickel and welding. *IARC monographs on the evaluation of carcinogenic risks to humans*, *49*. https://www.ncbi.nlm.nih.gov/books/NBK294452/

Ivask, A., Titma, T., Visnapuu, M., Vija, H., Kakinen, A., Sihtmae, M., Pokhrel, S., Madler, L., Heinlaan, M., & Kisand, V. (2015). Toxicity of 11 metal oxide nanoparticles to three mammalian cell types in vitro. *Current topics in medicinal chemistry*, *15*(18), 1914-1929. https://doi.org/10.2174/1568026615666150506150109

Jaakkola, M. S., Sripaiboonkij, P., & Jaakkola, J. J. (2011). Effects of occupational exposures and smoking on lung function in tile factory workers. *Int Arch Occup Environ Health*, *84*(2), 151-158. https://doi.org/10.1007/s00420-010-0603-6

Jederlinic, P. J., Abraham, J. L., Churg, A., Himmelstein, J. S., Epler, G. R., & Gaensler, E. A. (1990). Pulmonary fibrosis in aluminum oxide workers. Investigation

of nine workers, with pathologic examination and microanalysis in three of them. *Am Rev Respir Dis*, *142*(5), 1179-1184. https://doi.org/10.1164/ajrccm/142.5.1179

Karanasiou, A., Viana, M., Querol, X., Moreno, T., & de Leeuw, F. (2014). Assessment of personal exposure to particulate air pollution during commuting in European cities--recommendations and policy implications. *Sci Total Environ*, *490*, 785-797. https://doi.org/10.1016/j.scitotenv.2014.05.036

Kargar, F., Shahtaheri, S. J., Golbabaei, F., Barkhordari, A., Rahimi-Froushani, A., & Khadem, M. (2013). Evaluation of Occupational Exposure of Glazers of a Ceramic Industry to Cobalt Blue Dye. *Iranian journal of public health*, *42*(8), 868-875. https://www.ncbi.nlm.nih.gov/pmc/articles/PMC4441918/

Kim, I.-S., Baek, M., & Choi, S.-J. (2010). Comparative cytotoxicity of Al2O3, CeO2, TiO2 and ZnO nanoparticles to human lung cells. *Journal of Nanoscience and Nanotechnology*, *10*(5), 3453-3458. https://doi.org/10.1166/jnn.2010.2340

Kim, S., Jaques, P. A., Chang, M., Froines, J. R., & Sioutas, C. (2001). Versatile aerosol concentration enrichment system (VACES) for simultaneous in vivo and in vitro evaluation of toxic effects of ultrafine, fine and coarse ambient particles Part I: Development and laboratory characterization. *Journal of Aerosol Science*, *32*(11), 1281-1297. https://doi.org/10.1016/S0021-8502(01)00057-X

Kim, Y.-S., Chung, Y.-H., Seo, D.-S., Choi, H.-S., & Lim, C.-H. (2018). Twenty-Eight-Day Repeated Inhalation Toxicity Study of Aluminum Oxide Nanoparticles in Male Sprague-Dawley Rats. *Toxicological research*, *34*(4), 343-354. https://doi.org/10.5487/TR.2018.34.3.343

Lacroix, G., Koch, W., Ritter, D., Gutleb, A. C., Larsen, S. T., Loret, T., Zanetti, F., Constant, S., Chortarea, S., Rothen-Rutishauser, B., Hiemstra, P. S., Frejafon, E., Hubert, P., Gribaldo, L., Kearns, P., Aublant, J.-M., Diabaté, S., Weiss, C., de Groot, A., & Kooter, I. (2018). Air–Liquid Interface In Vitro Models for Respiratory Toxicology Research: Consensus Workshop and Recommendations. *Applied In Vitro Toxicology*, *4*(2), 91-106. https://doi.org/10.1089/aivt.2017.0034

Lippmann, M., & Chen, L.-C. (2009). Health effects of concentrated ambient air particulate matter (CAPs) and its components. *Critical Reviews in Toxicology*, *39*(10), 865-913. https://doi.org/10.3109/10408440903300080

Loret, T., Peyret, E., Dubreuil, M., Aguerre-Chariol, O., Bressot, C., le Bihan, O., Amodeo, T., Trouiller, B., Braun, A., Egles, C., & Lacroix, G. (2016). Air-liquid interface exposure to aerosols of poorly soluble nanomaterials induces different biological activation levels compared to exposure to suspensions. *Particle and Fibre Toxicology*, *13*(1), 58. https://doi.org/10.1186/s12989-016-0171-3

Ma, A., & Dai, X. (2018). The relationship between DNA single-stranded damage response and double-stranded damage response. *Cell cycle (Georgetown, Tex.)*, *17*(1), 73-79. https://doi.org/10.1080/15384101.2017.1403681

Manke, A., Wang, L., & Rojanasakul, Y. (2013). Mechanisms of nanoparticle-induced oxidative stress and toxicity. *BioMed research international*, *2013*, 942916-942916. https://doi.org/10.1155/2013/942916

Mjelle, R., Hegre, S. A., Aas, P. A., Slupphaug, G., Drabløs, F., Saetrom, P., & Krokan, H. E. (2015). Cell cycle regulation of human DNA repair and chromatin remodeling genes. *DNA Repair (Amst)*, *30*, 53-67. https://doi.org/10.1016/j.dnarep.2015.03.007

Mo, Y., Zhang, Y., Zhang, Y., Yuan, J., Mo, L., & Zhang, Q. (2021). Nickel nanoparticle-induced cell transformation: involvement of DNA damage and DNA repair defect through HIF-1α/miR-210/Rad52 pathway. *Journal of Nanobiotechnology*, *19*(1), 370. https://doi.org/10.1186/s12951-021-01117-7

Møller, P., Azqueta, A., Boutet-Robinet, E., Koppen, G., Bonassi, S., Milić, M., Gajski, G., Costa, S., Teixeira, J. P., Costa Pereira, C., Dusinska, M., Godschalk, R., Brunborg, G., Gutzkow, K. B., Giovannelli, L., Cooke, M. S., Richling, E., Laffon, B., Valdiglesias, V., Basaran, N., Del Bo', C., Zegura, B., Novak, M., Stopper, H., Vodicka, P., Vodenkova, S., de Andrade, V. M., Sramkova, M., Gabelova, A., Collins, A., & Langie, S. A. S. (2020). Minimum Information for Reporting on the Comet Assay (MIRCA): recommendations for describing comet assay procedures and results. *Nature Protocols*, *15*(12), 3817-3826. https://doi.org/10.1038/s41596-020-0398-1

Morimoto, Y., Hirohashi, M., Ogami, A., Oyabu, T., Myojo, T., Hashiba, M., Mizuguchi, Y., Kambara, T., Lee, B. W., & Kuroda, E. (2011). Pulmonary toxicity following an intratracheal instillation of nickel oxide nanoparticle agglomerates. *Journal of occupational health*, *53*(4), 293-295. https://doi.org/10.1539/joh.11-0034-BR

NanoToxclass. (2017). *Standard Operation Procedure - Preparation of nanoparticle suspensions by cup horn sonication.* https://www.nanopartikel.info/files/projekte/NanoToxClass/NanoToxClass -SOP_Dispersion_by_cup_horn_sonication_V2.0.pdf

Park, E. J., Lee, S. J., Lee, G. H., Kim, D. W., Yoon, C., Lee, B. S., Kim, Y., Chang, J., & Lee, K. (2018). Comparison of subchronic immunotoxicity of four different types of aluminum-based nanoparticles. *J Appl Toxicol*, *38*(4), 575-584. https://doi.org/10.1002/jat.3564

Paur, H.-R., Cassee, F. R., Teeguarden, J., Fissan, H., Diabate, S., Aufderheide, M., Kreyling, W. G., Hänninen, O., Kasper, G., & Riediker, M. (2011). In-vitro cell exposure studies for the assessment of nanoparticle toxicity in the lung - A dialog between aerosol science and biology. *Journal of Aerosol Science*, *42*(10), 668-692. https://doi.org/10.1016/j.jaerosci.2011.06.005

Pavlovska, I., Ramata-Stunda, A., Martinsone, Z., Boroduskis, M., Patetko, L., Martinsone, I., Seile, A., & Vanadzins, I. (2021). In vitro impact preliminary assessment of airborne particulate from metalworking and woodworking industries. *Scientific Reports*, *11*(1), 20181. https://doi.org/10.1038/s41598-021-99815-7

Peixoto, M. S., de Oliveira Galvão, M. F., & Batistuzzo de Medeiros, S. R. (2017). Cell death pathways of particulate matter toxicity. *Chemosphere*, *188*, 32-48. https://doi.org/10.1016/j.chemosphere.2017.08.076

Phillips, J. I., Green, F. Y., Davies, J. C., & Murray, J. (2010). Pulmonary and systemic toxicity following exposure to nickel nanoparticles. *American journal of industrial medicine*, *53*(8), 763-767. https://doi.org/10.1002/ajim.20855

Podhorecka, M., Skladanowski, A., & Bozko, P. (2010). H2AX Phosphorylation: Its Role in DNA Damage Response and Cancer Therapy. *J Nucleic Acids*, *2010*. https://doi.org/10.4061/2010/920161

Reynolds, M., Armknecht, S., Johnston, T., & Zhitkovich, A. (2012). Undetectable role of oxidative DNA damage in cell cycle, cytotoxic and clastogenic effects of Cr(VI) in human lung cells with restored ascorbate levels. *Mutagenesis*, *27*(4), 437-443. https://doi.org/10.1093/mutage/ger095

Ribalta, C., Koivisto, A. J., Salmatonidis, A., López-Lilao, A., Monfort, E., & Viana, M. (2019). Modeling of High Nanoparticle Exposure in an Indoor Industrial Scenario with a One-Box Model. *International journal of environmental research and public health*, *16*(10), 1695. https://doi.org/10.3390/ijerph16101695

Roedel, E. Q., Cafasso, D. E., Lee, K. W. M., & Pierce, L. M. (2012). Pulmonary toxicity after exposure to military-relevant heavy metal tungsten alloy particles. *Toxicology and Applied Pharmacology*, *259*(1), 74-86. https://doi.org/10.1016/j.taap.2011.12.008

Rosário, F., Bessa, M. J., Brandão, F., Costa, C., Lopes, C. B., Estrada, A. C., Tavares, D. S., Teixeira, J. P., & Reis, A. T. (2020). Unravelling the Potential Cytotoxic Effects of Metal Oxide Nanoparticles and Metal(Loid) Mixtures on A549 Human Cell Line. *Nanomaterials*, *10*(3), 447. https://doi.org/10.3390/nano10030447

Salmatonidis, A., Ribalta, C., Sanfélix, V., Bezantakos, S., Biskos, G., Vulpoi, A., Simion, S., Monfort, E., & Viana, M. (2018a). Workplace Exposure to Nanoparticles during Thermal Spraying of Ceramic Coatings. *Annals of Work Exposures and Health*, *63*(1), 91-106. https://doi.org/10.1093/annweh/wxy094

Salmatonidis, A., Viana, M., Biskos, G., & Bezantakos, S. (2020). Particle size distributions and hygroscopic restructuring of ultrafine particles emitted during thermal spraying. *Aerosol Science and Technology*, *54*(12), 1359-1372. https://doi.org/10.1080/02786826.2020.1784837

Salmatonidis, A., Viana, M., Pérez, N., Alastuey, A., Germán, F., Angurel, L. A., Sanfélix, V., & Monfort, E. (2018b). Nanoparticle formation and emission during laser ablation of ceramic tiles. *Journal of Aerosol Science*, *126*, 152-168. https://doi.org/10.1016/j.jaerosci.2018.09.006

Salnikow, K., & Zhitkovich, A. (2008). Genetic and Epigenetic Mechanisms in Metal Carcinogenesis and Cocarcinogenesis: Nickel, Arsenic, and Chromium. *Chemical Research in Toxicology*, *21*(1), 28-44. https://doi.org/10.1021/tx700198a

Schraufnagel, D. E. (2020). The health effects of ultrafine particles. *Experimental & Molecular Medicine*, *52*(3), 311-317. https://doi.org/10.1038/s12276-020-0403-3

Stone, V., Miller, M. R., Clift, M. J. D., Elder, A., Mills, N. L., Moller, P., Schins, R. P. F., Vogel, U., Kreyling, W. G., Alstrup Jensen, K., Kuhlbusch, T. A. J., Schwarze, P. E., Hoet, P., Pietroiusti, A., De Vizcaya-Ruiz, A., Baeza-Squiban, A., Teixeira, J. P., Tran, C. L., & Cassee, F. R. (2017). Nanomaterials Versus Ambient Ultrafine Particles: An Opportunity to Exchange Toxicology Knowledge. *Environ Health Perspect*, *125*(10), 106002. https://doi.org/10.1289/EHP424

Stuart, B. O. (1984). Deposition and clearance of inhaled particles. *Environ Health Perspect*, *55*, 369-390. https://doi.org/10.1289/ehp.8455369

Suzuki, H., Toyooka, T., & Ibuki, Y. (2007). Simple and easy method to evaluate uptake potential of nanoparticles in mammalian cells using a flow cytometric light scatter analysis. *Environ Sci Technol*, *41*(8), 3018-3024. https://doi.org/10.1021/es0625632

Thomassen, Y., Koch, W., Dunkhorst, W., Ellingsen, D. G., Skaugset, N. P., Jordbekken, L., Arne Drabløs, P., & Weinbruch, S. (2006). Ultrafine particles at workplaces of a primary aluminium smelter. *J Environ Monit*, *8*(1), 127-133. https://doi.org/10.1039/b514939h

Trethowan, W. N., Burge, P. S., Rossiter, C. E., Harrington, J. M., & Calvert, I. A. (1995). Study of the respiratory health of employees in seven European plants that manufacture ceramic fibres. *Occup Environ Med*, *52*(2), 97-104. https://doi.org/10.1136/oem.52.2.97

Tsaousi, A., Jones, E., & Case, C. P. (2010). The in vitro genotoxicity of orthopaedic ceramic (Al2O3) and metal (CoCr alloy) particles. *Mutation Research/Genetic Toxicology and Environmental Mutagenesis*, *697*(1), 1-9. https://doi.org/10.1016/j.mrgentox.2010.01.012

Valdiglesias, V., Laffon, B., Pásaro, E., & Méndez, J. (2011). Evaluation of okadaic acid-induced genotoxicity in human cells using the micronucleus test and γH2AX analysis. *J Toxicol Environ Health A*, *74*(15-16), 980-992. https://doi.org/10.1080/15287394.2011.582026

Viana, M., Fonseca, A. S., Querol, X., López-Lilao, A., Carpio, P., Salmatonidis, A., & Monfort, E. (2017). Workplace exposure and release of ultrafine particles during atmospheric plasma spraying in the ceramic industry. *Science of The Total Environment*, *599-600*, 2065-2073. https://doi.org/10.1016/j.scitotenv.2017.05.132

Viana, M., Salmatonidis, A., Bezantakos, S., Ribalta, C., Moreno, N., Córdoba, P., Cassee, F. R., Boere, J., Fraga, S., Teixeira, J. P., Bessa, M. J., & Monfort, E. (2021). Characterizing the Chemical Profile of Incidental Ultrafine Particles for Toxicity Assessment Using an Aerosol Concentrator. *Ann Work Expo Health*, *65*(8), 966-978. https://doi.org/10.1093/annweh/wxab011

Wise, J. P., Wise, S. S., & Little, J. E. (2002). The cytotoxicity and genotoxicity of particulate and soluble hexavalent chromium in human lung cells. *Mutation Research/Genetic Toxicology and Environmental Mutagenesis*, *517*(1), 221-229. https://doi.org/10.1016/S1383-5718(02)00071-2

Xing, Y.-F., Xu, Y.-H., Shi, M.-H., & Lian, Y.-X. (2016). The impact of PM2.5 on the human respiratory system. *Journal of thoracic disease*, *8*(1), E69-E74. https://doi.org/10.3978/j.issn.2072-1439.2016.01.19

Zhang, Q., Kusaka, Y., Zhu, X., Sato, K., Mo, Y., Kluz, T., & Donaldson, K. (2003). Comparative toxicity of standard nickel and ultrafine nickel in lung after intratracheal instillation. *Journal of occupational health*, *45*(1), 23-30. https://doi.org/10.1539/joh.45.23

Zhang, X. Q., Yin, L. H., Tang, M., & Pu, Y. P. (2011). ZnO, TiO2, SiO2, and Al2O3 Nanoparticles-induced Toxic Effects on Human Fetal Lung Fibroblasts. *Biomedical and Environmental Sciences*, *24*(6), 661-669. https://doi.org/10.3967/0895-3988.2011.06.011

Zhang, Z., Leonard, S. S., Wang, S., Vallyathan, V., Castranova, V., & Shi, X. (2001). Cr (VI) induces cell growth arrest through hydrogen peroxide-mediated reactions. *Mol Cell Biochem*, *222*(1-2), 77-83. https://doi.org/10.1023/A:1017963307358

B.3. *In vitro* toxicity of industrially relevant engineered nanoparticles in human alveolar epithelial (A549) cells: air-liquid interface *vs* submerged cultures

Bessa M. J., Brandão F., Fokkens P. H. B., Leseman D. L. A. C., Boere A. J. F., Cassee F. R., Salmatonidis A., Viana M., Vulpoi A., Simon S., Monfort E., Teixeira J. P., & Fraga S.

The PhD candidate contributed for the methodology, investigation, formal analysis and writing of the manuscript.

In Vitro Toxicity of Industrially Relevant Engineered Nanoparticles in Human Alveolar Epithelial Cells: Air–Liquid Interface *versus* Submerged Cultures

Maria João Bessa [1,2,3,4], Fátima Brandão [1,2,3,4], Paul H. B. Fokkens [5], Daan L. A. C. Leseman [5], A. John F. Boere [5], Flemming R. Cassee [5,6], Apostolos Salmatonidis [7,8], Mar Viana [7], Adriana Vulpoi [9], Simion Simon [9], Eliseo Monfort [10], João Paulo Teixeira [1,2,3,*] and Sónia Fraga [1,2,3]

[1] Department of Environmental Health, National Institute of Health Dr. Ricardo Jorge, 4000-053 Porto, Portugal; mjbessa8@gmail.com (M.J.B.); fatimabrandao988@gmail.com (F.B.); sonia.fraga@insa.min-saude.pt (S.F.)
[2] EPIUnit-Instituto de Saúde Pública, Universidade do Porto, 4050-091 Porto, Portugal
[3] Laboratório para a Investigação Integrativa e Translacional em Saúde Populacional (ITR), 4050-091 Porto, Portugal
[4] Instituto de Ciências Biomédicas Abel Salazar (ICBAS), Universidade do Porto, 4050-313 Porto, Portugal
[5] National Institute for Public Health and Environment (RIVM), 3721 Bilthoven, The Netherlands; paul.fokkens@rivm.nl (P.H.B.F.); daan.leseman@rivm.nl (D.L.A.C.L.); john.boere@rivm.nl (A.J.F.B.); flemming.cassee@rivm.nl (F.R.C.)
[6] Institute for Risk Assessment Sciences (IRAS), Utrecht University, 3584 Utrecht, The Netherlands
[7] Institute of Environmental Assessment and Water Research, Spanish Research Council (IDAEA-CSIC), 08034 Barcelona, Spain; asalmatonidis@leitat.org (A.S.); mar.viana@idaea.csic.es (M.V.)
[8] LEITAT Technological Center, C/de la Innovació 2, 08225 Terrassa, Spain
[9] Nanostructured Materials and Bio-Nano-Interfaces Center, Interdisciplinary Research Institute on Bio-Nano-Sciences, Babes-Bolyai University, 400271 Cluj-Napoca, Romania; adrianavulpoilazar@gmail.com (A.V.); simon49nmr@gmail.com (S.S.)
[10] Institute of Ceramic Technology (ITC), Universitat Jaume I, 12006 Castellón, Spain; eliseo.monfort@itc.uji.es
[*] Correspondence: jpft12@gmail.com; Tel.: +351-223-401-141

Abstract: Diverse industries have already incorporated within their production processes engineered nanoparticles (ENP), increasing the potential risk of worker inhalation exposure. *In vitro* models have been widely used to investigate ENP toxicity. Air–liquid interface (ALI) cell cultures have been emerging as a valuable alternative to submerged cultures as they are more representative of the inhalation exposure to airborne nano-sized particles. We compared the *in vitro* toxicity of four ENP used as raw materials in the advanced ceramics sector in human alveolar epithelial-like cells cultured under submerged or ALI conditions. Submerged cultures were exposed to ENP liquid suspensions or to aerosolised ENP at ALI. Toxicity was assessed by determining LDH release, WST-1 metabolisation and DNA damage. Overall, cells were more sensitive to ENP cytotoxic effects when cultured and exposed under ALI. No significant cytotoxicity was observed after 24 h exposure to ENP liquid suspensions, although aerosolised ENP clearly affected cell viability and LDH release. In general, all ENP increased primary DNA damage regardless of the exposure mode, where an increase in DNA strand-breaks was only detected under submerged conditions. Our data show that at relevant occupational concentrations, the selected ENP exert mild toxicity to alveolar epithelial cells and exposure at ALI might be the most suitable choice when assessing ENP toxicity in respiratory models under realistic exposure conditions.

Keywords: engineered nanoparticles; submerged cultures; air-liquid interface; *in vitro* cytotoxicity; DNA damage; genotoxicity

1. Introduction

Nanotechnology is one of the key technologies of the 21st century that is revolutionizing various fields of activity through the production and application of engineered

nanomaterials (ENM). Carbon-based nanomaterials (NM), metal and metal oxide nanoparticles (NP) are amongst the most used ENM in the industrial sector, which are consequently being produced in high volumes [1,2]. Accordingly, nano-sized materials are considered an emerging risk for occupational safety and health [3,4] and there is an urgent need to clearly identify the adverse health effects associated with workplace exposure to NP. In this context, the ceramic sector is a relevant case of occupational exposure to NP. Indeed, a wide range of ENM are already being used as raw materials in advanced ceramics manufacture, including carbon-based NM (e.g., graphene, carbon nanotubes and carbon black) for their reinforcing ability or metal/metal oxide NP [e.g., aluminium oxide (Al_2O_3), antimony-tin oxide (ATO; $Sb_2O_3 \bullet SnO_2$), cerium oxide (CeO_2), chromium oxide (Cr_2O_3), silica (SiO_2), tin oxide (SnO_2), titanium oxide (TiO_2) and zirconium oxide (ZrO_2)] for ceramic coatings, as insulators, cutting tools and polishing agents [5]. In addition, nano-sized particles may be unintentionally released to workplace air during advanced, as well as traditional ceramics manufacturing processes such as machining, combustion/heating processes, thermal coating, etc. [5–15]. This has also been observed in other industrial sectors [16].

Inhalation is considered a major route of exposure to NP in occupational settings, though dermal contact and ingestion are also likely to occur [17,18]. Depending on physiological factors (breathing pattern and lung health status) [19] but also on NP physicochemical properties (size, shape, surface chemistry) [20], airborne NP will deposit at different locations along the respiratory tree, where they might or might not exert toxicity. The available studies on the toxicity of ENM show that cell injury may arise from particle–cell interactions, plasma membrane perturbation and/or loss of integrity, mitochondrial function disruption, elevation of reactive oxygen species (ROS) levels, among others [21–23].

A large proportion of the existing information on ENM-induced biological effects derives from *in vitro* studies using lung models. Human airway epithelial cell lines from the bronchial (e.g., 16HBE14o, BEAS-2B or Calu-3 cells) and alveolar regions (e.g., A549 cells) are the most used culture systems [24–26]. In this regard, human alveolar epithelial A549 cells are often employed for assessing the toxicity of nano-sized materials [27,28]. Indeed, alterations in alveolar epithelial cells integrity and function, which might occur from the presence of ENM in the lung tissue, are in the basis of severe pulmonary diseases [29].

Metal oxide NP are amongst the most widely investigated ENM for *in vitro* pulmonary toxicity. In this regard, Lanone et al. [30] evaluated the *in vitro* toxicity of 24 manufactured NP, including metal oxide NP, in both human alveolar epithelial (A549) and macrophage (THP-1) cells at 24 h after exposure. These authors found that chemical composition was an important determinant of ENM toxicity, while no correlation between cytotoxicity and NP equivalent spherical diameter or specific surface area was found. While copper oxide (CuO) and zinc oxide (ZnO) NP were the most cytotoxic NP, TiO_2, Al_2O_3, CeO_2 and ZrO_2 NP induced moderated cytotoxicity. On the one hand, tungsten carbide (WC) NP did not cause any significant cytotoxicity. Importantly, A549 and THP-1 cells exhibited different sensitivity to the tested NP. In addition, Titma et al. [31] investigated the *in vitro* cytotoxicity of six metal oxide NP (antimony oxide (Sb_2O_3), manganese oxide (Mn_3O_4), TiO_2, cobalt oxide (Co_3O_4), ZnO and CuO NP) in human alveolar epithelial (A549) but also in intestinal epithelial (Caco-2) cells. In both cell models, no toxic effects were observed in cells exposed for 24 h to Sb_2O_3, Mn_3O_4 and TiO_2 NP, while Co_3O_4 and ZnO NP had moderate effects, and CuO NP were toxic below 100 µg/mL. Nevertheless, toxicity effects of Mn_3O_4 and Sb_2O_3 NP remarkably increased over time, up to nine days. Overall, the sensitivity of the cell lines to the tested NP was comparable considering the viability data, as assessed by the resazurin assay. However, transepithelial electrical resistance (TEER) measurements showed that Caco-2 cells were more susceptible to the toxic effects of the tested NP than A549 cells.

Most of the available *in vitro* studies addressing the pulmonary toxicity of ENM were performed under submerged conditions, i.e., cultured cells are immersed in liquid media [32,33]. However, innovative approaches using advanced exposure systems that more accurately replicate the physiological aspects of the airway exposure to airborne

particles and more precisely control dose deposition have emerged over the last few years [34,35]. Cellular models cultured under air-liquid interface (ALI) conditions, where aerosolised particles are directly delivered onto the cells' surface, are regarded as a more realistic and relevant exposure system, offering a valuable alternative to the traditional submerged cultures [33,36], although most of the *in vitro* toxicology laboratories worldwide are not equipped to conduct these studies as dedicated equipment and aerosol technology is needed. Notwithstanding, several studies to assess the pulmonary toxicity of ENM under submerged and ALI conditions have been already conducted and showed that ENM hazard might be different depending on the exposure conditions [37–40].

In the present study, we comparatively investigated the *in vitro* toxicity of occupationally relevant doses of four engineered nanoparticles (ENP) used for advanced ceramics manufacture (SnO_2, ATO, CeO_2 and ZrO_2 NP) in human alveolar epithelial (A549) cells under submerged vs. ALI conditions. We hypothesised that the tested ENP would be more hazardous to alveolar epithelial cells under ALI conditions compared to cells exposed under submerged conditions. To assess *in vitro* toxicity, plasma membrane integrity, cell metabolic activity (WST-1 reduction), primary and oxidative DNA damage were evaluated after exposure to the test ENP.

2. Materials and Methods

2.1. Chemicals

All chemicals used were of high purity or analytical grade. Dimethyl sulfoxide (DMSO), sodium hydroxide (NaOH), sodium chloride (NaCl), potassium chloride (KCl) and potassium hydroxide (KOH) were purchased from Merck KGaA (Darmstadt, Germany). Triton X-100, bovine serum albumin (BSA), low melting point (LMP) agarose, Tris hydrochloride (Tris-HCl), 4-(2-hydroxyethyl)piperazine-1-ethanesulfonic acid (HEPES), methyl methanesulfonate (MMS) and water TraceSELECT™ Ultra were bought from Sigma-Aldrich (Madrid, Spain). Tris-base and disodium salt dihydrate (Na_2EDTA) were supplied from Merck Millipore (Madrid, Spain). Normal melting point (NMP) agarose was purchased from Bioline (London, UK). Potassium bromate ($KBrO_3$) was supplied from Alfa Aesar (Karlsruhe, Germany). Formamidopyrimidine-DNA glycosylase (FPG) was purchased from New England Biolabs (Ipswich, MA, USA). Invitrogen™ SYBR® Gold dye and CM-H_2DCFDA (General Oxidative Stress Indicator) were bought from Thermo Fisher Scientific (Madrid, Spain). All cell culture reagents were purchased from Gibco, Thermo Fisher Scientific (Madrid, Spain).

2.2. Nanoparticle's Suspensions, Aerosols Generation and Characterisation

All NP were commercial products and obtained from different suppliers in the liquid form: superlite grade SnO_2 (10% *w/v*; Keeling and Walker, Stoke-on-Trent, UK), $Sb_2O_3 \bullet SnO_2$ (ATO; 10% *w/v*; Keeling and Walker, Stoke-on-Trent, UK), CeO_2 (5% *w/v*; PlasmaChem GmbH, Berlin, Germany) and ZrO_2 (10% *w/v*; Sigma-Aldrich, Madrid, Spain). All NP suspensions under study were subjected to gamma-ray irradiation to ensure the required sterility for *in vitro* toxicity testing.

Hydrodynamic size and concentration (number of particles/mL) of the aqueous ENP suspensions under study were determined by Dynamic Light Scattering using a ZetaSizer Ultra (Malvern Panalytical, Malvern, UK) and Nanoparticle Tracking Analysis (NTA) using a NanoSight LM20 (NANOSIGHT Ltd., Salisbury, UK), respectively. The effective density of ENP suspensions was determined by measuring the pellet volume of the ENP stock suspensions after centrifugation at 2000× *g* for 2 h at 20 °C. In addition, the ENP oxidative potential (acellular ROS production) was determined by Electron Spin Resonance (ESR) based on the trapping of NP-induced hydroxyl radicals (OH) generated in the presence of hydrogen peroxide (H_2O_2) using DMPO (5,5-dimethyl-1-pyrroline-N-oxide) as spin trap, as previously described [39]. Briefly, NP suspensions were mixed with 0.5 M H_2O_2 and 0.05 M DMPO, followed by incubation for 15 min at 37 °C in a heated shaking water bath prior to ESR (MS400, Magnettech GmbH, Berlin, Germany) analysis. The ESR quantification was

159

conducted with the Analysis Software (2.0 or higher, Magnettech GmbH, Berlin, Germany) on first derivation of ESR signals of DMPOeOH quartet as the average of total amplitudes and expressed in arbitrary units (A.U.) per sampled volume.

ENP aerosols were generated as previously described [41], with minor modifications. Briefly, the ENP aqueous suspensions were fed by a syringe pump to a spray nozzle (Schlick spray-nozzle) were the liquid was nebulized using pre-heated compressed air as depicted in Figure 1. This aerosol was further dried and mixed in a nebulising cylinder. This setup was connected to an automated exposurestation (VitroCell Systems GmbH, Waldkirch, Germany) through a copper tube. Gravimetric mass concentration was determined by weighing the deposited particle mass in Teflon filters using a microbalance under controlled relative humidity (40–70%) and temperature (21–23 °C) conditions. For that purpose, the Teflon filters were weighted before and after the exposure. In addition, the aerosolised ENP deposited in grids placed in the exposure module were analysed by transmission electron microscopy (TEM) analysis and energy-dispersive X-ray spectroscopy (EDS), using a Tecnai F20 XTWIN (FEI Company, Eindhoven, The Netherlands) field emission, high-resolution transmission electron microscope operating at an accelerating voltage of 200 kV, equipped with Eagle 4k CCD camera and an EDX detector (Thermo Fisher Scientific, Waltham, MA, USA).
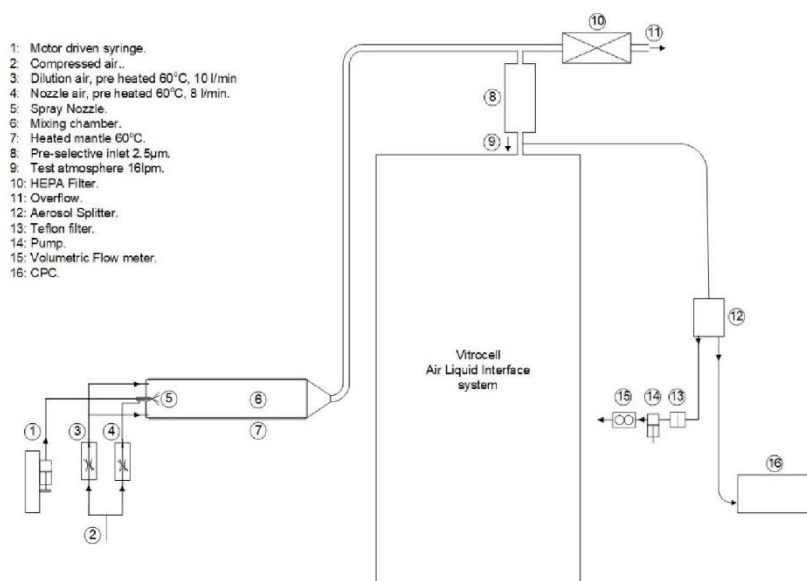

Figure 1. Aerosol generation set-up. Engineered nanoparticles (ENP) aerosols were generated by controlled injection of the ENP aqueous suspensions by means of a syringe pump to a spray nozzle were the liquid was nebulised using pre-heated compressed air. This aerosol was further dried and mixed in a nebulising cylinder connected to the Vitrocell® automated exposure station (AES). Just before entering the AES, a Teflon filter and a condensation particle counter (CPC) were connected for aerosol characterisation.

2.3. Cell Culture

Lung adenocarcinoma epithelial A549 cells from the American Type Culture Collection (ATCC®, CCL-185™) were cultured with RPMI 1640 medium with Glutamax™, 25 mM HEPES and supplemented with 10% heat-inactivated foetal bovine serum (FBS), 50 U/mL penicillin and 50 µg/mL streptomycin. Cells were maintained in a humidified atmosphere with 5% CO_2 at 37 °C. To carry out the submerged exposure experiments, cells were seeded in 96-well (1.0×10^4 cells/well) or 12-well plates (1.0×10^5 cells/well) and allowed to adhere for 48 h at 37 °C, 5% CO_2. For ALI exposure, cells were seeded onto 0.4 µm Corning® Transwell® polyester (PES) inserts (5×10^3 cells/cm²) placed in 6- or 12-well plates and grown for 7 days.

2.4. Submerged vs. Air-Liquid Interface (ALI) Exposure

All NP stock suspensions under study were dispersed by indirect probe sonication using a Branson sonifier (model 450) equipped with a disruptor cup horn according with the Standard Operation Procedure (SOP) for preparation of NP suspensions developed within the NanoToxClass project (NanoToxclass, 2017). A schematic representation of the experimental protocol is depicted in Figure 2. For submerged exposure (Figure 2A), NP working concentrations were prepared from an intermediate NP suspension (300 µg/mL) by serial dilution in incubation medium (serum-free cell culture medium). Cells were immediately incubated for 24 h with the NP suspensions at 5% CO_2 at 37 °C. For ALI exposure (Figure 2B), polarised cells grown on Transwell® permeable membranes were placed inside temperature-controlled exposure modules of an automated exposure station and the cultures exposed to the NP aerosol or clean air (exposure control) at an air flow rate of 25 mL/h, under electrostatic field (1 Kv), for different timepoints (2 and 4 h) to achieve different deposited doses. The culture medium at the apical side was removed 24 h before exposure to allow cells adaptation to the ALI conditions. Cells kept in the incubator during exposure served as non-exposed controls (incubator control). Following exposure, cells were returned to the incubator, the basal compartment medium was replaced, and cells allowed to incubate for an additional 24 h (recovery time).
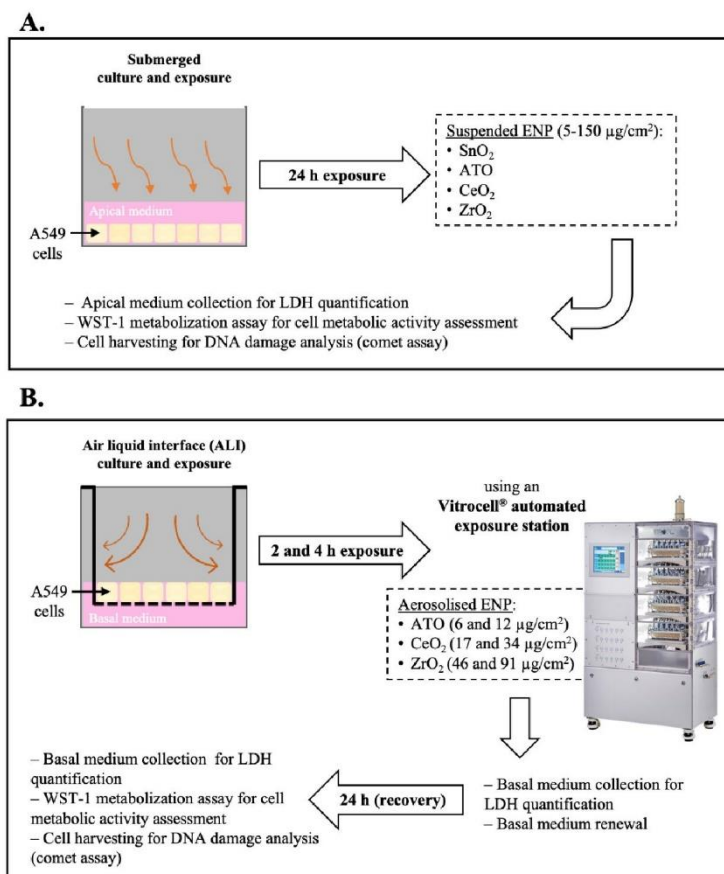

Figure 2. Experimental protocol scheme. (**A**) Human alveolar epithelial cultures under submerged conditions were exposed for 24 h to the tested engineered nanoparticles (ENP) dispersed in serum-free incubation medium. (**B**) Cell cultures under air-liquid interface (ALI) conditions were exposed to either clean air or ENP aerosols using an Automated Exposure Station (AES) for 2 and 4 h to achieve different deposited doses. It was not possible to generate a stable aerosol from SnO_2 NP, though they were not tested under ALI. As depicted, samples for cytotoxicity (LDH release and WST-1 metabolisation) and genotoxicity (DNA damage) assessment were collected at different timepoints.

2.5. Cytotoxicity Assessment

Two endpoints were evaluated to assess the impact of the tested NP in human alveolar epithelial cells: LDH release as an indicator of plasma membrane integrity, and WST-1 reduction to evaluate the cell viability. Under submerged conditions, cells were incubated with different concentrations of the tested NP (5, 10, 25, 50, 100, 150 $\mu g/cm^2$) and both assays carried out at 24 h after exposure. On the other hand, under ALI conditions, LDH release was assessed before exposure (to assess cell health status before exposure), immediately after exposure (basal medium from the exposure chambers was collected) and at the recovery time (24 h after exposure), while the WST-1 reduction was assessed only in the recovery time.

LDH release was determined using Roche Cytotoxicity Detection Kit (Roche, Mannheim, Germany), according to manufacturer's instructions. Briefly, at each assessed time-point, incubation media (submerged exposure) or basolateral media (ALI exposure) were collected for analysis. Before analysis, samples from the submerged exposures were centrifuged in 96-well round bottom plates at $2210\times g$ for 5 min to remove the cell debris and residual NP. Cells lysed with 2% Triton X-100 (30 min) were used as positive controls (PC). Briefly, 100 μL of freshly prepared reaction mixture was added to 100 μL of each sample and incubated up to 30 min at room temperature and protected from light. Absorbance was measured at 490 nm and 630/690 nm (reference wavelength) in a microplate reader (Spectramax M2 Molecular Devices, San Jose, CA, USA). LDH release values were normalised considering the PC mean value (total LDH release). To test for possible NP interferences with the assay, total LDH release, i.e., PC was determined in the absence and in the presence of the highest tested concentration of ENP or ENP aerosols.

Cell viability was evaluated using WST-1 Cell Proliferation Reagent Kit (Roche, Mannheim, Germany), according to the manufacturer's instructions. For submerged samples, cells were washed with PBS pH 7.4 prior incubation with 100 $\mu L/well$ of WST-1 reagent diluted 1:10 for 2 h at 37 °C, 5% CO_2. For ALI samples, 250 $\mu L/insert$ of WST-1 reagent diluted 1:10 was added to the apical compartment and let incubate for 30 min at 37 °C, 5% CO_2. At the end of the incubation time, 100 μL were transferred to a 96-well plate. Sample's absorbance was measured at 450 nm and 630/690 nm (reference wavelength) in a microplate reader (SpectraMax® iD3 Molecular Devices, San Jose, CA, USA). WST-1 reduction values were normalised considering the control (incubator control for ALI samples) mean value.

2.6. Genotoxicity Assessment

Primary and oxidative DNA damage were assessed by the standard alkaline and formamidopyrimidine-DNA glycosylase (FPG)-modified comet assay versions, respectively. Cells were collected using a cell scrapper after 24 h of submerged or ALI exposure. ALI samples were suspended in cryoprotective medium (cell culture medium supplemented with 10% DMSO) and frozen at −80 °C until analysis. Cells from submerged exposures were washed 2× with PBS pH 7.4, scrapped and suspended in PBS. For submerged conditions, cells exposed to 500 μM MMS and 2.5 mM of $KBrO_3$ for 30 min were included as PC of the primary and oxidative DNA damage, respectively, whereas for ALI cells exposed to 1 mM H_2O_2 for 30 min were used as PC. Cells were counted in a Neubauer's chamber and 6.0×10^3 cells were transferred to a microcentrifuge tube and centrifuged at $700\times g$ for 5 min. Supernatant was removed and cells were resuspended in 100 μL of 1% LMP agarose. Five microliters were placed onto microscope slides precoated with 1% NMP, using a high-throughput system of 12-minigel comet assay unit (Severn Biotech Ltd.®, Kidderminster, UK). Three slides were prepared, one for the standard alkaline comet assay and two for the enzyme-modified version (with or without FPG-enzyme), and duplicates of each sample were added to each slide. The alkaline comet assay procedure was performed as previously described (Bessa et al., 2019). After agarose solidification at 4 °C for 5 min, slides were immersed in ice-cold lysis solution (2.5 M NaCl, 100 mM Na_2EDTA, 10 mM Tris-base, 10 M NaOH, pH 10, 1% Triton-X 100) during 1 h at

4 °C, protected from light. After lysis, FPG-modified comet assay slides were washed three times for 5 min with buffer F (0.1 M KCl, 0.5 mM Na_2EDTA, 40 mM HEPES, 0.2 mg/mL BSA, pH 8) prior incubation for 30 min at 37 °C with 2.7 U/mL of FPG enzyme or with buffer F alone. After incubation, FPG and buffer F slides were washed with PBS pH 7.4. The alkaline comet assay slides were washed 3 times with PBS pH 7.4 for 5 min. For DNA unwinding, all slides were immersed in electrophoresis solution (1 mM Na_2EDTA, 0.3 M NaOH, pH 13) for 40 min at 4 °C, followed by electrophoresis in the same solution for 30 min at a constant 25 V (0.9 V/cm) and 400 mA. At the end of electrophoresis, slides were neutralised and fixed as described elsewhere [42]. For the comet scoring, slides were initially hydrated in Tris-EDTA (TE) buffer (10 mM Tris-HCl, 1 mM Na_2EDTA, pH 7.5–8) and then stained with 1:10,000 dilution of SYBR® Gold in TE buffer for 40 min at room temperature. Comets were visualised in a Motic BA410 ELITE series microscope equipped with a complete EPI-fluorescence kit and scored using the Comet Assay IV image analysis software (Perceptive Instruments, Staffordshire, UK). At least 100 cells/experimental group (50 in each replicate gel) were scored and the mean of the percentage of DNA in the comet tail (% tail intensity) was used as a DNA damage descriptor.

2.7. Statistical Analysis

Statistical analysis was performed using SPSS (version 26.0, Armonk, NY, USA) and GraphPad Prism (version 6.0, San Diego, CA, USA) statistical software. Experimental data were expressed as mean ± standard deviation (SD). Data were tested for normality and homogeneity of variances by Shapiro–Wilk and Levene's tests, respectively. For each assessed timepoint, differences between tested doses and controls were estimated using a one-way analysis of variance (ANOVA) followed by post-hoc Dunnett's test for multiple comparisons. A *p* value < 0.05 was considered significant.

3. Results

3.1. Nanoparticle's Suspensions and Aerosols Characterisation

In Table 1 are presented the main physicochemical features of the tested ENP suspensions. As shown, mean particle sizes of 455.5 nm, 688.5 nm, 305.6 nm and 406.0 nm were obtained for SnO_2, ATO, CeO_2 and ZrO_2 NP, respectively. A slight increase compared to the negative control but no significant differences in the oxidative potential of the four tested ENP were detected suggesting that all tested particles have a low ability to produce •OH in a cell-free environment.

Table 1. Physicochemical characteristics of the tested engineered nanoparticles (ENP) stock suspensions.

ENP	Hydrodynamic Size (nm)	Concentration (Number of Particles/mL)	Oxidative Potential (A.U.) *	Effective Density (mg/mL)
SnO_2	455.5 ± 17.98	2.70×10^8	4958	6.7
ATO	688.5 ± 97.80	12.28×10^8	4081	17.4
CeO_2	305.6 ± 79.72	8.07×10^8	4806	1.5
ZrO_2	406.0 ± 1.79	22.05×10^8	3408	3.5

Data are presented as mean ± SD. Hydrodynamic size was measured by Dynamic Light Scattering (DLS). Concentration was determined by Nanoparticle Tracking Analysis (NTA). Oxidative potential was measured by Electronic Spin Resonance (ERS). A.U.: arbitrary units. * Negative control (ultrapure water) = 3191 A.U.; Positive control (DOFA) = 48,041 A.U.
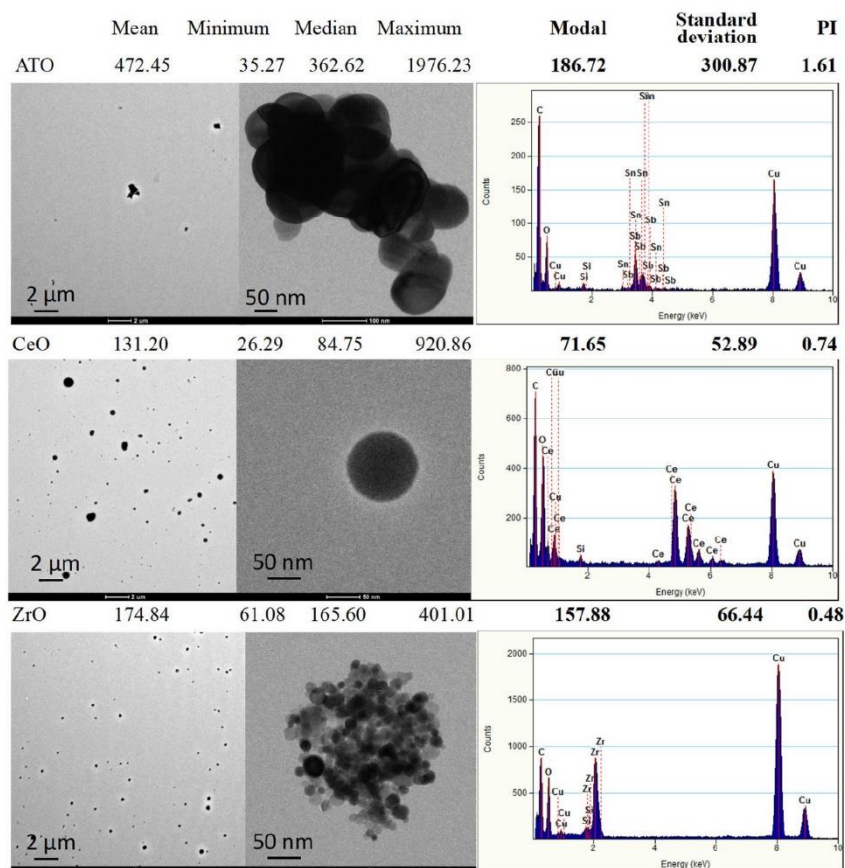
Under submerged conditions, all ENP are expected to settle onto the cells after 24 h of exposure since ENP effective density is substantially higher compared to cell culture medium. Regarding ALI exposure, it was not possible with the limited available amount of test material to generate a stable aerosol from the SnO_2 NP, thus this NP was not tested under these conditions. Table 2 shows NP aerosolisation conditions and aerosol deposition in human alveolar epithelial cultures. The deposited doses were calculated from the gravimetric data. Average single doses ranged between 6 to 12 $\mu g/cm^2$ for ATO NP, 46 to 92 $\mu g/cm^2$ for CeO_2 NP, 17 to 34 $\mu g/cm^2$ for ZrO_2 NP.

Table 2. Aerosolisation conditions and exposure concentrations of the tested aerosolised engineered nanoparticles in human alveolar epithelial-like cultures.

		ATO	CeO$_2$	ZrO$_2$
Liquid suspension flow rate (mL/h)		0.6	1.2	0.6
Aerosol flow through the insert (mL/min)		25	25	25
Aerosol concentration (mg/m^3)		2.3	6.4	17.0
Number of particles		4×10^5	1×10^5	1×10^5
Deposited mass	2 h	6	46	17
	4 h	12	92	34

Aerosol mass concentration determined by gravimetry; Number of particles determined using a condensation particle counter (CPC); Deposited mass = mass concentration of aerosol/volume of aerosol passing through exposure chambers during exposure.

Analysis of the generated aerosols collected on TEM grids (Figure 3) showed that NP exhibited different shapes and size distributions. The ATO aerosolised sample is composed of larger, irregular agglomerations (up to 2 μm) of fused small spheroidal NP (50–100 nm) with mean particle sizes of 472.45 nm and a modal value (value with maximum count) of 186.72 nm that give rise to a calculated PI polydispersity index) of 1.61. CeO$_2$ aerosols present themselves as spherical but with broad distribution NP (from 26 to 920 nm) with a mean value of 131.2 nm and a modal value of 71.65 nm associated with a PI of 0.74. ZrO$_2$ aerosols are formed of apparently spherical agglomerations (up to 400 nm) of very small round NP (10–25 nm) giving a mean value of the agglomerations of 174.8 nm, a modal value of 157.88 nm with a PI of 0.48.

	Mean	Minimum	Median	Maximum	Modal	Standard deviation	PI
ATO	472.45	35.27	362.62	1976.23	**186.72**	300.87	1.61
CeO	131.20	26.29	84.75	920.86	**71.65**	52.89	0.74
ZrO	174.84	61.08	165.60	401.01	**157.88**	66.44	0.48

Figure 3. Representative transmission electron microscopy (TEM) images of the generated aerosols (EDS spectra) with respective size distribution values. The size distribution of aerosol generated particles was determined from TEM images by using the ImageJ software.

164

3.2. Cytotoxicity: Submerged vs. ALI Conditions

Figure 4 shows the cytotoxicity data for the SnO_2, ATO, CeO_2 and ZrO_2 NP under study, as assessed by the LDH release and WST-1 viability assays. As depicted, no significant changes in plasma membrane integrity of human alveolar epithelial cells exposed to SnO_2 or ATO NP compared to control cells were observed under submerged conditions at 24 h after exposure (Figure 4A). On the other hand, a clear concentration-dependent decrease in LDH release was observed in cells exposed to CeO_2 or ZrO_2 NP compared to the negative controls ($p \leq 0.001$). However, CeO_2 NP seem to interfere in the LDH assay, as total LDH release of the cells exposed to the highest tested concentration (PC + 150; 4.08 ± 2.23%) was far below the total LDH release in the absence of CeO_2 NP (PC; 100.00 ± 2.37%). This finding is most likely caused by CeO_2 NP deposition onto the cell monolayer preventing LDH leakage into the extracellular environment. Regarding cellular viability, significant increases in WST-1 reduction were observed in cells exposed to all tested NP at 24 h exposure ($p \leq 0.001$) (Figure 4B). Taken together, these results seem to indicate that all tested NP did not induce significant cytotoxic responses in human alveolar epithelial cells under submerged conditions.
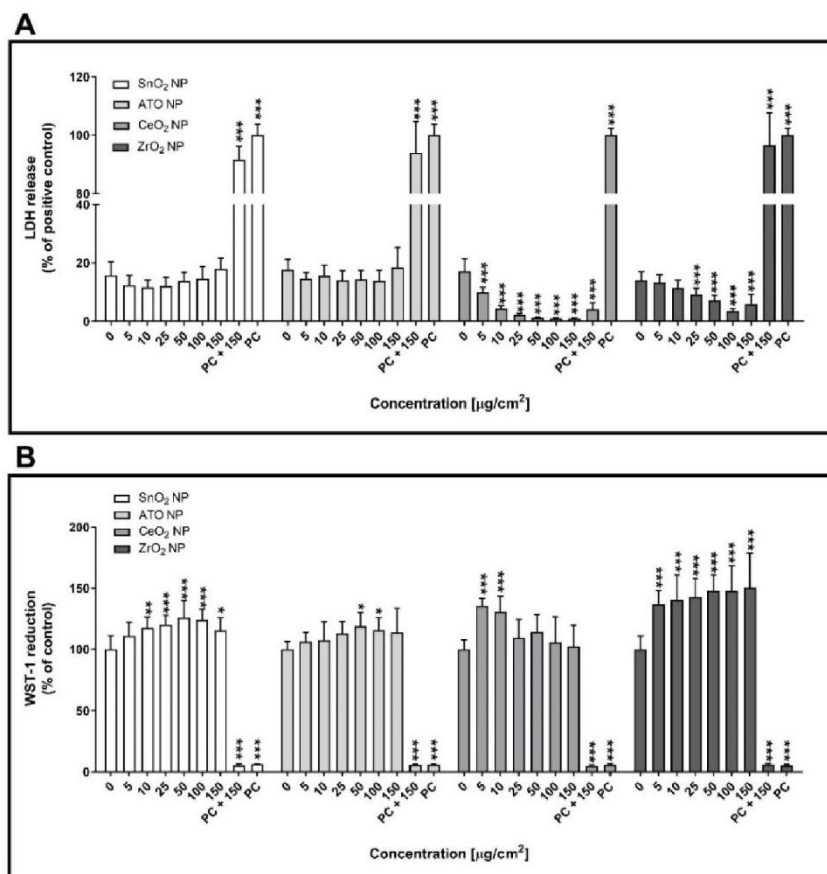

Figure 4. Cytotoxicity of the tested engineered nanoparticles (ENP) (SnO_2, ATO, CeO_2 and ZrO_2) in human alveolar epithelial cells under submerged conditions being exposed for 24 h. Lactate dehydrogenase release (LDH) release (**A**) and WST-1 reduction (**B**) assays were carried out after 24 h exposure to the NP suspensions prepared in serum-free cell culture medium. Data are expressed as mean ± standard deviation (n = 3–4). LDH release values were normalised considering the positive control (total LDH release; cells lysed with 2% Triton X-100), while WST-1 reduction values were normalised considering the negative control. Data was analysed by the one-way analysis of variance (ANOVA) test followed by the Dunnett's post hoc test for multiple comparisons. * $p \leq 0.05$, ** $p \leq 0.01$ and *** $p \leq 0.001$ vs. negative control. PC: Positive control.

Figure 5 refers to the cytotoxicity of the aerosolised ATO, CeO_2 and ZrO_2 NP in human alveolar epithelial cells at ALI. As expected, before exposure, no effects on the LDH release were observed in control, an indicator of cell health (data not shown). Immediately after exposure to all the tested aerosolised NP, a significant increase in LDH release was observed compared to cells exposed to clean air (exposure control). This detrimental effect on plasma membrane integrity was more marked in cells exposed to the highest deposited dose of CeO_2 (34 μg/cm^2; 52.36 ± 3.15%) and ZrO_2 (92 μg/cm^2; 59.77 ± 2.46%) NP aerosols than to ATO NP (12 μg/cm^2; 19.11 ± 3.43%) (Figure 5A). Based on LDH release data, calculated half-maximal effective concentrations (EC_{50}) were of 74.77 (CI 95%: 66.51–84.05), 32.97 (CI 95%: 31.01–35.04) and 20.70 (CI 95%: 12.60–33.98) μg/cm^2 for ATO, CeO_2 and ZrO_2 NP respectively. Nevertheless, at 24 h after exposure, no differences in LDH release levels were observed among the exposed cells (i.e., exposure control and NP aerosol-exposed cells), although those were significantly higher than the incubator control (Figure 5B). However, a significant decrease in cellular metabolic activity of similar magnitude, as assessed by the WST-1 assay, was observed at 24 h after exposure to all tested aerosolised NP (Figure 5C).
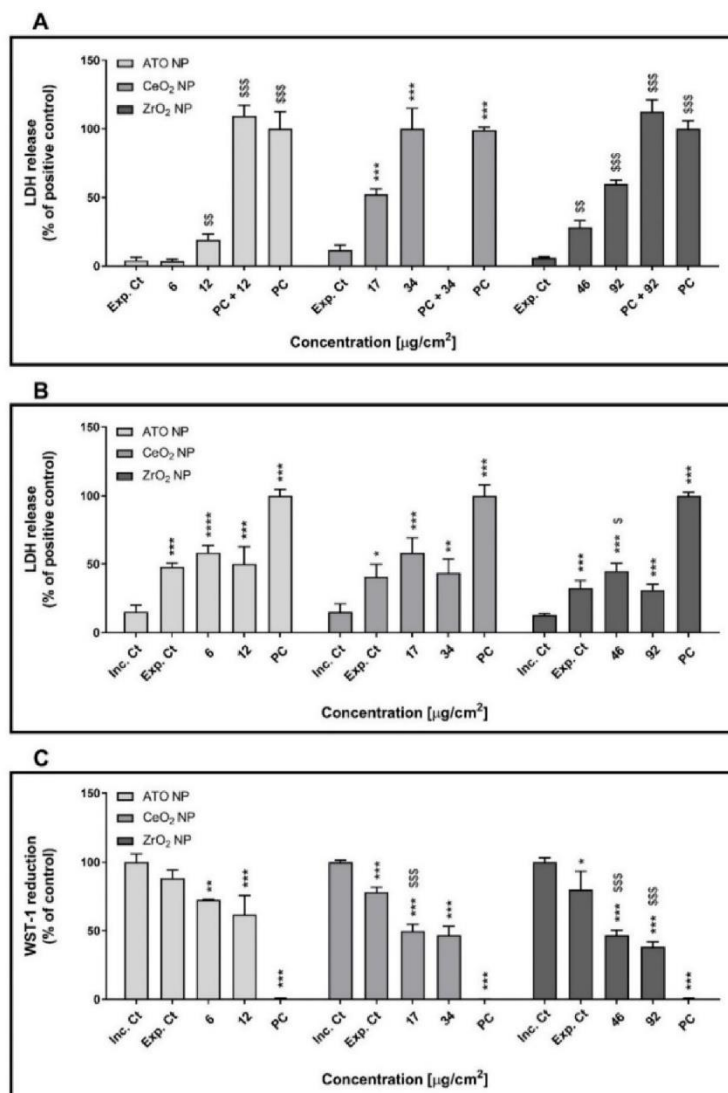

Figure 5. Cytotoxicity of the aerosolised engineered nanoparticles (ENP) (ATO, CeO_2 and ZrO_2) in polarised cultures of human alveolar epithelial cells at air-liquid interface (ALI) conditions. Lactate dehydrogenase release (LDH) was assessed immediately after (0 h) (**A**) and at 24 h (**B**) after exposure.

(**C**) WST-1 reduction assay was carried out only in the recovery period (24 h after exposure). Data are expressed as mean $\pm$ standard deviation (n = 3). LDH values were normalised considering positive control (total LDH release; cells lysed with 2% Triton X-100), while WST-1 values were normalised considering the incubator control. Data was analysed by the one-way analysis of variance (ANOVA) test followed by the Dunnett's post hoc test for multiple comparisons. * $p \leq 0.05$, ** $p \leq 0.01$ and *** $p \leq 0.001$ vs. Inc. Ct; $^{\$}$ $p \leq 0.05$, $^{\$\$}$ $p \leq 0.01$ and $^{\$\$\$}$ $p \leq 0.001$ vs. Exp. Ct. Inc. Ct: Incubator control; Exp. Ct: Exposure control; Positive Ct: Positive control.

3.3. Genotoxicity: Submerged vs. ALI Conditions

The comet assay was performed to assess the primary (strand breaks) and oxidative (FPG-sensitive sites) DNA damage levels of cells exposed to suspended or aerosolised NP (Figure 6). For cells cultured under submerged conditions, three non-cytotoxic concentrations of ATO, CeO_2 and ZrO_2 NP were tested: 10, 25 and 50 $\mu g/cm^2$. At 24 h post-exposure, increased levels of DNA strand breaks were observed in cells incubated with the highest concentration (50 $\mu g/cm^2$) of any tested NP compared to control cells (Figure 6A). On the other hand, cells exposed to SnO_2 and ATO NP but not to CeO_2 and ZrO_2 NP exhibited a significant increase of DNA oxidative lesions compared to control cells (Figure 6B). While cells exposed to 10 or 25 $\mu g/cm^2$ of SnO_2 NP (9.14 ± 3.11 and $9.47 \pm 2.00\%$ tDNA, respectively) showed increased levels of FPG-sensitive sites, only cells exposed to the highest tested concentration of ATO NP (50 $\mu g/cm^2$; $9.77 \pm 3.79\%$ tDNA) exhibited increased levels of DNA oxidative lesions compared to control cells ($5.80 \pm 2.60\%$ tDNA). As expected, high levels of primary and oxidative DNA damage were detected for submerged cells exposed to the corresponding PC (MMS 500 μM: $62.23 \pm 8.85\%$ tDNA; $KBrO_3$ 2.5 mM: $58.16 \pm 11.73\%$ tDNA, respectively).

The data obtained for human alveolar epithelial cells exposed to the NP aerosols at ALI is depicted in Figure 6C,D. As shown, exposure to aerosolised ATO NP failed to affect DNA integrity. However, cells exposed to the highest deposited dose of CeO_2 NP aerosols exhibited increased levels of DNA strand breaks (34 $\mu g/cm^2$; $15.48 \pm 3.64\%$ tDNA) (Figure 6C). Regarding ZrO_2 NP, a concentration-dependent increase of DNA strand breaks was detected in cells exposed to these aerosols compared to control cultures (Figure 6C). Notwithstanding this, no significant changes in oxidative DNA damage were detected for all the tested NP aerosols (Figure 6D).

Representative comet images of human alveolar epithelial cells exposed to ZrO_2 NP, which were able to induce DNA damage both under submerged and ALI conditions are depicted Figure 7.

As shown, wider comet tails were observed in cells exposed to the highest concentration of ZrO_2 NP, either in submerged or ALI conditions, when compared to those obtained in the negative controls. A pronounced DNA damage in relation to control was observed in cells at ALI exposed to the PC (1 mM H_2O_2, 30 min), which could not be quantified using the comet image analysis software (data not shown).
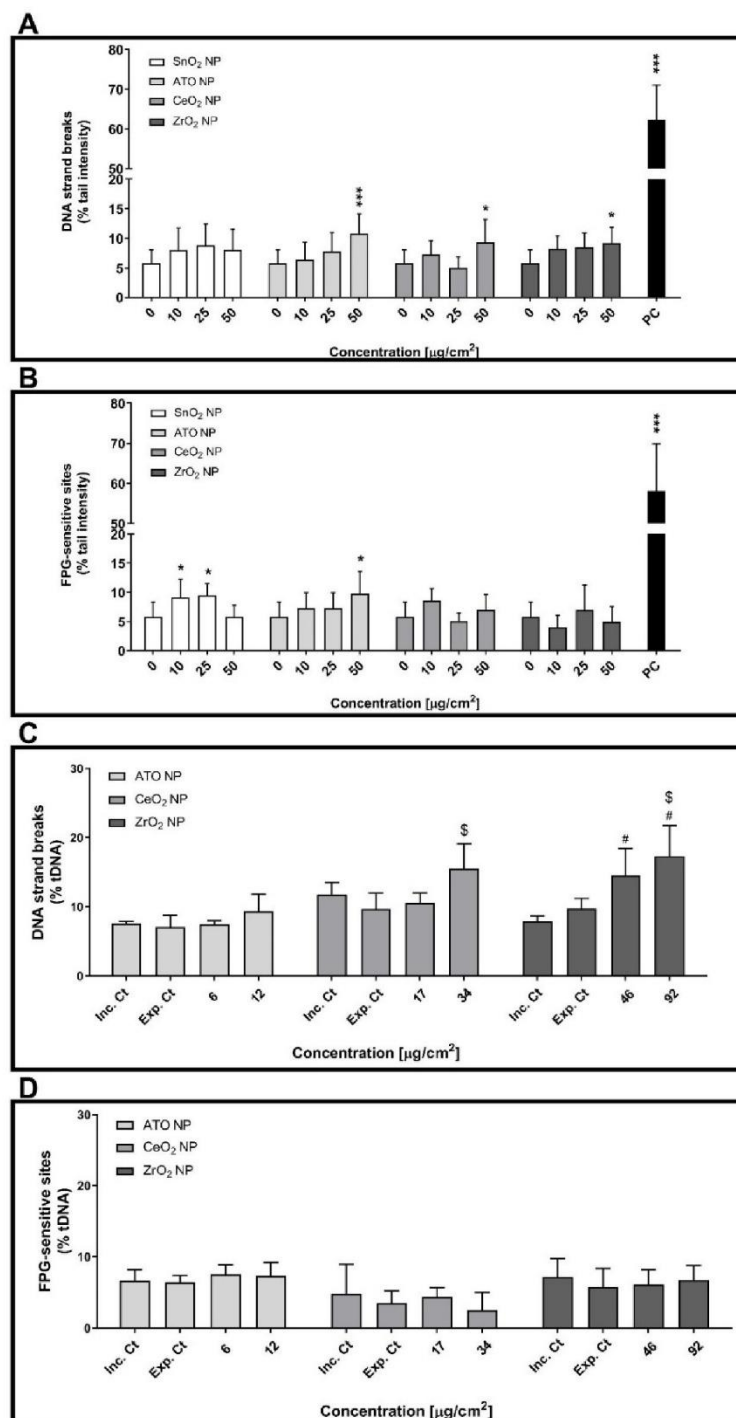
Figure 6. Genotoxicity of the tested engineered nanoparticles (ENP) in human alveolar epithelial cells under submerged (**A,B**) and ALI (**C,D**) conditions. Primary (**A,C**) and oxidative (**B,D**) DNA damage were assessed at 24 h after exposure to the ENP suspensions by the alkaline and FPG-modified comet assay versions, respectively. Data are expressed as mean $\pm$ standard deviation ($n = 3$–4). Data was analysed by one-way ANOVA followed by Dunnett's post-hoc test. * $p \leq 0.05$ and *** $p \leq 0.001$ vs. negative control. # $p \leq 0.05$ vs. incubator control and $ $p \leq 0.05$ vs. exposure control. PC: Positive control; 500 μM MMS and 2.5 mM KBrO$_3$ for primary (**A**) and oxidative (**B**) DNA damage under submerged conditions, respectively.
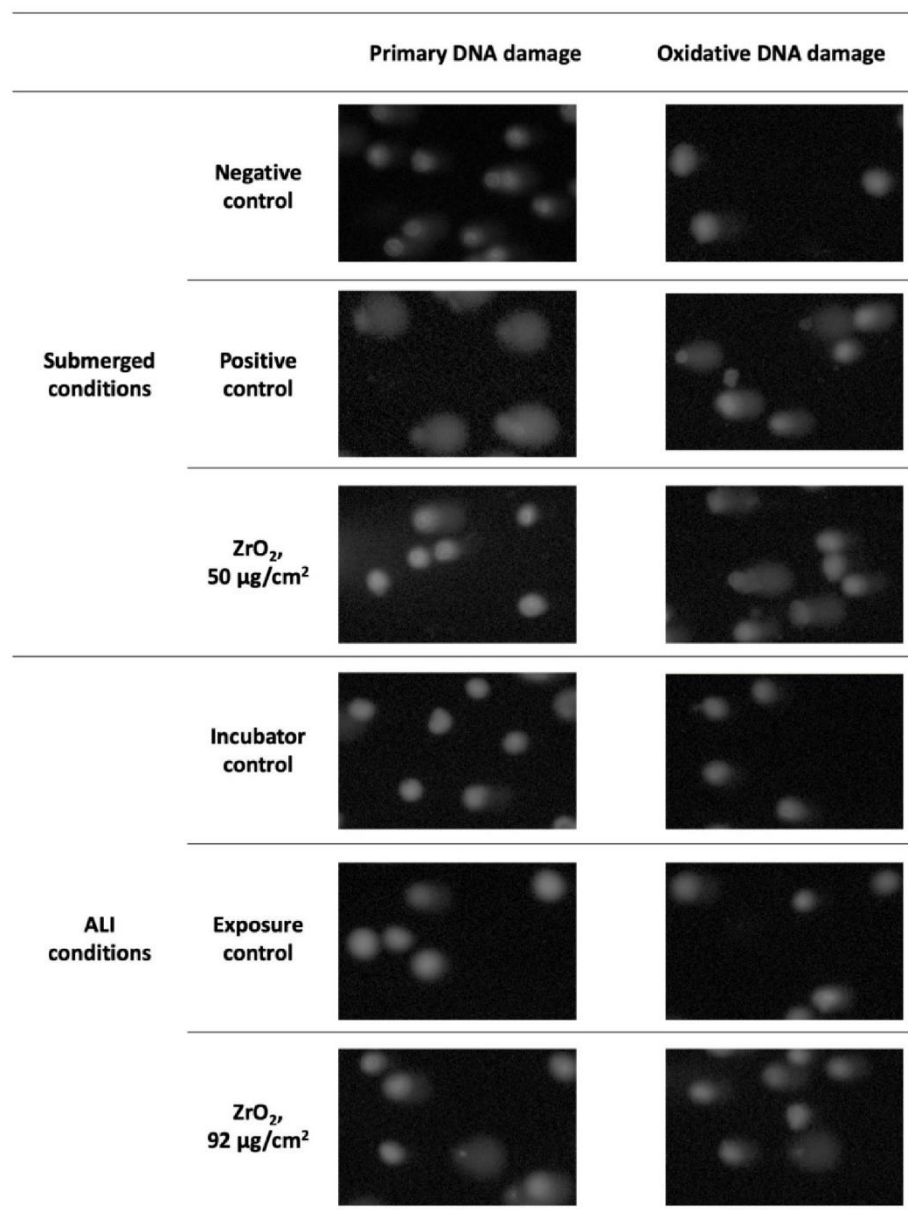
Figure 7. Comet assay representative images (100× magnification) of human alveolar epithelial cells under submerged and ALI conditions exposed to the highest tested concentration of ZrO_2 NP and respective experimental controls.

4. Discussion

Herein, we have comparatively evaluated the *in vitro* toxicity of four industrially relevant ENP in human alveolar epithelial-like submerged cultures exposed to liquid suspensions or in ALI cultures exposed to aerosolised ENP. Although not exactly the same, the tested dose levels were comparable as they were within the same range: 5–150 μg/cm^2 for submerged cultures and 6–92 μg/cm^2 for ALI cultures. From a human exposure scenario point of view, these values are relevant considering that the estimated lifetime dose under realistic ambient conditions is 6.6 μg/cm^2, while for a worst-case occupational exposure scenario a daily alveolar mass dose of 0.13 μg/cm^2 and a maximum accumulated lifetime dose of 420 μg/cm^2 are expected to be achieved [36].

169

Overall, our data showed that ENP cytotoxicity in human alveolar epithelial cells was more evident under ALI than at submerged conditions. Under ALI conditions, based on the EC_{50} values for LDH release immediately after exposure, ENP can be ranked for their toxicity hazard as follows: ZrO_2 NP > CeO_2 NP > ATO NP. Interestingly, no significant differences in the LDH release at 24 h post-exposure (recovery time) between cells exposed to clean air (exposure control) and cells exposed to the ENP aerosols were detected. However, a slight increase in LDH release in exposure control cells was detected compared to the incubator control, suggesting that plasma membrane integrity might have been affected by the air flow across the cells, considering the lack of tight intercellular junctions that polarised A549 cells exhibit [28,41]. Accordingly, other respiratory cell models such as bronchial epithelial Calu-3 cells have been shown to be more suitable for continuous flow exposure systems such as the one employed in the present study [41,43]. Notwithstanding, a significant decrease in cellular metabolic activity of cells exposed to ENP aerosols compared to the exposure control has been detected at 24 h post-exposure, meaning that the aerosolised ENP negatively affected the cell physiology.

In submerged conditions, no significant cytotoxic effects were observed in human alveolar epithelial cells exposed to the liquid suspensions of ENP. This difference in the cytotoxic potential of the tested ENP in submerged vs. ALI exposure conditions may obviously arise from differences in the attained deposited doses in both exposure conditions. One important aspect that also differed between exposure conditions is the potential for NP interference in the LDH release assay, in particular for CeO_2 NP that clearly affected the assay as evidenced by the low levels of LDH release comparing with the control and the evident difference in the PC value that corresponds to the maximum release of LDH, in the absence and in the presence of CeO_2 NP.

Regarding the genotoxic potential of the tested ENP, our data showed that all tested ENP seem to increase the primary DNA damage of human alveolar epithelial cells regardless of the exposure mode, except for ATO NP, where cells exposed in ALI conditions did not show significant changes in the level of DNA strand breaks comparing with the controls. Moreover, human alveolar epithelial cells seem to be more sensitive to the genotoxic effects of ZrO_2 NP aerosols than to the same NP in liquid medium. Nonetheless, as stated above, this apparent difference in sensitivity to the tested ZrO_2 NP might be related with differences in the physicochemical features and/or deposited doses under the two exposure conditions. However, while SnO_2 and ATO NP caused DNA oxidative lesions in cells under submerged cultures, no changes in FPG-sensitive sites were detected at ALI exposure.

Our data are in line with previous reports on *in vitro* toxicity of the tested ENP in human alveolar epithelial-like A549 cells under submerged conditions. Tabei, et al. [44] have reported low levels of NP uptake and no evident cytotoxic effects in A549 cells exposed for 6 and 24 h to indium-doped SnO_2 NP (30 nm; 1–1000 μg/mL), in spite of a markedly increase in ROS levels, expression of heme oxygenase 1 (HO-1) gene and DNA damage have been observed [44]. Titma, Shimmo, Siigur and Kahru [31] also reported no significant cytotoxicity in A549 cells exposed for 24 h to 3–100 μg/mL of Sb_2O_3 NP, though a marked increase in toxicity has been observed after long-term exposure (up to 9 days) [31]. Regarding CeO_2 NP, some studies in the literature showed that these NP are relatively non-cytotoxic. Indeed, minimal or no effects on cell viability and LDH release were detected in A549 alveolar epithelial cells exposed to CeO_2 NP in liquid incubation medium (concentrations up to 100 μg/mL [45–47] and 1000 μg/mL [48]), although some authors observed induction of genotoxicity (DNA damage; 0.5 μg/mL to 5000 μg/mL) [49]. On the other hand, some studies demonstrated that CeO_2 NP induced plausible toxicity effects towards A549 cells. For instance, Mittal and Pandey [50] suggested that CeO_2 NP produced an increased amount of ROS, which majorly contributed to extensive DNA damage and cell cycle arrest, responsible for apoptotic cell death in A549 cells [50]. According to these authors, CeO_2 NP induced a concentration-dependent increase in ROS production up to 6 h, however this tendency was strongly attenuated after 24 h exposure [50], in

opposition to what was found in the present study. Lanone, Rogerieux, Geys, Dupont, Maillot-Marechal, Boczkowski, Lacroix and Hoet [30] assessed the toxicity of CeO_2 and ZrO_2 (0–5000 µg/mL) in the human alveolar epithelial A549 and macrophage THP-1 cell lines at 24 h after exposure and found that both CeO_2 and ZrO_2 NP caused moderate cytotoxicity [30]. Recently, our lab has observed a mild cytotoxicity after exposure to aerosolised ATO and ZrO_2 NP at early timepoints (24 h; 5.56 µg ATO/cm^2 and 10.98 µg ZrO_2/cm^2) but no significant changes for late timepoints (72 h) in human 3D cultures of bronchial epithelial MucilAir™ cultures, with no meaningful effects regarding DNA damage [51].

Our data support the view that the ENP are more toxic to human alveolar epithelial cells when aerosolised rather than applied as a liquid suspension in submerged cell cultures. Lenz, et al. [38] compared the oxidative stress and proinflammatory responses of A549 exposed to aerosolised zinc oxide (ZnO) nanoparticles under ALI and submerged conditions. Lower levels of proinflammatory markers (IL-8, IL-6, and GM-CSF) were found in cells exposed under ALI conditions compared to submerged cultures, accompanied by no significant effects on the transcript levels of oxidative stress markers (0.7 and 2.5 µg ZnO/cm^2) [38]. Panas, et al. have also compared the biological responses of A549 cells under ALI or submerged cultures after exposure to two types of amorphous SiO_2 NP [40]. Amorphous SiO_2 NP induced similar cellular responses in both cultures systems, although submerged exposure to SiO_2 NP triggers stronger effects at much lower cellular doses [40]. On the other hand, Medina-Reyes, et al. [33] investigated the biological responses in A549 cells exposed to TiO_2 nanofibers and NP. These authors found that cytotoxicity of TiO_2 nanofibers and NP was similar in both types of A549 culture, although their uptake was higher in submerged compared to ALI cultures. TiO_2 nanofibers induced higher DNA double strand breaks (DSB) in A549 cells under ALI conditions than in submerged cultures, though TiO_2 NP caused similar levels of DSB in both culture conditions [39]. Recently, Diabaté, et al. [48] evaluated the *in vitro* toxicity of CeO_2 and TiO_2 NP in monocultures of A549 cultured at ALI vs. co-cultures of A549 and THP-1 macrophages under submerged conditions. Similar to our study, cells under ALI conditions were more sensitive to NP-induced toxicity when compared to those cultured under submerged conditions. Moreover, CeO_2 NP induced moderate *in vitro* toxicity, whilst TiO_2 NP caused evident cytotoxicity, pro-inflammatory gene expression and genotoxicity [52]. Taken together, these studies suggest that cell response to NM is dependent upon the exposure conditions that includes sample preparation but also upon the physicochemical properties of the NM. It is important to point out that *in vitro* pulmonary models in submerged systems do not fully recapitulate relevant cellular and physiological airway epithelia features [33,36]. In vivo, airways are not fully covered by pulmonary fluid to allow the gas-exchange between cells and the environment. Indeed, exposure to inhaled toxicants such as airborne NP mainly occurs under ALI conditions [53]. Thus, *in vitro* exposure systems able to deliver aerosolised particles to cells cultured at ALI is of major importance for a more reliable *in vitro* testing of NP effects in pulmonary nanotoxicity studies, and more accurately mimicking the human in vivo cells in the respiratory tract rather than the conventional approaches using *in vitro* submerged cell cultures [25,54].

More pronounced cytotoxic effects were observed after exposure to the aerosolised NP, while a similar DNA damage after NP exposure was found for both types of exposure conditions (except for ATO NP). The observed differences in toxicity may arise from different deposited doses attained in the cell surface when covered in culture medium or air, which consequently influences the toxic potency of these NP, as well as their capacity to interfere with the assay components. The dose levels tested herein are within the lifetime dose under realistic occupational exposure to NP, and the results obtained reflect the negative impact these aerosolised nano-sized materials inadvertently have on the workers' health. Although both submerged and ALI cell culture systems enable the evaluation of NP toxicity *in vitro*, the present study highlights how realistic dose levels under ALI conditions provide more biologically valuable data regarding occupational exposure to airborne NP.

So far, it has been difficult to assert with certainty whether airborne ENP constitute a higher or lower hazard to humans compared to incidental, process-generated NP since there are few toxicity studies on the latter. We have recently showed that both fine and NP fractions released and collected during high-velocity oxy-fuel (HVOF) spraying at an industrial facility induced higher toxicity than two ENP (ATO and ZrO_2 NP) on bronchial epithelial MucilAir^{TM} cultures under ALI conditions, most likely due to their chemical complexity [51]. These findings emphasize the importance of investigating not only ENP but also incidental, process-generated NP hazards, to have a deeper understanding of the toxicity mechanisms and potential risks for workers' health from occupational exposure to these NP.

5. Conclusions

Different toxicity effects induced by ENP used as raw materials in the advanced ceramics industry were observed in human alveolar epithelial cells under both types of culture condition. As hypothesised, ENP seemed more hazardous to human alveolar epithelial cells cultured under ALI compared to submerged conditions. ALI cultures are a key strategy for future occupational inhalation NP toxicity studies as it also has more potential to extrapolate the finding for human risk assessment. Additionally, from an occupational health management point of view, the study of the toxicity in different exposure systems is of utmost importance to better assess the potential impact on workers' health of a material in various exposure scenarios, to identify their hazards and put them in their true perspective.

References

1. Mohajerani, A.; Burnett, L.; Smith, J.V.; Kurmus, H.; Milas, J.; Arulrajah, A.; Horpibulsuk, S.; Kadir, A.A. Nanoparticles in Construction Materials and Other Applications, and Implications of Nanoparticle Use. *Materials* **2019**, *12*, 3052. [CrossRef]
2. Piccinno, F.; Gottschalk, F.; Seeger, S.; Nowack, B. Industrial production quantities and uses of ten engineered nanomaterials in Europe and the world. *J. Nanoparticle Res.* **2012**, *14*, 1109. [CrossRef]

3. Dolez, P.I.; Debia, M. Overview of Workplace Exposure to Nanomaterials. In *Nanoengineering*; Elsevier: Amsterdam, The Netherlands, 2015; pp. 427–484.

4. World Health Organization. *WHO Guidelines on Protecting Workers from Potential Risks of Manufactured Nanomaterials*; World Health Organization: Geneve, Switzerland, 2017; Licence: CC BY-NC-SA 3.0 IGO.

5. Bessa, M.J.; Brandão, F.; Viana, M.; Gomes, J.F.; Monfort, E.; Cassee, F.R.; Fraga, S.; Teixeira, J.P. Nanoparticle exposure and hazard in the ceramic industry: An overview of potential sources, toxicity and health effects. *Environ. Res.* **2020**, *184*, 109297. [CrossRef]

6. Fonseca, A.S.; Viana, M.; Querol, X.; Moreno, N.; De Francisco, I.; Estepa, C.; De La Fuente, G.F. Workplace Exposure to Process-Generated Ultrafine and Nanoparticles in Ceramic Processes Using Laser Technology. In *the Handbook of Environmental Chemistry*; Springer: Singapore, 2015; pp. 159–179.

7. Fonseca, A.; Viana, M.; Querol, X.; Moreno, N.; de Francisco, I.; Estepa, C.; de la Fuente, G.F. Ultrafine and nanoparticle formation and emission mechanisms during laser processing of ceramic materials. *J. Aerosol Sci.* **2015**, *88*, 48–57. [CrossRef]

8. Fonseca, A.; Maragkidou, A.; Viana, M.; Querol, X.; Hämeri, K.; de Francisco, I.; Estepa, C.; Borrell, C.; Lennikov, V.; de la Fuente, G.F. Process-generated nanoparticles from ceramic tile sintering: Emissions, exposure and environmental release. *Sci. Total Environ.* **2016**, *565*, 922–932. [CrossRef]

9. Salmatonidis, A.; Ribalta, C.; Sanfélix, V.; Bezantakos, S.; Biskos, G.; Vulpoi, A.; Simion, S.; Monfort, E.; Viana, M. Workplace Exposure to Nanoparticles during Thermal Spraying of Ceramic Coatings. *Ann. Work. Expo. Health* **2018**, *63*, 91–106. [CrossRef]

10. Salmatonidis, A.; Sanfélix, V.; Carpio, P.; Pawłowski, L.; Viana, M.; Monfort, E. Effectiveness of nanoparticle exposure mitigation measures in industrial settings. *Int. J. Hyg. Environ. Health* **2019**, *222*, 926–935. [CrossRef]

11. Salmatonidis, A.; Viana, M.; Pérez, N.; Alastuey, A.; de la Fuente, G.F.; Angurel, L.A.; Sanfélix, V.; Monfort, E. Nanoparticle formation and emission during laser ablation of ceramic tiles. *J. Aerosol Sci.* **2018**, *126*, 152–168. [CrossRef]

12. Viana, M.; Fonseca, A.S.; Querol, X.; López-Lilao, A.; Carpio, P.; Salmatonidis, A.; Monfort, E. Workplace exposure and release of ultrafine particles during atmospheric plasma spraying in the ceramic industry. *Sci. Total Environ.* **2017**, *599–600*, 2065–2073. [CrossRef]

13. Ribalta, C.; Koivisto, A.J.; Salmatonidis, A.; López-Lilao, A.; Monfort, E.; Viana, M. Modeling of High Nanoparticle Exposure in an Indoor Industrial Scenario with a One-Box Model. *Int. J. Environ. Res. Public Health* **2019**, *16*, 1695. [CrossRef]

14. Salmatonidis, A.; Viana, M.; Biskos, G.; Bezantakos, S. Particle size distributions and hygroscopic restructuring of ultrafine particles emitted during thermal spraying. *Aerosol Sci. Technol.* **2020**, *54*, 1359–1372. [CrossRef]

15. Viana, M.; Salmatonidis, A.; Bezantakos, S.; Ribalta, C.; Moreno, N.; Córdoba, P.; Cassee, F.R.; Boere, J.; Fraga, S.; Teixeira, J.P.; et al. Characterizing the Chemical Profile of Incidental Ultrafine Particles for Toxicity Assessment Using an Aerosol Concentrator. *Ann. Work. Expo. Health* **2021**, *65*, 966–978. [CrossRef]

16. López, M.; Lilao, A.L.; Ribalta, C.; Martínez, Y.; Piña, N.; Ballesteros, A.; Fito, C.; Koehler, K.; Newton, A.; Monfort, E.; et al. Particle release from refit operations in shipyards: Exposure, toxicity and environmental implications. *Sci. Total Environ.* **2022**, *804*, 150216. [CrossRef]

17. Oberdörster, G.; Maynard, A.; Donaldson, K.; Castranova, V.; Fitzpatrick, J.; Ausman, K.; Carter, J.; Karn, B.; Kreyling, W.; Lai, D.; et al. Principles for characterizing the potential human health effects from exposure to nanomaterials: Elements of a screening strategy. *Part. Fibre Toxicol.* **2005**, *2*, 8. [CrossRef]

18. Pietroiusti, A.; Stockmann-Juvala, H.; Lucaroni, F.; Savolainen, K. Nanomaterial exposure, toxicity, and impact on human health. *Wiley Interdiscip. Rev. Nanomed. Nanobiotechnol.* **2018**, *10*, e1513. [CrossRef]

19. Kim, C. Deposition of Aerosols in the Lung: Physiological Factors. In *ISAM Textbook of Aerosol Medicine*; Dhand, R., Ed.; International Society for Aerosols in Medicine (ISAM): Gemünden, Germany, 2015; Volume 1, pp. 115–136.

20. Carvalho, T.C.; Peters, J.I.; Williams, R.O., III. Influence of particle size on regional lung deposition—What evidence is there? *Int. J. Pharm.* **2011**, *406*, 1–10. [CrossRef]

21. Bakand, S.; Hayes, A. Finance Dechsakulthorn Nanoparticles: A review of particle toxicology following inhalation exposure. *Inhal. Toxicol.* **2012**, *24*, 125–135. [CrossRef]

22. Kurjane, N.; Zvagule, T.; Reste, J.; Žanna, M.; Pavlovska, I.; Martinsone, I.; Vanadziņš, I. The effect of different workplace nanoparticles on the immune systems of employees. *J. Nanoparticle Res.* **2017**, *19*, 320. [CrossRef]

23. Li, J.J.; Muralikrishnan, S.; Ng, C.-T.; Yung, L.-Y.L.; Bay, B.-H. Nanoparticle-induced pulmonary toxicity. *Exp. Biol. Med.* **2010**, *235*, 1025–1033. [CrossRef]

24. Fröhlich, E. Comparison of conventional and advanced in vitro models in the toxicity testing of nanoparticles. *Artif. Cells, Nanomed. Biotechnol.* **2018**, *46*, 1091–1107. [CrossRef]

25. Hiemstra, P.S.; Grootaers, G.; van der Does, A.M.; Krul, C.A.; Kooter, I.M. Human lung epithelial cell cultures for analysis of inhaled toxicants: Lessons learned and future directions. *Toxicol. Vitr.* **2018**, *47*, 137–146. [CrossRef]

26. Rothen-Rutishauser, B.; Blank, F.; Mühlfeld, C.; Gehr, P. In vitro models of the human epithelial airway barrier to study the toxic potential of particulate matter. *Expert Opin. Drug Metab. Toxicol.* **2008**, *4*, 1075–1089. [CrossRef]

27. Blank, F.; Gehr, P.; Rothen-Rutishauser, B. In vitro human lung cell culture models to study the toxic potential of nanoparticles. In *Nanotoxicity: From In Vitro, In Vivo Models to Health Risks*; Wiley: Hoboken, NJ, USA, 2009; pp. 379–395. [CrossRef]

28. Leibrock, L.; Wagener, S.; Singh, A.V.; Laux, P.; Luch, A. Nanoparticle induced barrier function assessment at liquid–liquid and air–liquid interface in novel human lung epithelia cell lines. *Toxicol. Res.* **2019**, *8*, 1016–1027. [CrossRef]

29. Whitsett, J.A.; Wert, S.E.; Weaver, T.E. Alveolar Surfactant Homeostasis and the Pathogenesis of Pulmonary Disease. *Annu. Rev. Med.* **2010**, *61*, 105–119. [CrossRef]

30. Lanone, S.; Rogerieux, F.; Geys, J.; Dupont, A.; Maillot-Marechal, E.; Boczkowski, J.; Lacroix, G.; Hoet, P. Comparative toxicity of 24 manufactured nanoparticles in human alveolar epithelial and macrophage cell lines. *Part. Fibre Toxicol.* **2009**, *6*, 14. [CrossRef]

31. Titma, T.; Shimmo, R.; Siigur, J.; Kahru, A. Toxicity of antimony, copper, cobalt, manganese, titanium and zinc oxide nanoparticles for the alveolar and intestinal epithelial barrier cells in vitro. *Cytotechnology* **2016**, *68*, 2363–2377. [CrossRef]

32. Bierkandt, F.S.; Leibrock, L.; Wagener, S.; Laux, P.; Luch, A. The impact of nanomaterial characteristics on inhalation toxicity. *Toxicol. Res.* **2018**, *7*, 321–346. [CrossRef]

33. Lacroix, G.; Koch, W.; Ritter, D.; Gutleb, A.; Larsen, S.T.; Loret, T.; Zanetti, F.; Constant, S.; Chortarea, S.; Rothen-Rutishauser, B.; et al. Air–Liquid Interface In Vitro Models for Respiratory Toxicology Research: Consensus Workshop and Recommendations. *Appl. Vitr. Toxicol.* **2018**, *4*, 91–106. [CrossRef]

34. Polk, W.W.; Sharma, M.; Sayes, C.M.; Hotchkiss, J.A.; Clippinger, A.J. Aerosol generation and characterization of multi-walled carbon nanotubes exposed to cells cultured at the air-liquid interface. *Part. Fibre Toxicol.* **2015**, *13*, 20. [CrossRef]

35. Secondo, L.E.; Liu, N.J.; Lewinski, N.A. Methodological considerations when conducting in vitro, air–liquid interface exposures to engineered nanoparticle aerosols. *Crit. Rev. Toxicol.* **2017**, *47*, 225–262. [CrossRef]

36. Paur, H.-R.; Cassee, F.R.; Teeguarden, J.; Fissan, H.; Diabate, S.; Aufderheide, M.; Kreyling, W.G.; Hänninen, O.; Kasper, G.; Riediker, M.; et al. In-vitro cell exposure studies for the assessment of nanoparticle toxicity in the lung—A dialog between aerosol science and biology. *J. Aerosol Sci.* **2011**, *42*, 668–692. [CrossRef]

37. Ghio, A.J.; Dailey, L.A.; Soukup, J.M.; Stonehuerner, J.; Richards, J.H.; Devlin, R.B. Growth of human bronchial epithelial cells at an air-liquid interface alters the response to particle exposure. *Part. Fibre Toxicol.* **2013**, *10*, 25–28. [CrossRef]

38. Lenz, A.-G.; Karg, E.; Brendel, E.; Hinze-Heyn, H.; Maier, K.L.; Eickelberg, O.; Stoeger, T.; Schmid, O. Inflammatory and Oxidative Stress Responses of an Alveolar Epithelial Cell Line to Airborne Zinc Oxide Nanoparticles at the Air-Liquid Interface: A Comparison with Conventional, Submerged Cell-Culture Conditions. *BioMed Res. Int.* **2013**, *2013*, 652632. [CrossRef]

39. Medina-Reyes, E.I.; Delgado-Buenrostro, N.L.; Leseman, D.L.; Déciga-Alcaraz, A.; He, R.; Gremmer, E.R.; Fokkens, P.H.; Flores-Flores, J.O.; Cassee, F.R.; Chirino, Y.I. Differences in cytotoxicity of lung epithelial cells exposed to titanium dioxide nanofibers and nanoparticles: Comparison of air-liquid interface and submerged cell cultures. *Toxicol. Vitr.* **2020**, *65*, 104798. [CrossRef]

40. Panas, A.; Comouth, A.; Saathoff, H.; Leisner, T.; Al-Rawi, M.; Simon, M.; Seemann, G.; Dössel, O.; Mülhopt, S.; Paur, H.-R.; et al. Silica nanoparticles are less toxic to human lung cells when deposited at the air–liquid interface compared to conventional submerged exposure. *Beilstein J. Nanotechnol.* **2014**, *5*, 1590–1602. [CrossRef]

41. Braakhuis, H.M.; He, R.; Vandebriel, R.J.; Gremmer, E.R.; Zwart, E.; Vermeulen, J.P.; Fokkens, P.; Boere, J.; Gosens, I.; Cassee, F.R. An Air-liquid Interface Bronchial Epithelial Model for Realistic, Repeated Inhalation Exposure to Airborne Particles for Toxicity Testing. *J. Vis. Exp.* **2020**, *159*, e61210. [CrossRef]

42. Bessa, M.J.; Brandão, F.; Querido, M.M.; Costa, C.; Pereira, C.C.; Valdiglesias, V.; Laffon, B.; Carriere, M.; Teixeira, J.P.; Fraga, S. Optimization of the harvesting and freezing conditions of human cell lines for DNA damage analysis by the alkaline comet assay. *Mutat. Res. Toxicol. Environ. Mutagen.* **2019**, *845*, 402994. [CrossRef]

43. Martens, K.; Hellings, P.W.; Steelant, B. Calu-3 epithelial cells exhibit different immune and epithelial barrier responses from freshly isolated primary nasal epithelial cells in vitro. *Clin. Transl. Allergy* **2018**, *8*, 40. [CrossRef]

44. Tabei, Y.; Sonoda, A.; Nakajima, Y.; Biju, V.; Makita, Y.; Yoshida, Y.; Horie, M. In vitro evaluation of the cellular effect of indium tin oxide nanoparticles using the human lung adenocarcinoma A549 cells. *Metallomics* **2015**, *7*, 816–827. [CrossRef]

45. Demokritou, P.; Gass, S.; Pyrgiotakis, G.; Cohen, J.M.; Goldsmith, W.; McKinney, W.; Frazer, D.; Ma, J.; Schwegler-Berry, D.; Brain, J.; et al. An in vivo and in vitro toxicological characterization of realistic nanoscale CeO$_2$ inhalation exposures. *Nanotoxicology* **2012**, *7*, 1338–1350. [CrossRef]

46. Kroll, A.; Dierker, C.; Rommel, C.; Hahn, D.; Wohlleben, W.; Schulze-Isfort, C.; Göbbert, C.; Voetz, M.; Hardinghaus, F.; Schnekenburger, J. Cytotoxicity screening of 23 engineered nanomaterials using a test matrix of ten cell lines and three different assays. *Part. Fibre Toxicol.* **2011**, *8*, 9. [CrossRef]

47. Park, B.; Donaldson, K.; Duffin, R.; Tran, L.; Kelly, F.; Mudway, I.; Morin, J.-P.; Guest, R.; Jenkinson, P.; Samaras, Z.; et al. Hazard and Risk Assessment of a Nanoparticulate Cerium Oxide-Based Diesel Fuel Additive—A Case Study. *Inhal. Toxicol.* **2008**, *20*, 547–566. [CrossRef]

48. Kim, I.-S.; Baek, M.; Choi, S.-J. Comparative cytotoxicity of Al2O3, CeO2, TiO2 and ZnO nanoparticles to human lung cells. *J. Nanosci. Nanotechnol.* **2010**, *10*, 3453–3458. [CrossRef]

49. De Marzi, L.; Monaco, A.; De Lapuente, J.; Ramos, D.; Borras, M.; Di Gioacchino, M.; Santucci, S.; Poma, A. Cytotoxicity and Genotoxicity of Ceria Nanoparticles on Different Cell Lines in Vitro. *Int. J. Mol. Sci.* **2013**, *14*, 3065–3077. [CrossRef]

50. Mittal, S.; Pandey, A.K. Cerium Oxide Nanoparticles Induced Toxicity in Human Lung Cells: Role of ROS Mediated DNA Damage and Apoptosis. *BioMed Res. Int.* **2014**, *2014*, 891934. [CrossRef]

51. Bessa, M.J.; Brandão, F.; Fokkens, P.; Cassee, F.R.; Salmatonidis, A.; Viana, M.; Vulpoi, A.; Simon, S.; Monfort, E.; Teixeira, J.P.; et al. Toxicity assessment of industrial engineered and airborne process-generated nanoparticles in a 3D human airway epithelial in vitro model. *Nanotoxicology* **2021**, *15*, 542–557. [CrossRef]

52. Diabaté, S.; Armand, L.; Murugadoss, S.; Dilger, M.; Fritsch-Decker, S.; Schlager, C.; Béal, D.; Arnal, M.-E.; Biola-Clier, M.; Ambrose, S.; et al. Air–Liquid Interface Exposure of Lung Epithelial Cells to Low Doses of Nanoparticles to Assess Pulmonary Adverse Effects. *Nanomaterials* **2020**, *11*, 65. [CrossRef]

53. Ji, J.; Hedelin, A.; Malmlöf, M.; Kessler, V.; Seisenbaeva, G.; Gerde, P.; Palmberg, L. Development of Combining of Human Bronchial Mucosa Models with XposeALI®for Exposure of Air Pollution Nanoparticles. *PLoS ONE* **2017**, *12*, e0170428. [CrossRef]

54. Drasler, B.; Sayre, P.; Steinhäuser, K.G.; Fink, A.; Rothen-Rutishauser, B. In vitro approaches to assess the hazard of nanomaterials. *NanoImpact* **2017**, *8*, 99–116. [CrossRef]

B.4. Toxicity assessment of industrial engineered and airborne process-generated nanoparticles in a 3D human airway epithelial *in vitro* model

Bessa M. J., Brandão F., Fokkens P., Cassee F. R., Salmatonidis A., Viana M., Vulpoi A., Simon S., Monfort E., Teixeira J. P., & Fraga S.

The PhD candidate contributed for the methodology, investigation, formal analysis and writing of the manuscript.

Taylor & Francis
Taylor & Francis Group

ARTICLE

Check for updates

Toxicity assessment of industrial engineered and airborne process-generated nanoparticles in a 3D human airway epithelial *in vitro* model

Maria João Bessa[a,b,c] (ID), Fátima Brandão[a,b,c] (ID), Paul Fokkens[d], Flemming R. Cassee[d,e] (ID), Apostolos Salmatonidis[f,g] (ID), Mar Viana[f] (ID), Adriana Vulpoi[h] (ID), Simion Simon[h], Eliseo Monfort[i] (ID), João Paulo Teixeira[a,b] (ID) and Sónia Fraga[a,b] (ID)

[a]Departamento de Saúde Ambiental, Instituto Nacional de Saúde Doutor Ricardo Jorge, Porto, Portugal; [b]EPIUnit-Instituto de Saúde Pública, Universidade do Porto, Porto, Portugal; [c]Instituto de Ciências Biomédicas Abel Salazar (ICBAS), Universidade do Porto, Porto, Portugal; [d]National Institute for Public Health and Environment (RIVM), Bilthoven, The Netherlands; [e]Institute for Risk Assessment Sciences (IRAS), Utrecht, The Netherlands; [f]Institute of Environmental Assessment and Water Research, Spanish Research Council (IDAEA-CSIC), Barcelona, Spain; [g]LEITAT Technological Center, Barcelona, Spain; [h]Nanostructured Materials and Bio-Nano-Interfaces Center, Interdisciplinary Research Institute on Bio-Nano-Sciences, Babes-Bolyai University, Cluj-Napoca, Romania; [i]Institute of Ceramic Technology (ITC), Universitat Jaume I, Castellón, Spain

ABSTRACT

The advanced ceramic technology has been pointed out as a potentially relevant case of occupational exposure to nanoparticles (NP). Not only when nanoscale powders are being used for production, but also in the high-temperature processing of ceramic materials there is also a high potential for NP release into the workplace environment. *In vitro* toxicity of engineered NP (ENP) [antimony tin oxide ($Sb_2O_3 \bullet SnO_2$; ATO); zirconium oxide (ZrO_2)], as well as process-generated NP (PGNP), and fine particles (PGFP), was assessed in MucilAir™ cultures at air–liquid interface (ALI). Cultures were exposed during three consecutive days to varying doses of the aerosolized NP. General cytotoxicity [lactate dehydrogenase (LDH) release, WST-1 metabolization], (oxidative) DNA damage, and the levels of pro-inflammatory mediators (IL-8 and MCP-1) were assessed. Data revealed that ENP (5.56 µg ATO/cm^2 and 10.98 µg ZrO$_2$/cm^2) only caused mild cytotoxicity at early timepoints (24 h), whereas cells seemed to recover quickly since no significant changes in cytotoxicity were observed at late timepoints (72 h). No meaningful effects of the ENP were observed regarding DNA damage and cytokine levels. PGFP affected cell viability at dose levels as low as ∼9 µg/cm^2, which was not seen for PGNP. However, exposure to PGNP (∼4.5 µg/cm^2) caused an increase in oxidative DNA damage. These results indicated that PGFP and PGNP exhibit higher toxicity potential than ENP in mass per area unit. However, the presence of a mucociliary apparatus, as it occurs *in vivo* as a defense mechanism, seems to considerably attenuate the observed toxic effects. Our findings highlight the potential hazard associated with exposure to incidental NP in industrial settings.

1. Introduction

Nanotechnology has enabled many industrial advances through the creation and development of processes and nanoscale materials with innovative physicochemical properties that are revolutionizing different fields such as electronics, optics, food industry, biomedicine, among others (De Jong and Borm 2008; Tran and Webster 2010; Jariwala et al. 2013; Thiruvengadam, Rajakumar, and Chung 2018). In this context, the demand for advanced ceramic materials, especially nano-sized ones, is also a growing trend that is benefitting from advances made available through nanotechnology and innovative industrial processes. Many ceramic nanomaterials (NM) are currently being used as raw materials for different purposes that include nanosized clays for nanocomposites and inks; metal and metal oxide nanoparticles (NP) for high-performance ceramic coatings (e.g. titanium dioxide [TiO_2], zirconium dioxide (ZrO_2), and antimony tin oxide [ATO; $Sb_2O_3 \bullet SnO_2$]), polishing agents [e.g. alumina (Al_2O_3) and ceria (CeO_2)] and insulators (e.g. silica

179

[SiO$_2$]) (Bessa et al. 2020). In addition, several processes employing ceramic materials have the potential to generate and release incidental fine (<2.5 μm mass median aerodynamic diameter [MMAD]) and ultrafine particles (<0.250 μm MMAD) into the air, potentially exposing workers to micro-sized matter (Monfort et al. 2014; Ribalta et al. 2019a, 2019b). There are already a few studies in the literature reporting occupational exposure to nano-sized airborne particles emitted when ceramic materials are processed with very different technologies and applications, mainly at high temperature, for instance during ceramics firing (Voliotis et al. 2014), laser-based surface treatment of ceramic tiles (Fonseca et al. 2015a, 2015b; Fonseca et al. 2016; Salmatonidis et al. 2018a, 2018b; Salmatonidis et al. 2019) and thermal spraying of ceramic coatings on metals (Viana et al. 2017; Salmatonidis et al. 2018a; Salmatonidis et al. 2020). In this regard, Salmatonidis et al. monitored particle emissions along with exposure quantification during two different types of thermal spraying of ceramic coatings onto metallic surfaces, namely atmospheric plasma spraying (APS) and high-velocity oxy-fuel spraying (HVOF) (Salmatonidis et al. 2018a). The authors reported high particle number concentrations (>10^6 particles/cm^3) inside the thermal spraying booths. These findings indicate the great need for information on the potential harmful effects of workplace exposure to intentionally employed and/or process-generated nanoparticles (PGNP).

Nowadays, there are numerous in vitro lung models that can be used to assess the toxicity of inhaled agents, ranging from more traditional and simple monoculture models to more advanced systems such as 3D organotypic, organoid, and lung-on-chip cultures (Miller and Spence 2017; Faber and Mccullough 2018). Balogh Sivars et al. demonstrated that MucilAir™ is a reliable and predictive model for in vivo respiratory response either too toxic (e.g. salmeterol free base) or nontoxic drugs (e.g. budesonide) (Balogh Sivars et al. 2018). Most of these studies were carried out under submerged conditions, i.e. test compound solutions are applied in the apical and/or basolateral compartment. However, air–liquid interface (ALI) exposures, where the test compound is delivered as an aerosol, are increasingly being recognized as a more relevant and realistic exposure scenario to assess inhalation

toxicity (Paur et al. 2011; Lacroix et al. 2018). Moreover, ALI exposure is particularly advantageous since it allows for a more accurate dose delivery allied with a high degree of preservation of NP intrinsic physicochemical properties (Paur et al. 2011; Lacroix et al. 2018).

This study aimed to compare the in vitro toxicity of two types of engineered nanoparticles (ENP) used in advanced ceramics as raw materials – ATO and ZrO$_2$ NP, with PGNP and fine particles (PGFP) released and collected during HVOF spraying at an industrial facility (Salmatonidis et al. 2018a). Considering the complex composition of HVOF-generated particles, we hypothesized that they would be more hazardous to human bronchial epithelium cells than ENP. To test our hypothesis, MucilAir™ bronchial epithelial cultures from healthy donors were exposed for three consecutive days to different doses of aerosolized ENP and HVOF-generated NP and fine particles in a Vitrocell® Cloud 12 exposure system and tested for alterations in barrier integrity, cyto- and genotoxicity, and inflammatory response.

2. Materials and methods

2.1. Chemicals and reagents

Dimethyl sulfoxide (DMSO), sodium hydroxide (NaOH), sodium chloride (NaCl), and potassium chloride (KCl) were obtained from Merck KGaA (Darmstadt, Germany). Tris base and disodium salt dihydrate (Na$_2$EDTA) were supplied from Merck Millipore (Madrid, Spain). Water TraceSELECT™ Ultra, Triton X-100, bovine serum albumin (BSA), low melting point (LMP) agarose, Tris–hydrochloride (Tris–HCl), 4-(2-Hydroxyethyl)piperazine-1-ethanesulfonic acid, N-(2-Hydroxyethyl)piperazine-N′-(2-ethanesulfonic acid) (HEPES), and lipopolysaccharide (LPS) were brought from Sigma-Aldrich (St Louis, MO). Normal melting point (NMP) agarose was purchased from Bioline (London, UK). Formamidopyrimidine-DNA glycosylase (FPG) enzyme was obtained from New England Biolabs (Ipswich, MA). Invitrogen™ SYBR® Gold stain was bought from Thermo Fisher Scientific (Madrid, Spain).

2.2. Nanoparticle suspension, aerosol generation, and characterization

ATO and ZrO_2 NP suspensions were obtained from Keeling & Walker (Stoke-on-Trent, UK) and Sigma-Aldrich (Madrid, Spain), respectively. Incidental PGFP and PGNP emitted during HVOF were collected directly from the inside of the spraying booths at an industrial-scale precision engineering workshop during injection of a tungsten carbide (WC)– nickel (Ni)–chromium (Cr) blend as described in (Salmatonidis et al. 2018a). Airborne PGFP and PGNP fractions were sampled directly as liquid suspensions for toxicity testing, using an aerosol concentration enrichment system (VACES), as previously described (Kim et al. 2001). All particle suspensions under study were subjected to gamma-ray irradiation to ensure the required sterility for *in vitro* toxicity testing. Moreover, these were dispersed by indirect probe sonication using a Branson sonifier (model 450) equipped with a disruptor cup horn according to the standard operation procedure (SOP) for preparation of NP suspensions developed within the NanoToxClass project (Nanotoxclass 2017). For ALI exposures, all (nano)particle suspensions were aerosolized using a Vitrocell® Cloud 12 system. The generated aerosols were collected in grids for characterization by Transmission Electron Microscopy (TEM) analysis and Energy Dispersive X-Ray Spectroscopy (EDS), using a Tecnai F20 XTWIN field emission, high-resolution transmission electron microscope operating at an accelerating voltage of 200 kV, equipped with Eagle 4k CCD camera and an EDX detector.

2.3. MucilAir™ cultures

In this study, primary cultures from upper airway epithelium were chosen for *in vitro* toxicity testing based on the expected particle size range. Thus, fully differentiated MucilAir™ bronchial epithelial cultures from three healthy male Caucasian donors (donor #1: 15-year-old, nonsmoker, donor #2: 30-year-old, smoker, and donor #3: 58-year-old, smoker) were purchased from Epithelix Sárl (Geneva, Switzerland). Cultures were grown onto Transwell® inserts (polyester, 12 mm, 0.4 µm pore size, Corning, MA) in MucilAir™ serum-free culture medium (Epithelix Sárl, Geneva, Switzerland)

supplemented with 50 U/mL penicillin and 50 µg/mL streptomycin, and maintained in a humidified atmosphere with 5% CO_2 at 37 °C under ALI conditions. Upon receipt, cultures were allowed to stabilize for 1 week prior to performing the experiments. Cell culture medium in the basolateral compartment was changed every 2–3 d. The apical side was washed with a saline solution (NaCl 0.9%) containing 10 mM HEPES and 1.25 mM $CaCl_2$ once week and 24 h prior to exposure, to remove mucus and surface dead cells, as recommended by the supplier.

2.4. MucilAir™ aerosol exposure

The basolateral culture medium was refreshed 24 h before the first exposure (E1). Cultures were exposed (∼5 min) for three consecutive days (E1, E2, and E3) to three concentrations of aerosolized particles using a Vitrocell® Cloud 12 exposure system (Figure 1). This system is equipped with a nebulizer, an exposure chamber, and a quartz crystal microbalance (QCM) that allows real-time deposited dose monitoring. Direct dilutions of the stock particle suspensions were prepared in ultra-trace H_2O. For aerosolization, 200 µL of each test suspension containing 1% (v/v) of saline solution (0.9% NaCl) were added to the nebulizer. MucilAir™ cultures exposed to dispersant (1% saline solution in ultra-trace H_2O) (exposure control; Exp. Ct) or kept inside the incubator (5% CO_2 at 37 °C) (incubator control; Inc. Ct) served as controls. Aerosolized crystalline Dörentruper Quartz (DQ12; ≤5 µm) was employed as a positive pro-inflammatory particle control (Clouter et al. 2001). After exposure, the basolateral medium was refreshed, and cultures returned to the incubator. Table 1 shows the single (per day) and total deposited doses achieved for each test aerosol.

2.5. Transepithelial electrical resistance (TEER)

Transepithelial electrical resistance (TEER) was measured with an EVOM2 voltohmmeter (WPI, UK) at 24 h before the initial exposure (E1) and at 24 h after the last exposure (E3) to assess changes in cell permeability. Briefly, Transwell® inserts were transferred to a test plate with 1.4 mL/well of saline solution containing 10 mM HEPES and 1.25 mM $CaCl_2$
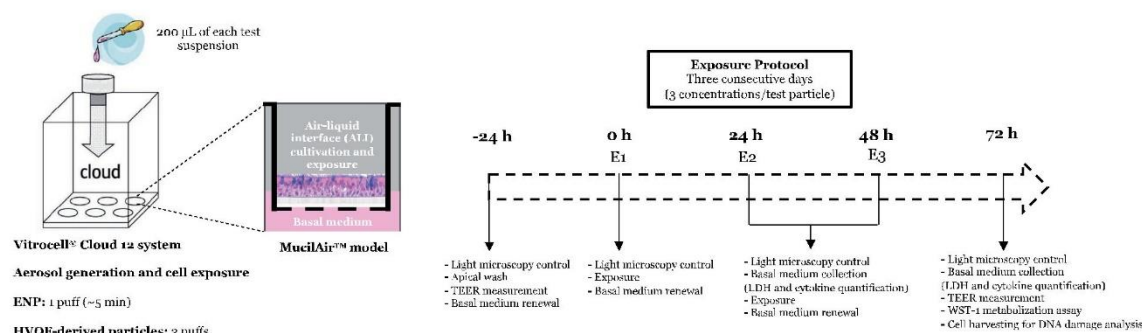
Figure 1. Scheme of the experimental protocol. MucilAir™ cultures under air–liquid interface (ALI) conditions were exposed for three consecutive days (E1, E2, and E3) to the test aerosols in the VitroCell™ Cloud 12 system. At 24 h before the initial exposure (E1) and at 24 h after the last exposure (E3), the transepithelial electrical resistance (TEER) was measured. As depicted, samples for cytotoxicity (LDH release and WST-1 metabolization), genotoxicity (DNA damage), and inflammatory response assessment (cytokine measurements) were collected at different timepoints (24, 48, and 72 h).

and 600 μL of the same solution were added to the apical compartment. The electrode tips were immersed in the apical and basolateral solution avoiding contact with cells and the resistance (Ω) was measured. The resistance means value of a 'blank' insert (without cells) (~135 Ω) was subtracted from the measured values, the obtained values normalized to the insert area (1.12 cm^2) and expressed as Ω·cm^2.

2.6. General toxicity assessment

2.6.1. Lactate dehydrogenase (LDH) assay

Lactate dehydrogenase (LDH) release was determined in the basolateral medium at 24, 48, and 72 h using the LDH Cytotoxicity Detection Kit (Roche, Mannheim, Germany), according to the manufacturer's instructions. Cells lysed with 2% Triton X-100 were used as positive controls (PC). Briefly, 100 μL of freshly prepared reaction mixture was added to 100 μL of each sample and incubated for 20 min at room temperature and protected from light. Absorbance was measured at 490 and 690 nm (reference wavelength) in a microplate reader (Spectramax M2 Molecular Devices, San Jose, CA). LDH release values were normalized considering the PC mean value (total LDH release).

2.6.2. WST-1 metabolization assay

Metabolic activity was assessed using the Cell Proliferation Reagent WST-1 (Roche, Mannheim, Germany) at 72 h. Cell incubated for 30 min with 70% ethanol served as PC. Briefly, 500 μL of WST-1

Table 1. Single (per exposure) and total average deposition (μg/cm^2) of the tested engineered nanoparticles (ENP; antimony-tin oxide [Sb$_2$O$_3$•SnO$_2$; ATO], and zirconium oxide [ZrO$_2$]), high-velocity oxygen fuel spraying (HVOF)-generated PGFP and PGNP] and Dörentruper Quartz (DQ12; ≤5 μm) as measured by the quartz crystal microbalance (QCM).

Particle suspension concentration (mg/mL)	Mean deposited dose (μg/cm^2/exposure)	Total deposited dose (μg/cm^2)
ENP		
ATO (10.00)		
Dose 1	2.45 ± 1.11	7.34
Dose 2	5.56 ± 0.93	16.67
Dose 3	26.00 ± 3.27	78.00
ZrO$_2$ (10.00)		
Dose 1	5.36 ± 0.46	16.09
Dose 2	10.98 ± 0.93	32.94
Dose 3	49.21 ± 8.90	147.62
HVOF-derived		
PGFP (1.07)		
Dose 1	~1	~3
Dose 2	~2	~6
Dose 3	~3	~9
PGNP (0.14)		
Dose 1	~0.5	~1.5
Dose 2	~1	~3
Dose 3	~1.5	~4.5
Positive control		
DQ12 (1.00)		
Dose 1	0.47 ± 0.05	1.41

reagent diluted 1:10 in serum-free culture medium was added to the apical compartment and cultures incubated for 30 min at 37 °C, 5% CO$_2$. One hundred microliters were transferred to a 96 well plate and absorbance read at 450 and 650 nm (reference wavelength), in a microplate reader (Spectramax M2, Molecular Devices, San Jose, CA). WST-1 reduction values were normalized considering the incubator control mean value.

2.7. Genotoxicity assessment

2.7.1. Alkaline and enzyme-modified comet assay

Primary and oxidative DNA damage of MucilAir™ cultures were assessed at 72 h by the standard alkaline and FPG-modified comet assay versions, respectively. Cells were gently scrapped in cryoprotective medium (90% MucilAir™ culture medium, 10% DMSO), transferred to a microcentrifuge tube and frozen at −80 °C until analysis. Frozen samples were thawed at 37 °C, centrifuged at 700 g for 5 min (Universal 320, Hettich, Tuttlingen, Germany) and the pellet resuspended in PBS pH 7.4. Cells were counted in a Neubauer's chamber and 6.0×10^3 cells were transferred to a microcentrifuge tube and centrifuged at 700 g for 5 min. Supernatant was removed and cells were resuspended in 100 μL of 1% LMP agarose. Five microliters were placed onto microscope slides precoated with 1% NMP, using a high-throughput system of 12-minigel comet assay unit (Severn Biotech Ltd®, Kidderminster, UK). Three slides were prepared, one for the standard alkaline comet assay and two for the enzyme-modified version (with or without FPG-enzyme), and duplicates of each sample were added to each slide. The alkaline comet assay procedure was performed as previously described (Bessa et al. 2019). After agarose solidification at 4 °C for 5 min, slides were immersed in ice-cold lysis solution (2.5 M NaCl, 100 mM Na$_2$EDTA, 10 mM Tris-base, 10 M NaOH, pH 10, 1% Triton-X 100) during 1 h at 4 °C, protected from light. After lysis, FPG-modified comet assay slides were washed three times for 5 min with buffer F (0.1 M KCl, 0.5 mM Na$_2$EDTA, 40 mM HEPES, 0.2 mg/mL BSA, pH 8) prior incubation for 30 min at 37 °C with 2.7 U/mL of FPG enzyme or with buffer F alone. After incubation, FPG and buffer F slides were washed with PBS pH 7.4. The alkaline comet assay slides were washed three times with PBS pH 7.4 for 5 min. For DNA unwinding, all slides were immersed in electrophoresis solution (1 mM Na$_2$EDTA, 0.3 M NaOH, pH 13) for 40 min at 4 °C, followed by electrophoresis in the same solution for 30 min at constant 25 V (0.9 V/cm) and 400 mA. At the end of electrophoresis, slides were neutralized and fixed as described elsewhere (Bessa et al. 2019). For the comet scoring, slides were initially hydrated in Tris-EDTA (TE) buffer (10 mM Tris–HCl, 1 mM Na$_2$EDTA, pH 7.5–8) and then stained with 1:10 000 dilution of SYBR® Gold in TE buffer for 40 min at room temperature. Comets were visualized in a Motic BA410 ELITE series microscope equipped with a complete EPI-fluorescence kit and scored using the Comet Assay IV image analysis software (Perceptive Instruments, Staffordshire, UK). At least 100 cells/experimental group (50 in each replicate gel) were scored and the mean of the percentage of DNA in the comet tail (% tail intensity) was used as a DNA damage descriptor.

2.8. Inflammatory responses: IL-8 and MCP-1 levels

The release of human interleukin-8 (IL-8) and monocyte chemoattractant protein-1 (MCP-1) pro-inflammatory mediators was quantified in the basolateral media at 72 h using enzyme-linked immunosorbent assays (ELISA) kits (Invitrogen™, Thermo Fisher Scientific, Viena, Austria), according to the manufacturer's instructions. Cultures exposed to aerosolized DQ12 or incubated with 10 μg/mL LPS for 24 h served as PC.

2.9. Statistical analysis

Statistical analysis was performed using SPSS version 26.0 (Armonk, NY) and GraphPad Prism version 6.0 (San Diego, CA) statistical software. Experimental data were expressed as mean ± standard deviation (SD). Data were tested for normality and homogeneity of variances by Shapiro–Wilk and Levene's tests, respectively. To meet these assumptions, mathematical transformations (e.g. logarithmic) were attempted whenever necessary. For each assessed timepoint, differences between tested doses and controls (incubation and exposure controls) were estimated using a one-way analysis of variance (ANOVA) followed by post-hoc Dunnett's test for multiple comparisons. A two-way ANOVA followed by HSD Tukey test was performed to test the effect of time and dose in variation of IL-8 and MCP-1 levels. A p value < 0.05 was considered significant.

3. Results

3.1. Aerosol characterization and deposition

Liquid suspensions of the tested ENP and HVOF-derived particles (PGFP and PGNP) were successfully aerosolized using a VitroCell® Cloud 12 system. Analysis of the generated aerosols collected on TEM grids showed that ENP exhibited a spheroidal shape. A bimodal size distribution with mean values of 16.8 ± 2.4 and 92.4 ± 2.7 nm was observed for ATO NP samples, consistent with its high polydispersity index (PI) value of 0.81 (Figure 2(A)), while ZrO_2 NP aerosols exhibited a monomodal size distribution with a mean value of 18 ± 0.3 nm (Figure 2(B)). Regarding HVOF aerosols, mean particle sizes of 9.1 ± 0.3 and 57.3 ± 1.4 nm were obtained for PGFP (Figure 2(C)), while for PGNP aerosols three peaks corresponding to mean sizes of 10.2 ± 0.3, 20.3 ± 2.8, and 79.0 ± 0.9 nm have been detected (Figure 2(D)). As expected, EDS spectra of the ENP aerosols revealed that their chemical composition were in good agreement with that reported in the ENP suspensions technical specification sheets. On the other hand, PGFP aerosols were mainly constituted by W and Cr, while aerosolized PGNP were composed of Ni and Cr, evidencing that the particles sourced from the feedstock used in the thermal spraying processes, as reported elsewhere (Salmatonidis et al. 2018a).

Table 1 shows that average single doses for ATO NP ranged between 2.45 and $26 \mu g/cm^2$, while for ZrO_2 NP values of $5.36-49.21 \mu g/cm^2$ were achieved. In turn, the low concentrations and chemical nature of the stock suspensions of both fractions of HVOF-generated particles did not allow an accurate determination of the deposited dose, thus the values shown are approximate values. Moreover, exposure to aerosolized DQ12 resulted in an average deposited dose of $0.47 \pm 0.05 \mu g/cm^2$.

3.2. TEER measurements

TEER values obtained before exposure of all MucilAir™ cultures used for cytotoxicity and genotoxicity experiments are shown in Table 2. As shown, TEER mean values of MucilAir™ cultures derived from donor #3 (1128.63 ± 22.03 $\Omega \cdot cm^2$; $n = 27$) were significantly higher ($p < 0.0001$) compared to the primary bronchial cultures established

from donor #1 (828.30 ± 9.66 $\Omega \cdot cm^2$; $n = 30$) and donor #2 (810.14 ± 9.64 $\Omega \cdot cm^2$; $n = 47$). These TEER values are indicative of fully differentiated cultures with well-developed tight junctions. Upon exposure, no significant changes in TEER values as compared to the respective control cultures were observed for any tested aerosolized ENP or HVOF-derived particles, at any tested dose (Table 2).

3.3. Cytotoxicity

Two cytotoxicity endpoints were determined at different timepoints: plasma membrane integrity using the LDH release assay (at 24, 48, and 72 h) and cellular metabolic activity by the WST-1 reduction test (at 72 h after E1). A significant increase in LDH leakage was observed in ATO NP-exposed cultures (donor #3) for 24 h to 10.98 $\mu g/cm^2$ (Dose 2; 1.08 ± 0.19) (Figure 3(A)), while in primary bronchial cultures (donor #1) exposed to the aerosolized ZrO_2 NP (5.6 $\mu g/cm^2$/per exposure; Dose 2) this effect has been detected both at 24 h (0.88 ± 0.25) and 48 h (0.82 ± 0.10) (Figure 3(B)). Moreover, no significant changes upon cell metabolic activity were detected at 72 h in both ENP-exposed cultures (Figure 3(A,B)). Regarding the airborne HVOF particles, exposure to the aerosolized PGFP fraction failed to affect plasma membrane integrity of the MucilAir™ cultures (donor #2) as evaluated by the LDH release (Figure 3(C)). However, at 72 h (~9 $\mu g/cm^2$; Dose 3) a significant decrease in cellular metabolic activity ($62.17 \pm 11.62\%$ of control) in human bronchial epithelium exposed cultures compared to the control cultures was observed, as assessed by the WST-1 assay (Figure 3(C)). On the other hand, MucilAir™ cultures exposed to the lowest tested dose of the aerosolized PGNP exhibited a significant increase in LDH release only visible at 24 h (~0.5 $\mu g/cm^2$; Dose 1), whereas no changes in the metabolic activity were detected (Figure 3(D)).

3.4. Genotoxicity

As shown in Figure 4(A), no significant alterations of primary (strand breaks) and oxidative (FPG-sensitive sites) DNA damage levels were detected following exposure to the ATO and ZrO_2 NP aerosols compared to the controls. Regarding the HVOF-generated particles, cultures exposed to the PGNP
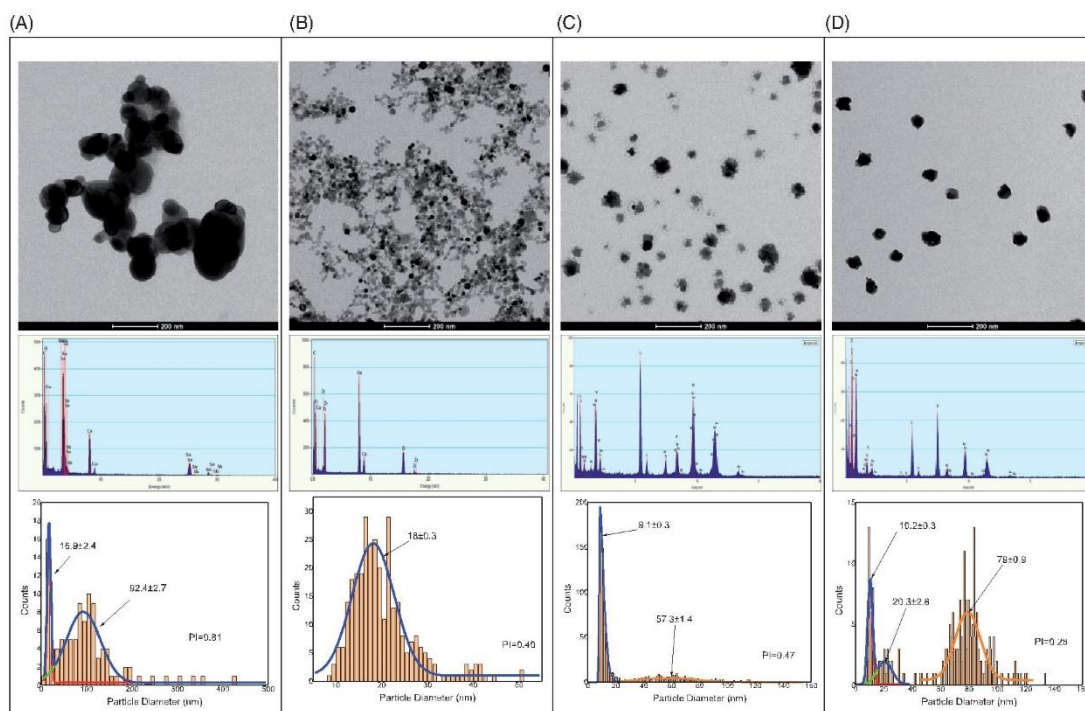
Figure 2. Representative TEM images (scale bar 200 nm), EDS spectra, and size distribution histograms of the generated aerosols. Antimony-tin oxide ($Sb_2O_3\bullet SnO_2$; ATO) NP (A), zirconium oxide (ZrO_2) NP (B) and high-velocity oxygen fuel (HVOF)-derived PGFP (C) and PGNP (D). PI: polydispersity index.

fraction aerosols exhibited increased levels of FPG-sensitive sites (Dose 3; $22.25 \pm 0.77\%$ tail intensity) compared to the incubator (15.66 ± 1.96) and exposure (15.05 ± 2.05) controls, though the differences were not significant (Figure 4(B)). Similar findings were detected for DNA strand break levels of PGNP-exposed cultures. On the other hand, exposure to the PGFP aerosols did not seem to affect DNA integrity of the human bronchial cultures. A pronounced DNA damage in relation to control was observed in cells exposed to the PC (1 mM H_2O_2, 30 min), which was not possible to quantify using the comet image analysis software (data not shown).

3.5. Cytokine release

The inflammatory response of MucilAir™ cultures after exposure to the aerosolized ENP and HVOF particles was investigated by quantifying the levels of pro-inflammatory IL-8 and MCP-1 cytokines in the basolateral media at 24, 48, and 72 h. Figure 5(A,B) shows the levels of IL-8 and MCP-1 (ng/mL) released by MucilAir™ cultures following exposure

Table 2. Transepithelial electrical resistance ($\Omega\cdot cm^2$) values of MucilAir™ cultures derived from different donors, at 24 h before initial exposure and at 24 h after the last exposure to the test aerosols.

Test aerosol	Experimental group	TEER ($\Omega\cdot cm^2$)
ATO (donor #3)	Before exposure	1128.63 ± 22.03[****]
	After exposure	
	Inc. Ct	1120.39 ± 12.30
	Exp. Ct	1160.29 ± 13.19
	Dose 1	1124.99 ± 19.86
	Dose 2	1128.76 ± 13.71
	Dose 3	1114.48 ± 9.94
ZrO2 (donor #1)	Before exposure	828.30 ± 9.66
	After exposure	
	Inc. Ct	834.94 ± 10.90
	Exp. Ct	844.79 ± 16.34
	Dose 1	877.13 ± 11.84
	Dose 2	872.86 ± 13.24
	Dose 3	823.11 ± 27.05
HVOF-derived (donor #2)	Before exposure	810.14 ± 9.64
	After exposure	
	Inc. Ct	854.44 ± 15.10
	Exp. Ct	880.65 ± 6.24
	PGFP Dose 1	893.22 ± 30.81
	PGFP Dose 2	934.44 ± 21.76
	PGFP Dose 3	885.97 ± 14.77
	PGNP Dose 1	847.00 ± 44.48
	PGNP Dose 2	852.50 ± 44.73
	PGNP Dose 3	891.75 ± 26.93

HVOF: high-velocity oxy-fuel spraying; Inc. Ct: Incubator control; Exp. Ct: Exposure control; PGFP: process-generated fine particles; PGNP: process-generated nanoparticles.
Data are expressed as mean ± SD.
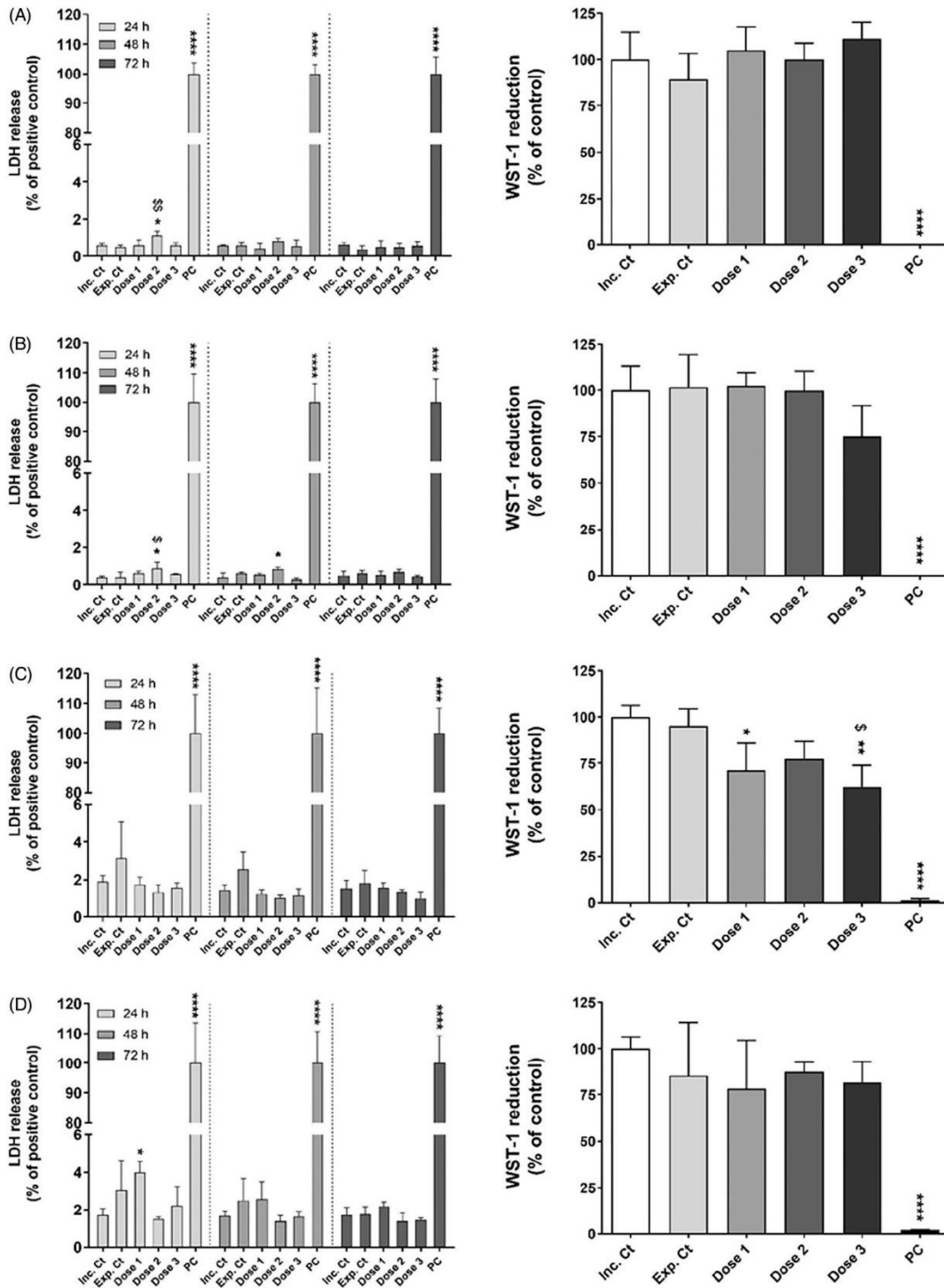[****]$p < 0.0001$ vs. donor#1 and donor#2 values before exposure.

Figure 3. Cytotoxicity of the aerosolized particles under study in polarized 3D human bronchial epithelial MucilAir™ cultures under air–liquid interface (ALI) conditions. Cultures were exposed three consecutive days to aerosolized antimony-tin oxide ($Sb_2O_3 \bullet SnO_2$; ATO) NP (A), zirconium oxide (ZrO_2) NP (B) and to the airborne PGFP (C) and PGNP (D) released during high-velocity oxygen-fuel spraying (HVOF). Lactate dehydrogenase release (LDH) was assessed at 24, 48, and 72 h after the initial exposure, while WST-1 reduction was evaluated only at 72 h. Data were analyzed by the one-way analysis of variance (ANOVA) test followed by Dunnett's *post hoc* test for multiple comparisons. $*p < 0.05$ and $****p < 0.0001$ *vs.* Inc. Ct; $^\$p < 0.05$ and $^{\$\$}p < 0.01$ *vs.* Exp. Ct. Inc. Ct: Incubator control; Exp. Ct: Exposure control; PC: Positive control.
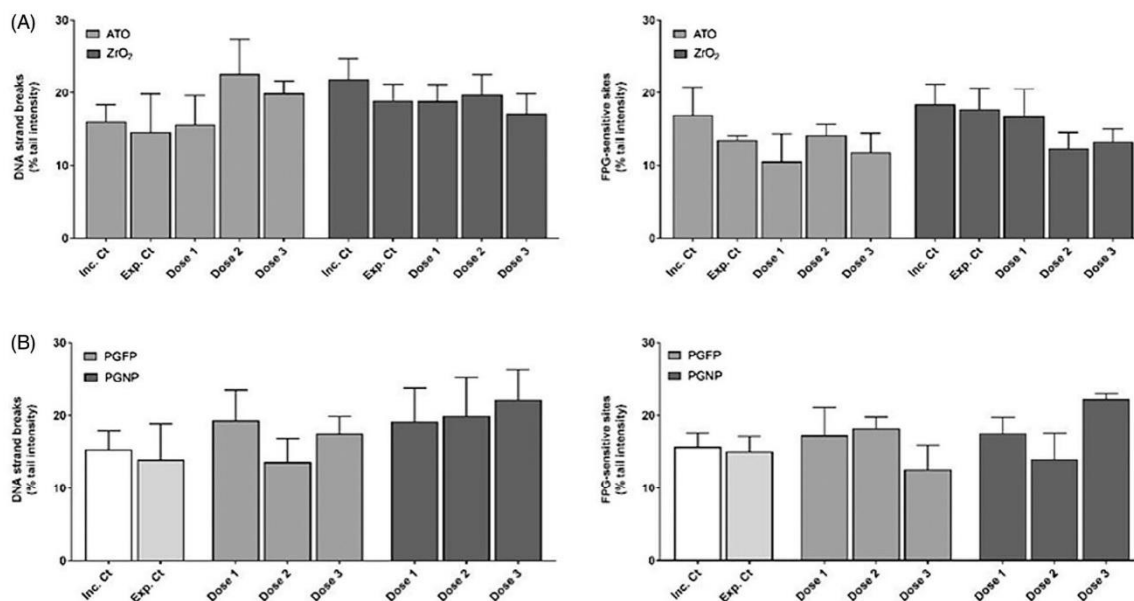
Figure 4. Genotoxicity of the aerosolized particles under study in polarized 3 D human bronchial epithelial MucilAir™ cultures under air–liquid interface (ALI) conditions. Cultures were exposed three consecutive days to the aerosolized engineered nanoparticles (ENP) (A) and HVOF-derived particles (B). Primary (left) and oxidative (right) DNA damage was assessed by the comet assay at 72 h after the initial exposure. Data were analyzed by the one-way analysis of variance (ANOVA) test followed by Dunnett's post hoc test for multiple comparisons. No significant differences were found compared to the control cultures. Inc. Ct: Incubator control, Exp. Ct: Exposure control.

to the ENP aerosols. No major differences were observed between exposed cells and controls. Notwithstanding, in ATO and ZrO_2 NP-exposed cultures, significantly higher levels of IL-8 release at the initial assessed timepoint, i.e. at 24 h were found compared to later timepoints (48 and 72 h) ($p < 0.001$) (Figure 5(A)). At the same time, no significant changes in MCP-1 release were observed in ENP-exposed 3D cultures compared to controls at any assessed timepoint (Figure 5(B)). MucilAir™ cultures exposed to HVOF-derived PGFP and PGNP fractions were also evaluated in terms of IL-8 (Figure 5(C)) and MCP-1 (Figure 5(D)) release. Overall, significantly higher levels of IL-8 release were detected at 72 h compared to the other assessed timepoints ($p < .001$). Exposure to Doses 1 and 2 of PGFP fraction aerosols significantly decreased IL-8 levels comparing with control cultures at 72 h (Figure 5(C)). On the other hand, exposure to the aerosolized PGNP fraction did not significantly alter IL-8 release in MucilAir™ cultures. Regarding MCP-1 measurements, as represented in Figure 5(D), a similar pattern of release was detected, i.e. significantly higher levels at 72 h *vs.*

24 h and 48 h timepoints ($p = 0.001$). Once again, a significant decrease in MCP-1 levels of bronchial epithelial cultures exposed to Doses 1 and 2 of PGFP aerosols has been detected at 72 h. LPS and DQ12 served as PC. Human bronchial cells incubated with LPS (10 µg/mL; 24 h) secreted significant higher levels of both IL-8 (21.024 ± 3.995 ng/mL) and MCP-1 (7.023 ± 0.289 ng/mL) compared to control cells. Overall, exposure to aerosolized DQ12 significantly elevated IL-8 and MCP-1 levels at 24 and 72 h (Figure 5(A–C)) but failed to increase MCP-1 secretion in donor #2 cultures (Figure 5(D)) at all assessed timepoints.

4. Discussion

We have investigated the *in vitro* toxicity of ENP and HVOF-derived particles (PGFP and PGNP) relevant to the ceramic industry in a respiratory model, as inhalation is the major exposure route in occupational settings. Our findings show that exposure to either aerosolized ENP or HVOF-derived particles did not significantly affect MucilAir™ cultures in terms of barrier integrity, cell viability, metabolic
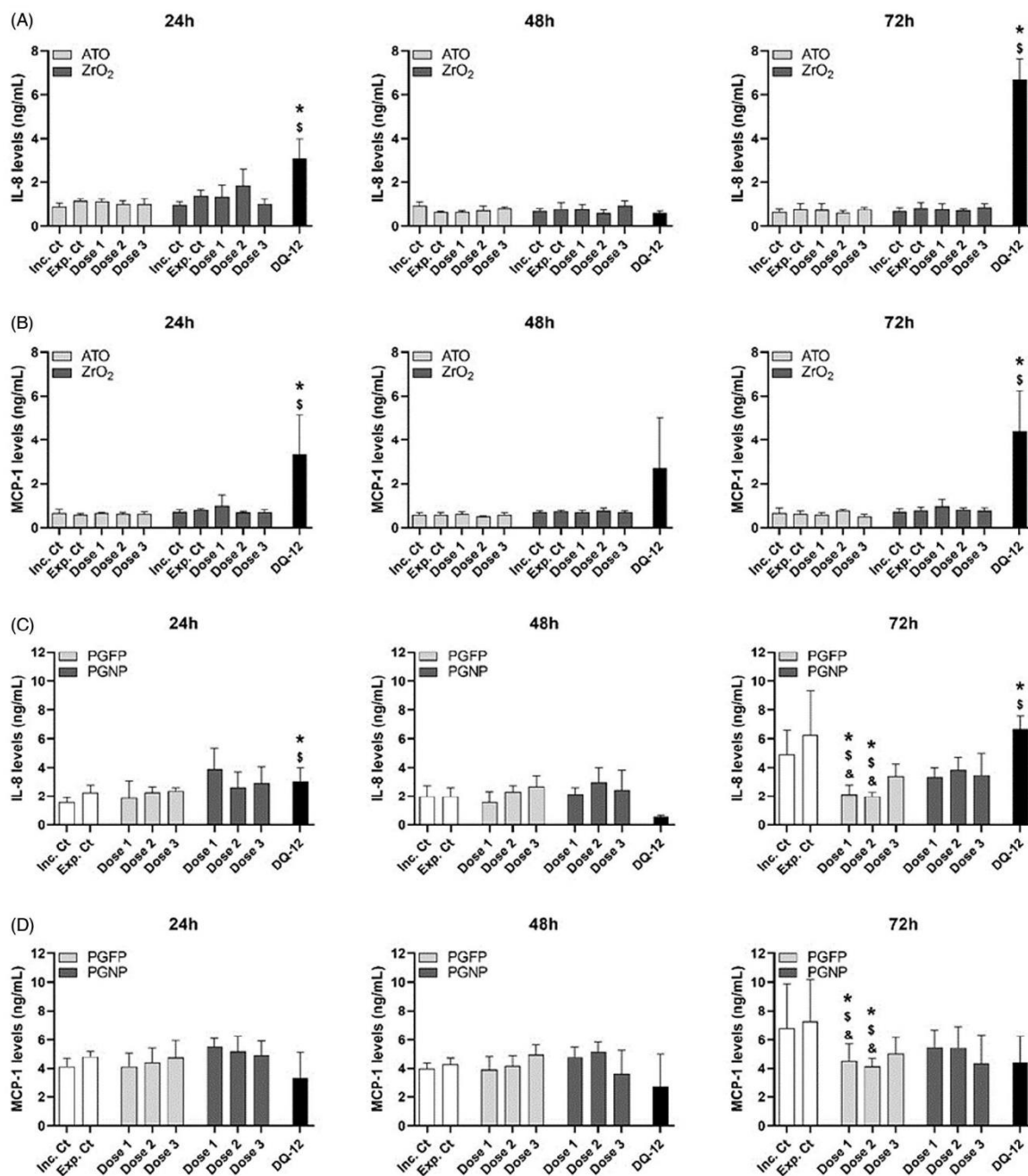
Figure 5. Interleukin-8 (IL-8) and monocyte chemoattractant protein-1 (MCP-1) levels in 3D human bronchial epithelial MucilAir[TM] cultures exposed to the aerosolized engineered nanoparticles (ENP: antimony-tin oxide [$Sb_2O_3 \bullet SnO_2$; ATO] and zirconium oxide [ZrO_2] NP) or high-velocity oxygen-fuel spraying (HVOF)-derived particles. IL-8 (A) and MCP-1 (B) levels in ENP-exposed cultures; IL-8 (C) and MCP-1 (D) levels in cultures exposed to aerosolized HVOF-derived PGFP and PGNP. Aerosolized crystalline Dörentruper Quartz (DQ12; $\leq 5\,\mu m$) was employed as a positive pro-inflammatory particle control. Values are presented as mean $\pm$ SD of three biological replicates, each run in duplicate. A two-way ANOVA analysis was performed to compare differences between timepoints and tested doses. $^*p \leq 0.05$ *vs.* Inc. Ct, $^\$p \leq 0.05$ *vs.* Exp. Ct and $^\&p \leq 0.05$ *vs.* Dose 3. Inc. Ct: Incubator control; Exp. Ct: Exposure control.

188

activity, and cytokine release. However, a few interesting changes in cells were detected, especially at early timepoints. Exposure to aerosolized ATO ($Sb_2O_3 \bullet SnO_2$) or ZrO_2 NP only caused a mild cytotoxicity (significant increase in LDH release) at 24 h, at doses of 5.56 and 10.98 $\mu g/cm^2$, respectively. Nonetheless, cells seemed to quickly recover since no significant changes in LDH release and cell viability were observed at late timepoints. In addition, no significant changes in both primary and oxidative DNA damage, as well as no relevant alterations in pro-inflammatory IL-8 and MCP-1 levels of MucilAir™ cultures were detected following exposure to ATO or ZrO_2 NP aerosols, compared to control, at any assessed time point. These findings support the view that under our experimental conditions, human primary bronchial cultures cope with the potential adverse effects caused by exposure to the deposited doses of both tested ENP.

In the literature, studies on the toxicity of ATO ($Sb_2O_3 \bullet SnO_2$) NP are scarce. Titma et al. reported no toxic effects of Sb_2O_3 NP on A549 cells exposed for a short period (24 h) to NP concentrations from 3 to 100 μg metal/mL, as assessed by the resazurin assay. However, long-term exposure up to 9 d markedly increased toxicity over time, with an EC50 value of 22 $\mu g/mL$ (Titma et al. 2016). On the other hand, Tabei et al. investigated the cellular uptake, cytotoxicity, genotoxicity, and oxidative stress in A549 cells exposed for 6 and 24 h to indium-doped SnO_2 (ITO) NP (30 nm; 1–1000 $\mu g/mL$) (Tabei et al. 2015). These authors reported low levels of NP uptake and no cytotoxic effects in A549 cells, in spite of a markedly increase in reactive oxygen species (ROS) levels, expression of heme oxygenase 1 (HO-1) gene, and DNA damage have been observed. These studies were performed in conventional cell lines that have shown to be more prone to NP effects when compared to more advanced cultures such as 3D in vitro cell models (Fröhlich 2018). On the other hand, our findings on the toxicological potential of the ZrO_2 NP were, in general, in agreement with those reported in the literature. Brunner et al. evaluated the toxicity of metal NP, including ZrO_2 NP, with different degrees of solubility in human lung mesothelioma (MSTO). In this study, cells were exposed for 3 and 6 d to either insoluble (ZrO_2, cerium oxide [CeO_2], TiO_2 NP) or slightly soluble (ZnO, uncoated iron oxide [Fe_2O_3],

and tricalcium phosphate [$Ca_3(PO_4)_2$]) NP at concentrations up to 30 ppm (Brunner et al. 2006). ZrO_2 NP induced similar responses as CeO_2, TiO_2, and $Ca_3(PO_4)_2$ NP, while ZnO NP were the most cytotoxic among the tested NP, supporting the view that ions arising from NP dissolution contribute to the toxic responses to NP. Interestingly, exposure to ZrO_2 NP caused a marked decrease in cell proliferation and viability (~50%) at 3 d, while at 6 d, MSTO cells almost fully recovered to control levels. By its turn, Lanone et al. (2009) investigated the toxicity of 24 NM, including ZrO_2-based and SnO_2 NP in human alveolar epithelial (A549) and macrophage (THP-1) cell lines. At 24 h after exposure, ZrO_2-based and SnO_2 NP up to 5000 $\mu g/mL$ caused moderate to low toxicity in both cell lines, with A549 cells showing less sensitivity than THP- cells.

To the best of our knowledge, this is the first report on in vitro toxicity of airborne PGFP and PGNP collected in a real-world industrial scenario. The collected HVOF liquid suspensions were highly diluted, which limited the concentration range to be tested. As hypothesized, aerosolized PGFP and PGNP seemed to induce higher toxicity on MucilAir™ cultures when compared to ENP, though their total deposited doses (up to 9 $\mu g/cm^2$) were far below the ones achieved in MucilAir™ cultures exposed to ENP aerosols (up to 148 $\mu g/cm^2$), especially in PGNP-exposed cultures. While PGFP aerosols significantly affected cell viability at mean deposited dose levels as low as ~3 $\mu g/cm^2$, exposure to the aerosolized PGNP increased DNA damage at 72 h after the first aerosolization. On the other hand, a low but significant decrease in the secretion of IL-8 and MCP-1 has been detected in cultures exposed to PGFP aerosols (Doses 1 and 2) at 72 h, while no changes in the levels of both pro-inflammatory chemokines have been detected following exposure to PGNP aerosols at any assessed timepoint. These findings indicate that under our experimental conditions, exposure to both fractions of HVOF-derived particles did not elicit an evident pro-inflammatory response in MucilAir™ cultures.

The toxicity of ambient airborne particles is strongly dependent on their size and chemical nature (Cassee et al. 2013). Chemical composition analyses of HVOF particles revealed that they were mainly constituted by the elements present in the feedstock material used (WC, Ni, and Cr) and not

from secondary sources, being Ni and Cr the major components found on both fine (PGFP) and ultrafine (PGNP) fractions (Salmatonidis et al. 2018a). Considering the ample epidemiological evidence of adverse human health outcomes from inhalation of W (Coates and Watson 1971; Sprince et al. 1984; Armstead, Arena, and Li 2014; Wasel and Freeman 2018), Cr (Salnikow and Zhitkovich 2008; Halasova et al. 2010), and Ni (Salnikow and Zhitkovich 2008; Lippmann and Chen 2009; Phillips et al. 2010), all these constituents will likely contribute for the observed *in vitro* toxicity, either additively or synergistically. This view is supported by several reports in the literature on W, Cr, and Ni *in vitro* and *in vivo* pulmonary toxicity (IARC 1990; Wise, Wise, and Little 2002; Zhang et al. 2003; Morimoto et al. 2011; Wasel and Freeman 2018; George et al. 2019). Higher Ni content in PM 2.5 has been associated with increased occurrence of cardiovascular events and respiratory diseases (Salnikow and Zhitkovich 2008; Lippmann and Chen 2009). In the occupational context, there is even a report of a 38-years-old healthy male death from adult respiratory distress syndrome (ARDS), caused by inhalation of Ni-NP during spraying onto bushes for turbin bearing using a metal arc process (Phillips et al. 2010). On the other hand, occupational exposure to inhalable Cr has long been associated with airway irritation, obstruction and increased incidence of respiratory tract malignancies (Salnikow and Zhitkovich 2008; Halasova et al. 2010).

A more intense toxicity was expected to be detected in human bronchial cultures exposed to the ENP or the HVOF particles tested herein. Different aspects may account for the low toxicity observed. One plausible explanation is an effective particle mucociliary clearance, similar to what occurs *in vivo*, that considerably attenuates the uptake and the cellular effects of the tested particles. Indeed, this defense mechanism has been previously reported to prevent/mitigate NP toxicity in the MucilAir[TM] model (Frieke Kuper et al. 2015; George et al. 2019). At the same time, despite its complexity and unique features, MucilAir[TM] cultures lack other cell types such as fibroblasts or macrophages, known to play an important role on the observed cellular responses to inhaled NP, namely in inflammatory responses (Movia et al. 2017), which may also account for its resistance to NP. In

the present study, MucilAir[TM] cultures were exposed for three consecutive days to the aerosolized particles. Considering the available evidence from both experimental studies (Murgia et al. 2016) and mathematical models for predicting the behavior of particles in the mucus (Ernst et al. 2017), NP < 100 nm seem to have a greater chance to penetrate into the mucus layer. Accordingly, one should expect that all the tested particles, whose mean size fall in this category, would be able to cross the mucus layer and reach the epithelial cell surface. Notwithstanding, assessment of mucus secretion and cilia beating in response to airborne NP will be valuable to better understand the role of these defense mechanisms for protecting against airborne NP exposure in complex *in vitro* systems such as MucilAir[TM] cultures.

Recent studies showed that the adverse effects of conventional chemicals and NP on MucilAir[TM] cultures are mostly limited to long-term exposures, making this model suitable for studying the effects of chronic exposures (Baxter et al. 2015; Chortarea et al. 2017). Therefore, a longer exposure would probably be necessary to reveal the negative effects of the tested NP on MucilAir[TM] cultures. Finally, we also cannot discard the possibility that sampling and aerosolization procedures might have affected the original properties of the tested particles, in particular of HVOF particles, reducing their toxic potency.

In vitro NM toxicity studies must rely on a realistic concentration testing, i.e. assess the toxicity of NP concentrations expected to be found in an *in vivo* setting. In this study, single exposure and total deposited doses of ENP and HVOF-derived particles ranged from $0.5 - 49.1$ to $1.5 - 147.6$ μg/cm^3, respectively. For a healthy, moderately active adult, the estimated lifetime deposited alveolar dose under realistic ambient conditions is of 6.6 μg/cm^2 (Paur et al. 2011). On the other hand, in a worst-case exposure scenario, a daily alveolar mass dose of 0.13 μg/cm^2 is expected to be achieved, while its maximum lifetime value would be close to 420 μg/cm^2 (Paur et al. 2011). Thus, we can assume that the deposited doses achieved in our study are realistic from an occupational perspective. Currently, regulatory occupational exposure limit (OEL) values are only available for specific types of ENP (e.g. for TiO_2 from the National Institute for

Occupational Safety and Health [NIOSH] or for nano-SiO$_2$ fumes from the European Chemical Agency [ECHA]). For PGNP, the most frequently used guidance is referred to as nano-reference values (NRV)(Van Broekhuizen et al. 2012), non-regulatory reference values for NM based on the precautionary approach, which is set to 4×10^4/cm^3 for non-biodegradable granular NM in the range 1–100 nm and density <6 g/cm^3. At the industrial-scale precision engineering workshop where the tested HVOF-derived particles were collected, particle number concentration measured in the near (inside booth) and far (worker area) fields was of 3.4×10^6/cm^3 and 2×10^5/cm^3, respectively (Salmatonidis et al. 2018a), values that largely exceeded the recommended NRV.

5. Conclusions

The present work highlights the impact that advanced ceramic technologies (materials and/or processes) have on workplace air quality and worker's exposure to airborne nano-sized particles, a matter that had been largely overlooked. PGFP and PGNP exhibit higher toxicity than ENP in mass per area unit, the presence of a mucociliary apparatus, as it occurs *in vivo* as defense mechanism, seems to substantially decrease the detected toxic effects. Generally, NM toxicity studies focus on ENP that are getting increasingly used as input materials but our data shows that PGNP might constitute a higher hazard to workers health not only due to its chemical complexity and unknown hazard, but also to the high levels of emitted particles that often exceed the recommended NRV. Therefore, more studies are urgently needed to identify occupational exposure scenarios and to establish the hazardous potential of NP incidentally released from industrial technologies and/or processes, which is of paramount importance for setting OEL s for NP and protecting workers' health.

Disclosure statement

The authors declare that the original work described is approved by all co-authors, has not been previously published and is not under consideration for publication elsewhere. In addition, the authors also declare that they have no conflicts of interest concerning this article.

ORCID

Maria João Bessa http://orcid.org/0000-0001-5357-6167
Fátima Brandão http://orcid.org/0000-0002-2933-8561
Flemming R. Cassee http://orcid.org/0000-0001-9958-8630
Apostolos Salmatonidis http://orcid.org/0000-0002-9999-3836
Mar Viana http://orcid.org/0000-0002-4073-3802
Adriana Vulpoi http://orcid.org/0000-0001-5334-4980
Eliseo Monfort http://orcid.org/0000-0003-3995-2378
João Paulo Teixeira http://orcid.org/0000-0001-8693-5250
Sónia Fraga http://orcid.org/0000-0001-9386-2336

References

Armstead, A. L., C. B. Arena, and B. Li. 2014. "Exploring the Potential Role of Tungsten Carbide Cobalt (WC-Co) Nanoparticle Internalization in Observed Toxicity toward Lung Epithelial Cells in Vitro." *Toxicology and Applied Pharmacology* 278 (1): 1–8. doi:10.1016/j.taap.2014.04.008.

Balogh Sivars, K., U. Sivars, E. Hornberg, H. Zhang, L. Brändén, R. Bonfante, S. Huang, et al. 2018. "A 3D Human

Airway Model Enables Prediction of Respiratory Toxicity of Inhaled Drugs in Vitro." *Toxicological Sciences: An Official Journal of the Society of Toxicology* 162 (1): 301–308. doi:10.1093/toxsci/kfx255.

Baxter, A., S. Thain, A. Banerjee, L. Haswell, A. Parmar, G. Phillips, and E. Minet. 2015. "Targeted Omics Analyses, and Metabolic Enzyme Activity Assays Demonstrate Maintenance of Key Mucociliary Characteristics in Long Term Cultures of Reconstituted Human Airway Epithelia." *Toxicology in Vitro: An International Journal Published in Association with BIBRA* 29 (5): 864–875. doi:10.1016/j.tiv.2015.03.004.

Bessa, M. J., F. Brandão, M. M. Querido, C. Costa, C. C. Pereira, V. Valdiglesias, B. Laffon, M. Carriere, J. P. Teixeira, and S. Fraga. 2019. "Optimization of the Harvesting and Freezing Conditions of Human Cell Lines for DNA Damage Analysis by the Alkaline Comet Assay." *Mutation Research* 845: 402994. doi:10.1016/j.mrgentox.2018.12.002.

Bessa, M. J., F. Brandão, M. Viana, J. F. Gomes, E. Monfort, F. R. Cassee, S. Fraga, and J. P. Teixeira. 2020. "Nanoparticle Exposure and Hazard in the Ceramic Industry: An Overview of Potential Sources, Toxicity and Health effects." *Environmental Research* 184: 109297. doi:10.1016/j.envres.2020.109297.

Brunner, T. J., P. Wick, P. Manser, P. Spohn, R. N. Grass, L. K. Limbach, A. Bruinink, and W. J. Stark. 2006. "In Vitro Cytotoxicity of Oxide Nanoparticles: comparison to Asbestos, Silica, and the Effect of Particle solubility." *Environmental Science & Technology* 40 (14): 4374–4381. doi:10.1021/es052069i.

Cassee, F. R., M.-E. Héroux, M. E. Gerlofs-Nijland, and F. J. Kelly. 2013. "Particulate Matter beyond Mass: Recent Health Evidence on the Role of Fractions, Chemical Constituents and Sources of Emission." *Inhalation Toxicology* 25 (14): 802–812. doi:10.3109/08958378.2013.850127.

Chortarea, S., H. Barosova, M. J. D. Clift, P. Wick, A. Petri-Fink, and B. Rothen-Rutishauser. 2017. "Human Asthmatic Bronchial Cells Are More Susceptible to Subchronic Repeated Exposures of Aerosolized Carbon Nanotubes at Occupationally Relevant Doses than Healthy Cells." *ACS Nano* 11 (8): 7615–7625. doi:10.1021/acsnano.7b01992.

Clouter, A., D. Brown, D. Höhr, P. Borm, and K. Donaldson. 2001. "Inflammatory Effects of Respirable Quartz Collected in Workplaces versus Standard DQ12 Quartz: Particle Surface Correlates." *Toxicological Sciences: An Official Journal of the Society of Toxicology* 63 (1): 90–98. doi:10.1093/toxsci/63.1.90.

Coates, E. O., and J. H. Watson. 1971. "Diffuse Interstitial Lung Disease in Tungsten Carbide Workers." *Annals of Internal Medicine* 75 (5): 709–716. doi:10.7326/0003-4819-75-5-709.

De Jong, W. H., and P. J. A. Borm. 2008. "Drug Delivery and Nanoparticles: Applications and Hazards." *International Journal of Nanomedicine* 3 (2): 133–149. doi:10.2147/ijn.s596.

Ernst, M., T. John, M. Guenther, C. Wagner, U. F. Schaefer, and C. M. Lehr. 2017. "A Model for the Transient Subdiffusive Behavior of Particles in Mucus." *Biophysical Journal* 112 (1): 172–179. doi:10.1016/j.bpj.2016.11.900.

Faber, S. C., and S. D. Mccullough. 2018. "Through the Looking Glass: In Vitro Models for Inhalation Toxicology and Interindividual Variability in the Airway." *Applied in Vitro Toxicology* 4 (2): 115–128. doi:10.1089/aivt.2018.0002.

Fonseca, A., M. Viana, X. Querol, N. Moreno, I. De Francisco, C. Estepa, and G. De La Fuente. 2015a. *Workplace Exposure to Process-Generated Ultrafine and Nanoparticles in Ceramic Processes Using Laser Technology. Indoor and Outdoor Nanoparticles*, 159–179. Berlin, Germany: Springer.

Fonseca, A. S., A. Maragkidou, M. Viana, X. Querol, K. Hameri, I. De Francisco, C. Estepa, C. Borrell, V. Lennikov, and G. F. De La Fuente. 2016. "Process-Generated Nanoparticles from Ceramic Tile Sintering: Emissions, Exposure and Environmental Release." *Science of the Total Environment* 565: 922–932. doi:10.1016/j.scitotenv.2016.01.106.

Fonseca, A. S., M. Viana, X. Querol, N. Moreno, I. De Francisco, C. Estepa, and G. F. De La Fuente. 2015b. "Ultrafine and Nanoparticle Formation and Emission Mechanisms during Laser Processing of Ceramic Materials." *Journal of Aerosol Science* 88: 48–57. doi:10.1016/j.jaerosci.2015.05.013.

Frieke Kuper, C., M. Gröllers-Mulderij, T. Maarschalkerweerd, N. M. M. Meulendijks, A. Reus, F. Van Acker, E. K. Zondervan-Van Den Beuken, M. E. L. Wouters, S. Bijlsma, and I. M. Kooter. 2015. "Toxicity Assessment of Aggregated/Agglomerated Cerium Oxide Nanoparticles in an in Vitro 3D Airway Model: The Influence of Mucociliary Clearance." *Toxicology in Vitro: An International Journal Published in Association with BIBRA* 29 (2): 389–397. doi:10.1016/j.tiv.2014.10.017.

Fröhlich, E. 2018. "Comparison of Conventional and Advanced in Vitro Models in the Toxicity Testing of Nanoparticles." *Artificial Cells, Nanomedicine, and Biotechnology* 46 (2): 1091–1107. doi:10.1080/21691401.2018.1479709.

George, I., C. Uboldi, E. Bernard, M. S. Sobrido, S. Dine, A. Hagège, D. Vrel, et al. 2019. "Toxicological Assessment of ITER-Like Tungsten Nanoparticles Using an in Vitro 3D Human Airway Epithelium Model." *Nanomaterials* 9 (10): 1374. doi:10.3390/nano9101374.

Halasova, E., M. Adamkov, T. Matakova, E. Kavcova, I. Poliacek, and A. Singliar. 2010. "Lung Cancer Incidence and Survival in Chromium Exposed Individuals with Respect to Expression of anti-Apoptotic Protein Survivin and Tumor Suppressor P53 Protein." *European Journal of Medical Research* 15(2): 55–59. doi:10.1186/2047-783x-15-s2-55.

IARC. 1990. "Chromium, Nickel and Welding." *IARC Monographs on the Evaluation of Carcinogenic Risks to Humans* 49: 1–648. https://publications.iarc.fr/Book-And-Report-Series/Iarc-Monographs-On-The-Identification-Of-

Carcinogenic-Hazards-To-Humans/Chromium-Nickel-And-Welding-1990

Jariwala, D., V. K. Sangwan, L. J. Lauhon, T. J. Marks, and M. C. Hersam. 2013. "Carbon Nanomaterials for Electronics, Optoelectronics, Photovoltaics, and Sensing." *Chemical Society Reviews* 42 (7): 2824–2860. doi:10.1039/c2cs35335k.

Kim, S., P. A. Jaques, M. Chang, J. R. Froines, and C. Sioutas. 2001. "Versatile Aerosol Concentration Enrichment System (VACES) for Simultaneous in Vivo and in Vitro Evaluation of Toxic Effects of Ultrafine, Fine and Coarse Ambient Particles Part I: Development and Laboratory Characterization." *Journal of Aerosol Science* 32 (11): 1281–1297. doi:10.1016/S0021-8502(01)00057-X.

Lacroix, G., W. Koch, D. Ritter, A. C. Gutleb, S. T. Larsen, T. Loret, F. Zanetti, et al. 2018. " Air-Liquid Interface In Vitro Models for Respiratory Toxicology Research: Consensus Workshop and Recommendations." *Applied in Vitro Toxicology* 4 (2): 91–106. doi:10.1089/aivt.2017.0034.

Lanone, S., F. Rogerieux, J. Geys, A. Dupont, E. Maillot-Marechal, J. Boczkowski, G. Lacroix, and P. Hoet. 2009. "Comparative Toxicity of 24 Manufactured Nanoparticles in Human Alveolar Epithelial and Macrophage Cell Lines." *Particle and Fibre Toxicology* 6: 14. doi:10.1186/1743-8977-6-14.

Lippmann, M., and L. C. Chen. 2009. "Health Effects of Concentrated Ambient Air Particulate Matter (CAPs) and Its components." *Critical Reviews in Toxicology* 39 (10): 865–913. doi:10.3109/10408440903300080.

Miller, A. J., and J. R. Spence. 2017. "In Vitro Models to Study Human Lung Development, Disease and Homeostasis." *Physiology (Bethesda, MD)* 32 (3): 246–260. doi:10.1152/physiol.00041.2016.

Monfort, E., A. Mezquita, E. Vaquer, I. Celades, V. Sanfelix, and A. Escrig. 2014. "Ceramic Manufacturing Processes: Energy, Environmental, and Occupational Health Issues." *Comprehensive Materials Processing* 8: 71–102.doi:10.1016/B978-0-08-096532-1.00809-8.

Morimoto, Y., M. Hirohashi, A. Ogami, T. Oyabu, T. Myojo, M. Hashiba, Y. Mizuguchi, et al. 2011. "Pulmonary Toxicity following an Intratracheal Instillation of Nickel Oxide Nanoparticle Agglomerates." *Journal of Occupational Health* 53 (4): 293–295. doi:10.1539/joh.11-0034-br.

Movia, D., L. Di Cristo, R. Alnemari, J. E. Mccarthy, H. Moustaoui, M. Lamy De La Chapelle, J. Spadavecchia, Y. Volkov, and A. Prina-Mello. 2017. "The Curious Case of How Mimicking Physiological Complexity in in Vitro Models of the Human Respiratory System Influences the Inflammatory Responses. A Preliminary Study Focused on Gold Nanoparticles." *Journal of Interdisciplinary Nanomedicine* 2 (2): 110–130. doi:10.1002/jin2.25.

Murgia, X., P. Pawelzyk, U. F. Schaefer, C. Wagner, N. Willenbacher, and C.-M. Lehr. 2016. "Size-Limited Penetration of Nanoparticles into Porcine Respiratory Mucus after Aerosol Deposition." *Biomacromolecules* 17 (4): 1536–1542. doi:10.1021/acs.biomac.6b00164.

Nanotoxclass. 2017. *Standard Operation Procedure – Preparation of Nanoparticle Suspensions by Cup Horn Sonication.* https://www.nanopartikel.info/data/projekte/NanoToxClass/NanoToxClass-SOP_Dispersion_by_cup_horn_sonication_V2.0.pdf

Paur, H. R., F. R. Cassee, J. Teeguarden, H. Fissan, S. Diabate, M. Aufderheide, W. G. Kreyling, et al. 2011. "In-Vitro Cell Exposure Studies for the Assessment of Nanoparticle Toxicity in the Lung—a Dialog between Aerosol Science and Biology." *Journal of Aerosol Science* 42 (10): 668–692. doi:10.1016/j.jaerosci.2011.06.005.

Phillips, J. I., F. Y. Green, J. C. Davies, and J. Murray. 2010. "Pulmonary and Systemic Toxicity following Exposure to Nickel Nanoparticles." *American Journal of Industrial Medicine.* 53: 763–767. doi:10.1002/ajim.20855.

Ribalta, C., A. López-Lilao, S. Estupiñá, A. S. Fonseca, A. Tobías, A. García-Cobos, M. C. Minguillón, E. Monfort, and M. Viana. 2019a. "Health Risk Assessment from Exposure to Particles during Packing in Working Environments." *The Science of the Total Environment* 671: 474–487. doi:10.1016/j.scitotenv.2019.03.347.

Ribalta, C., M. Viana, A. López-Lilao, S. Estupiñá, M. C. Minguillón, J. Mendoza, J. Díaz, D. Dahmann, and E. Monfort. 2019b. "On the Relationship between Exposure to Particles and Dustiness during Handling of Powders in Industrial Settings." *Annals of Work Exposures and Health* 63 (1): 107–123. doi:10.1093/annweh/wxy092.

Salmatonidis, A., C. Ribalta, V. Sanfélix, S. Bezantakos, G. Biskos, A. Vulpoi, S. Simion, E. Monfort, and M. Viana. 2018a. "Workplace Exposure to Nanoparticles during Thermal Spraying of Ceramic Coatings." *Annals of Work Exposures and Health* 63 (1): 91–106. doi:10.1093/annweh/wxy094.

Salmatonidis, A., V. Sanfélix, P. Carpio, L. Pawłowski, M. Viana, and E. Monfort. 2019. "Effectiveness of Nanoparticle Exposure Mitigation Measures in Industrial Settings." *International Journal of Hygiene and Environmental Health* 222 (6): 926–935. doi:10.1016/j.ijheh.2019.06.009.

Salmatonidis, A., M. Viana, G. Biskos, and S. Bezantakos. 2020. "Particle Size Distributions and Hygroscopic Restructuring of Ultrafine Particles Emitted during Thermal Spraying." *Aerosol Science and Technology* 54 (12): 1314–1359. doi:10.1080/02786826.2020.1784837.

Salmatonidis, A., M. Viana, N. Pérez, A. Alastuey, G. F. De La Fuente, L. A. Angurel, V. Sanfélix, and E. Monfort. 2018b. "Nanoparticle Formation and Emission during Laser Ablation of Ceramic Tiles." *Journal of Aerosol Science* 126: 152–168. doi:10.1016/j.jaerosci.2018.09.006.

Salnikow, K., and A. Zhitkovich. 2008. "Genetic and Epigenetic Mechanisms in Metal Carcinogenesis and Cocarcinogenesis: Nickel, Arsenic, and Chromium." *Chemical Research in Toxicology* 21 (1): 28–44. doi:10.1021/tx700198a.

Sprince, N. L., R. I. Chamberlin, C. A. Hales, A. L. Weber, and H. Kazemi. 1984. "Respiratory Disease in Tungsten Carbide Production Workers." *Chest* 86 (4): 549–557. doi:10.1378/chest.86.4.549.

Tabei, Y., A. Sonoda, Y. Nakajima, V. Biju, Y. Makita, Y. Yoshida, and M. Horie. 2015. "In Vitro Evaluation of the Cellular Effect of Indium Tin Oxide Nanoparticles Using the Human Lung Adenocarcinoma A549 Cells." *Metallomics: Integrated Biometal Science* 7 (5): 816–827. doi:10.1039/c5mt00031a.

Thiruvengadam, M., G. Rajakumar, and I.-M. Chung. 2018. "Nanotechnology: current Uses and Future Applications in the Food Industry." *3 Biotech* 8 (1): 74. doi:10.1007/s13205-018-1104-7.

Titma, T., R. Shimmo, J. Siigur, and A. Kahru. 2016. "Toxicity of Antimony, Copper, Cobalt, Manganese, Titanium and Zinc Oxide Nanoparticles for the Alveolar and Intestinal Epithelial Barrier Cells in vitro." *Cytotechnology* 68 (6): 2363–2377. doi:10.1007/s10616-016-0032-9.

Tran, N., and T. J. Webster. 2010. "Magnetic Nanoparticles: Biomedical Applications and Challenges." *Journal of Materials Chemistry* 20 (40): 8760–8767. doi:10.1039/c0jm00994f.

Van Broekhuizen, P., W. Van Veelen, W. H. Streekstra, P. Schulte, and L. Reijnders. 2012. "Exposure Limits for Nanoparticles: Report of an International Workshop on Nano Reference Values." *The Annals of Occupational Hygiene* 56 (5): 515–524. doi:10.1093/annhyg/mes043.

Viana, M., A. S. Fonseca, X. Querol, A. Lopez-Lilao, P. Carpio, A. Salmatonidis, and E. Monfort. 2017. "Workplace Exposure and Release of Ultrafine Particles during Atmospheric Plasma Spraying in the Ceramic Industry." *Science of the Total Environment*. 599–600: 2065–2073. doi:10.1016/j.scitotenv.2017.05.132.

Voliotis, A., S. Bezantakos, M. Giamarelou, M. Valenti, P. Kumar, and G. Biskos. 2014. "Nanoparticle Emissions from Traditional Pottery Manufacturing." *Environmental Science Processes & Impacts* 16 (6): 1489–1494. doi:10.1039/c3em00709j.

Wasel, O., and J. L. Freeman. 2018. "Comparative Assessment of Tungsten Toxicity in the Absence or Presence of Other Metals." *Toxics* 6 (4): 66. doi:10.3390/toxics6040066.

Wise, J. P., Sr., S. S. Wise, and J. E. Little. 2002. "The Cytotoxicity and Genotoxicity of Particulate and Soluble Hexavalent Chromium in Human Lung Cells." *Mutation Research* 517 (1–2): 221–229. doi:10.1016/S1383-5718(02)00071-2.

Zhang, Q., Y. Kusaka, X. Zhu, K. Sato, Y. Mo, T. Kluz, and K. Donaldson. 2003. "Comparative Toxicity of Standard Nickel and Ultrafine Nickel in Lung after Intratracheal Instillation." *Journal of Occupational Health* 45 (1): 23–30. doi:10.1539/joh.45.23.

Chapter III.

Integrated Discussion, Conclusions and Final Considerations

A. Integrated Discussion

Occupational exposure to inhalable particles is a cause of great concern for workers' health. In this regard, the ceramic industry is an extremely relevant case of worker exposure to airborne fine and nano-sized particles that can be originated from the manipulation of powdered raw materials, but also from manufacturing processes where incidental generation and release of particles to the workplace air occurs (Bessa *et al.*, 2020).

In the present thesis, the toxicity of PGFP and PGNP, and industrial ENP commonly used as input materials for ceramics production were tested in *in vitro* models and exposure conditions of different complexity. PGFP and PGNP were collected in a real industrial scenario during two spraying processes of ceramic powders onto metal surfaces to produce thermal-resistant coatings, namely APS and HVOF. Relevant biological endpoints were assessed to address their potential hazard in conventional or advanced human pulmonary *in vitro* models, either in the liquid or aerosolised form. From a human exposure scenario point of view, the particle concentrations tested herein were occupationally relevant considering that the estimated lifetime deposited alveolar dose under realistic ambient conditions for a healthy male adult is 6.60 µg/cm^2, while for a worst-case occupational exposure scenario a daily alveolar mass dose of 0.13 µg/cm^2 and a maximum accumulated lifetime dose of 420 µg/cm^2 are expected to be achieved (Paur *et al.*, 2011).

Optimisation of the Cell Harvesting and Freezing Procedures for DNA Damage Analysis

The collection, handling, and storage of cell samples may have a profound impact on DNA integrity and its suitability for use in downstream analysis (Shao *et al.*, 2012). A preliminary study for the optimisation of the harvesting and freezing protocol of human cell line samples for DNA damage analysis by the alkaline comet assay was performed (Chapter II, Section B.1.). For comparative purposes, two human cell lines have been selected, the alveolar epithelial A549 cells (one of the chosen models for the *in vitro* toxicity testing studies) and glioma A172 cells. Overall, no significant differences between the two investigated cell harvesting methods - mechanical (by scraping) and chemical (by trypsinisation)-, were found in terms of DNA integrity. Moreover, both tested cryoprotective media [10 %

dimethyl sulfoxide (DMSO) in fetal bovine serum (FBS) and 10 % DMSO in cell culture media supplemented with 10 % FBS] were found suitable (Bessa *et al.*, 2019). Importantly, no differences in DNA integrity were found between freshly collected and frozen cells up to eight weeks, irrespective of the harvesting method and freezing medium used. Accordingly, A549 cells and MucilAir™ cultures from ALI exposure studies, collected at RIVM and shipped to INSA for DNA damage analysis, were frozen in 10 % DMSO + 90 % cell culture media supplemented with 10 % FBS, the most cost-effective cryoprotective medium tested. Considering the tightness of the MucilAir™ monolayer, mechanical harvesting by scraping was the chosen harvesting method that was also adopted for human A549 cells detachment.

In Vitro Toxicity Assessment of the Airborne Process-Generated (Nano)Particles

An innovative aspect of this thesis was the testing of real scenario airborne particles collected at an industrial metallurgical plant using a versatile aerosol concentration enrichment system (VACES) system that allows collecting particles directly to liquid suspensions while preserving their biologically active components, which is a great advantage for toxicological assessment purposes (Kim *et al.*, 2001).

The collected airborne process-generated particles were initially tested using conventional cultures of A549 cells under submerged conditions (Chapter II, Section B.2.). As shown in **Table 1**, pronounced cytotoxicity together with increased reactive oxygen species (ROS) levels and oxidative DNA damage were found at 24 h after exposure to both fractions of HVOF-derived particles, being these effects, particularly evident at low concentrations of PGNP. On the other hand, only the fine fraction of the APS-derived particles slightly decreased cell viability at the highest tested concentration (5 µg/cm²). Notwithstanding, both APS- and HVOF-derived fine, and nano-sized particles were able to induce cell cycle arrest at S and G_2/M phases in human alveolar epithelial A549 cells, most likely triggered in response to DNA damage. Also, increased levels of histone H2AX phosphorylation (γ-H2AX) were found in A549 cells, especially in cells at S and G_2/M phases for all tested process-generated particles, although much more prominent in cells exposed to the particles emitted during APS. Therefore, our data suggest that both APS- and HVOF-derived particles induce genotoxic effects on human alveolar epithelial-like cells through different mechanisms: while APS-particles caused phosphorylation of histone H2AX at serine-139 (γ-H2AX) as an early cellular response to the induction

of DNA double-strand breaks, HVOF-particles induced 8-oxo-G oxidative DNA lesions, most likely caused by the increased intracellular ROS levels observed.

These differences in the cellular responses to both types of airborne process-generated particles are likely related to their physicochemical composition. As described in Chapter II, Section A.1., APS-derived particles were majorly enriched in aluminium (Al), Cr, and Ni, while Cr and Ni were the dominant elements found in both fractions of the HVOF-derived particles (Viana *et al.*, 2021). These elements have been previously linked with increased risk of cardiovascular and respiratory disease in humans exposed via inhalation (Halasova *et al.*, 2010; Lippmann *et al.*, 2009; Phillips *et al.*, 2010; Salnikow *et al.*, 2008). Moreover, our data are in accordance with previous *in vitro* studies in human lung cells incubated with Cr(VI) that reported increased levels of oxidative DNA damage (Reynolds *et al.*, 2012) and H2AX-Ser139 phosphorylation (DeLoughery *et al.*, 2015), as well as cell cycle arrest at G_2/M (Zhang *et al.*, 2001). In addition, *in vitro* exposure to Ni was related to G_2/M cell cycle arrest (Ding *et al.*, 2009), while in the nanoscale form (Ni NP) activation of DNA damage response mechanisms through the phosphorylation of ATM serine/threonine protein kinase (Ser1981), p53 tumour protein (Ser15) and H2AX (ser139) has been detected in human bronchial epithelial cells (Mo *et al.*, 2021).

A follow-up study in MucilAir™ bronchial epithelial cultures from healthy donors cultured at ALI was carried out to investigate the effects of repeated exposure to HVOF-derived particles' aerosols since those proven to be more toxic to A549 submerged cultures compared to the APS-emitted particles (Chapter II, Section B.4.). As shown in **Table 1**, while PGFP aerosols significantly affected cell viability and slightly reduced interleukin-8 (IL-8) and monocyte chemoattractant protein-1 (MCP-1) levels at dose levels up to ~9 µg/cm², exposure to the aerosolised PGNP (4.5 µg/cm²) increased primary and oxidative DNA damage at 72 h after the first exposure (Bessa *et al.*, 2021a). Notwithstanding, the magnitude of the responses to the HVOF particles in the advanced 3D cultures was far below compared to the observed responses in conventional human alveolar epithelial A549 submerged cultures. The complexity and sensitivity of the used cell model play a crucial role in the observed effects. While cultures of A549 cells are much more simplistic models representing only one cell type, MucilAir™ cultures present a higher degree of complexity containing different cells of the human airway epithelium. These 3D cultures produce mucus that is propelled by the continuous beating of cilia, as it occurs *in vivo* (Hoffmann *et al.*, 2018). Therefore, the presence of these mucociliary clearance mechanisms may have considerably attenuated and

mitigated the cellular effects of the tested particles, as previously reported in other studies using this model (Frieke Kuper *et al.*, 2015; George *et al.*, 2019).

Table 1. *In vitro* toxicity testing main findings in human A549 alveolar epithelial cells and 3D bronchial epithelial MucilAir™ cultures exposed to atmospheric plasma spraying (APS) and high velocity oxy-fuel spraying (HVOF)-derived fine (PGFP) and nanoparticles (PGNP).

	APS-derived		HVOF-derived	
	PGFP	**PGNP**	**PGFP**	**PGNP**
A549 cells (Submerged, Apical medium)	Not cytotoxic (up to 5 $\mu g/cm^2$)	No cytotoxic	↑ Cytotoxicity (IC_{50}: 20.18 $\mu g/cm^2$)	↑ Cytotoxicity (IC_{50}: 1.79 $\mu g/cm^2$)
	No ROS release	No ROS release	↑ ROS levels (40 $\mu g/cm^2$)	↑ ROS levels (20 $\mu g/cm^2$)
	Cellular uptake (5 $\mu g/cm^2$)	Cellular uptake (2.5 $\mu g/cm^2$)	Cellular uptake (5 $\mu g/cm^2$)	Cellular uptake (1.25 $\mu g/cm^2$)
	↑ S+G_2/M; ↑ Sub-G_1 subpopulations	↑ S+G_2/M; ↑ Sub-G_1 subpopulations	↑ S+G_2/M; ↑ Sub-G_1 subpopulations	↑ S+G_2/M; ↑ Sub-G_1 subpopulations
	↑ γ-H2AX levels	↑ γ-H2AX levels	↑ γ-H2AX levels	↑ γ-H2AX levels
	No changes in DNA strand breaks	No changes in DNA strand breaks and oxidative lesions	No changes in DNA strand breaks	No changes in DNA strand breaks
	↑ Oxidative DNA damage (2.5 and 5 $\mu g/cm^2$)		↑ Oxidative DNA damage (2.5 and 5 $\mu g/cm^2$)	↑ Oxidative DNA damage (up to 1.25 $\mu g/cm^2$)
MucilAir™ (ALI, Basal medium)	n.a.	n.a.	↑ Cytotoxicity (3 and 9 $\mu g/cm^2$; 72 h)	Not cytotoxic (up to 1.5 $\mu g/cm^2$; 24 h)
			Slight ↓ IL-8 and MCP-1 (3 and 6 $\mu g/cm^2$; 72 h)	No changes in IL-8 and MCP-1 levels
			No changes in DNA strand breaks and oxidative lesions	No changes in DNA strand breaks and oxidative lesions

In vitro complexity

ALI: air-liquid interface; **IC_{50}:** half-maximal inhibitory concentration, calculated through WST-1 metabolization results; **n.a:** not assessed; **ROS:** reactive oxygen species

Overall, airborne process-generated HVOF particles caused greater cytotoxicity than those derived from the APS thermal spraying. Notwithstanding, both fractions of PGFP and PGNP emitted during the two thermal spraying processes under study were able to induce significant levels of γ-H2AX and/or 8-oxo-G oxidative DNA damage in alveolar epithelial submerged cultures. HVOF nano-sized fraction seemed to induce greater cyto- and genotoxicity in A549 cells exposed under submerged conditions than in MucilAir™ cultures under ALI, through the decrease of cellular viability, increased DNA strand breaks and oxidative lesions, and the impairment of the plasma membrane. On the other hand, PGFP were more cytotoxic to MucilAir™ cultures than PGNP, although both did not induce significant primary or oxidative DNA damage.

In Vitro Toxicity Assessment of the Engineered Nanoparticles (ENP)

In Section B.3. from Chapter II, a set of four ENP widely used as raw materials in the ceramic industrial sector were tested in A549 submerged cells as liquid suspensions, or as aerosols directly delivered onto the A549 cells cultured under ALI. However, due to the limitations regarding the available amount of test material, it was not possible to generate a stable aerosol of SnO_2 NP, thus this ENP was not tested under ALI conditions. As depicted in **Table 2**, no significant cytotoxic effects were observed in human alveolar epithelial A549 cells exposed to the liquid suspensions of ENP, while pronounced cytotoxic effects, through decreased plasma membrane integrity and cellular viability, were observed after exposure to all aerosolised ENP compared to the controls. Based on the half-maximal effective concentration (EC_{50}) values with respect to the lactate dehydrogenase (LDH) release in A549 cultures at ALI after 4 h exposure, aerosolised ENP can be ranked for their cytotoxicity hazard as follows: ZrO_2 NP > CeO_2 NP > ATO NP. On the other hand, all tested ENP caused similar DNA damage in alveolar epithelial cells under both exposure conditions, except ATO NP that did not significantly increase DNA strand breaks of A549 cells under ALI conditions. Amongst all tested ENP, ZrO_2 NP aerosols seemed to induce more genotoxic effects in human alveolar epithelial-like cells than to the same ENP in liquid suspension. Taken together, our results support the view that ENP are more toxic to human alveolar epithelial cells when aerosolised rather than applied as a liquid suspension in submerged cell cultures (Bessa *et al.*, 2021b).

At submerged conditions, (nano)particles in suspension may react with the culture medium and agglomerate/aggregate into larger particles, which impacts cell-particle interactions (Loret *et al.*, 2016). In ALI systems, on the other hand, aerosolised particles directly deposit on cells' surface as occurs in the human respiratory tract, which makes this system more reliable for *in vitro* testing of (nano)particle toxicity (Fröhlich, 2018; Lacroix *et al.*, 2018). Therefore, the magnitude of the toxic responses observed might be related to differences in the deposited doses attained in cells under submerged and ALI conditions. Consequently, the reports found in the literature on the magnitude of the effects induced by exposure to NP in submerged *vs* ALI conditions are not consensual.
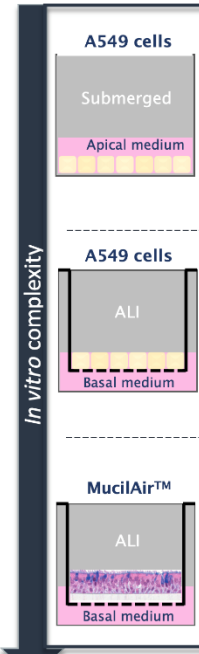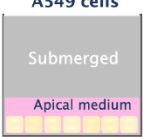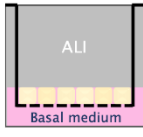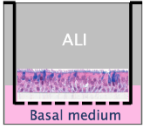
Moving on to advanced 3D models of the human airway epithelium cultured at ALI, ATO, and ZrO_2 ENP were selected based on the toxicity profiles obtained in cultures of A549 cells (Chapter II, Section B.4.). According to our findings, exposure

to the ENP aerosols for three consecutive days failed to significantly affect MucilAir™ cultures in terms of barrier integrity, cell viability, metabolic activity, cytokine (IL-8 and MCP-1) release, and DNA integrity. Only mild cytotoxicity was found at the first 24 h after exposure to the aerosolised ATO or ZrO_2 NP, but cells were able to quickly recover at later timepoints (**Table 2**) (Bessa *et al.*, 2021a). Considering the toxicity data obtained for A549 cells at ALI, marked toxicity of the aerosolised ENP in 3D MucilAir™ cultures was expected to be detected, which was possibly attenuated by mucociliary transport, as previously mentioned. Frieke Kuper *et al.* (2015) also found that CeO_2 NP did not induce evident toxic effects in 3D human bronchial epithelial model (MucilAir™) at ALI, although significant toxicity was detected in BEAS-2B and A549 cell cultures under submerged conditions (Frieke Kuper *et al.*, 2015). Another study also reported minor effects on human airway epithelium MucilAir™ cultures exposed to occupationally relevant doses of milled W-NP (10-50 µg/cm^2), with no impact on metabolic activity and cell viability but with a transient increase in IL-8 secretion (George *et al.*, 2019). These findings underline that cellular models' features and the exposure mode are determinant factors for (nano)particle-cell interactions and mediated biological effects.

As displayed in **Table 2**, although ENP induced DNA damage in A549 cells cultured at both submerged and ALI conditions, aerosolised ENP seemed to induce greater cytotoxicity than the same ENP as liquid suspensions. Moreover, aerosolised ENP induced more cyto- and genotoxic responses in A549 cells than in MucilAir™ cultures.

Table 2. Summary table of the *in vitro* toxicity testing main findings in human A549 alveolar epithelial cultures under submerged or air-liquid interface (ALI) conditions, and in human 3D bronchial epithelial MucilAir™ cultures exposed to the tested engineered nanoparticles (ENP).

	SnO$_2$	ATO	CeO$_2$	ZrO$_2$
A549 cells Submerged Apical medium	Not cytotoxic No changes in DNA strand breaks ↑ Oxidative DNA damage (10 and 25 µg/cm^2)	Not cytotoxic ↑ Primary and oxidative DNA damage (50 µg/cm^2)	Not cytotoxic ↑ Primary DNA damage (50 µg/cm^2) No changes in DNA oxidative lesions	Not cytotoxic ↑ Primary DNA damage (50 µg/cm^2) No changes in DNA oxidative lesions
A549 cells ALI Basal medium	**n.a.**	↑ Cytotoxicity (EC$_{50}$: 74.77 µg/cm^2) No changes in DNA strand breaks and oxidative lesions	↑ Cytotoxicity (EC$_{50}$: 32.97 µg/cm^2) ↑ Primary DNA damage (34 µg/cm^2) No changes in DNA oxidative lesions	↑ Cytotoxicity (EC$_{50}$: 20.70 µg/cm^2) ↑ Primary DNA damage (46 and 92 µg/cm^2) No changes in DNA oxidative lesions
MucilAir™ ALI Basal medium	**n.a.**	Not cytotoxic (up to 16.67 µg/cm^2; 24 h) No changes in IL-8 and MCP-1 levels No changes in DNA strand breaks and oxidative lesions	**n.a.**	Not cytotoxic (up to 32.94 µg/cm^2; 24 and 48 h) No changes in IL-8 and MCP-1 levels No changes in DNA strand breaks and oxidative lesions

ALI: air-liquid interface; EC$_{50}$: half-maximal effective concentration, calculated through LDH release results; **n.a:** not assessed; ROS: reactive oxygen species

In Vitro Hazard of the Airborne Process-Generated vs Engineered (Nano)Particles

Overall, both process-generated and engineered (nano)particles under study were able to induce adverse biological effects in the human pulmonary cell cultures evaluated. Upon contacting the cells, these particles were able to trigger a cascade of events responsible for the disturbance of the normal function and homeostasis of these lung cells. These included the imbalance of intracellular ROS levels, DNA strand breaks leading to the γ-H2AX, 8-oxo-G oxidative lesions, and ultimately the decrease in cell viability and plasma membrane disruption. However, the degree of these effects largely depended on the type and origin of the tested particles, as well as on the complexity and sensitivity of the *in vitro* cell model and/or exposure system.

When comparing PGFP and PGNP derived from each thermal spraying process *vs* ENP, the latter induced lower toxicity on both conventional A549 and advanced MucilAir™ cultures. In submerged human alveolar epithelial-like cells, though all particles induced increased levels of DNA damage, those effects were

more pronounced at lower concentrations for both APS and HVOF fine and nano-sized particles. Besides, the HVOF-derived particles induced noticeable cytotoxic effects, contrary to what was observed after exposure to ENP. A similar trend was observed in MucilAir™ cultures where the aerosolised PGFP and PGNP from HVOF spraying seemed to induce higher toxicity compared to ENP, with far below total deposited doses (up to ~9 µg/cm^2). These differences in the toxicity patterns must rely on the chemical complexity of the process-generated particles compared to the selected ENP. As previously stated, process-generated particles are enriched with Cr and Ni metals that have been described as potentially hazardous for humans, which is supported by several *in vitro* and *in vivo* reports (Åkerlund *et al.*, 2018; International Agency for Research on Cancer, 1990; Mo *et al.*, 2021; Morimoto *et al.*, 2011; Wise *et al.*, 2002; Zhang *et al.*, 2003; Zhang *et al.*, 2001). On the other hand, previous *in vitro* studies using similar ENP to the ones tested herein reported only mild to moderate toxic responses (De Marzi *et al.*, 2013; Demokritou *et al.*, 2013; Kim *et al.*, 2010; Kroll *et al.*, 2011; Lanone *et al.*, 2009; Mittal *et al.*, 2014; Park *et al.*, 2008; Tabei *et al.*, 2015; Titma *et al.*, 2016).

Notwithstanding, it is important to stand out that only acute exposures to the (nano)particles have been evaluated in the present study. However, in occupational settings, exposure occurs over prolonged periods (chronic exposures). In the case of advanced MucilAir™ cultures, longer exposure periods would probably be necessary to reveal the negative effects of the tested (nano)particles. Regarding the tested process-generated particles, is important to mention that particle number concentrations of APS- and HVOF-derived particles in the workplace air largely exceeded the recommended NRV of $4x10^4$/cm^3 for non-biodegradable granular NM (1–100 nm; density < 6 g/cm^3) (Salmatonidis *et al.*, 2018a). Taken together, these data suggest that worker's health may be at risk.

B. Conclusions and Final Considerations

The present work highlights the hazard that airborne (nano)particles related to advanced ceramic technologies might represent for workers' health, as demonstrated by the obtained data of the toxicological assessment performed in conventional and/or cutting-edge *in vitro* models and exposure systems representative of human respiratory system. The cellular models and exposure conditions played a determinant role in the observed biological effects. This reinforces the importance of using physiologically relevant *in vitro* models in (nano)particle toxicity studies, for a better extrapolation to humans. All toxicological studies performed herein tested realistic occupational dose levels of the selected (nano)particles, and the obtained results alert for the risk these aerosolised fine and nano-sized particles might pose for the workers' health.

Based on these remarks, the main conclusions of the present PhD study are the following:

- Among the two evaluated thermal spraying processes, HVOF-particles seem to be more cytotoxic than APS-derived particles. Nevertheless, PGFP and PGNP derived from the two thermal spraying processes were able to induce measurable genotoxicity effects in submerged human alveolar epithelial cultures, either through H2AX phosphorylation (APS-particles) or oxidative DNA damage (HVOF-particles) mechanisms;

- ENP aerosols, in particular ZrO_2 NP, were more toxic to human alveolar epithelial A549 cells than in the liquid suspension form. Accordingly, while submerged cultures are useful models for an initial screening of NP toxicity, data originated from studies involving exposure to aerosolised NP under ALI conditions are more valuable and meaningful in terms of airborne NP hazard assessment;

- Advanced MucilAir™ cultures, which display *in vivo* defence mechanisms such as the mucociliary apparatus, exhibited attenuated response to either HVOF-derived particles or ENP aerosols, while the conventional A549 cultures were more sensitive to the studied (nano)particles.

- Most likely due to their increased chemical complexity, the tested process-generated particles caused greater toxicity than ENP commonly used as raw materials in the ceramic industry;

- Considering that in the present study process-generated particles emission levels largely exceeded the recommended NRV values, workers from industries employing high-energy processes may be at (increased) risk of adverse health effects depending on the actual inhaled dose, i.e. exposure levels and duration.

Therefore, the present study on the toxicity of industrially relevant airborne (nano)particle substantiated that the scientific community must not only focus on ENP but also investigate more thoroughly the toxicity of incidentally released particles that, due to their complexity, might present a greater hazard to the human health. The high level of uncertainty and lack of internationally recognised occupational standards and exposure limits, i.e., OEL, for NM must be surpassed. More studies on the identification of occupational exposure scenarios, as well as on the establishment of toxicological profiles of the potentially hazardous (nano)particles released from multiple industrial technologies and/or processes are urgently needed. This information will be vital for the establishment of more effective health and safety protocols to help preventing and/or mitigating workers' adverse health outcomes and will be paramount for setting definitive nano-OEL. Until a complete and detailed knowledge on the hazard of airborne (nano)particles is established, preventive measures and precautionary engineering controls should be implemented in industries of elevated risk of (nano)particles' workplace exposure.

Chapter IV.

References

Ahmad, I., Yazdani, B., & Zhu, Y. (2015). Recent Advances on Carbon Nanotubes and Graphene Reinforced Ceramics Nanocomposites. *Nanomaterials*, *5*(1), 90-114. https://doi.org/10.3390/nano5010090

Åkerlund, E., Cappellini, F., Di Bucchianico, S., Islam, S., Skoglund, S., Derr, R., Odnevall Wallinder, I., Hendriks, G., & Karlsson, H. L. (2018). Genotoxic and mutagenic properties of Ni and NiO nanoparticles investigated by comet assay, γ-H2AX staining, Hprt mutation assay and ToxTracker reporter cell lines. *Environ Mol Mutagen*, *59*(3), 211-222. https://doi.org/10.1002/em.22163

Bakand, S., & Hayes, A. (2010). Troubleshooting methods for toxicity testing of airborne chemicals in vitro. *J Pharmacol Toxicol Methods*, *61*(2), 76-85. https://doi.org/10.1016/j.vascn.2010.01.010

Bakand, S., & Hayes, A. (2016). Toxicological Considerations, Toxicity Assessment, and Risk Management of Inhaled Nanoparticles. *Int J Mol Sci*, *17*(6). https://doi.org/10.3390/ijms17060929

Bessa, M. J., Brandão, F., Fokkens, P., Cassee, F. R., Salmatonidis, A., Viana, M., Vulpoi, A., Simon, S., Monfort, E., Teixeira, J. P., & Fraga, S. (2021a). Toxicity assessment of industrial engineered and airborne process-generated nanoparticles in a 3D human airway epithelial in vitro model. *Nanotoxicology*, *15*(4), 542-557. https://doi.org/10.1080/17435390.2021.1897698

Bessa, M. J., Brandão, F., Fokkens, P. H. B., Leseman, D., Boere, A. J. F., Cassee, F. R., Salmatonidis, A., Viana, M., Vulpoi, A., Simon, S., Monfort, E., Teixeira, J. P., & Fraga, S. (2021b). In Vitro Toxicity of Industrially Relevant Engineered Nanoparticles in Human Alveolar Epithelial Cells: Air-Liquid Interface versus Submerged Cultures. *Nanomaterials (Basel)*, *11*(12). https://doi.org/10.3390/nano11123225

Bessa, M. J., Brandão, F., Querido, M. M., Costa, C., Pereira, C. C., Valdiglesias, V., Laffon, B., Carriere, M., Teixeira, J. P., & Fraga, S. (2019). Optimization of the harvesting and freezing conditions of human cell lines for DNA damage analysis by the alkaline comet assay. *Mutat Res Genet Toxicol Environ Mutagen*, *845*, 402994. https://doi.org/10.1016/j.mrgentox.2018.12.002

Bessa, M. J., Brandão, F., Viana, M., Gomes, J. F., Monfort, E., Cassee, F. R., Fraga, S., & Teixeira, J. P. (2020). Nanoparticle exposure and hazard in the ceramic industry: an overview of potential sources, toxicity and health effects. *Environ Res*, *184*, 109297. https://doi.org/10.1016/j.envres.2020.109297

Cain, M., & Morrell, R. (2001). Nanostructured ceramics: a review of their potential. *Applied Organometallic Chemistry*, *15*(5), 321-330. https://doi.org/10.1002/aoc.153

Carter, C. B., & Norton, M. G. (2007). *Ceramic materials: science and engineering*. Springer Science & Business Media. https://link.springer.com/book/10.1007/978-1-4614-3523-5

Cerame Unie - The European Ceramic Industry Association. (2021). *Ceramic Industry - Facts and Figures*. Retrieved 01 December 2021 from http://cerameunie.eu/ceramic-industry/facts-figures/

da Silva, A. L., Dondi, M., & Hotza, D. (2017). Self-cleaning ceramic tiles coated with Nb2O5-doped-TiO2 nanoparticles. *Ceramics International*, *43*(15), 11986-11991. https://doi.org/10.1016/j.ceramint.2017.06.049

De Marzi, L., Monaco, A., De Lapuente, J., Ramos, D., Borras, M., Di Gioacchino, M., Santucci, S., & Poma, A. (2013). Cytotoxicity and Genotoxicity of Ceria Nanoparticles on Different Cell Lines in Vitro. *International Journal of Molecular Sciences*, *14*(2), 3065-3077. https://doi.org/10.3390/ijms14023065

DeLoughery, Z., Luczak, M. W., Ortega-Atienza, S., & Zhitkovich, A. (2015). DNA double-strand breaks by Cr(VI) are targeted to euchromatin and cause ATR-dependent phosphorylation of histone H2AX and its ubiquitination. *Toxicol Sci*, *143*(1), 54-63. https://doi.org/10.1093/toxsci/kfu207

Demokritou, P., Gass, S., Pyrgiotakis, G., Cohen, J. M., Goldsmith, W., McKinney, W., Frazer, D., Ma, J., Schwegler-Berry, D., Brain, J., & Castranova, V. (2013). An in vivo and in vitro toxicological characterisation of realistic nanoscale CeO2 inhalation exposures. *Nanotoxicology*, *7*(8), 1338-1350. https://doi.org/10.3109/17435390.2012.739665

Ding, J., He, G., Gong, W., Wen, W., Sun, W., Ning, B., Huang, S., Wu, K., Huang, C., Wu, M., Xie, W., & Wang, H. (2009). Effects of nickel on cyclin expression, cell cycle progression and cell proliferation in human pulmonary cells. *Cancer epidemiology, biomarkers & prevention : a publication of the American Association for Cancer Research, cosponsored by the American Society of Preventive Oncology*, *18*(6), 1720-1729. https://doi.org/10.1158/1055-9965.EPI-09-0115

Commission Recommendation of 18 October 2011 on the definition of nanomaterial Text with EEA relevance, 38-40 275 (2011). https://eur-lex.europa.eu/legal-content/EN/TXT/?uri=CELEX:32011H0696

Fadeel, B. (2019). The Right Stuff: On the Future of Nanotoxicology [Specialty Grand Challenge]. *Frontiers in Toxicology*, *1*(1). https://doi.org/10.3389/ftox.2019.00001

Fonseca, A. S., Maragkidou, A., Viana, M., Querol, X., Hämeri, K., de Francisco, I., Estepa, C., Borrell, C., Lennikov, V., & de la Fuente, G. F. (2016). Process-generated nanoparticles from ceramic tile sintering: Emissions, exposure and environmental release. *Science of The Total Environment*, *565*, 922-932. https://doi.org/10.1016/j.scitotenv.2016.01.106

Fonseca, A. S., Viana, M., Querol, X., Moreno, N., de Francisco, I., Estepa, C., & de la Fuente, G. F. (2015). Ultrafine and nanoparticle formation and emission mechanisms during laser processing of ceramic materials. *Journal of Aerosol Science*, *88*, 48-57. https://doi.org/10.1016/j.jaerosci.2015.05.013

Frieke Kuper, C., Gröllers-Mulderij, M., Maarschalkerweerd, T., Meulendijks, N. M. M., Reus, A., van Acker, F., Zondervan-van den Beuken, E. K., Wouters, M. E. L., Bijlsma, S., & Kooter, I. M. (2015). Toxicity assessment of aggregated/agglomerated cerium oxide nanoparticles in an in vitro 3D airway model: The influence of mucociliary clearance. *Toxicology in Vitro*, *29*(2), 389-397. https://doi.org/10.1016/j.tiv.2014.10.017

Fröhlich, E. (2018). Comparison of conventional and advanced in vitro models in the toxicity testing of nanoparticles. *Artificial Cells, Nanomedicine, and Biotechnology*, *46*(sup2), 1091-1107. https://doi.org/10.1080/21691401.2018.1479709

George, I., Uboldi, C., Bernard, E., Sobrido, M. S., Dine, S., Hagège, A., Vrel, D., Herlin, N., Rose, J., Orsière, T., Grisolia, C., Rousseau, B., & Malard, V. (2019). Toxicological Assessment of ITER-Like Tungsten Nanoparticles Using an In Vitro 3D Human Airway Epithelium Model. *Nanomaterials*, *9*(10), 1374. https://doi.org/10.3390/nano9101374

Halasova, E., Adamkov, M., Matakova, T., Kavcova, E., Poliacek, I., & Singliar, A. (2010). Lung cancer incidence and survival in chromium exposed individuals with respect to expression of anti-apoptotic protein survivin and tumor suppressor P53 protein. *Eur J Med Res*, *15 Suppl 2*(Suppl 2), 55-59. https://doi.org/10.1186/2047-783x-15-s2-55

Hoffmann, W., Gradinaru, J., Farcal, L., Caul-Futy, M., Huang, S., Wiszniewski, L., Parissis, N., Morath, S., Fortaner, S., & Cole, T. (2018). Establishment of a human 3D tissue-based assay for upper respiratory tract absorption. *Applied in vitro toxicology*, *4*(2), 139-148. https://doi.org/10.1089/aivt.2017.0035

International Agency for Research on Cancer. (1990). Chromium, nickel and welding. *IARC monographs on the evaluation of carcinogenic risks to humans*, *49*. https://monographs.iarc.who.int/wp-content/uploads/2018/06/mono71.pdf

Kim, I.-S., Baek, M., & Choi, S.-J. (2010). Comparative cytotoxicity of Al2O3, CeO2, TiO2 and ZnO nanoparticles to human lung cells. *Journal of Nanoscience and Nanotechnology*, *10*(5), 3453-3458. https://doi.org/10.1166/jnn.2010.2340

Kim, S., Jaques, P. A., Chang, M., Barone, T., Xiong, C., Friedlander, S. K., & Sioutas, C. (2001). Versatile aerosol concentration enrichment system (VACES) for simultaneous in vivo and in vitro evaluation of toxic effects of ultrafine, fine and coarse ambient particles Part II: Field evaluation. *Journal of Aerosol Science*, *32*(11), 1299-1314. https://doi.org/10.1016/S0021-8502(01)00058-1

Kroll, A., Dierker, C., Rommel, C., Hahn, D., Wohlleben, W., Schulze-Isfort, C., Göbbert, C., Voetz, M., Hardinghaus, F., & Schnekenburger, J. (2011). Cytotoxicity screening of 23 engineered nanomaterials using a test matrix of ten cell lines and three different assays. *Particle and fibre toxicology*, *8*(1), 9. https://doi.org/10.1186/1743-8977-8-9

Krug, H. F. (2014). Nanosafety research—are we on the right track? *Angewandte Chemie International Edition*, *53*(46), 12304-12319. https://doi.org/10.1002/anie.201403367

Lacroix, G., Koch, W., Ritter, D., Gutleb, A. C., Larsen, S. T., Loret, T., Zanetti, F., Constant, S., Chortarea, S., & Rothen-Rutishauser, B. (2018). Air–liquid Interface in vitro models for respiratory toxicology research: consensus workshop and recommendations. *Applied in vitro toxicology*, *4*(2), 91-106. https://doi.org/10.1089/aivt.2017.0034

Lanone, S., Rogerieux, F., Geys, J., Dupont, A., Maillot-Marechal, E., Boczkowski, J., Lacroix, G., & Hoet, P. (2009). Comparative toxicity of 24 manufactured nanoparticles in human alveolar epithelial and macrophage cell lines. *Particle and fibre toxicology*, *6*, 14. https://doi.org/10.1186/1743-8977-6-14

Lee, J., Mahendra, S., & Alvarez, P. J. J. (2010). Nanomaterials in the Construction Industry: A Review of Their Applications and Environmental Health and Safety Considerations. *ACS Nano*, *4*(7), 3580-3590. https://doi.org/10.1021/nn100866w

Lippmann, M., & Chen, L. C. (2009). Health effects of concentrated ambient air particulate matter (CAPs) and its components. *Crit Rev Toxicol*, *39*(10), 865-913. https://doi.org/10.3109/10408440903300080

Loret, T., Peyret, E., Dubreuil, M., Aguerre-Chariol, O., Bressot, C., le Bihan, O., Amodeo, T., Trouiller, B., Braun, A., Egles, C., & Lacroix, G. (2016). Air-liquid interface exposure to aerosols of poorly soluble nanomaterials induces different biological activation levels compared to exposure to suspensions. *Particle and fibre toxicology*, *13*(1), 58-58. https://doi.org/10.1186/s12989-016-0171-3

Manivasakan, P., Rajendran, V., Rauta, P. R., Sahu, B. B., Sahu, P., Panda, B. K., Valiyaveettill, S., & Jegadesan, S. (2010). Effect of TiO2 nanoparticles on properties of silica refractory. *Journal of the American Ceramic Society*, *93*(8), 2236-2243. https://doi.org/10.1111/j.1551-2916.2010.03727.x

Matizamhuka, W. (2018). Advanced ceramics-the new frontier in modern-day technology: Part I. *Journal of the Southern African Institute of Mining and Metallurgy*, *118*(7), 757-764. https://doi.org/10.17159/2411-9717/2018/v118n7a9

Miller, A. J., & Spence, J. R. (2017). In Vitro Models to Study Human Lung Development, Disease and Homeostasis. *Physiology (Bethesda)*, *32*(3), 246-260. https://doi.org/10.1152/physiol.00041.2016

Mittal, S., & Pandey, A. K. (2014). Cerium Oxide Nanoparticles Induced Toxicity in Human Lung Cells: Role of ROS Mediated DNA Damage and Apoptosis. *BioMed research international*, *2014*, 891934. https://doi.org/10.1155/2014/891934

Mo, Y., Zhang, Y., Zhang, Y., Yuan, J., Mo, L., & Zhang, Q. (2021). Nickel nanoparticle-induced cell transformation: involvement of DNA damage and DNA repair defect through HIF-1α/miR-210/Rad52 pathway. *Journal of Nanobiotechnology*, *19*(1), 370. https://doi.org/10.1186/s12951-021-01117-7

Morimoto, Y., Hirohashi, M., Ogami, A., Oyabu, T., Myojo, T., Hashiba, M., Mizuguchi, Y., Kambara, T., Lee, B. W., & Kuroda, E. (2011). Pulmonary toxicity following an intratracheal instillation of nickel oxide nanoparticle agglomerates. *Journal of occupational health*, *53*(4), 293-295. https://doi.org/10.1539/joh.11-0034-BR

Munz, D., & Fett, T. (2000). Ceramics: mechanical properties, failure behaviour, materials selection. Annales de Chimie Science des Materiaux,

Nossa, R., Costa, J., Cacopardo, L., & Ahluwalia, A. (2021). Breathing in vitro: Designs and applications of engineered lung models. *Journal of Tissue Engineering*, *12*, 20417314211008696. https://doi.org/10.1177/20417314211008696

Palmero, P. (2015). Structural Ceramic Nanocomposites: A Review of Properties and Powders' Synthesis Methods. *Nanomaterials*, *5*(2), 656-696. https://doi.org/10.3390/nano5020656

Park, B., Donaldson, K., Duffin, R., Tran, L., Kelly, F., Mudway, I., Morin, J.-P., Guest, R., Jenkinson, P., Samaras, Z., Giannouli, M., Kouridis, H., & Martin, P. (2008). Hazard and Risk Assessment of a Nanoparticulate Cerium Oxide-Based Diesel Fuel Additive—A Case Study. *Inhalation Toxicology*, *20*(6), 547-566. https://doi.org/10.1080/08958370801915309

Paur, H.-R., Cassee, F. R., Teeguarden, J., Fissan, H., Diabate, S., Aufderheide, M., Kreyling, W. G., Hänninen, O., Kasper, G., Riediker, M., Rothen-Rutishauser, B., & Schmid, O. (2011). In-vitro cell exposure studies for the assessment of nanoparticle toxicity in the lung—A dialog between aerosol science and biology. *Journal of Aerosol Science*, *42*(10), 668-692. https://doi.org/10.1016/j.jaerosci.2011.06.005

Phillips, J. I., Green, F. Y., Davies, J. C., & Murray, J. (2010). Pulmonary and systemic toxicity following exposure to nickel nanoparticles. *Am J Ind Med*, *53*(8), 763-767. https://doi.org/10.1002/ajim.20855

Reynolds, M., Armknecht, S., Johnston, T., & Zhitkovich, A. (2012). Undetectable role of oxidative DNA damage in cell cycle, cytotoxic and clastogenic effects of Cr(VI) in human lung cells with restored ascorbate levels. *Mutagenesis*, *27*(4), 437-443. https://doi.org/10.1093/mutage/ger095

Riediker, M., Zink, D., Kreyling, W., Oberdörster, G., Elder, A., Graham, U., Lynch, I., Duschl, A., Ichihara, G., Ichihara, S., Kobayashi, T., Hisanaga, N., Umezawa, M., Cheng, T.-J., Handy, R., Gulumian, M., Tinkle, S., & Cassee, F. (2019). Particle toxicology and health - where are we? *Particle and fibre toxicology*, *16*(1), 19. https://doi.org/10.1186/s12989-019-0302-8

Riego Sintes, J., Roebben, G., Linsinger, T., Gibson, N., Rauscher, H., Kestens, V., & Mech, A. (2019). *An overview of concepts and terms used in the European Commission's definition of nanomaterial*. European Commission, Joint Research Centre Publications Office. https://doi.org/10.2760/459136

Salamon, D. (2014). Chapter 6 - Advanced Ceramics. In J. Z. Shen & T. Kosmač (Eds.), *Advanced Ceramics for Dentistry* (pp. 103-122). Butterworth-Heinemann. https://doi.org/10.1016/B978-0-12-394619-5.00006-7

Salmatonidis, A., Ribalta, C., Sanfélix, V., Bezantakos, S., Biskos, G., Vulpoi, A., Simion, S., Monfort, E., & Viana, M. (2018a). Workplace Exposure to Nanoparticles during Thermal Spraying of Ceramic Coatings. *Annals of Work Exposures and Health*, *63*(1), 91-106. https://doi.org/10.1093/annweh/wxy094

Salmatonidis, A., Sanfélix, V., Carpio, P., Pawłowski, L., Viana, M., & Monfort, E. (2019). Effectiveness of nanoparticle exposure mitigation measures in industrial settings. *International Journal of Hygiene and Environmental Health*, *222*(6), 926-935. https://doi.org/10.1016/j.ijheh.2019.06.009

Salmatonidis, A., Viana, M., Biskos, G., & Bezantakos, S. (2020). Particle size distributions and hygroscopic restructuring of ultrafine particles emitted during thermal spraying. *Aerosol Science and Technology*, *54*(12), 1359-1372. https://doi.org/10.1080/02786826.2020.1784837

Salmatonidis, A., Viana, M., Pérez, N., Alastuey, A., de la Fuente, G. F., Angurel, L. A., Sanfélix, V., & Monfort, E. (2018b). Nanoparticle formation and emission during laser ablation of ceramic tiles. *Journal of Aerosol Science*, *126*, 152-168. https://doi.org/10.1016/j.jaerosci.2018.09.006

Salnikow, K., & Zhitkovich, A. (2008). Genetic and epigenetic mechanisms in metal carcinogenesis and cocarcinogenesis: nickel, arsenic, and chromium. *Chemical research in toxicology*, *21*(1), 28-44. https://doi.org/10.1021/tx700198a

Schraufnagel, D. E. (2020). The health effects of ultrafine particles. *Experimental & Molecular Medicine*, *52*(3), 311-317. https://doi.org/10.1038/s12276-020-0403-3

Shao, W., Khin, S., & Kopp, W. C. (2012). Characterization of effect of repeated freeze and thaw cycles on stability of genomic DNA using pulsed field gel electrophoresis. *Biopreservation and biobanking*, *10*(1), 4-11. https://doi.org/10.1089/bio.2011.0016

Tabei, Y., Sonoda, A., Nakajima, Y., Biju, V., Makita, Y., Yoshida, Y., & Horie, M. (2015). In vitro evaluation of the cellular effect of indium tin oxide nanoparticles using the human lung adenocarcinoma A549 cells. *Metallomics*, *7*(5), 816-827. https://doi.org/10.1039/c5mt00031a

Titma, T., Shimmo, R., Siigur, J., & Kahru, A. (2016). Toxicity of antimony, copper, cobalt, manganese, titanium and zinc oxide nanoparticles for the alveolar and intestinal epithelial barrier cells in vitro. *Cytotechnology*, *68*(6), 2363-2377. https://doi.org/10.1007/s10616-016-0032-9

Valsami-Jones, E., & Lynch, I. (2015). How safe are nanomaterials? *Science*, *350*(6259), 388-389. https://doi.org/10.1126/science.aad0768

Viana, M., Fonseca, A. S., Querol, X., López-Lilao, A., Carpio, P., Salmatonidis, A., & Monfort, E. (2017). Workplace exposure and release of ultrafine particles during atmospheric plasma spraying in the ceramic industry. *Science of The Total Environment*, *599-600*, 2065-2073. https://doi.org/10.1016/j.scitotenv.2017.05.132

Viana, M., Salmatonidis, A., Bezantakos, S., Ribalta, C., Moreno, N., Córdoba, P., Cassee, F. R., Boere, J., Fraga, S., Teixeira, J. P., Bessa, M. J., & Monfort, E. (2021). Characterizing the Chemical Profile of Incidental Ultrafine Particles for Toxicity Assessment Using an Aerosol Concentrator. *Ann Work Expo Health*, *65*(8), 966-978. https://doi.org/10.1093/annweh/wxab011

Wise, J. P., Sr., Wise, S. S., & Little, J. E. (2002). The cytotoxicity and genotoxicity of particulate and soluble hexavalent chromium in human lung cells. *Mutat Res*, *517*(1-2), 221-229. https://doi.org/10.1016/s1383-5718(02)00071-2

Zhang, Q., Kusaka, Y., Zhu, X., Sato, K., Mo, Y., Kluz, T., & Donaldson, K. (2003). Comparative toxicity of standard nickel and ultrafine nickel in lung after intratracheal instillation. *J Occup Health*, *45*(1), 23-30. https://doi.org/10.1539/joh.45.23

Zhang, Z., Leonard, S. S., Wang, S., Vallyathan, V., Castranova, V., & Shi, X. (2001). Cr (VI) induces cell growth arrest through hydrogen peroxide-mediated reactions. *Mol Cell Biochem*, *222*(1-2), 77-83. https://doi.org/10.1023/A:1017963307358